

Orange, Red, Yellow: Biosynthesis of Azaphilone Pigments in *Monascus* Fungi

Wanping Chen^{1#}, Runfa Chen^{1#}, Qingpei Liu^{1,3#}, Yi He¹, Kun He¹, Xiaoli Ding¹, Lijing Kang¹, Xiaoxiao Guo¹, Nana Xie¹, Youxiang

Zhou^{2*}, Yuanyuan Lu^{3,4}, Russell J. Cox⁵, István Molnár^{3*}, Mu Li¹, Yanchun Shao¹, and Fusheng Chen^{1*}

¹ Key Laboratory of Environment Correlative Dietology, College of Food Science and Technology, Huazhong Agricultural University, Wuhan, Hubei Province, 430070, China

² Institute of Quality Standard and Testing Technology for Agro-Products, Hubei Academy of Agricultural Sciences, Wuhan, Hubei Province, 430064, China

³ Natural Products Center, The University of Arizona, 250 E. Valencia Rd., Tucson, Arizona 85706, U.S.A.

⁴ State Key Laboratory of Natural Medicines, School of Life Science and Technology, China Pharmaceutical University, 24 Tong Jia Xiang, Nanjing 210009, China

⁵ Institut für Organische Chemie and BMWZ, Leibniz Universität Hannover, Schneiderberg 1B, 30167 Hannover, Germany

These authors contributed equally to this work.

* Corresponding authors

E-mail: zhouyouxiang@gmail.com; imolnar@email.arizona.edu; chenfs@mail.hzau.edu.cn

ELECTRONIC SUPPLEMENTARY INFORMATION

Content

1. MonAzPs production in <i>Monascus ruber</i> M7	3
2. Gene map and annotation of the 54 kb MonAzPs gene cluster from <i>M. ruber</i> M7	4
3. Comparison of MonAzPs biosynthesis gene clusters from <i>M. ruber</i> M7, <i>Penicillium marneffei</i> ATCC18224, <i>Talaromyces stipitatus</i> ATCC10500	6
4. Construction of MonAzPs biosynthetic gene knockouts in <i>M. ruber</i> M7	8
5. Fermentation and MonAzPs detection	13
6. Spectral data for MonAzPs and intermediates	16
7. Heterologous production of MonAzPs biosynthetic intermediates	106
8. Enzyme assay for MrPigD	114
9. <i>In vitro</i> reaction of rubropunctatin (3), monascorubrin (4) and monascin (1) with 17 amino acids and ammonia	127
10. Domain analysis of MrPigA, the MonAzPs polyketide synthase from <i>M. ruber</i> M7	142
11. Mechanism of Knoevenagel cyclization	143
12. References	144

1. MonAzPs production in *Monascus ruber* M7

The wide type *M. ruber* M7 was isolated from red mold rice and used as a model strain in our lab to study the MonAzPs pathway. As shown in Figure 1-1, ten MonAzPs congeners are easily detected in the *M. ruber* M7 methanol extract, including six yellow pigments (monascin **1**, ankaflavin **2**, monasfluol A **7**, monasfluol B **8**, monasfluore A **9**, and monasfluore B **10**), two orange pigments (rubropunctatin **3** and monascorubrin **4**), and two red pigments (rubropunctamine **5** and monascorubramine **6**).

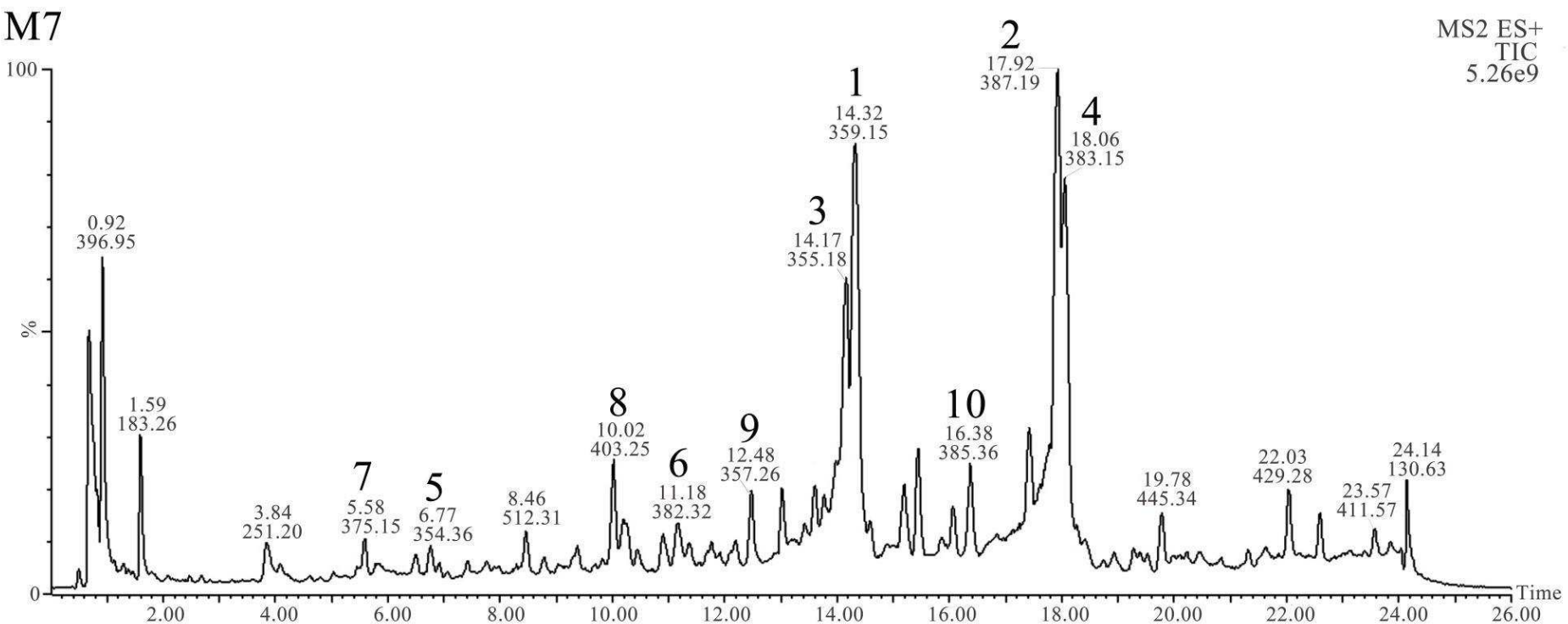
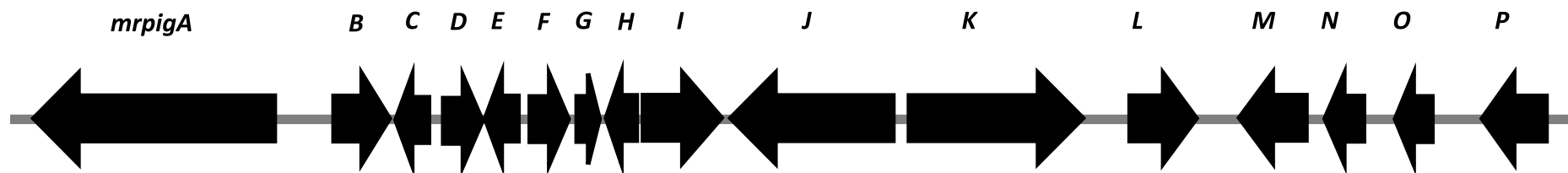


Figure 1-1. The total ion chromatogram of the *M. ruber* M7 methanol extract. The fermentation conditions and MonAzPs detection methods are presented in the later Section 5. The related spectral data are shown in Section 6.

2. Gene map and annotation of the 54 kb MonAzPs gene cluster from *M. ruber* M7

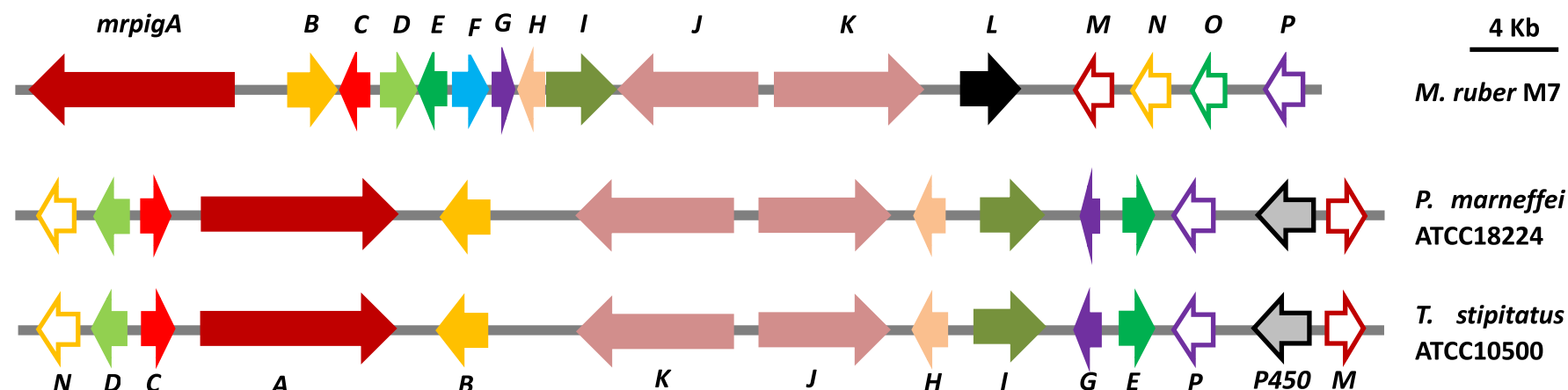


Gene	Size (bp/aa)	GenBank Accession	Plausible function	Protein with high similarity	Identity at amino acid level (%)
<i>mrpigA</i>	8146/2690	ALN44200.1	MonAzPs biosynthesis nrPKS	<i>M. pilosus</i> MonAzPs biosynthesis PKS (AGN71604.1)	97
<i>mrpigB</i>	1980/554	AGL44390.1	MonAzPs biosynthesis activator	<i>M. pilosus</i> MonAzPs biosynthesis transcriptional activator (AGN71605.1)	95
<i>mrpigC</i>	1057/303	ALN44201.1	C-11-Ketoreductase	<i>Talaromyces marneffei</i> oxoacyl-[ACP] reductase FabG (KFX50139.1)	50
<i>mrpigD</i>	1367/455	AGI63864.1	4-O-Acyltransferase	<i>M. pilosus</i> O-acetyltransferase (AGN71607.1)	96
<i>mrpigE</i>	1028/342	AHA93896.1	NAD(P)H-dependent oxidoreductase	<i>M. pilosus</i> aflatoxin aldehyde reductase (BAE44305.1)	98

<i>mrpigF</i>	1397/465	KX278306	FAD-dependent oxidoreductase	<i>M. pilosus</i> amino oxidase (AGN71609.1)	94
<i>mrpigG</i>	821/273	KX278307	Serine hydrolase	<i>Coccidioides immitis</i> citrinin biosynthesis oxydoreductase CtnB (XP_001246124.2)	54
<i>mrpigH</i>	1109/369	KX278308	Dehydrogenase	<i>M. pilosus</i> quinone oxidoreductase (AGN71610.1)	95
<i>mrpigI</i>	2795/812	KX278309	Transcription factor	<i>M. pilosus</i> transcriptional regulatory protein (AGN71612.1)	95
<i>mrpigJ</i>	5770/1842	JX675042	FAS alpha subunit	<i>M. pilosus</i> FAS alpha subunit (AGN71613.1)	90
<i>mrpigK</i>	6265/2027	JX675043	FAS beta subunit	<i>M. pilosus</i> FAS beta subunit (AGN71614.1)	93
<i>mrpigL</i>	2400/473	KX290843	Ankyrin repeat protein	<i>Penicillium chrysogenum</i> ankyrin repeat protein (KZN92140.1)	58
<i>mrpigM</i>	2574/508	KX278310	O-Acetyltransferase	<i>M. pilosus</i> hypothetical protein (AGN71622.1)	94
<i>mrpigN</i>	1371/436	ALT31754.1	FAD-dependent monooxygenase	<i>M. pilosus</i> salicylate hydroxylase (AGN71623.1)	97
<i>mrpigO</i>	1379/459	KX290844	Deacetylase	<i>M. pilosus</i> hypothetical protein (AGN71624.1)	93
<i>mrpigP</i>	2239/570	KX290845	MFS multidrug transporter	<i>Talaromyces stipitatus</i> MFS multidrug transporter (XP_002340049.1)	61

3. Comparison of MonAzPs biosynthesis gene clusters from *M. ruber* M7, *Penicillium marneffei* ATCC18224, *Talaromyces stipitatus* ATCC10500

P. marneffei produces soluble red pigments that have been shown to have the same structures as MonAzPs (Woo et al., 2014). To identify the core biosynthetic gene set for MonAzPs, we compared the *M. ruber* M7 MonAzPs biosynthesis gene cluster with similar clusters from *P. marneffei* ATCC18224 and its close relative *T. stipitatus* ATCC10500 (Nierman et al., 2015). The comparison shows that most MonAzPs pigment biosynthetic genes are conserved across these three strains within these clusters, with the exception of the *mrpigF*, *mrpigL* and *mrpigO* genes (emphasized in red font in the table). Similar genes to *mrpigF* and *mrpigO* are encoded outside the pigment gene clusters of *P. marneffei* ATCC18224 and *T. stipitatus* ATCC10500.



Genes in <i>M. ruber</i> M7 (1)	Identities between 1 and 2 at amino acid level (%)	Homologs in <i>P. marneffei</i> ATCC18224 (2)	Identities between 2 and 3 at amino acid level (%)	Homologs in <i>T. stipitatus</i> ATCC10500 (3)	Identities between 1 and 3 at amino acid level (%)
<i>mrpigA</i>	65	XP_002149769.1	83	XP_002340038.1	64

<i>mrpigB</i>	46	XP_002149768.1	84	XP_002340039.1	48
<i>mrpigC</i>	70	XP_002149770.1	87	XP_002340037.1	67
<i>mrpigD</i>	64	XP_002149771.1	84	XP_002340036.1	61
<i>mrpigE</i>	70	XP_002149761.1	92	XP_002340048.1	68
<i>mrpigF</i>	36	XP_002144367.1	76	XP_002479165.1	35
<i>mrpigG</i>	71	XP_002149762.1	84	XP_002340047.1	70
<i>mrpigH</i>	65	XP_002149765.1	95	XP_002340043.1	66
<i>mrpigI</i>	39	XP_002149763.1* XP_002149764.1*	66	XP_002340045.1* XP_002340046.1* XP_002340044.1*	42
<i>mrpigJ</i>	59	XP_002149766.1	81	XP_002340042.1	57
<i>mrpigK</i>	58	XP_002149767.1	80	XP_002340041.1	57
<i>mrpigL</i>	-	-	-	-	-
<i>mrpigM</i>	53	XP_002149758.1	85	XP_002340051.1	51
<i>mrpigN</i>	65	XP_002149772.1	85	XP_002340035.1	65
<i>mrpigO</i>	41	XP_002149741.1	70	XP_002340066.1	41
<i>mrpigP</i>	62	XP_002149760.1	85	XP_002340049.1	61

*: The multiple apparent homologs of *mrpigI* in *P. marneffei* ATCC18224 and *T. stipitatus* ATCC10500 probably arose from erroneous annotations in the *P. marneffei* ATCC18224 and *T. stipitatus* ATCC10500 genomes.

4. Construction of MonAzPs biosynthetic gene knockouts in *M. ruber* M7

4.1. Deletion of the target genes

The coding regions of the targeted genes were replaced with the neomycin phosphotransferase (*neo*) or the hygromycin B phosphotransferase (*hph*) resistance gene cassettes that were produced by double-joint PCR (Yu et al., 2004). First, the 5' and the 3' flanking regions of the targeted genes were PCR amplified with the appropriate primers (**Table 4-1**) using genomic DNA as the template. The 1,221-bp *neo* resistance marker cassette was amplified from plasmid pKN1 (He et al., 2013) with the primer pair neof–neor. Alternatively, the 2,137-bp *hph* resistance marker cassette was amplified from plasmid pSKH (He et al., 2013) with the primer pair hphf–hphr (**Table 4-1**). All PCR products were purified with the TransGen gel purification kit (TransGen, Beijing, China), and the three fragments (5' flanking region, resistance gene, and 3' flanking region) were mixed at a 1:2:1 molar ratio to perform a fusion PCR. The product of the fusion PCR was used as the template for a second round of PCR with the primers X5f–X3r (**Table 4-1**). This PCR product was then cloned into the pMD19-T vector (Takara, Dalian, China) and the cloned fragment was sequence-verified. Next, the fragment was subcloned into the pCAMBIA3300 vector (<http://www.cambia.org/daisy/cambia/home.html>), and the resulting deletion vector was transformed into *Agrobacterium tumefaciens* EHA105. *A. tumefaciens* EHA105 clones containing the deletion vector were induced using acetosyringone, and co-incubated for transformation with *M. ruber* M7 to obtain the deletion mutants (Shao et al., 2009). PDA supplemented with G418 or hygromycin B were utilized to select the deletion mutants, and these mutants were verified by PCR. The deletion mutants of *mrpigA*, *mrpigB*, and *mrpigE* were described previously (Xie et al., 2013; Liu et al., 2014; Xie et al., 2015).

Table 4-1. Primers used in this study

Name	Sequence (5'→3')	Descriptions
A5f	ACATCCAAGTCGAGATGGTCAGTC	For amplification of the 828-bp 5' flanking region

A5r	<u>CAATATCATCTTCTGTCGAC</u> ATGATGCCAGCTGAACGGAGT	of the <i>mrpigA</i> gene
A3f	<u>GAGGTAATCCTCTTTCTAG</u> GGGCGAGCTGGAACAGAAAGT	For amplification of the 878-bp 3' flanking region of the <i>mrpigA</i> gene
A3r	GCACGGCGTATTGAAATAGA	
B5f	CGGTCTTCCCACTCGATTGCCA	For amplification of the 866-bp 5' flanking region of the <i>mrpigB</i> gene
B5r	<u>CAATATCATCTTCTGTCGAC</u> AAATACCACTCGCGCTGTC	
B3f	<u>GAGGTAATCCTCTTTCTAG</u> GTCCATCCATTGATGCCGTTAC	For amplification of the 811-bp 3' flanking region of the <i>mrpigB</i> gene
B3r	CGCATCTTCTCAACCCGACTCT	
C5f	ACAGCTCGATGGCACCGCTC	For amplification of the 801-bp 5' flanking region of the <i>mrpigC</i> gene
C5r	<u>CAATATCATCTTCTGTCGAC</u> GGCTCTTTCTGGATCCT	
C3f	<u>GAGGTAATCCTCTTTCTAG</u> ACTGCCTTTATGACT	For amplification of the 712-bp 3' flanking region of the <i>mrpigC</i> gene
C3r	GATACCGGTGCACTGTTCT	
D5f	GCTGGGTAGGTGTCGTTG	For amplification of the 894-bp 5' flanking region of the <i>mrpigD</i> gene
D5r	<u>CAATATCATCTTCTGTCGAC</u> CCCTGACTGTGCGTTATTT	
D3f	<u>GAGGTAATCCTCTTTCTAG</u> TGTTAACCTCTGGTCAATG	For amplification of the 856-bp 3' flanking region of the <i>mrpigD</i> gene
D3r	TGGGCATCAGCAACTACAT	
E5f	ACGGCACCGGAAACGAAGTT	For amplification of the 885-bp 5' flanking region of the <i>mrpigE</i> gene
E5r	<u>CAATATCATCTTCTGTCGAC</u> GGATATCTGCCTTAT	
E3f	<u>GAGGTAATCCTCTTTCTAG</u> TCACTAGGGTCGGGTTGTTG	For amplification of the 856-bp 3' flanking region of the <i>mrpigE</i> gene
E3r	GCGATCCCCGCCAACCCCGTC	
F5f	TCGAGTTCGCGTGTCAA	For amplification of the 738-bp 5' flanking region of the <i>mrpigF</i> gene
F5r	<u>GGTTACGGTTCGATGGGTTGAG</u> TTGGCAACGGAGGACAGGATGAGAA	
F3f	<u>CATGCATGTTGCATGATGAT</u> CGGTGTTCTGGTGGCTGTAC	For amplification of the 878-bp 3' flanking region of the <i>mrpigF</i> gene
F3r	TTGAATGGCCCCGAACCTCTTGTA	
J5f	GCGATGACTCTGCCAATGCC	For amplification of the 738-bp 5' flanking region of the <i>mrpigJ</i> gene
J5r	<u>CAATATCATCTTCTGTCGAC</u> CCCTATGTTCCGGGATCA	
J3f	<u>GAGGTAATCCTCTTTCTAG</u> CCAGTGCCTAGCGGGATGTA	For amplification of the 878-bp 3' flanking region of the <i>mrpigJ</i> gene
J3r	GGCGCACAAAGCTCTGATTGAA	
K5f	AGACACCGTGCCCTAATTGTCC	For amplification of the 860-bp 5' flanking region of the <i>mrpigK</i> gene
K5r	<u>CAATATCATCTTCTGTCGACC</u> AGGTACCGCGTAATGT	

K3f	<u>GAGGTAATCCTCTTTCTAGATGCGGAGCAAGGGACTTATC</u>	For amplification of the 873-bp 3' flanking region of the <i>mrpigK</i> gene
K3r	ATATTGGGCTCTGCGTGATGTT	
L5f	TCACGCCATCTCTACCAC	For amplification of the 834-bp 5' flanking region of the <i>mrpigL</i> gene
L5r	<u>CAATATCATCTTCTGTCGAC</u> GCATCGCCTTGTCAACTTCT	
L3f	<u>GAGGTAATCCTCTTTCTAGG</u> CACCCAAAGGTAGAGAACTCAC	For amplification of the 802-bp 3' flanking region of the <i>mrpigL</i> gene
L3r	CTTCGCCACTCCATTACAAC	
M5f	TTGGTGTGCAACAGAACTAGA	For amplification of the 860-bp 5' flanking region of the <i>mrpigM</i> gene
M5r	<u>GGTTACGGTTCGATGGGGTTGAG</u> TTGGGCTTGAGGGTGCTATCTTA	
M3f	<u>CATGCATGTTGCATGATGATT</u> GAGCGGTTGAAGGATGTGAA	For amplification of the 873-bp 3' flanking region of the <i>mrpigM</i> gene
M3r	CGTGATAGACAGTGCCTAGAG	
N5f	CCCGCTCTCCAGATATTG	For amplification of the 928-bp 5' flanking region of the <i>mrpigN</i> gene
N5r	<u>CAATATCATCTTCTGTCGAC</u> GCAGGGCACTGGGATTGAAGAT	
N3f	<u>CATGCATGTTGCATGATGATG</u> TGTACCCGTCAACCCAA	For amplification of the 932-bp 3' flanking region of the <i>mrpigN</i> gene
N3r	TAGTTGCCGATTGCCA	
O5f	TTGTCAAATAGCGGGCTATCACC	For amplification of the 916-bp 5' flanking region of the <i>mrpigO</i> gene
O5r	<u>GGTTACGGTTCGATGGGGTTGAG</u> TTGGCACTGAGTTGGGATCAGAGATGA	
O3f	<u>CATGCATGTTGCATGATGATG</u> GGATGAGCACGATCTCCAATACT	For amplification of the 978-bp 3' flanking region of the <i>mrpigO</i> gene
O3r	CGCCCCAAACAACAGTAAGTGAG	
P5f	CGGGGTACCGCAGGAGACCAAGAACGAGA	For amplification of the 766-bp 5' flanking region of the <i>mrpigP</i> gene
P5r	<u>CAATATCATCTTCTGTCGAC</u> CGCAGCCATCTGGAGACGAAA	
P3f	<u>CATGCATGTTGCATGATGAT</u> TAGATCTTCCCGTCAGT	For amplification of the 758-bp 3' flanking region of the <i>mrpigP</i> gene
P3r	CCCAAGCTGCGGATCACCACCAAGGATATGT	
neof	CCAACCTAACCCCCATCGAACCGTAACC	For amplification of the 1,221-bp <i>neo</i> cassette from plasmid pKN1
neor	ATCATCATGCAACATGCATG	
hphf	GTCGACAGAAAGATGATATTG	For amplification of the 2,137-bp <i>hph</i> cassette from plasmid pSKH
hphr	CTAGAAAGAAGGATTACCTC	

Note: The sequences underlined with straight lines overlap with the primer sequences of either hphf or hphr. The sequences underlined by the wavy lines overlap with the primer sequences of either neof or neor.

4.2. Phenotypes of the knockout mutants of *M. ruber* M7

Knockout mutants of *M. ruber* M7 were cultivated on PDA, PDB and rice media, respectively, at 28°C for 12 days. Compared to the wild type M7, some knockout mutants show visually obvious differences in their MonAzPs production, confirming the roles of the corresponding genes in MonAzPs biosynthesis. However, none of the knockout mutants show differences in colonial morphology and growth rates (**Figure 4-1**). Similarly, all the knockout mutants show regular cleistothecia and conidia formation, except for $\Delta mrpigN$ that forms no cleistothecia (**Figure 4-2**).

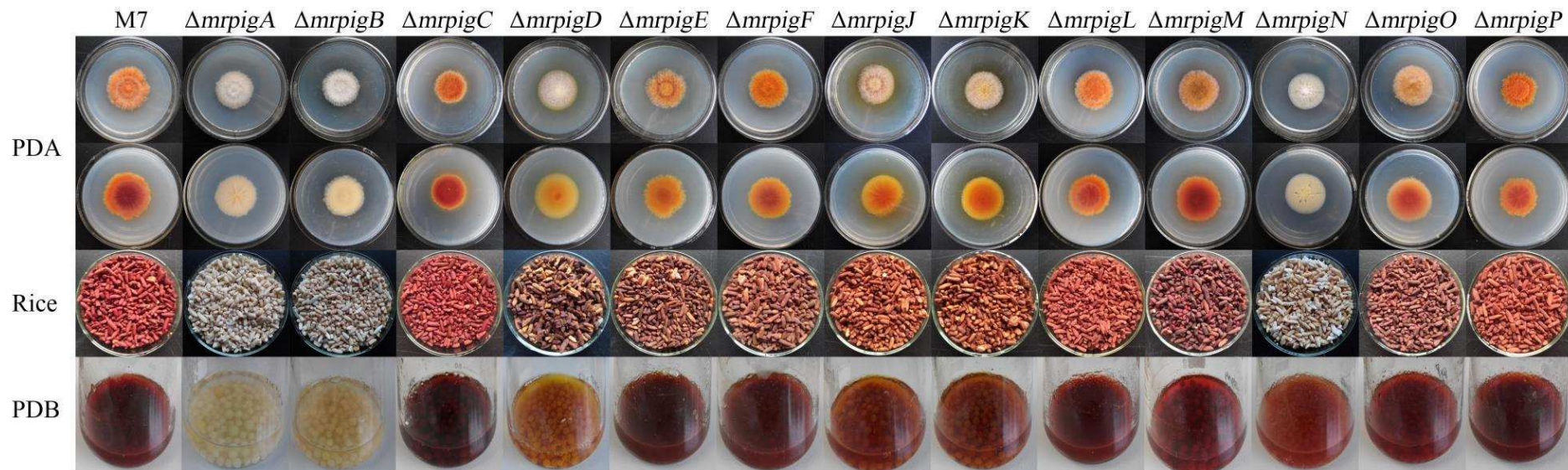


Figure 4-1. Colony phenotypes of *M. ruber* M7 and its knockout mutants on PDA, rice media, and PDB

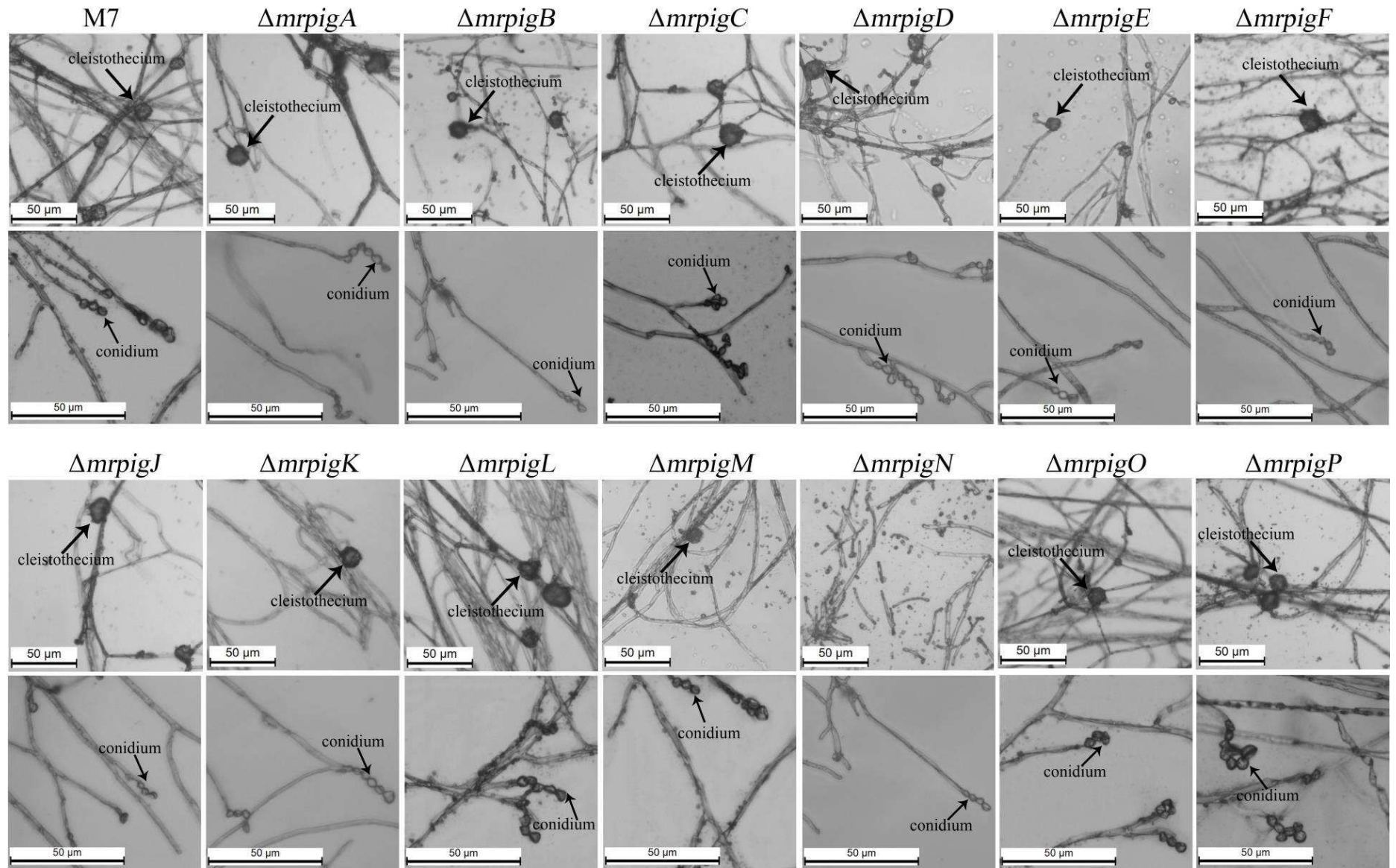


Figure 4-2. Cleistothecia and conidia formation by *M. ruber* M7 and its knockout mutants on PDA after incubation at 28 °C for 10 days

5. Fermentation and MonAzPs detection

5.1. *M. ruber* MonAzPs fermentation process

Fresh spore suspensions (10^5 /mL, 100 μ L) of *M. ruber* M7 or its knockout mutants were inoculated into 40 mL PDB and incubated at 28°C for 15 days with shaking at 120 rpm. The mycelia were harvested by filtration, and freeze-dried. 0.5 g dried mycelia were extracted with 80% methanol (4 mL) with sonication for 40 min, then centrifuged (Heal Force Neofuge 15R, Shanghai, China) at $10,000 \times g$ for 10 min to collect the supernatant.

5.2. MonAzPs detection methods

Pigment constituents were analyzed by Ultra Performance Liquid Chromatography - Photodiode Array Detector (UPLC-PDA), UPLC – mass spectrometry (UPLC-MS) and nuclear magnetic resonance (NMR) spectroscopy.

5.2.1. UPLC-PDA analysis method

The analytes were separated on a Waters ACQUITY UPLC system equipped with a PDA (Waters, Milford, MA, USA), using an ACQUITY BEH C18 column (2.1 mm × 100 mm, 1.7 μ m) with a flow rate of 0.3 mL/min. Mobile phases A and B were water and acetonitrile, respectively, both containing 0.1% formic acid. Five microliters of each sample were injected into the column. The temperatures of the column and the samples were held at 40°C and 4°C, respectively. Gradient elution was performed as follows: 35 % (v/v) solvent A with 65 % (v/v) solvent B for 3 min; solvent A 35% to 70% in 15 min; solvent A from 70% to 90% in 5 min; and finally, 35% solvent A for 3 min. The detection wavelength was 210 to 600 nm. The UPLC chromatograms and UV-VIS spectra recorded for the extracts of the different knockout mutants are shown in sections 6.1-6.2. The relative quantities of MonAzPs and their intermediates are in **Table 5-1**.

5.2.2. UPLC-MS analysis method

UPLC-MS analysis of MonAzPs were performed on a Waters ACQUITY UPLC system, equipped with Xevo tandem quadrupole mass spectrometer (Waters, Milford, MA, USA), using the UPLC conditions described in 5.2.1. Two microliters of each sample were injected into the column. Mass spectrometry was performed using a single quadrupole detector equipped with an electrospray ionization source (ESI). Positive ionization was used in the scan mode from 200 to 600 *m/z*. The capillary voltage was set to 2.5 kV. The source and desolvation temperatures were optimized and kept at 150 and 350°C, respectively. The desolvation gas was delivered at a flow rate of 10 L/min and the cone gas was set to 1 L/min. The mass spectra of MonAzPs and their intermediates are shown in section 6.3.

5.2.3. NMR analysis method

¹H-NMR, ¹³C-NMR, and 2D spectra (COSY, HSQC, HMBC) of the purified intermediates or pigments were acquired using an AV400 NMR spectrometer (Bruker, Germany). NMR spectra were referenced to the signals of the solvent, methanol-d₄. Chemical shifts (δ) are expressed in ppm, with the coupling constants (J) are reported in Hertz (Hz). The NMR spectra data of selected MonAzPs and their intermediates are shown in section 6.4.

5.3. Relative quantification of MonAzPs and their intermediates in *M. ruber* M7 and its deletion mutants

A total of 32 MonAzPs or their intermediates (**1-10, 12-30, 33-35**) were proposed in the pathway (see Scheme 2 in the main text). Among these, **12, 18, 26-28** are proposed intermediates that may be highly unstable. Compounds **20, 21, 29, 30**, and **33** were detected only by mass spectrometry. The relative quantities of the remaining 21 metabolites in *M. ruber* M7 and its deletion mutants were estimated based on the absorbance values at the applicable maximum absorption wavelengths (MAW, 254nm, 370nm or 470nm), and listed in Table 5-1.

Table 5-1. The relative quantities of MonAzPs and their intermediates in *M. ruber* M7 and its knockout mutants

MonAzPs/ intermediates	M7	$\Delta mrpigA$	$\Delta mrpigB$	$\Delta mrpigC$	$\Delta mrpigD$	$\Delta mrpigE$	$\Delta mrpigF$	$\Delta mrpigJ$	$\Delta mrpigK$	$\Delta mrpigL$	$\Delta mrpigM$	$\Delta mrpigN$	$\Delta mrpigO$	$\Delta mrpigP$	MAW(nm)
1	+++	-	-	-	-	++	+++	-	-	+++	-	-	-	+++	370
2	++	-	-	-	-	+	+++	-	-	++	-	-	-	++	370
3	++	-	-	-	-	-	-	-	-	++	-	-	-	+	470
4	++++	-	-	-	-	-	-	-	-	+++	-	-	-	+++	470
5	+	-	-	-	-	-	-	-	-	-	-	-	-	-	520
6	+	-	-	-	-	-	-	-	-	-	-	-	-	-	520
7	-	-	-	-	-	-	-	-	-	-	++	-	+/-	-	370
8	-	-	-	-	-	-	-	-	-	-	++++	-	++	-	370
9	+/-	-	-	-	-	++++	+	-	-	+/-	-	-	-	+/-	370
10	+/-	-	-	-	-	+++	+/-	-	-	+/-	-	-	-	+/-	370
13	-	-	-	-	-	-	-	-	-	-	-	++	-	-	254
14	-	-	-	++	-	-	-	-	-	-	-	-	-	-	254
15	-	-	-	++	-	-	-	-	-	-	-	-	-	-	254
16	-	-	-	+++	-	-	-	-	-	-	-	-	-	-	254
17	-	-	-	-	+	-	-	+	+	-	-	-	-	-	254
19	-	-	-	-	++	-	-	+	+	-	-	-	-	-	254
20	*	-	-	-	-	-	-	-	-	-	-	-	-	-	*
21	*	-	-	-	-	-	-	-	-	-	-	-	-	-	*
22	-	-	-	-	-	-	-	-	-	-	++	-	-	-	370
23	-	-	-	-	-	-	-	-	-	-	++	-	-	-	370
24	-	-	-	-	-	-	-	-	-	-	-	-	++	-	370
25	-	-	-	-	-	-	-	-	-	-	-	-	++	-	370
29	*	-	-	-	-	-	+	-	-	-	-	-	-	-	*
30	*	-	-	-	-	-	-	+	-	-	-	-	-	-	*
33	-	-	-	-	-	*	-	-	-	-	-	-	-	-	*
34	-	-	-	-	-	+	-	-	-	-	-	-	-	-	370
35	-	-	-	-	-	+	-	-	-	-	-	-	-	-	370

++++, A=1.0 – 1.4; +++, A=0.6 – 1.0 ; ++, A=0.2 – 0.6; +, A=0.1 – 0.2 ; +/-, A=0.05 – 0.1; -, A<0.05; *, detected by MS only.

6. Spectral data for MonAzPs and their intermediates

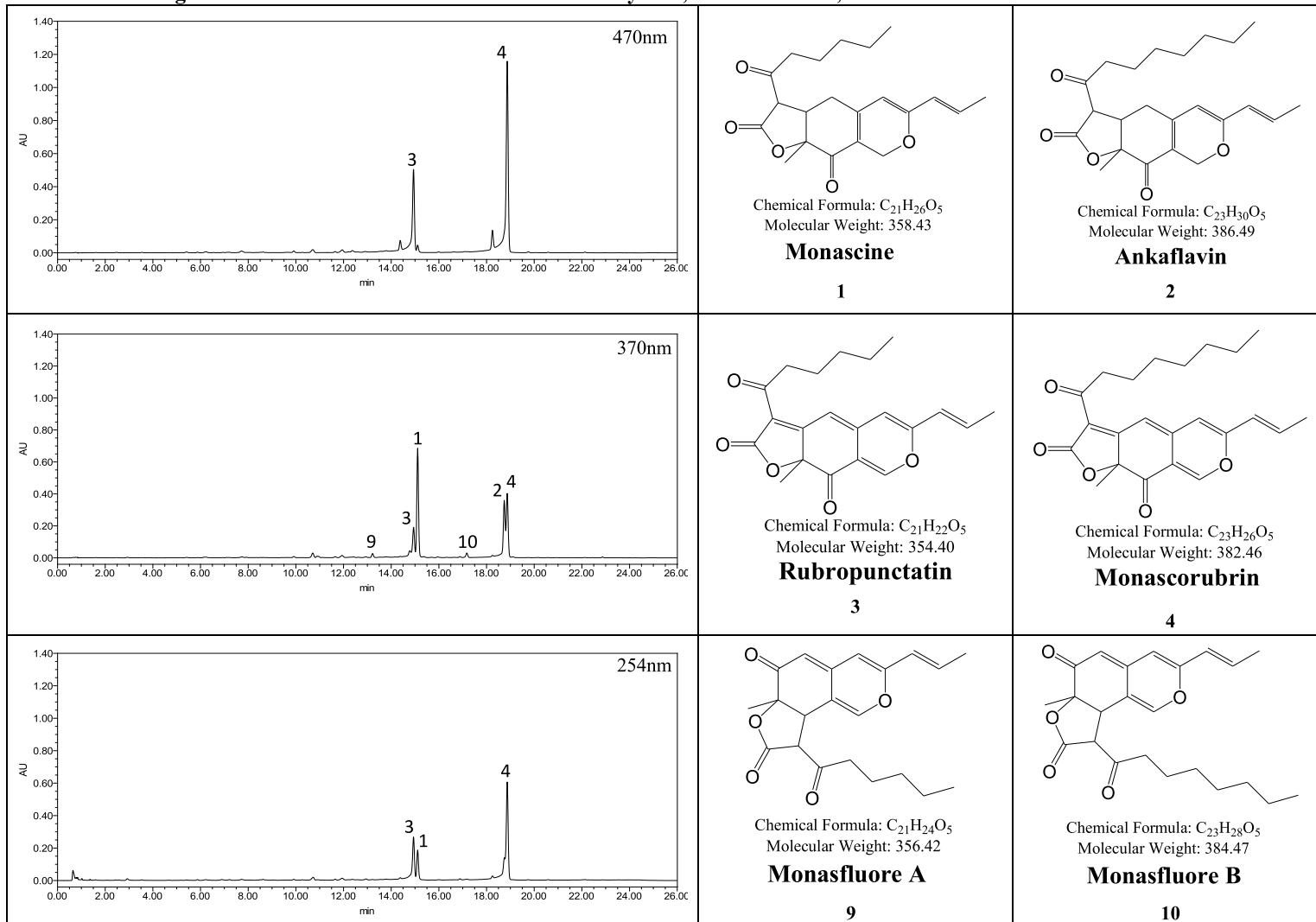
As described in **Section 5.3**, total 27 MonAzPs and their intermediates in *M. ruber* M7 and the knockouts were detected in this study. The spectral data are summarized in **Table 6-1** and presented in sections **6.1 – 6.4**. Among these compounds, **20**, **21**, **29**, **30** and **33** could be identified in the MS data, but were undetectable by UPLC as they were produced only at very low amounts in our fermentations (**Table 5-1**). In particular, detection of **20**, **21**, **22**, **23**, **25**, **29**, **30**, **33** and **34** are first reported in this study. The NMR spectra of MonAzPs **1–6** are not shown here as these have previously been reported in the literature as shown in the **Table 6-1**.

Table 6-1 Summary of MonAzPs and intermediates detected in this study

MonAzPs or intermediates	UPLC	UV-VIS	MS	NMR	Strains	Comments
1	✓	✓	✓		M7, ΔmrpigE, ΔmrpigF, ΔmrpigL, ΔmrpigP	This study, also Fielding <i>et al.</i> , 1961
2	✓	✓	✓		M7, ΔmrpigE, ΔmrpigF, ΔmrpigL, ΔmrpigP	This study, also Manchand <i>et al.</i> , 1973
3	✓	✓	✓		M7, ΔmrpigL, ΔmrpigP	This study, also Haws <i>et al.</i> , 1959
4	✓	✓	✓		M7, ΔmrpigL, ΔmrpigP	This study, also Kumasaki <i>et al.</i> , 1962
5	✓	✓	✓		M7	This study, also Sweeny <i>et al.</i> , 1981
6	✓	✓	✓		M7	This study, also Sweeny <i>et al.</i> , 1981
7	✓	✓	✓	✓	M7, ΔmrpigM, ΔmrpigO	This study, also Campoy <i>et al.</i> , 2006
8	✓	✓	✓	✓	M7, ΔmrpigM, ΔmrpigO	This study, also Bijinu <i>et al.</i> , 2014
9	✓	✓	✓	✓	M7, ΔmrpigE, ΔmrpigF, ΔmrpigL, ΔmrpigP	This study, also Huang <i>et al.</i> , 2008
10	✓	✓	✓	✓	M7, ΔmrpigE, ΔmrpigF, ΔmrpigL, ΔmrpigP	This study, also Huang <i>et al.</i> , 2008
13	✓	✓	✓	✓	ΔmrpigN	This study, also Liu <i>et al.</i> , 2016
14	✓	✓	✓	✓	ΔmrpigC	This study, also Bijinu <i>et al.</i> , 2014
15	✓	✓	✓	✓	ΔmrpigC	This study, also Bijinu <i>et al.</i> , 2014
16	✓	✓	✓	✓	ΔmrpigC	This study, also Bijinu <i>et al.</i> , 2014
17	✓	✓	✓		ΔmrpigD, ΔmrpigJ, ΔmrpigK	This study, also Zabala <i>et al.</i> , 2012
19	✓	✓	✓	✓	ΔmrpigD, ΔmrpigJ, ΔmrpigK	This study, also Jongrungruangchok <i>et al.</i> , 2004
20			✓		M7, ΔmrpigM	This study
21			✓		M7, ΔmrpigM	This study
22	✓	✓	✓		ΔmrpigM	This study
23	✓	✓	✓		ΔmrpigM	This study
24	✓	✓	✓	✓	ΔmrpigO	This study, also Wu <i>et al.</i> , 2013
25	✓	✓	✓	✓	ΔmrpigO	This study
29			✓		M7, ΔmrpigF	This study
30			✓		M7, ΔmrpigF	This study
33			✓		M7, ΔmrpigM	This study, also Bijinu <i>et al.</i> , 2014
34	✓	✓	✓		M7, ΔmrpigM	This study, also Bijinu <i>et al.</i> , 2014
35	✓	✓	✓	✓	ΔmrpigE	This study, also Jongrungruangchok <i>et al.</i> , 2004

6.1. UPLC chromatograms of fermentation extracts of various knockout mutants

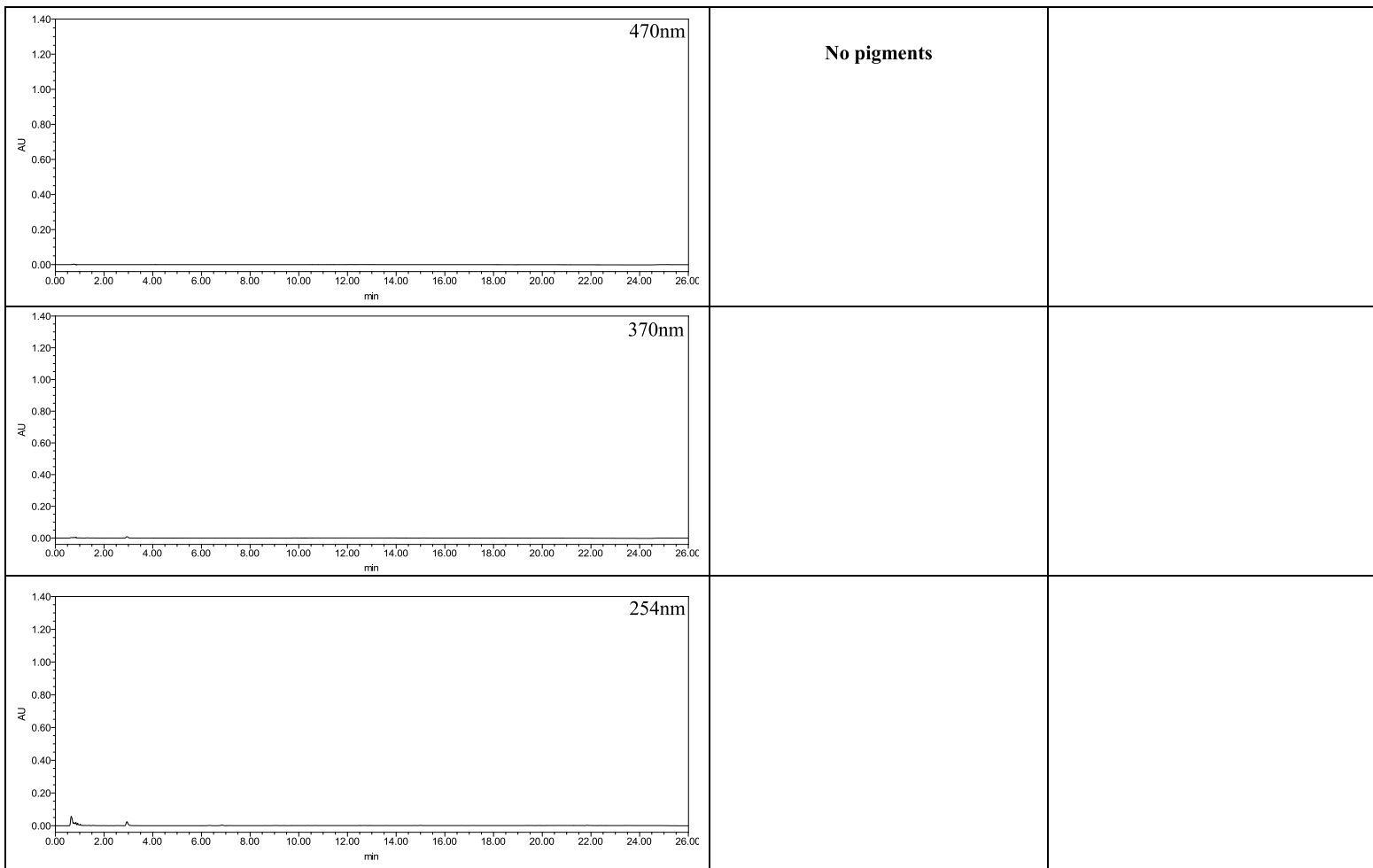
UPLC chromatogram of the methanol extract of *M. ruber* M7 mycelia, detected at 470, 370 and 254 nm.



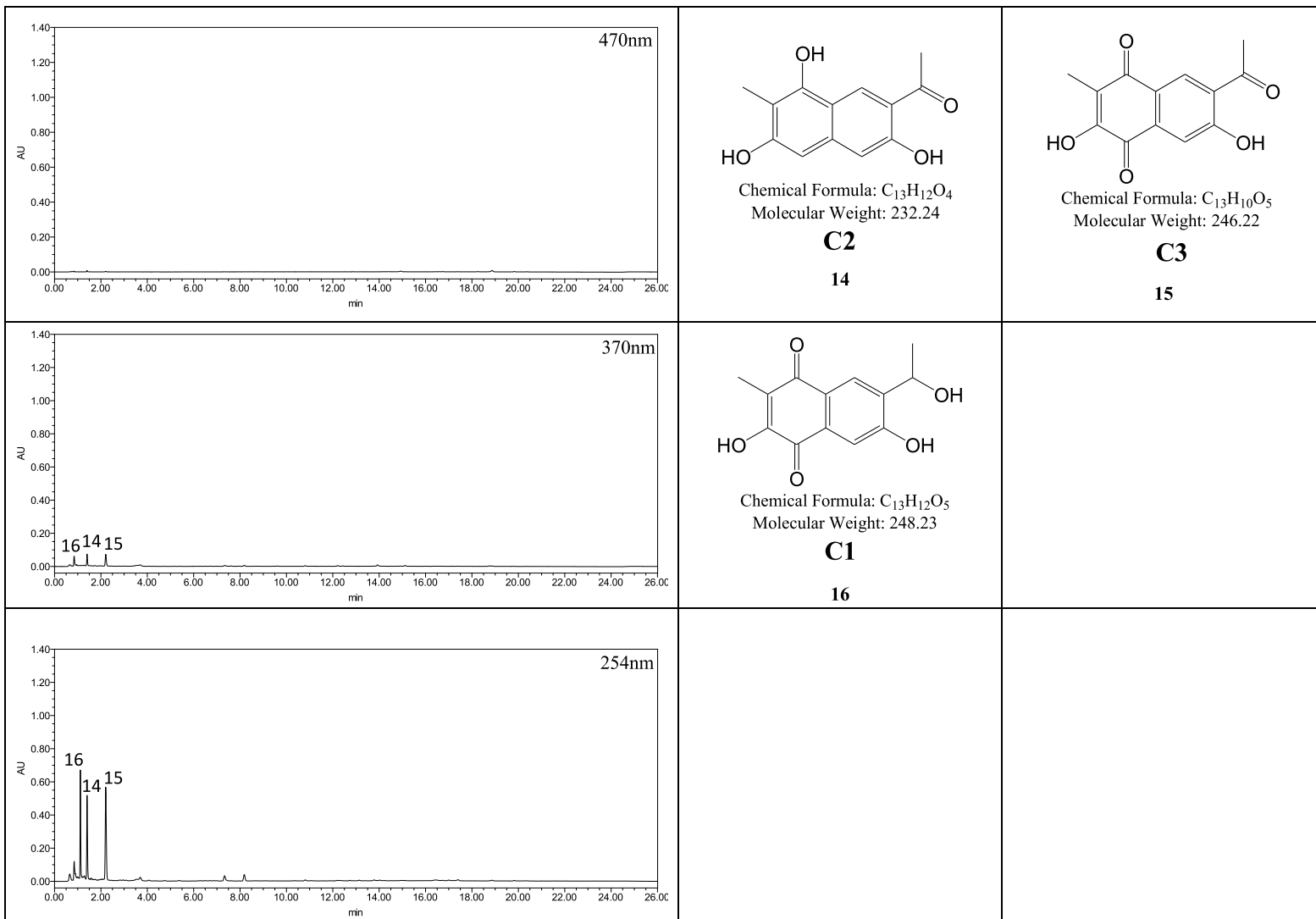
UPLC chromatogram of the methanol extract of the mycelia of the $\Delta mrpIGA$ mutant, detected at 470, 370 and 254 nm.



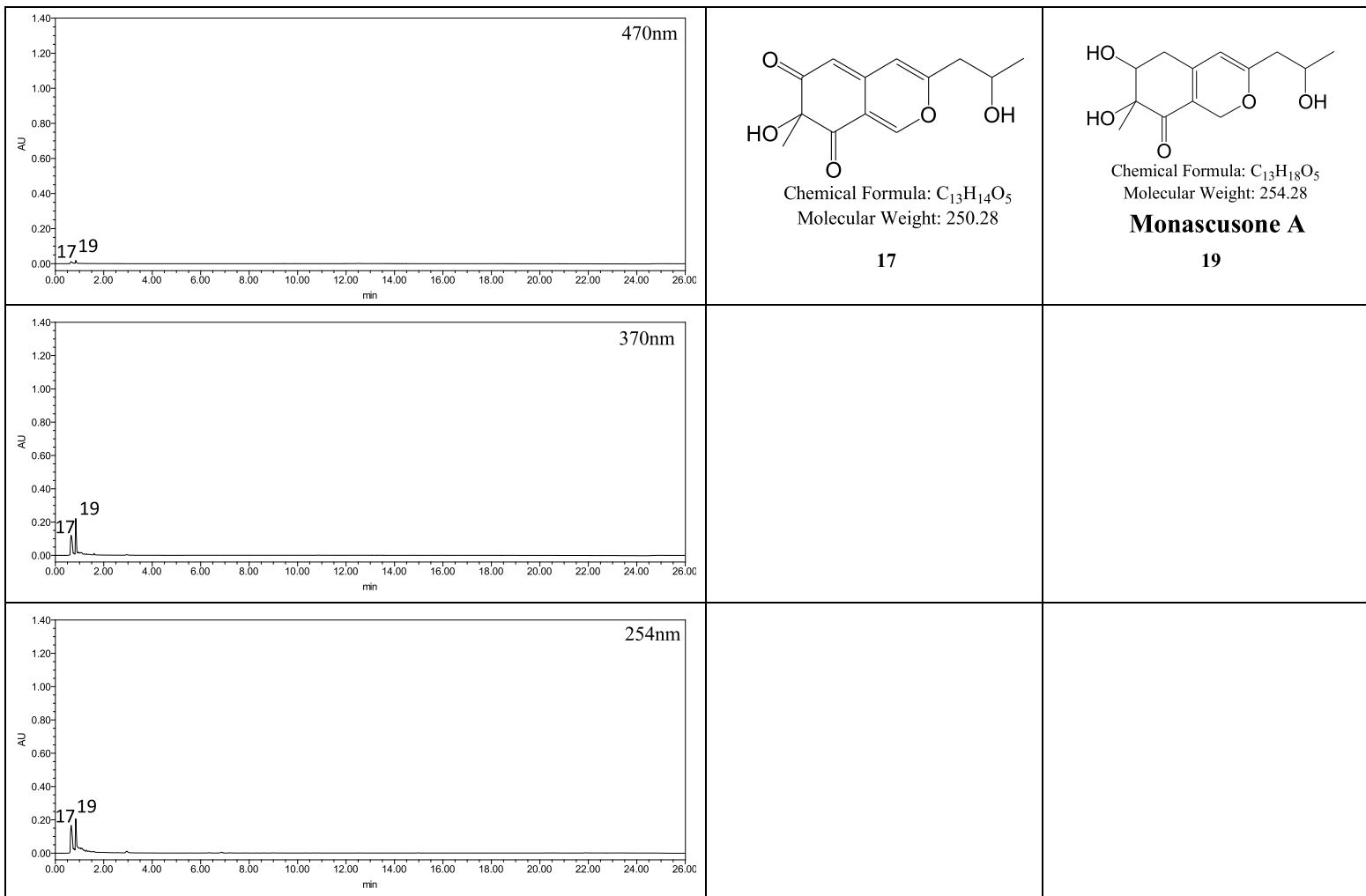
UPLC chromatogram of the methanol extract of the mycelia of the $\Delta mrpIGB$ mutant, detected at 470, 370 and 254 nm.



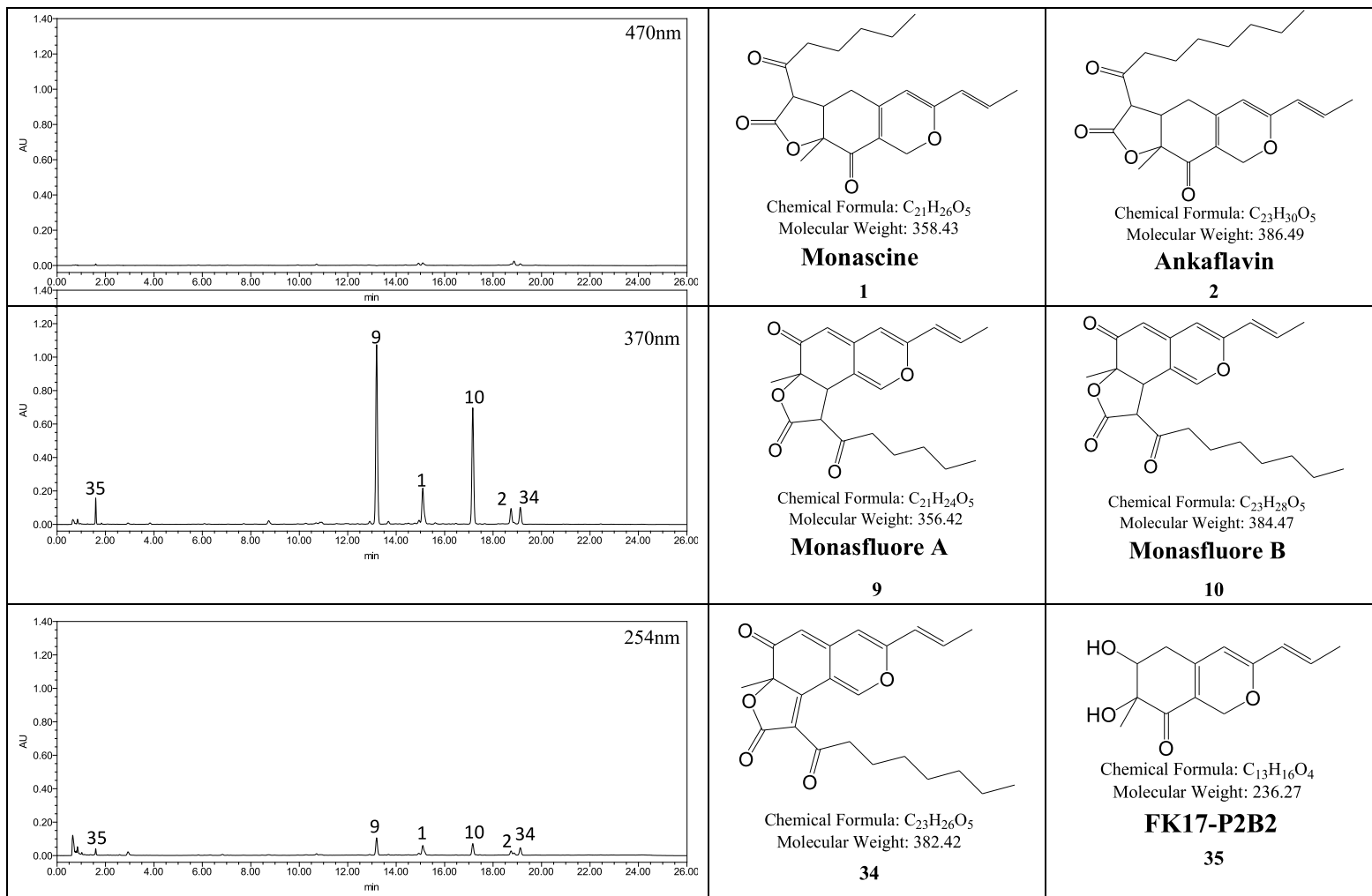
UPLC chromatogram of the methanol extract of the mycelia of the $\Delta mrpigC$ mutant, detected at 470, 370 and 254 nm.



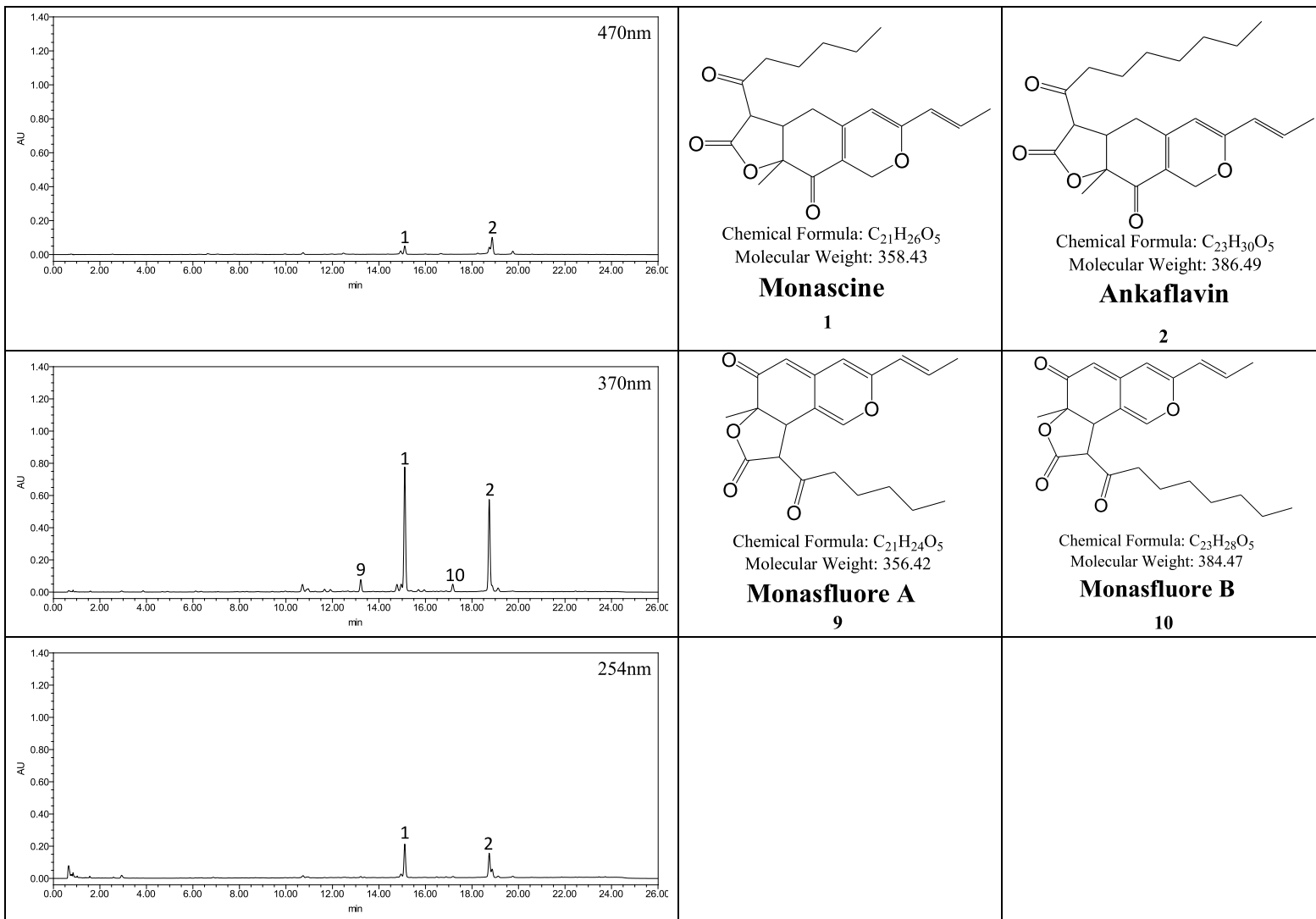
UPLC chromatogram of the methanol extract of the mycelia of the $\Delta mrpIGD$ mutant, detected at 470, 370 and 254 nm.



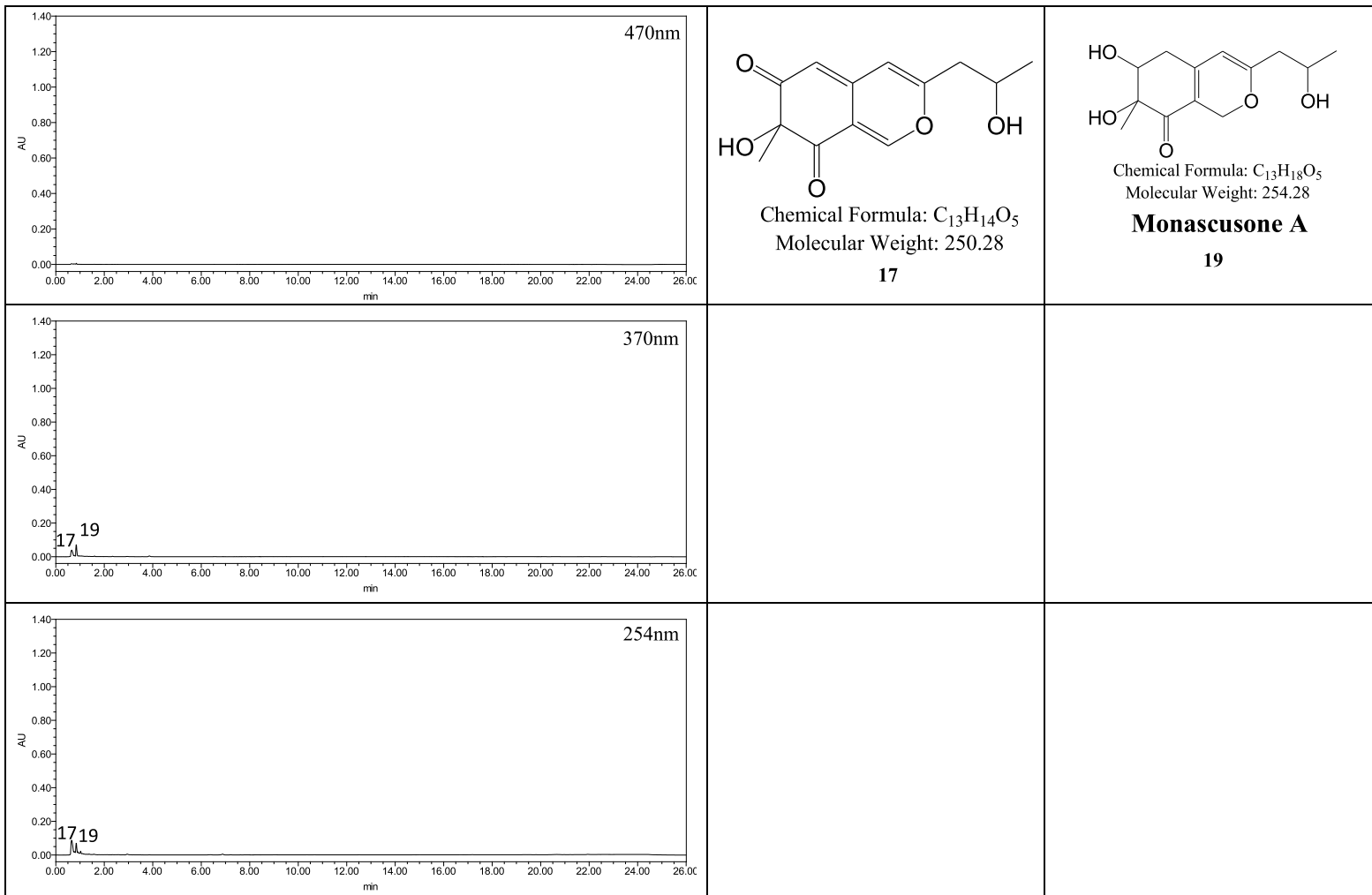
UPLC chromatogram of the methanol extract of the mycelia of the $\Delta mrpigE$ mutant, detected at 470, 370 and 254 nm.



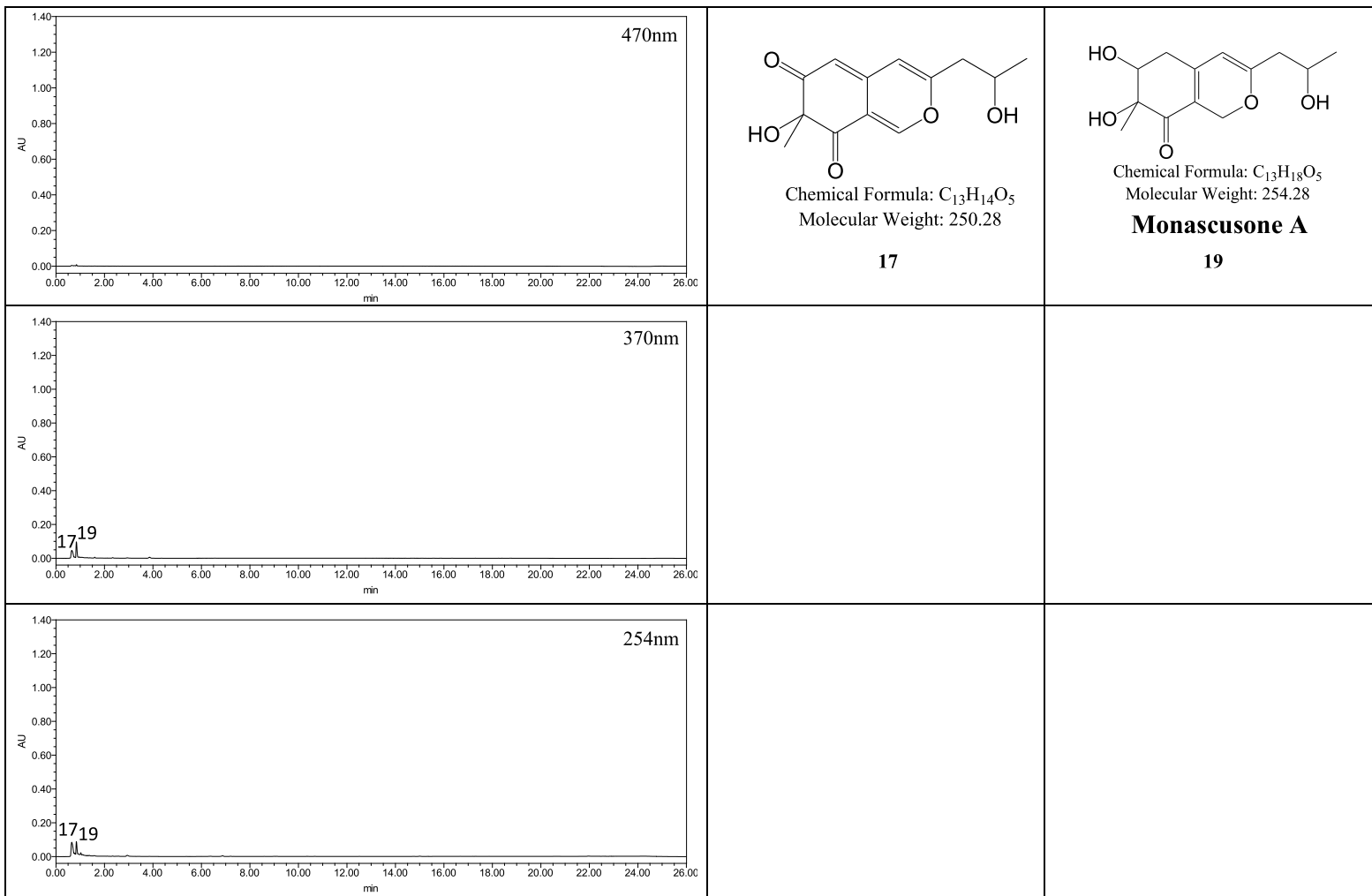
UPLC chromatogram of the methanol extract of the mycelia of the $\Delta mnpigF$ mutant, detected at 470, 370 and 254 nm.



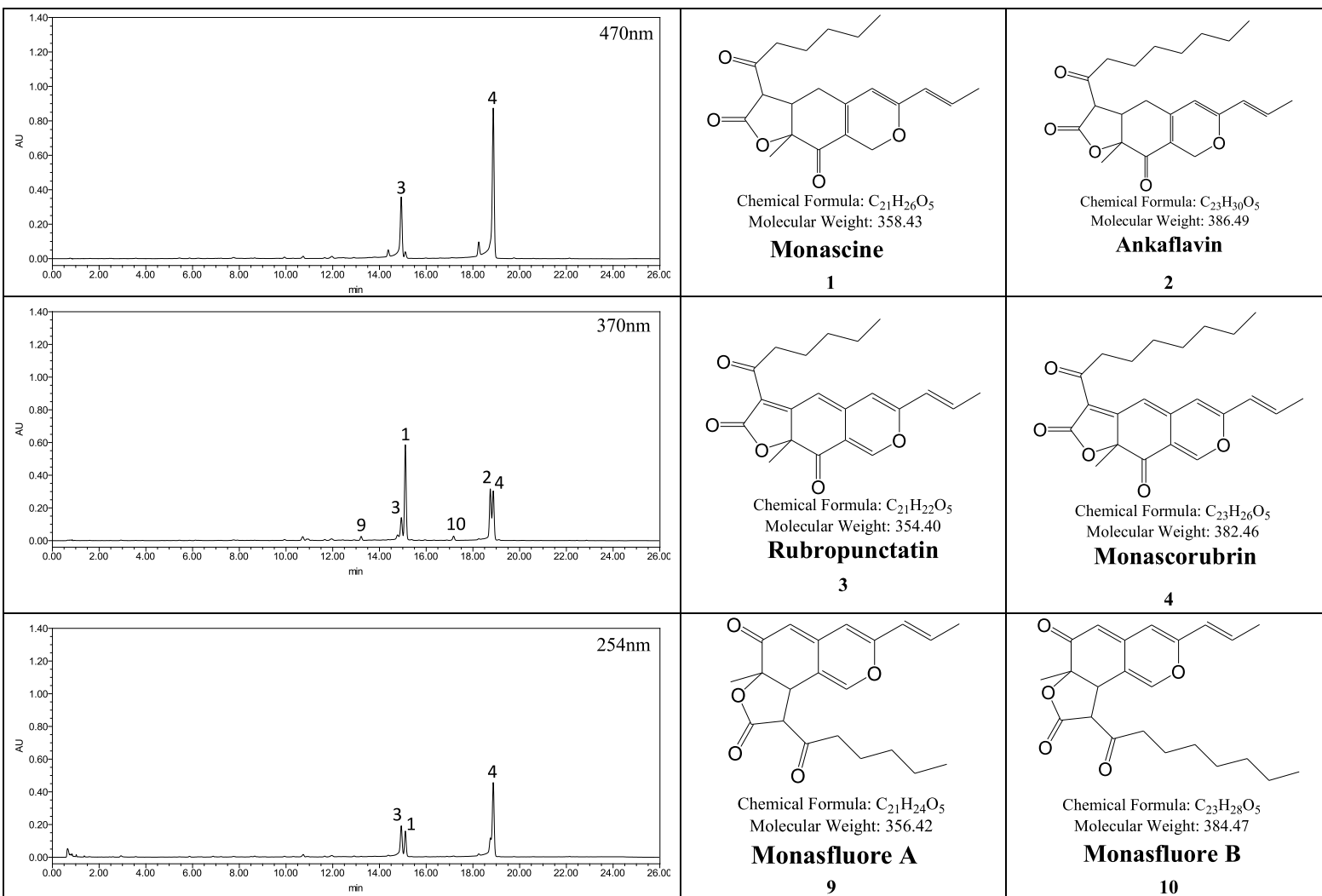
UPLC chromatogram of the methanol extract of the mycelia of the $\Delta mrrpigJ$ mutant, detected at 470, 370 and 254 nm.



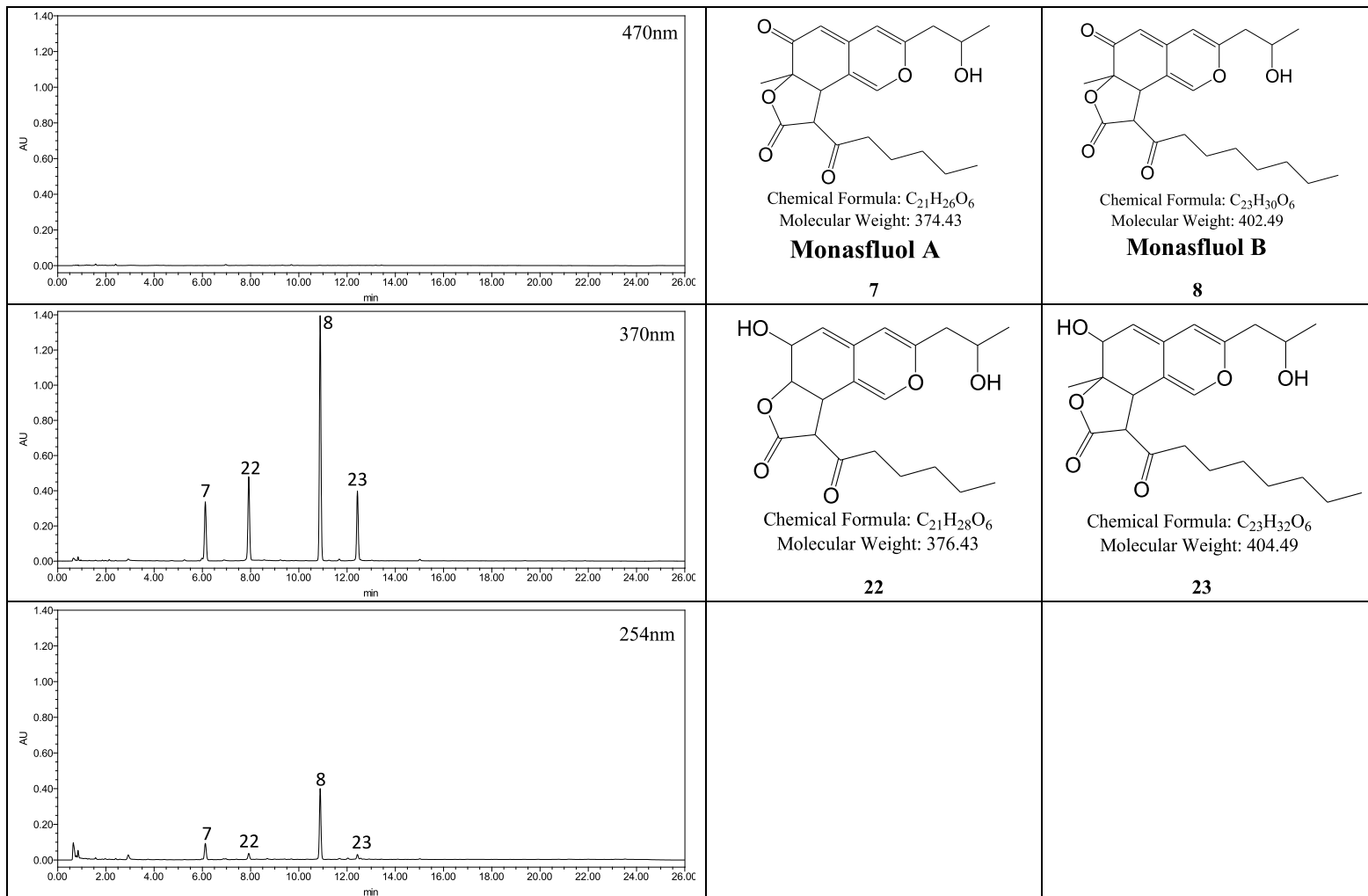
UPLC chromatogram of the methanol extract of the mycelia of the $\Delta mrpigK$ mutant, detected at 470, 370 and 254 nm.



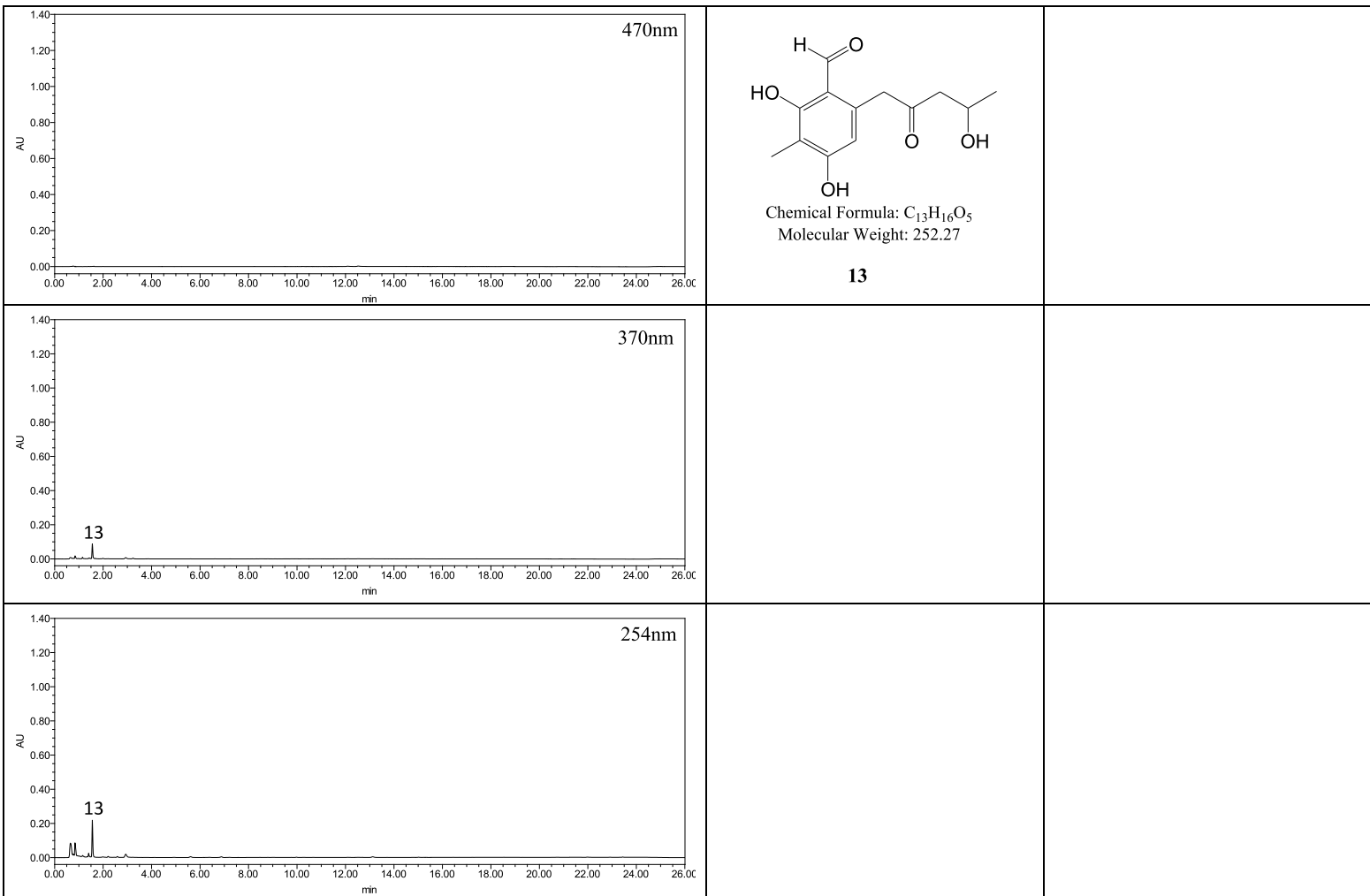
UPLC chromatogram of the methanol extract of the mycelia of the $\Delta mrpIGL$ mutant, detected at 470, 370 and 254 nm.



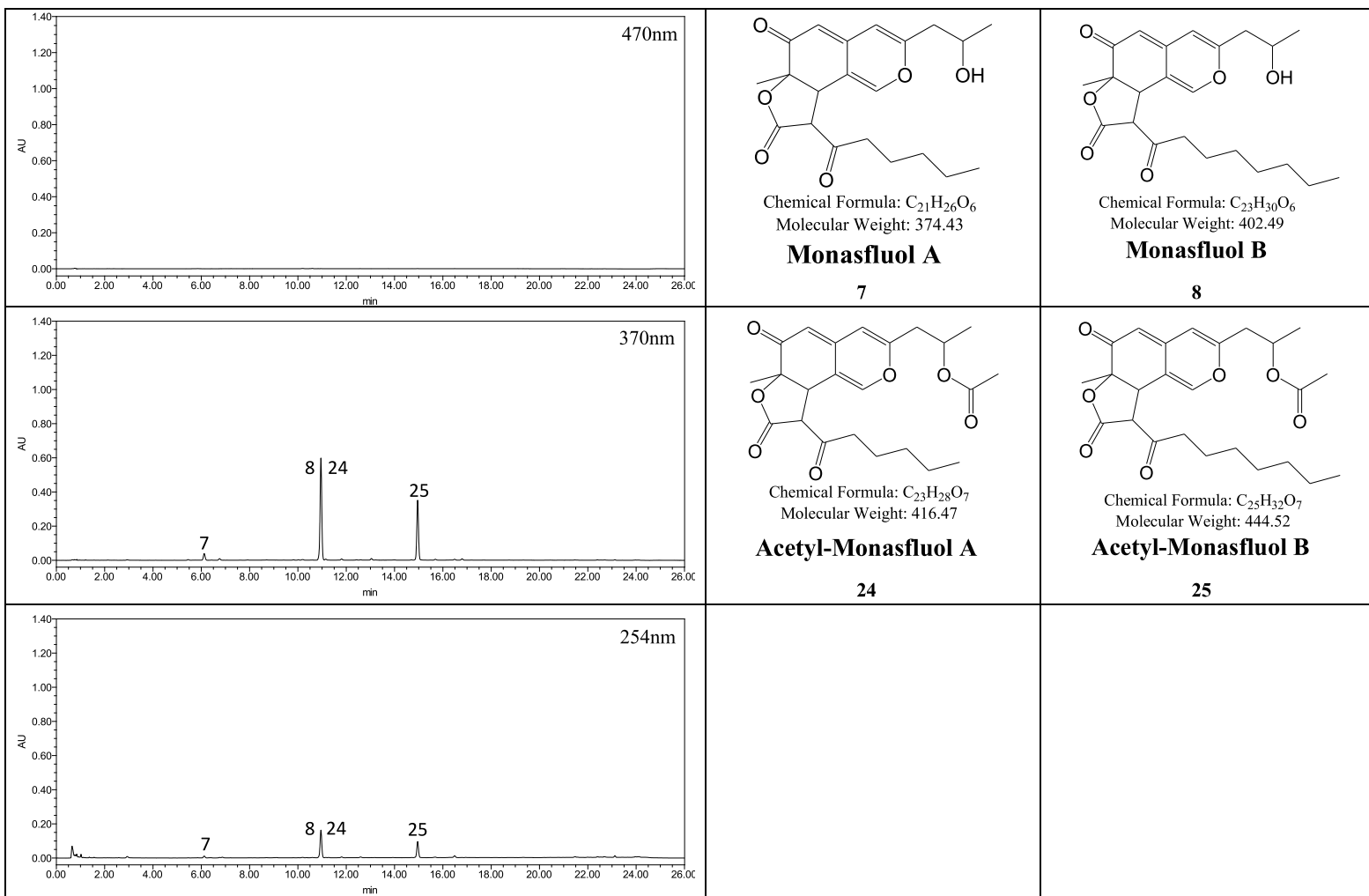
UPLC chromatogram of the methanol extract of the mycelia of the $\Delta mnpigM$ mutant, detected at 470, 370 and 254 nm.



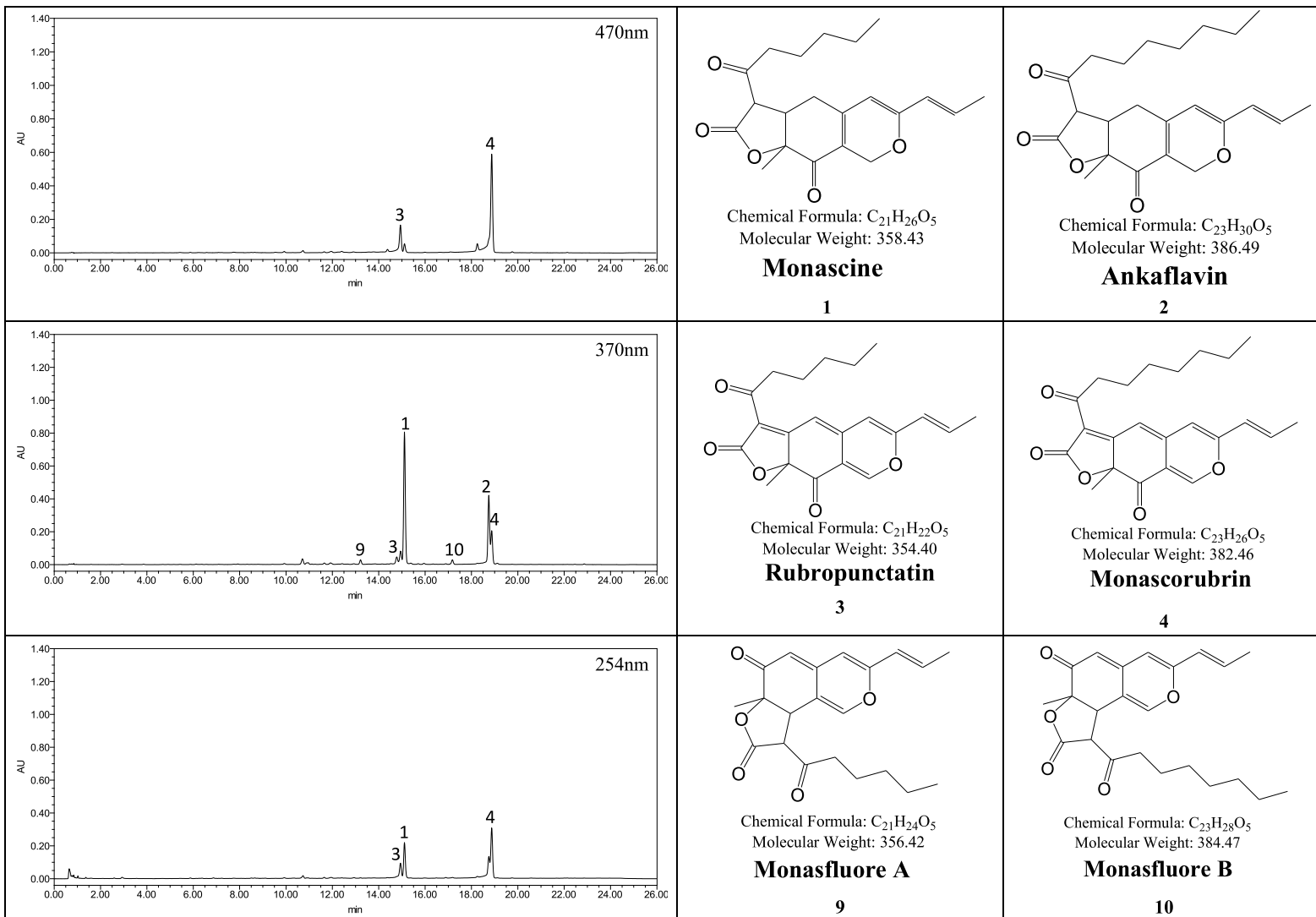
UPLC chromatogram of the methanol extract of the mycelia of the $\Delta mrpIGN$ mutant, detected at 470, 370 and 254 nm.



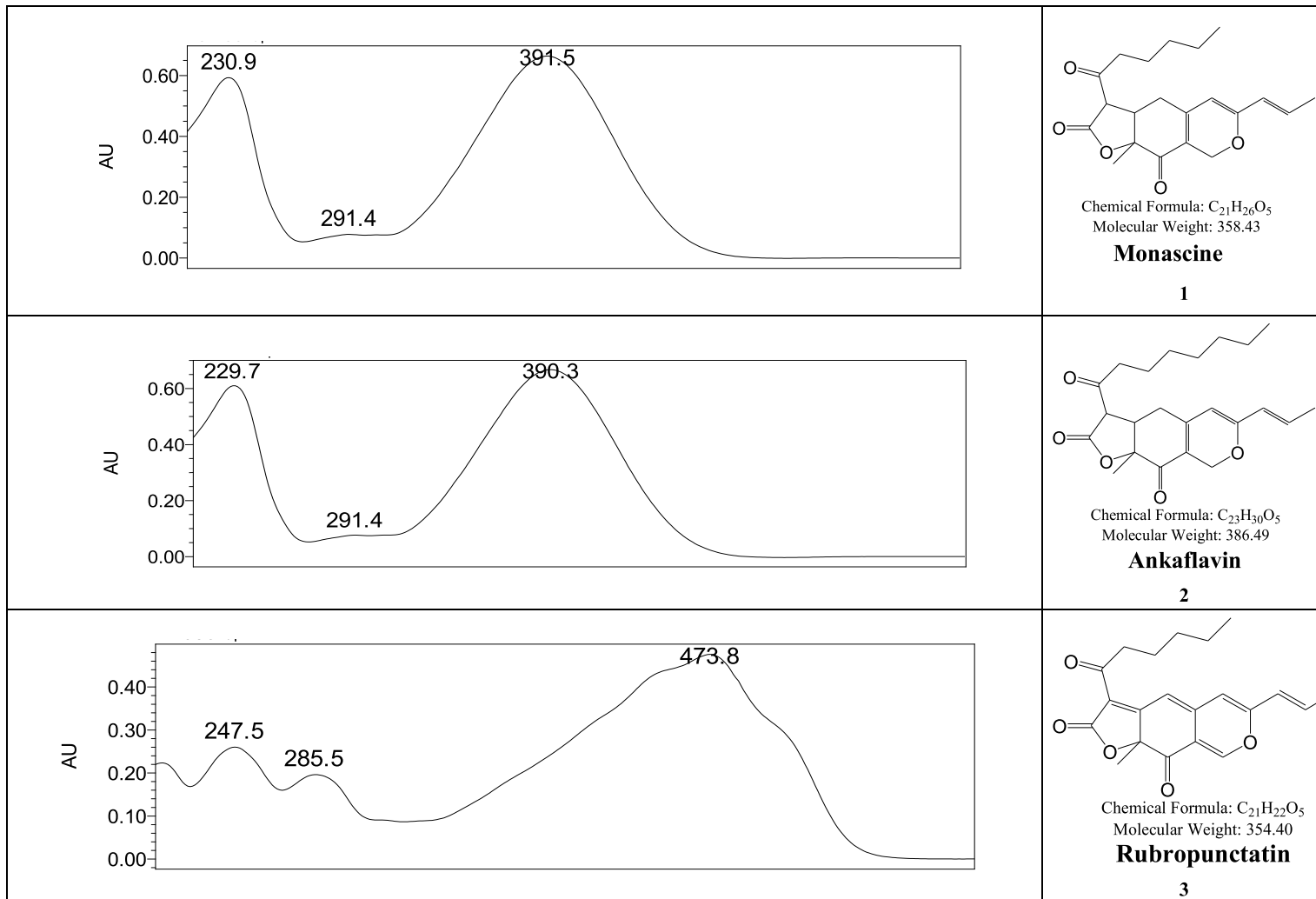
UPLC chromatogram of the methanol extract of the mycelia of the $\Delta mrpIG$ mutant, detected at 470, 370 and 254 nm.

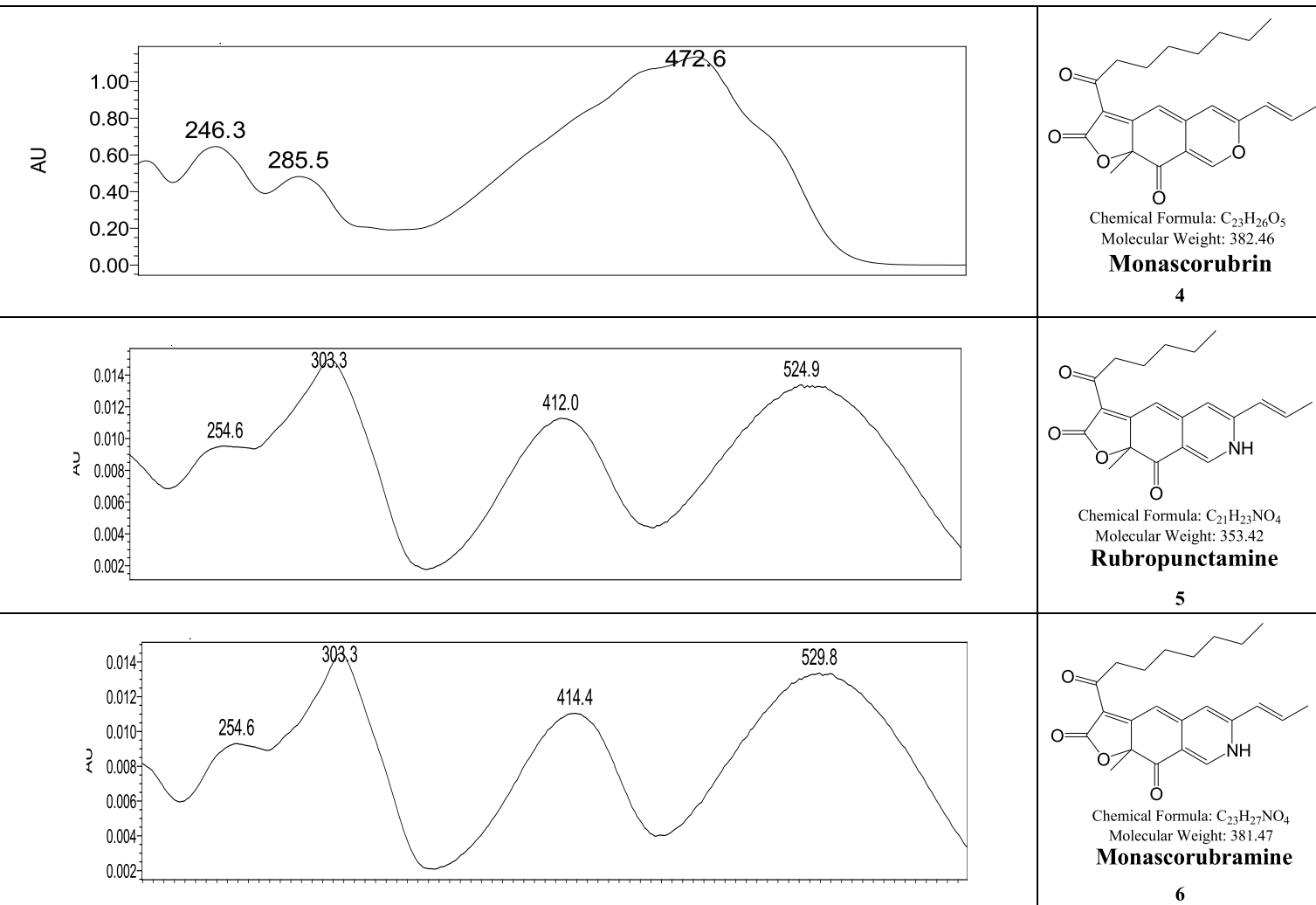


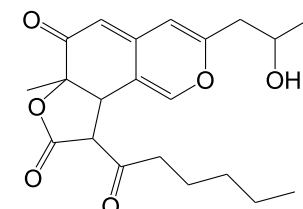
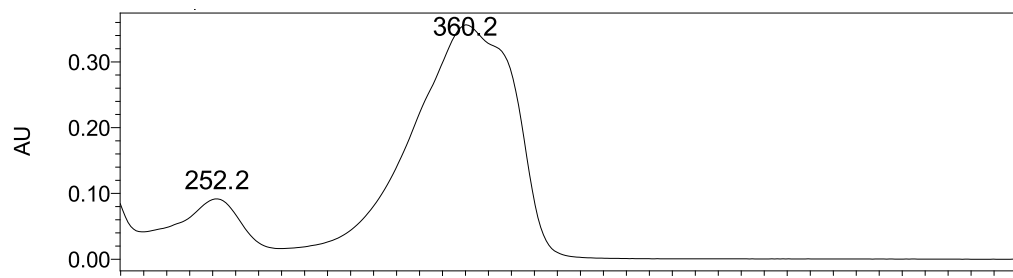
UPLC chromatogram of the methanol extract of the mycelia of the $\Delta mrpIGP$ mutant, detected at 470, 370 and 254 nm.



6.2. UV-VIS spectra of MonAzPs and intermediates



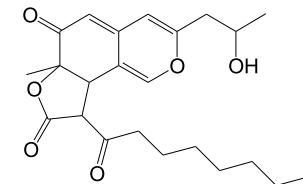
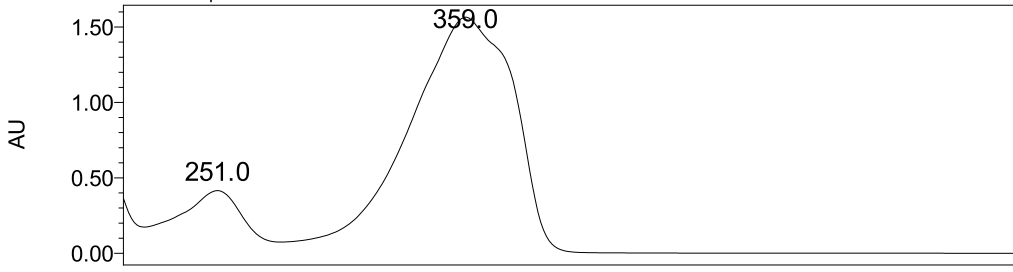




Chemical Formula: C₂₁H₂₆O₆
Molecular Weight: 374.43

Monasfluol A

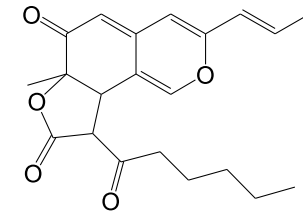
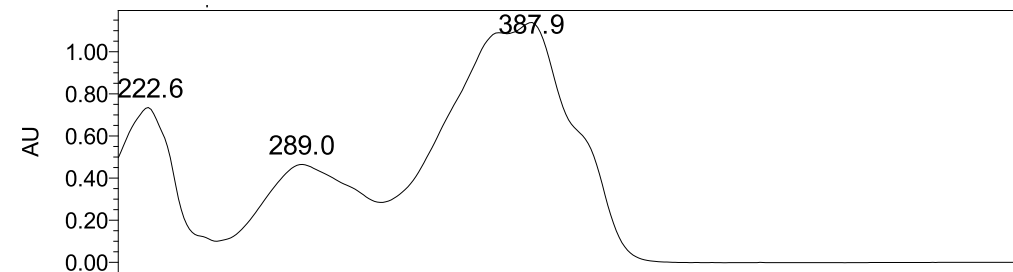
7



Chemical Formula: C₂₃H₃₀O₆
Molecular Weight: 402.49

Monasfluol B

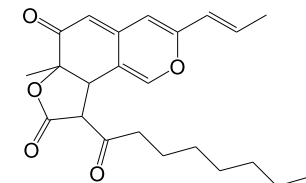
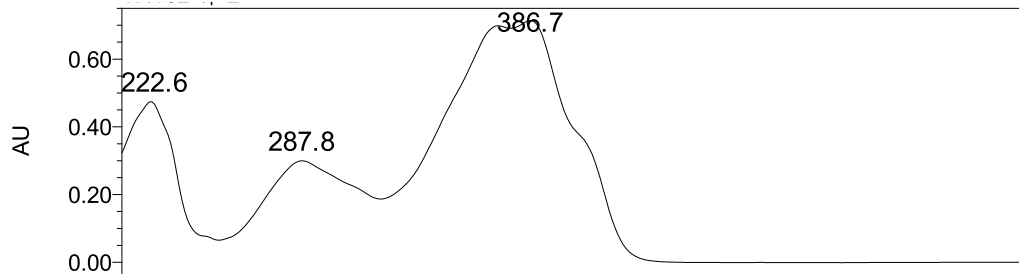
8



Chemical Formula: C₂₁H₂₄O₅
Molecular Weight: 356.42

Monasfluore A

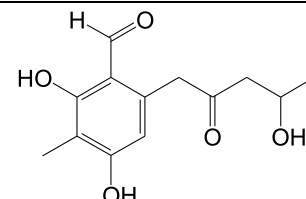
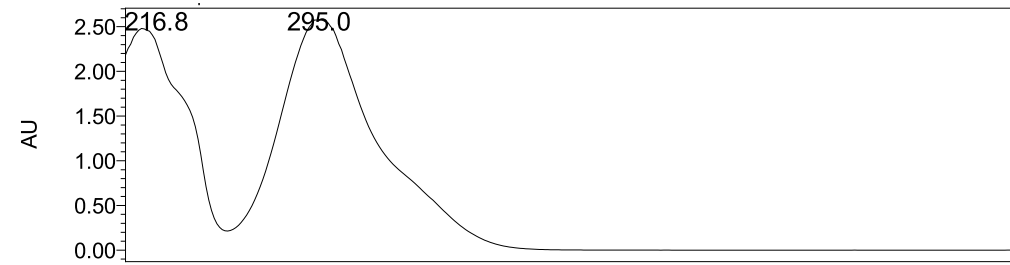
9



Chemical Formula: C₂₃H₂₈O₅
Molecular Weight: 384.47

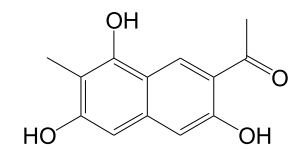
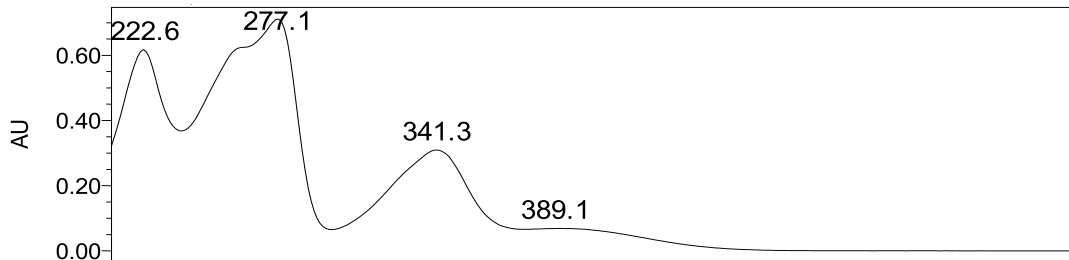
Monasfluore B

10



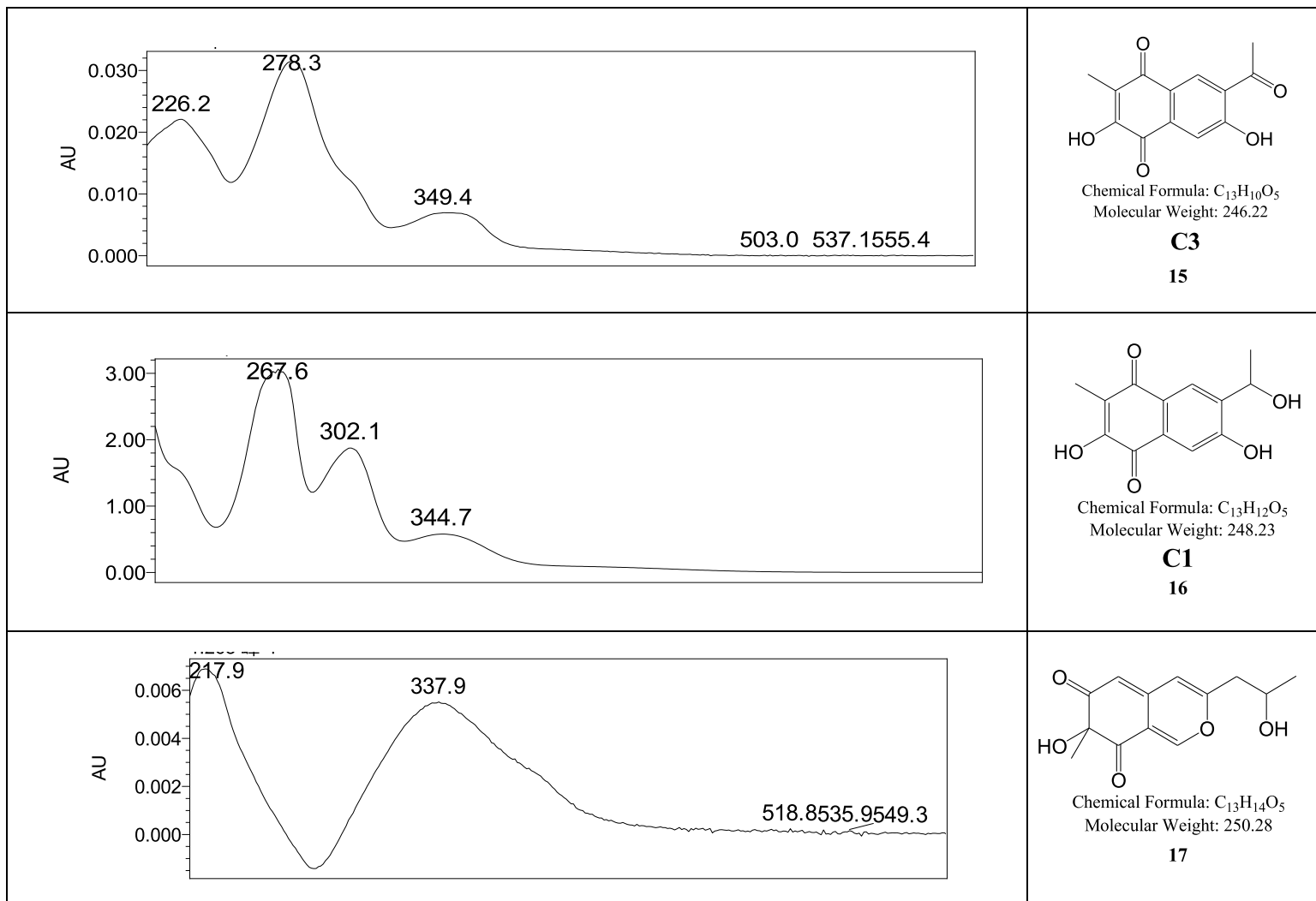
Chemical Formula: C₁₃H₁₆O₅
Molecular Weight: 252.27

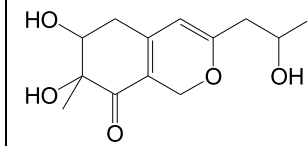
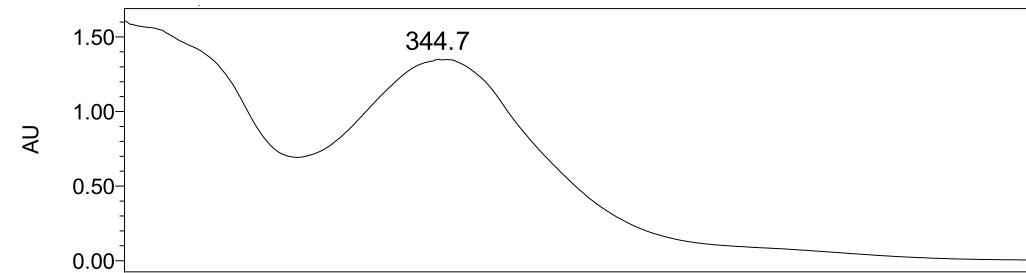
13



Chemical Formula: C₁₃H₁₂O₄
Molecular Weight: 232.24

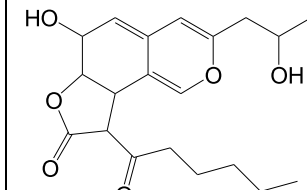
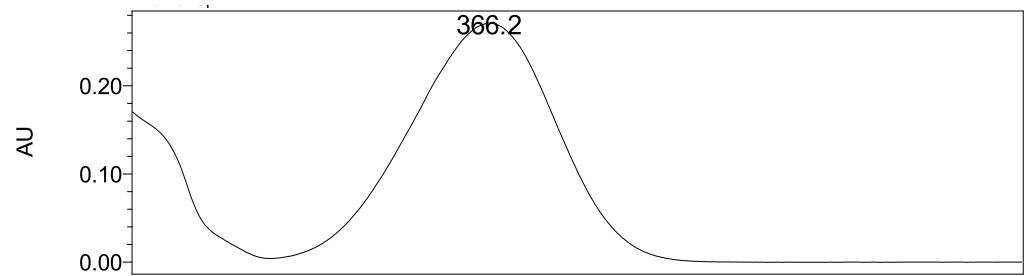
C2
14





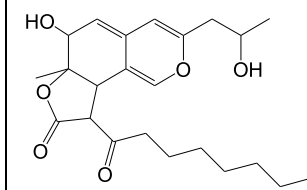
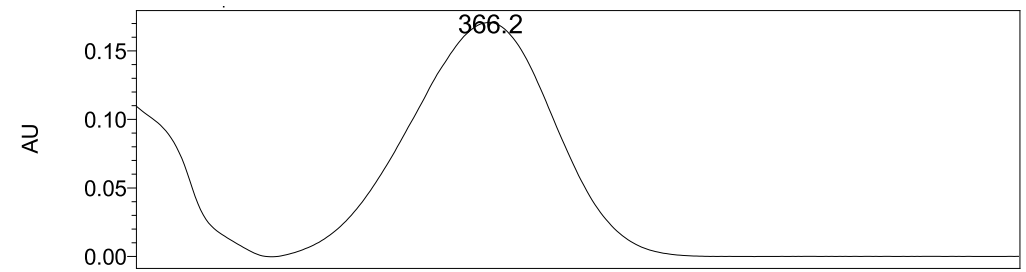
Chemical Formula: C₁₃H₁₈O₅
Molecular Weight: 254.28

Monascusone A
19



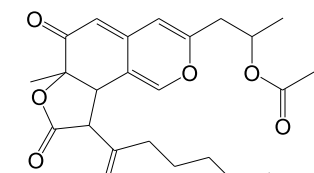
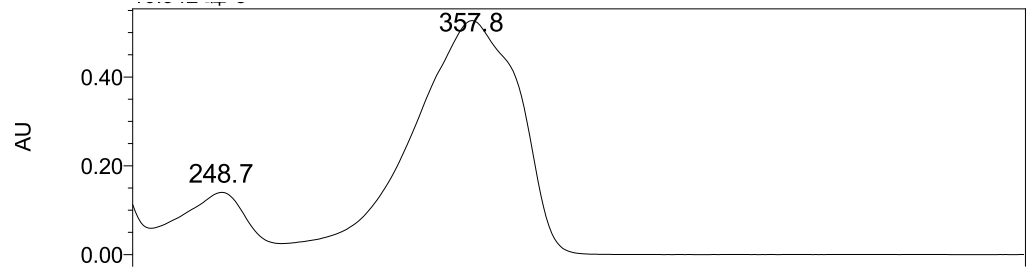
Chemical Formula: C₂₁H₂₈O₆
Molecular Weight: 376.43

22



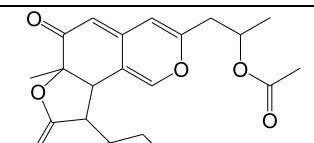
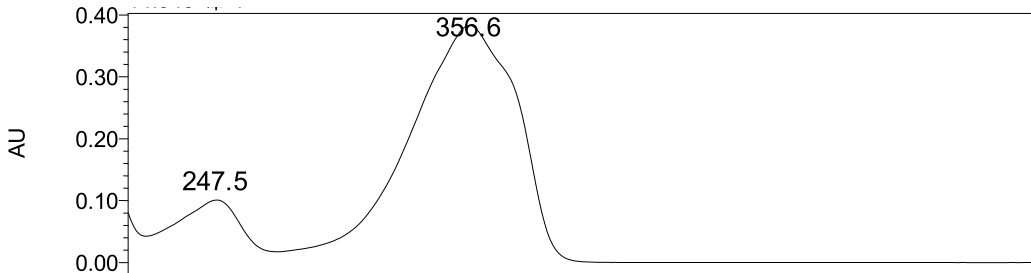
Chemical Formula: C₂₃H₃₂O₆
Molecular Weight: 404.49

23



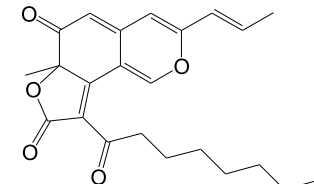
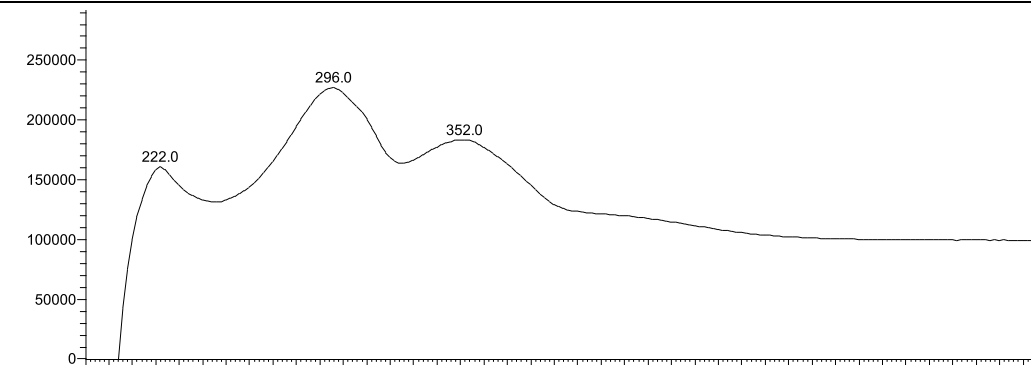
Chemical Formula: C₂₃H₂₈O₇
Molecular Weight: 416.47

24



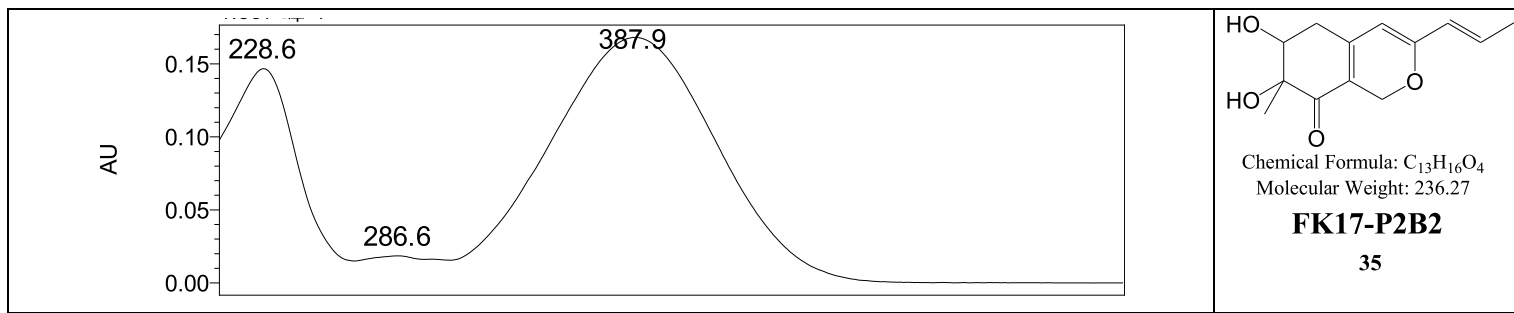
Chemical Formula: C₂₅H₃₂O₇
Molecular Weight: 444.52
Acetyl-Monasfluol B

25

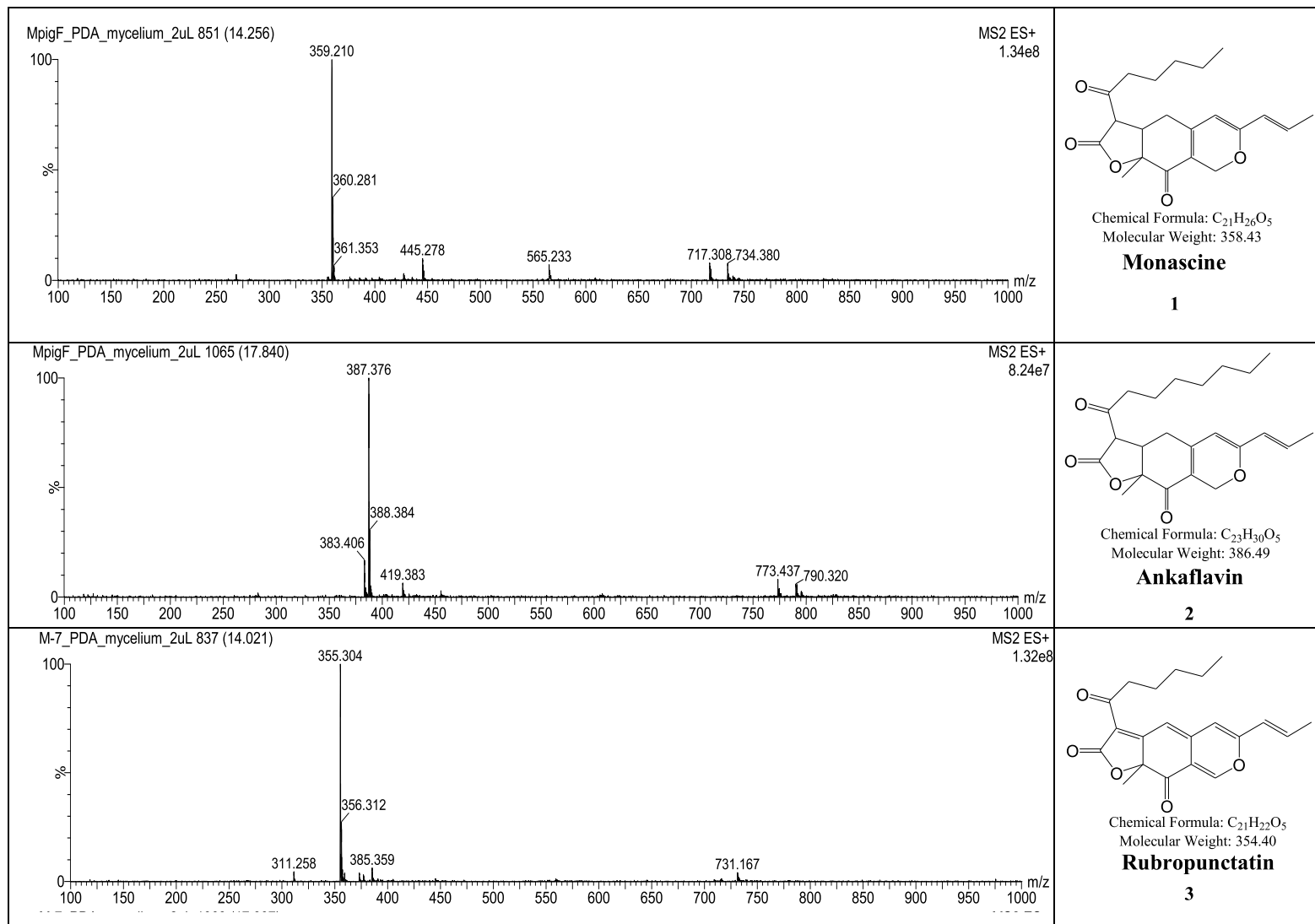


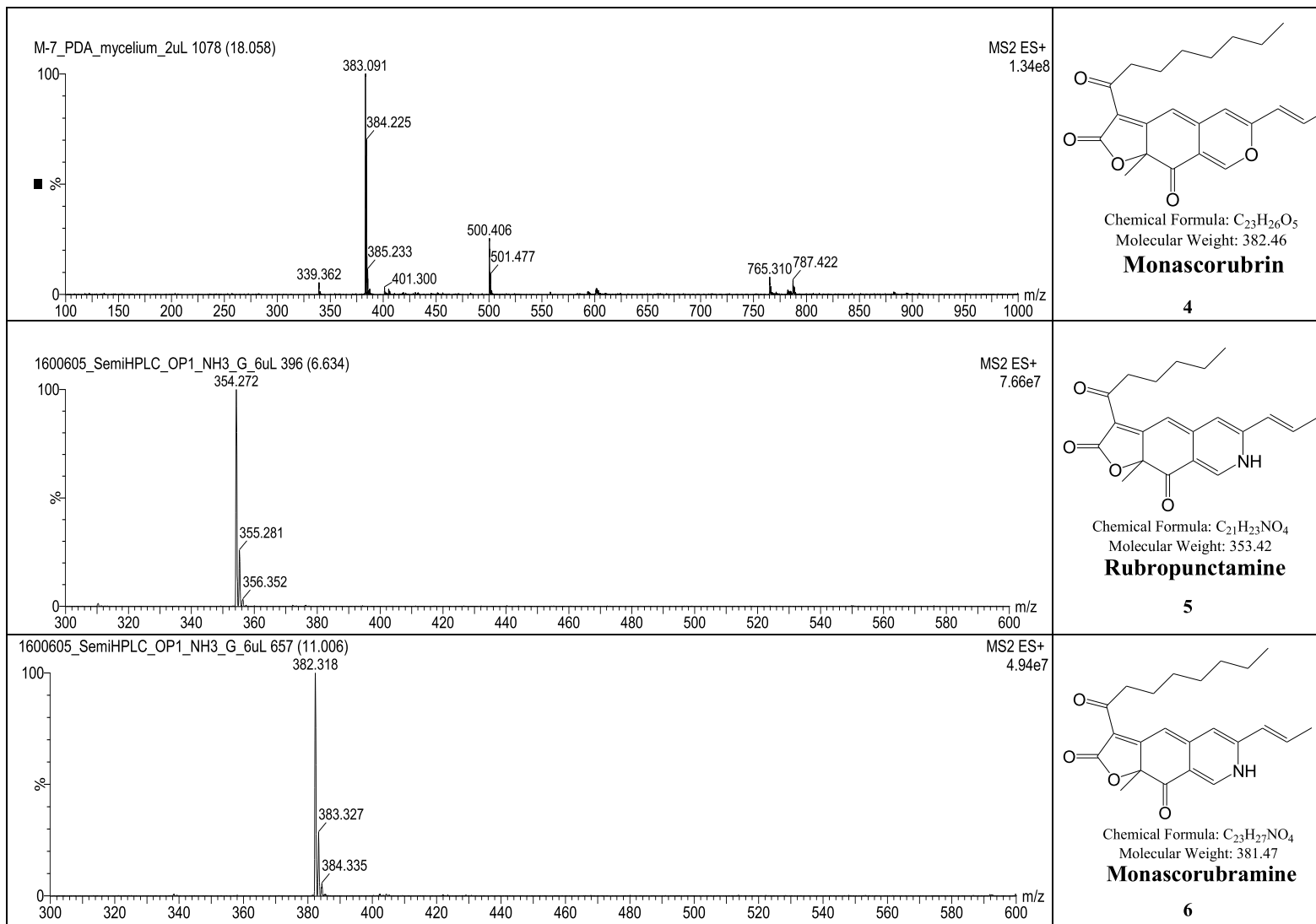
Chemical Formula: C₂₃H₂₆O₅
Molecular Weight: 382.42

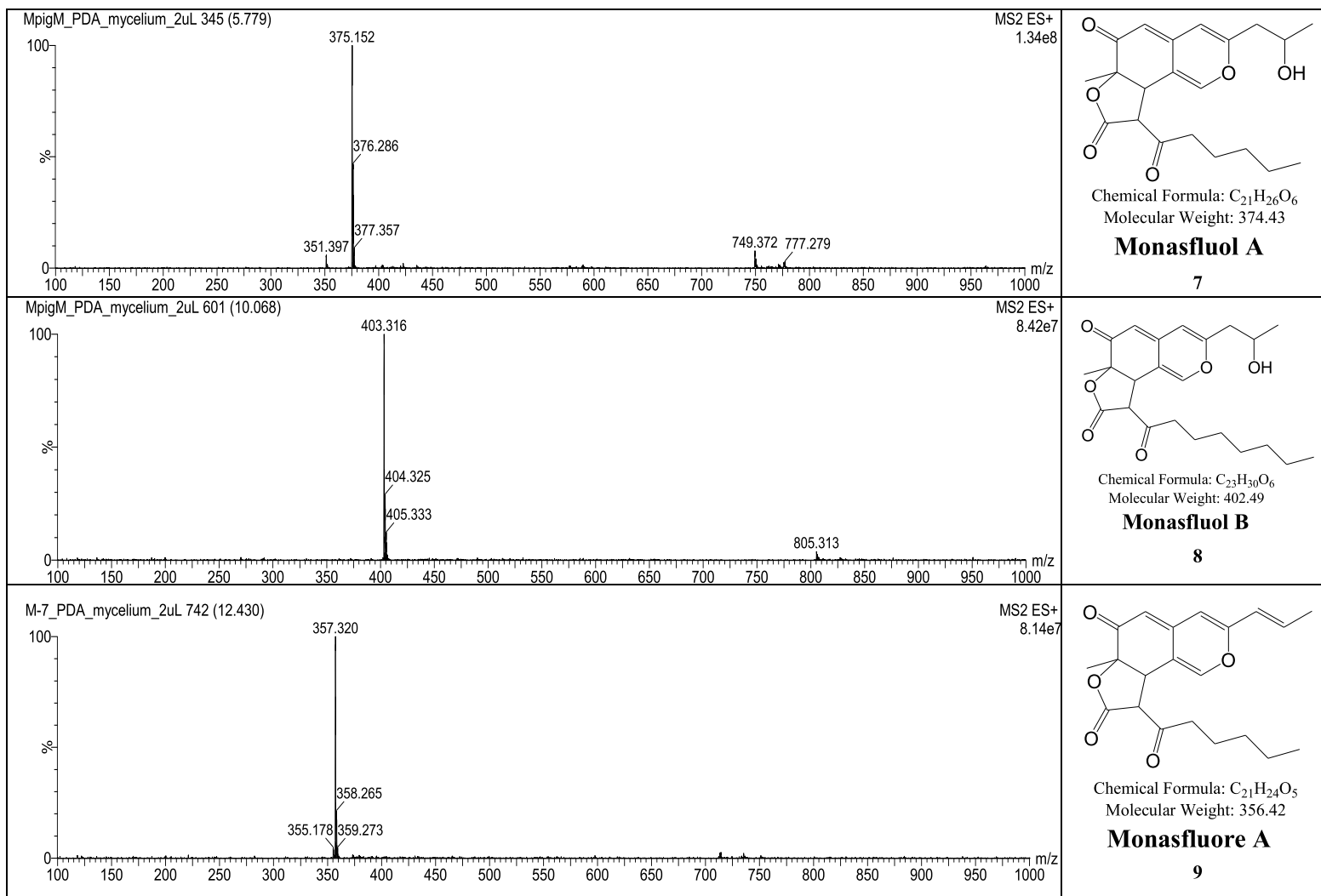
34

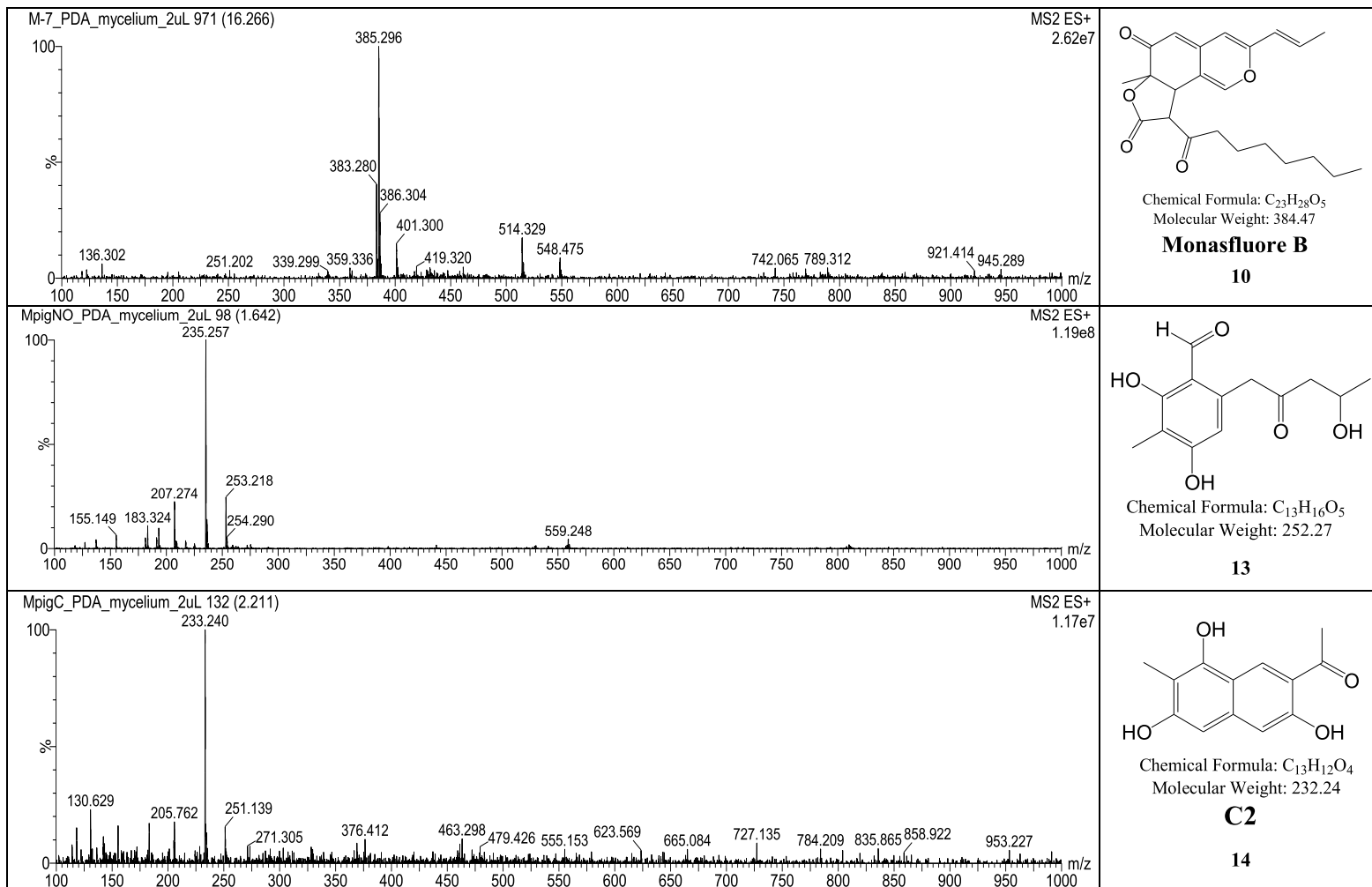


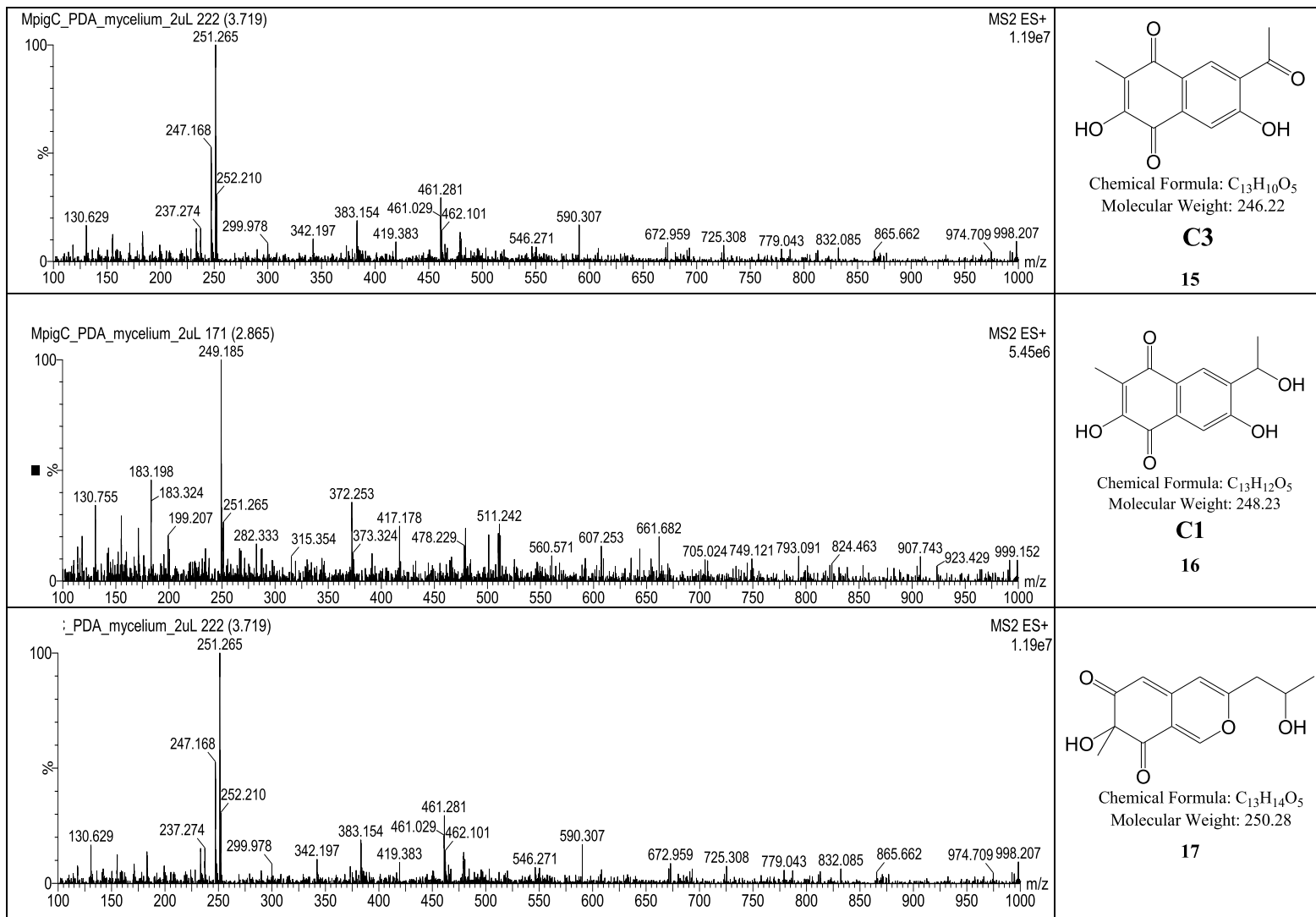
6.3. Mass spectra of MonAzPs and intermediates

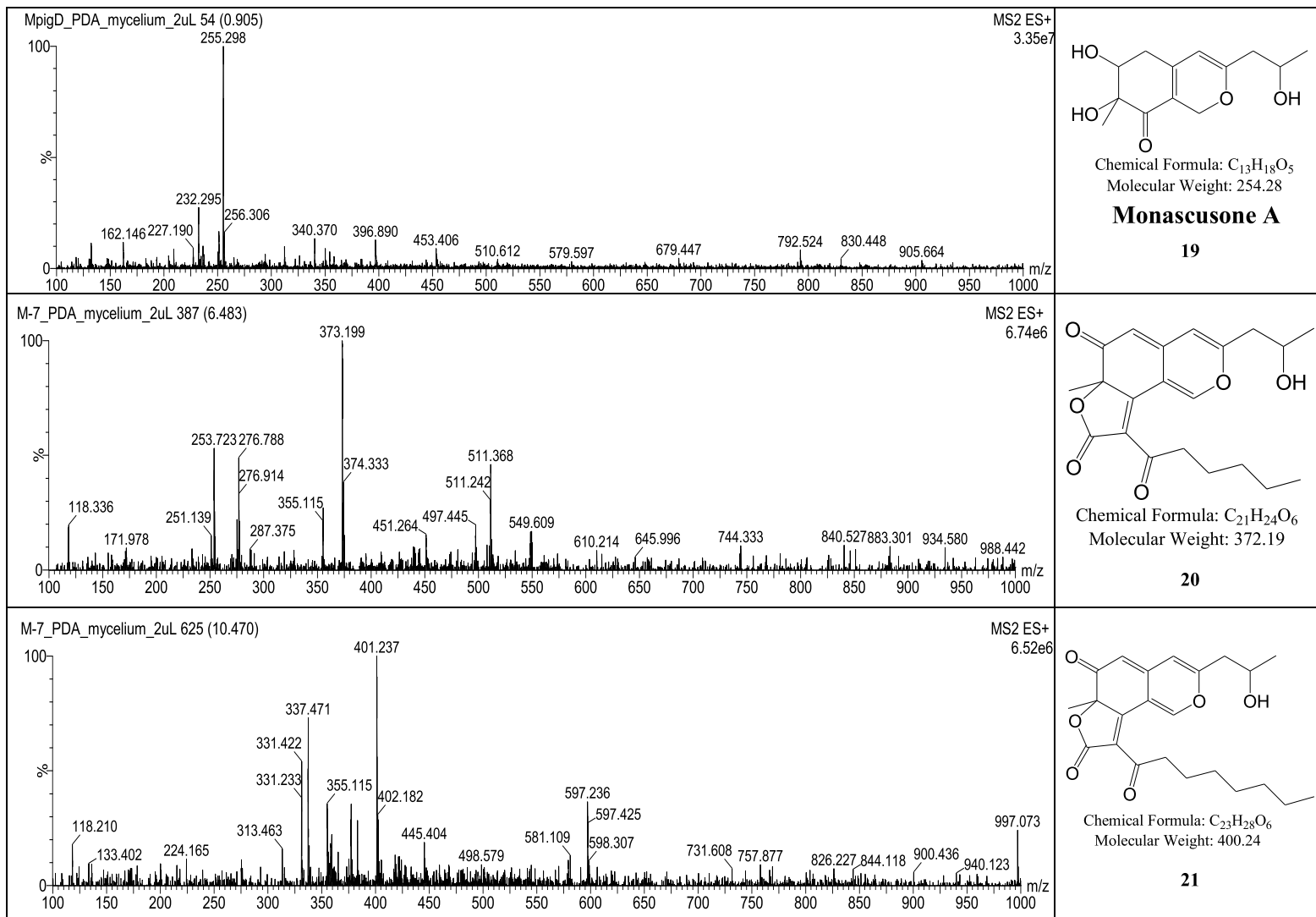


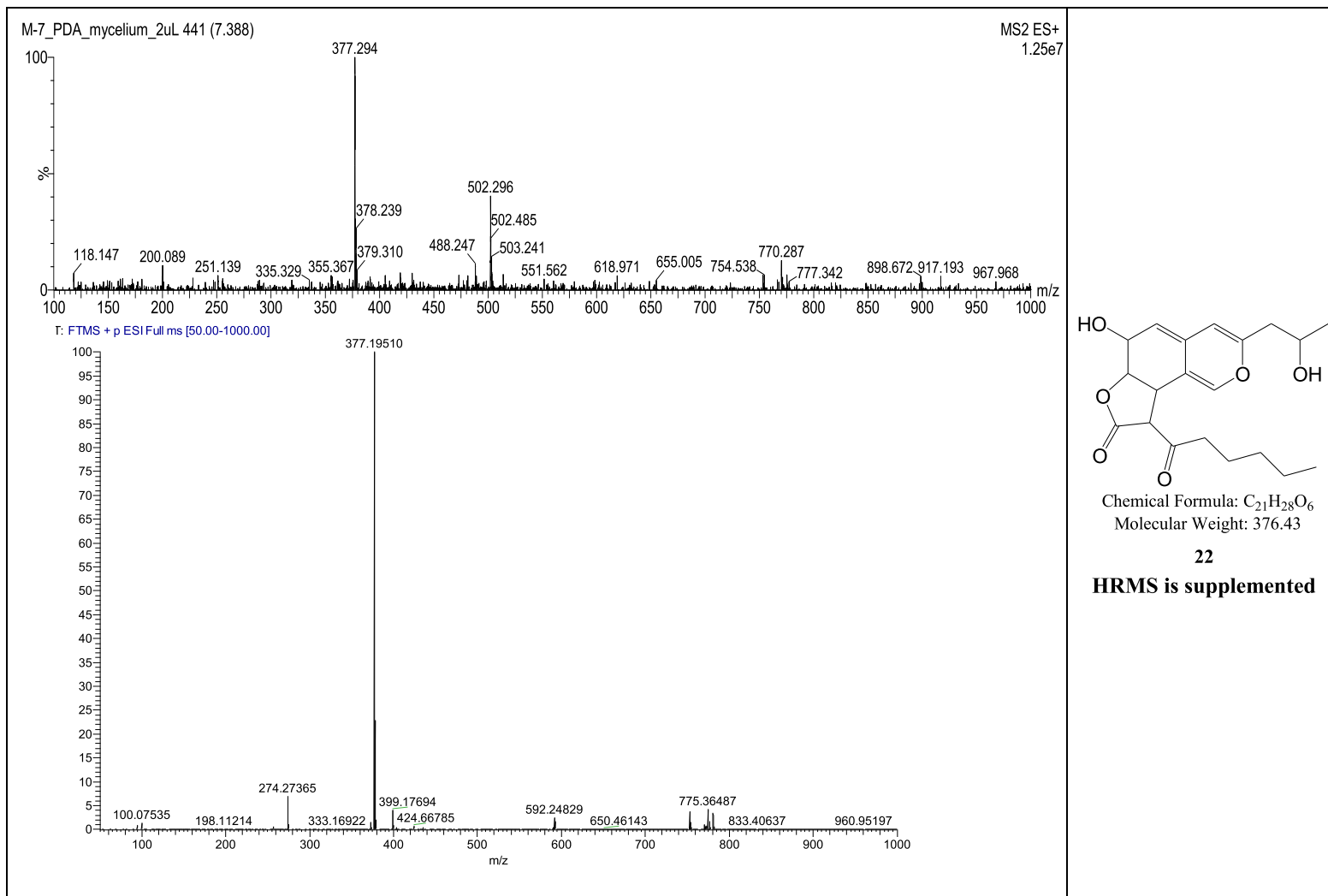


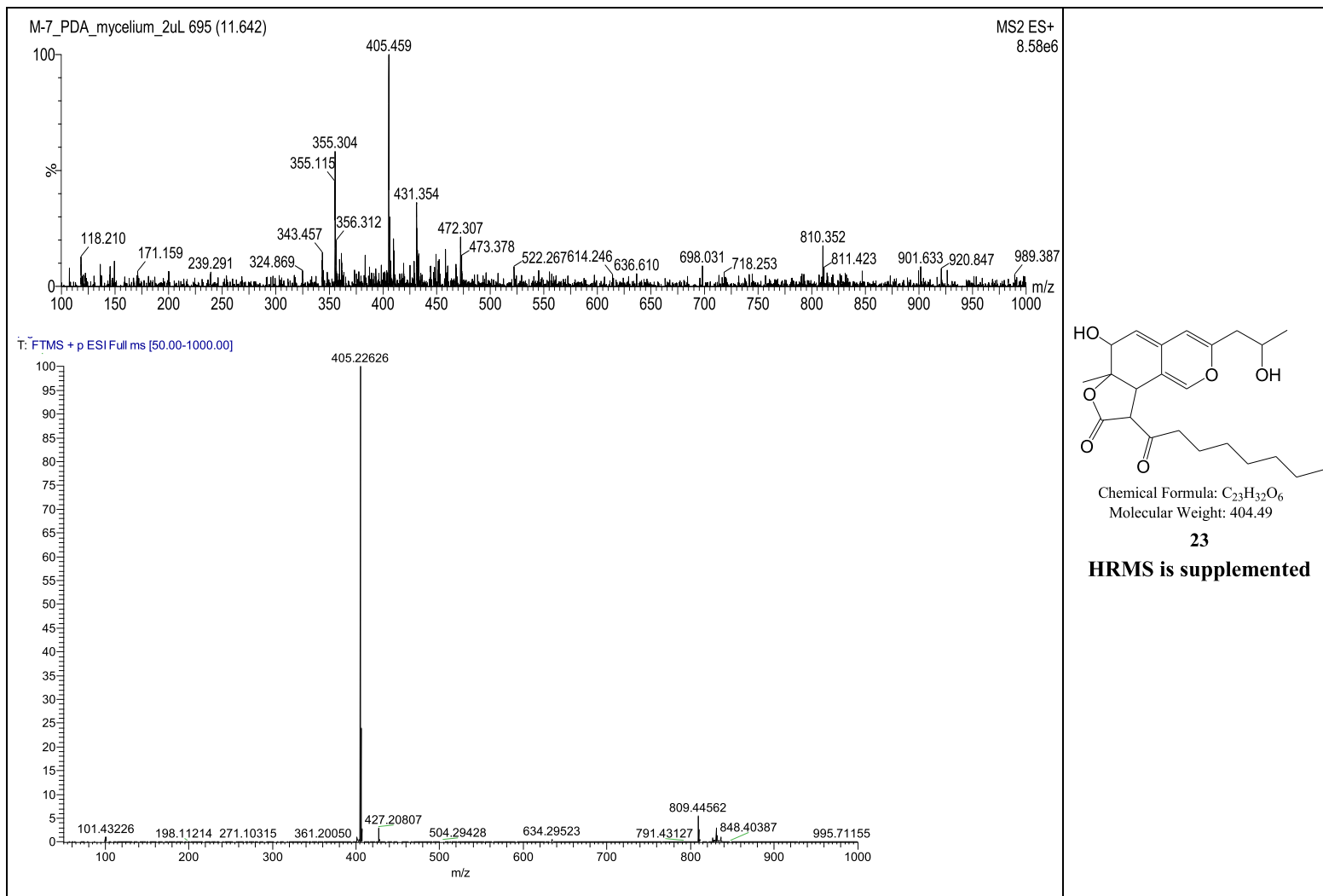


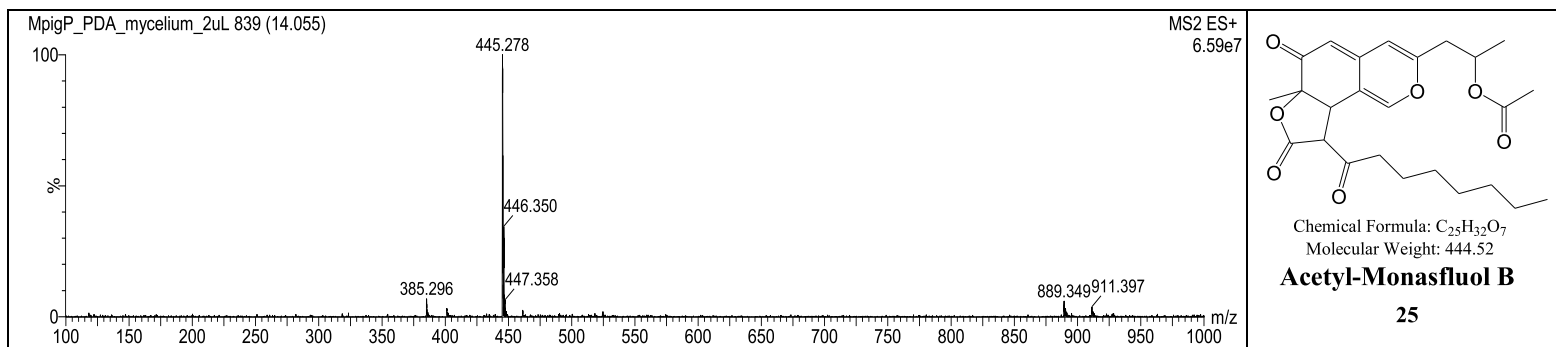
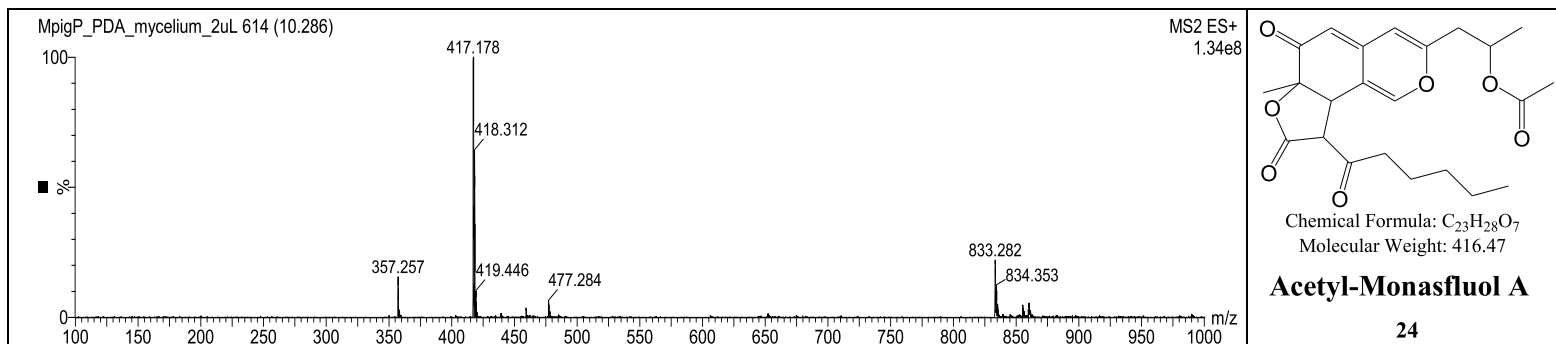


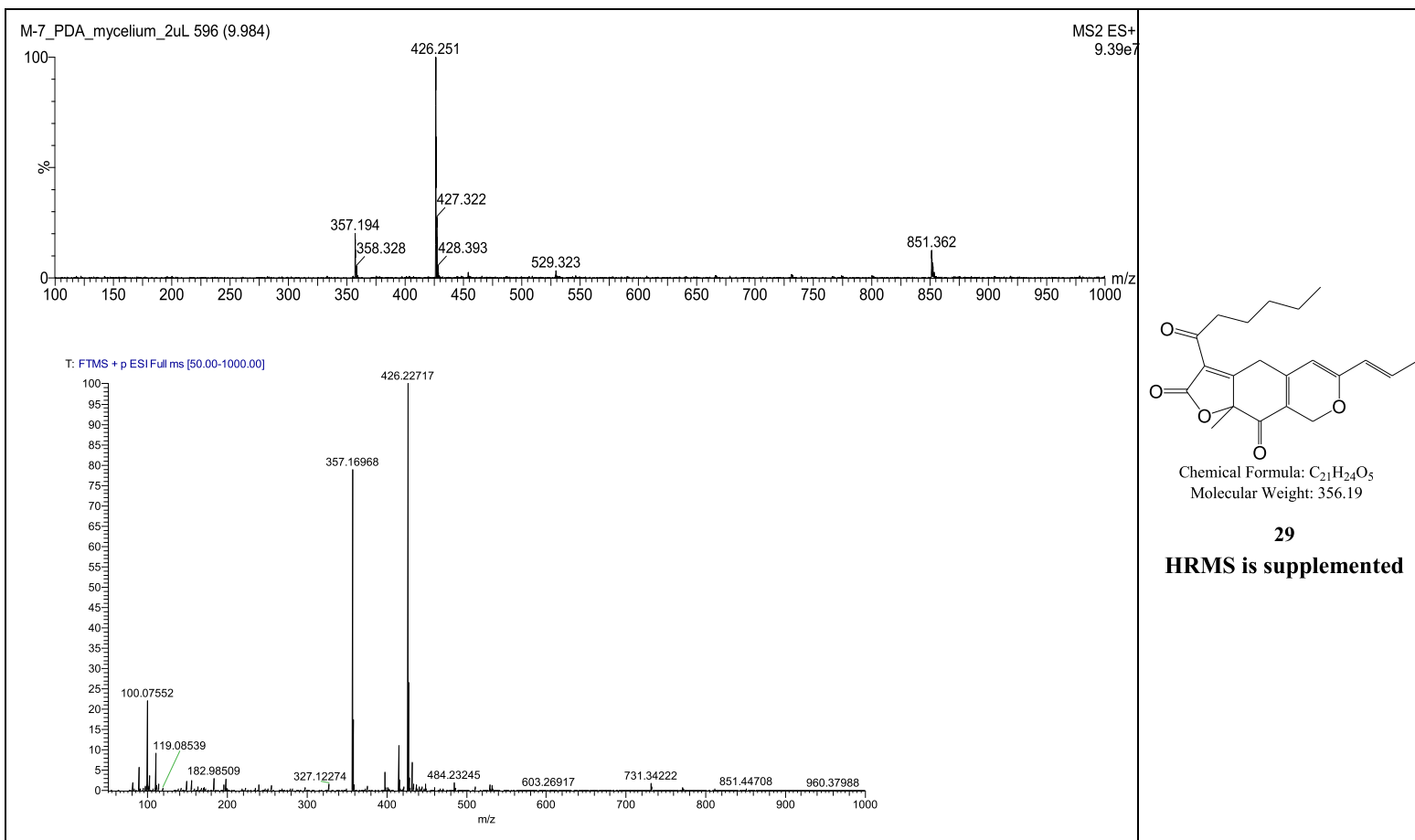


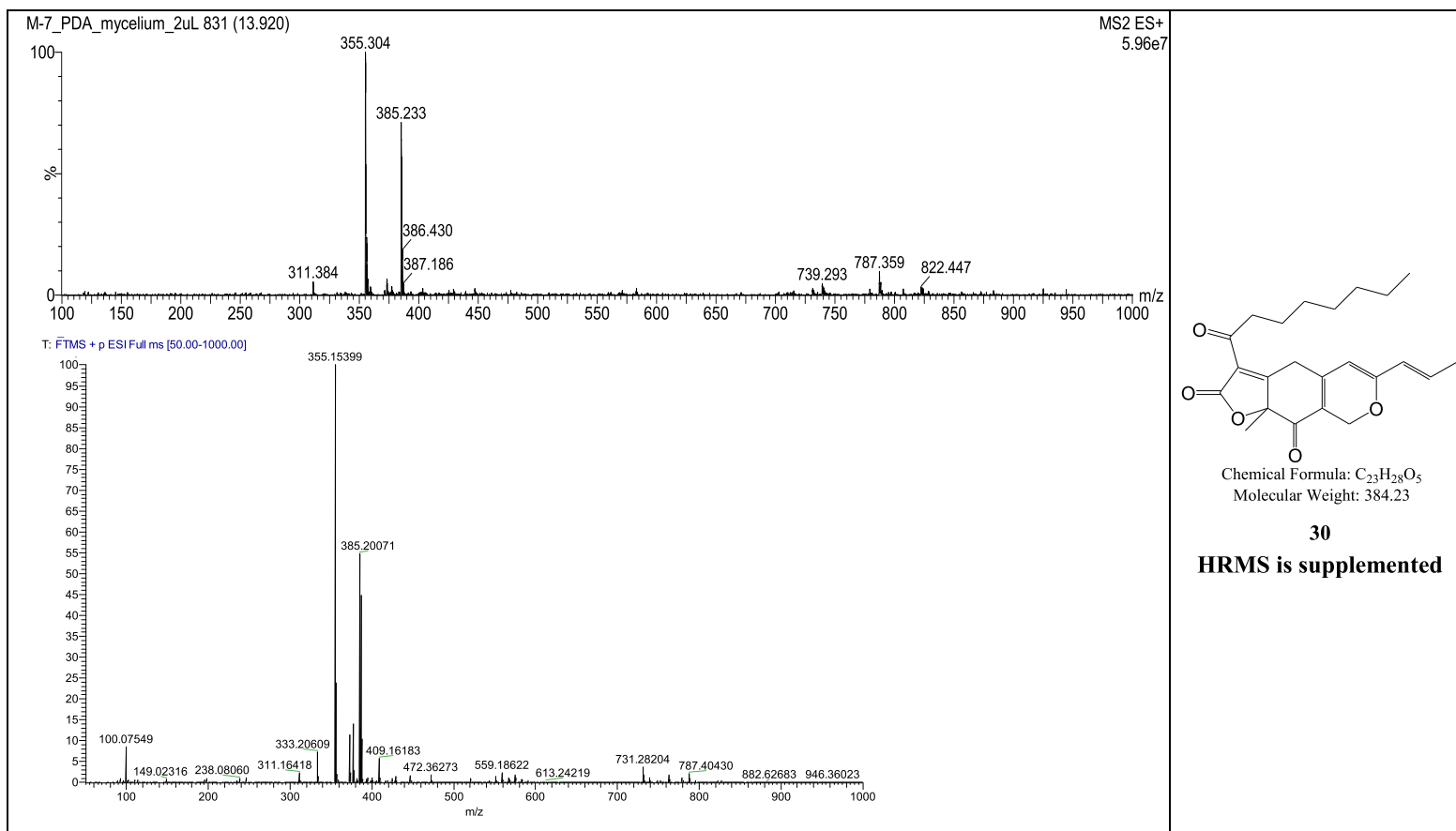


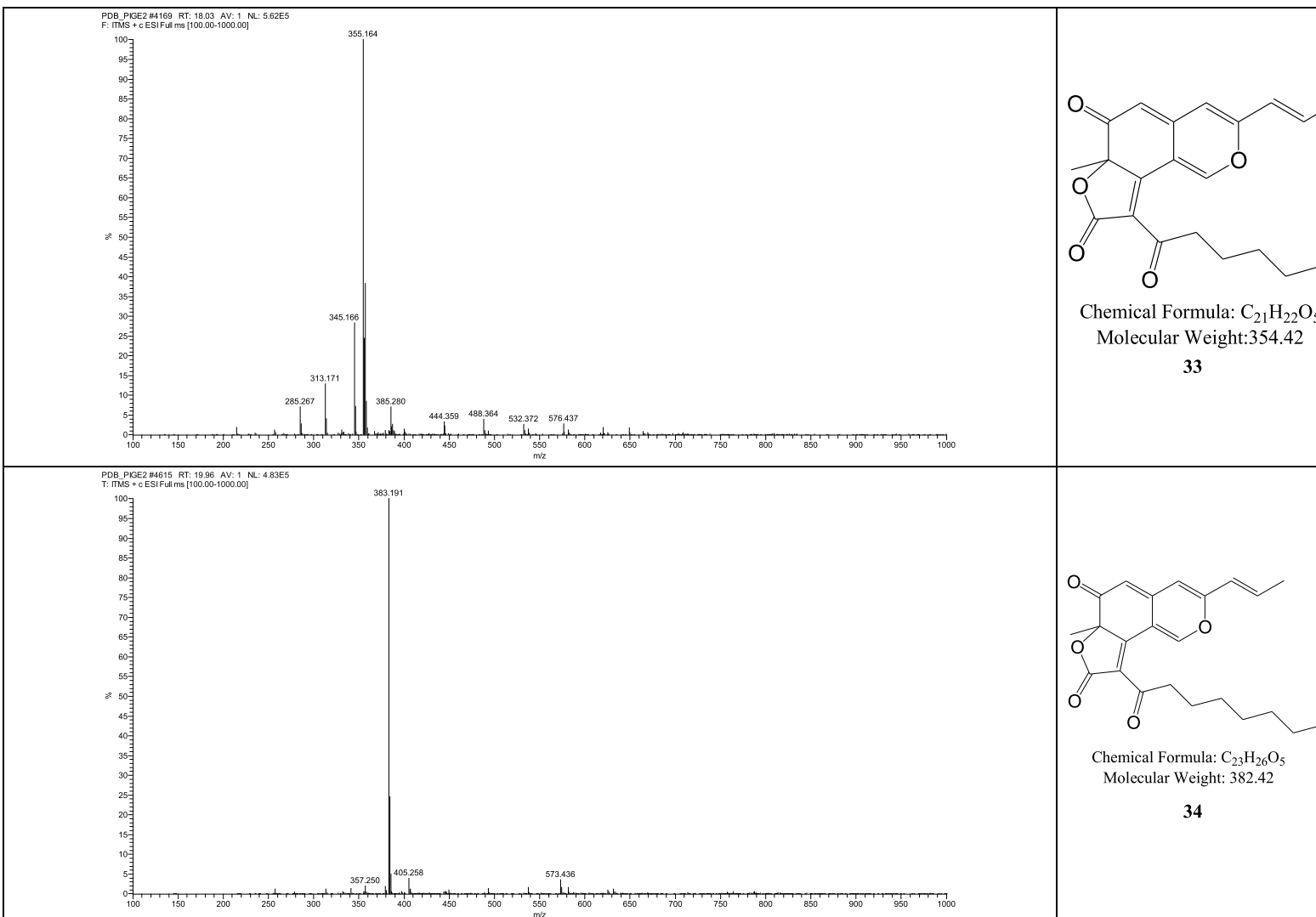


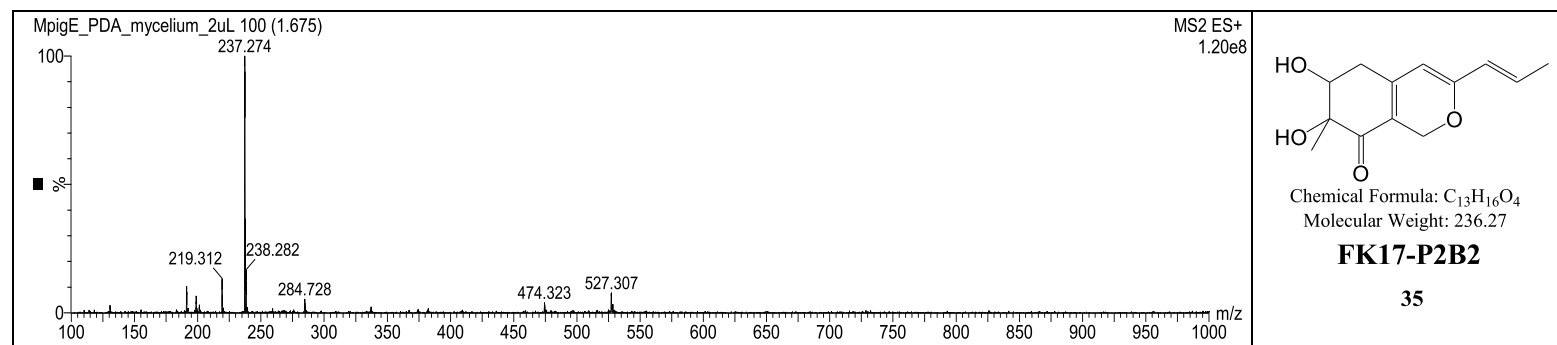








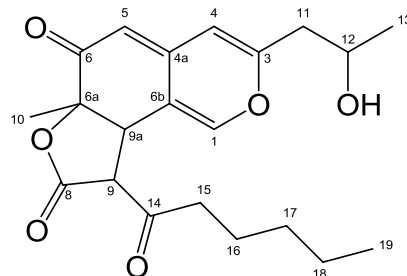




6.4. NMR spectra of MonAzPs and intermediates

Table 6-2 The NMR spectra of monasfluol A (7) (400 MHz, CD₃OD, δ in ppm, J in Hz)

No.	δ_{C}	δ_{H} (m, J_{HH} , area)
1	148.4	7.55 (s, 1H)
3	162.9	
4	105.6	6.33 (s, 1H)
4a	149.9	
5	109.9	5.38 (d, $J= 1.2$, 1H)
6	194.1	
6a	84.1	
6b	116.4	
8	169.1	
9	66.3	3.96 (s, 1H)
9a	43.7	3.31 (m, 1H)
10	23.5	1.53 (s, 3H)
11	43.9	2.68 (d, $J= 6.4$, 2H)
12	58.1	4.07 (m, 1H)
13	24.0	1.26 (d, $J= 6.3$, 3H)
14	203.8	
15	43.5	3.08 (dt, $J= 7.4, 2.21$, 2H)
16	23.7	1.58 (m, 2H)
17	30.2	1.30 (d, $J= 5.0$, 2H)
18	30.0	1.23 (d, $J= 6.4$, 2H)
19	14.4	0.90 (t, $J= 6.9$, 3H)



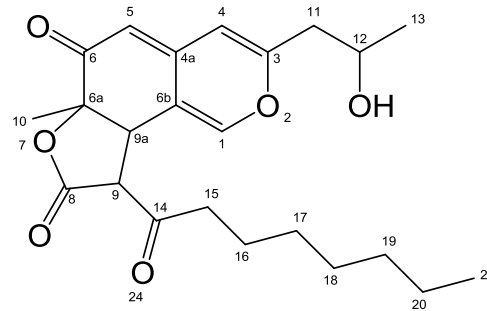
Chemical Formula: C₂₁H₂₆O₆
Molecular Weight: 374.43

Monasfluol A

7

Table 6-3 The NMR spectra of monasfluol B (**8**) (400 MHz, CD₃OD, δ in ppm, J in Hz)

No.	δ_{C}	δ_{H} (m, J _{HH} , area)
1	148.4	7.56 (s,1H)
3	163.0	
4	105.6	6.34 (s,1H)
4a	149.9	
5	109.9	5.39 (d,J=1.2,1H)
6	194.1	
6a	84.1	
6b	116.3	
8	170.1	
9	66.3	3.97 (s,1H)
9a	43.9	3.04(br s, 1H)
10	23.5	1.54 (s, 3H)
11	43.7	2.56 (ddd, $J_1=4.5$, $J_2=8.5$, $J_3=14.2$, 2H)
12	56.9	4.08(m,1H)
13	23.7	1.31(d,J=8.2, 3H)
14	203.8	
15	43.4	3.32 (dt, $J_1=1.6$, $J_2= 3.3$, 2H)
16	23.5	1.60 (d, $J=7.7$, 2H)
17	30.1	1.24 (o, 2H)
18	31.5	1.24 (o, 2H)
19	32.3	1.24 (o, 2H)
20	23.5	1.24 (o, 2H)
21	14.3	0.91 (t, $J= 7.1$, 3H)

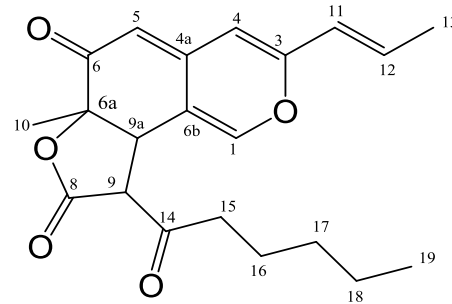


Chemical Formula: C₂₃H₃₀O₆
Molecular Weight: 402.49

Monasfluol B
8

Table 6-4 The NMR spectra of monasfluore A (**9**) (400 MHz, CD₃OD, δ in ppm, J in Hz)

No.	δ_{C}	δ_{H} (m, J_{HH} , area)
1	149.1	7.52 (s, 1H)
3	158.3	
4	108.3	6.13 (dd, $J_1=1.6$, $J_2=15.6$, 1H)
4a	148.3	
5	106.4	5.42 (s, 1H)
6	193.9	
6a	84.1	
6b	115.9	
8	171.0	
9	49.2	3.28 (dt, 1H)
9a	43.9	3.94 (s, 1H)
10	23.5	1.54 (s, 3H)
11	124.1	6.29 (s, 1H)
12	136.6	6.59 (dd, $J_1=6.9$, $J_2=15.6$, 1H)
13	18.6	1.88 (m, 3H)
14	203.8	
15	43.5	2.54 (dt, $J_1=9.1$, $J_2=16.2$, 1H), 2.97 (dt, $J_1=9.1$, $J_2=16.2$, 1H)
16	23.7	1.32 (o, 2H)
17	32.3	1.28 (o, 2H)
18	22.4	1.27 (o, 2H)
19	14.3	0.85 (t, $J=7.0$, 3H)



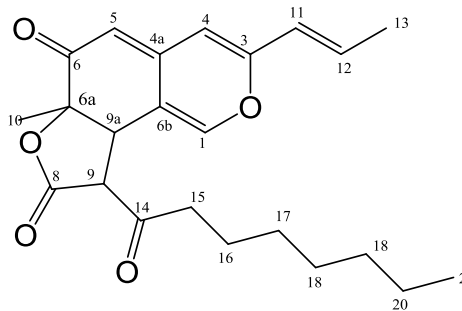
Chemical Formula: C₂₁H₂₄O₅
Molecular Weight: 356.42

Monasfluore A

9

Table 6-5 The NMR spectra of monasfluore B (**10**) (400 MHz , CD₃OD, δ in ppm, J in Hz)

No.	δ_{C}	δ_{H} (m, J , area)
1	149.1	7.50 (s, 1H)
3	158.3	
4	108.3	
4a	148.3	6.14 (dd, $J_1=1.6$, $J_2=15.6$, 1H)
5	106.5	5.41 (s, 1H)
6	193.9	
6a	84.1	
6b	116.0	
8	171.0	
9	49.2	3.29 (dt, $J_1=1.6$, $J_2=3.2$, 1H)
9a	43.9	3.94 (s, 1H)
10	23.5	1.51 (s, 3H)
11	124.1	6.30 (s, 1H)
12	136.6	6.60 (dd, $J_1=6.9$, $J_2=15.6$, 1H)
13	18.6	1.89 (dd, $J_1=1.4$, $J_2=6.9$, 3H)
14	203.9	
15	43.5	2.55(dt, $J_1=6.9$, $J_2=18.2$, 1H), 2.97 (dt, $J_1=6.9$, $J_2=18.2$, 1H)
16	24.1	1.26 (o, 2H)
17	30.0	1.26 (o, 2H)
18	30.2	1.26 (o, 2H)
19	32.9	1.26 (o, 2H)
20	23.5	1.26 (o, 2H)
21	14.5	0.86 (t, $J=6.8$, 3H)

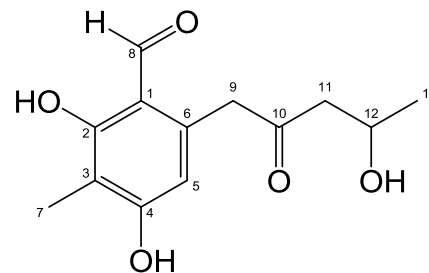


Chemical Formula: C₂₃H₂₈O₅
Molecular Weight: 384.47

Monasfluore B
10

Table 6-6 The NMR spectra of intermediate **13** (600 MHz, CD₃OD, δ in ppm, J in Hz)

No.	δ_{C}	δ_{H} (m, J , area)
1	13.09	
2	165.1	
3	111.5	
4	164.5	
5	111.92	6.23 (s, 1H)
6	113.8	
7	7.2	2.02 (s, 3H)
8	194.9	9.78 (s, 1H)
9	47.5	4.05(s, 2H)
10	208.8	
11	52.0	2.62 (d, $J_1=4.6$, $J_2=15.9$, 1H), 2.71 ($J_1=8.0$, $J_2=15.9$, 1H)
12	65.2	4.22(m, 1H)
13	23.5	1.18 (d, $J=6.26$, 3H)

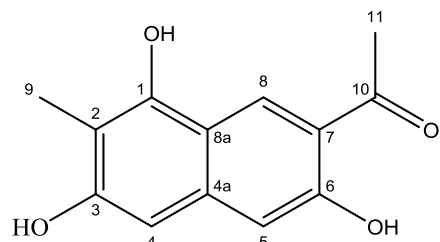


Chemical Formula: C₁₃H₁₆O₅
Molecular Weight: 252.27

13

Table 6-7 The NMR spectra of C2 (**14**) (400 MHz, CD₃OD, δ in ppm, J in Hz)

No.	δ_{C}	δ_{H} (m, J , area)
1	153.9	
2	109.5	
3	161.0	
4	100.2	6.48 (s, 1H)
a4	116.4	
5	109.7	6.79 (s, 1H)
6	158.3	
7	118.8	
8	129.8	8.70 (s, 1H)
8a	140.4	
9	8.9	2.16 (s, 3H)
10	206.0	
11	26.6	2.70 (s, 3H)

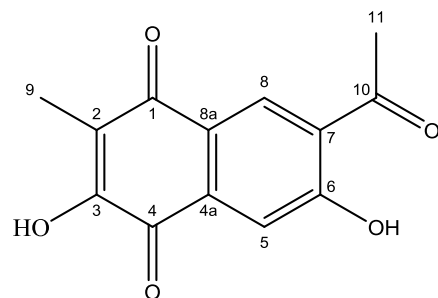


Chemical Formula: C₁₃H₁₂O₄
Molecular Weight: 232.24

C2
14

Table 6-8 The NMR spectra of C3 (**15**) (400 MHz, CD₃OD, δ in ppm, J in Hz)

No.	δ_{C}	δ_{H} (m, J , area)
1	183.9	
2	122.3	
3	154.9	;
4	180.2	
4a	135.3	
5	116.1	7.50 (s, 1H)
6	165.4	
7	122.3	
8	130.4	8.45 (s, 1H)
8a	124.0	
9	8.7	2.03 (s, 3H)
10	204.9	
11	27.2	2.70 (s, 3H)
3-OH		7.26 (s, 1H)
6-OH		12.62 (s, 1H)



Chemical Formula: C₁₃H₁₀O₅

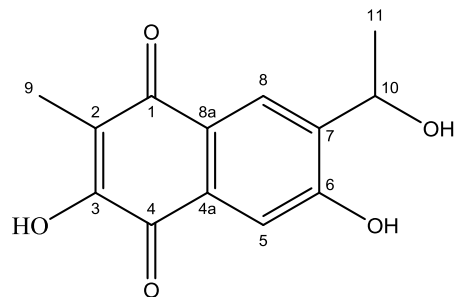
Molecular Weight: 246.22

C3

15

Table 6-9 The NMR spectra of C1 (**16**) (400 MHz, CD₃OD, δ in ppm, J in Hz)

No.	δ_{C}	δ_{H} (m, J , area)
1	184.4	
2	119.4	
3	154.9	
4	180.8	
4a	124.4	
5	111.2	7.33 (s, 1H)
6	157.6	
7	140.3	
8	124.1	8.03 (s, 1H)
8a	123.0	
9	8.6	1.90 (s, 3H)
10	62.9	4.98 (q, $J= 6.3$, 3H)
11	23.9	1.28 (d, $J= 6.4$, 3H)



Chemical Formula: C₁₃H₁₂O₅

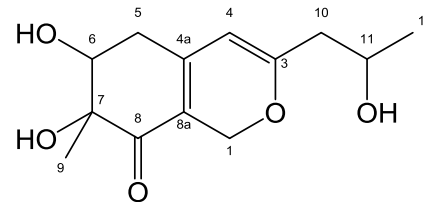
Molecular Weight: 248.23

C1

16

Table 6-10 The NMR spectra of monascusone A (**19**) (400 MHz, D₂O, δ in ppm, J in Hz)

No.	δ_{C}	δ_{H} (m, J_{HH} , area)
1	63.7	4.79 (d, $J=12.4$, 1H), 4.87 (d, $J=12.4$, 1H)
2	165.3	
3	102.9	5.38 (s, 1H)
4a	149.8	
5	34.0	2.43 (d, $J_1=10.0$, $J_2=18.0$, 1H), 2.65 (d, $J_1=5.2$, $J_2=18.0$, 1H)
6	72.1	3.91 (dd, $J_1=5.2$, $J_2=10.0$, 1H)
7	76.7	
8	197.6	
8a	112.8	
9	16.7	1.22 (s, 3H)
10	43.2	2.29 (dd, $J_1=7.4$, $J_2=14.0$, 1H) 2.36 (dd, $J_1=7.4$, $J_2=5.6$, 1H)
11	65.0	4.01 (ddd, $J_1=5.6$, $J_2=6.4$, $J_3=7.41$ H)
12	22.0	1.20 (d, $J=6.4$, 3H)



Chemical Formula: C₁₃H₁₈O₅

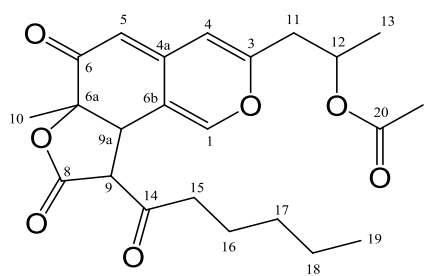
Molecular Weight: 254.28

Monascusone A

19

Table 6-11 The NMR spectra of acetyl-monasfluol A (**24**) (400 MHz , CD₃OD, δ in ppm, J in Hz)

No.	δ_{C}	δ_{H} (m, J_{HH} , area)
1	149.8	7.52 (s, 1H)
3	161.4	
4	110.1	6.33 (s, 1H)
4a	147.9	
5	106.1	5.36 (d, $J= 1.0$, 1H)
6	194.2	
6a	84.1	
6b	116.3	
8	171.1	
9	57.1	3.92 (s, 1H)
9a	43.6	3.28 (br s, 1H)
10	23.5	1.53 (s, 3H)
11	40.6	2.68 (d, $J= 6.4$, 2H)
12	69.4	5.16 (m, 1H)
13	20.1	1.26 (d, $J=6.3$, 3H)
14	203.9	
15	44.0	, 2.94 (dt, $J_1=7.4$, $J_2= 18.4$, 1H), 2.97 (dt, $J_1=7.4$, $J_2= 18.4$, 1H)
16	23.5	1.56 (m, 2H)
17	32.3	1.28 (m, 2H)
18	23.7	1.33 (m, 2H)
19	14.3	0.86 (t, $J= 7.1$, 3H)
20	172.0	
21	21.0	1.99 (s, 3H)



Chemical Formula: C₂₃H₂₈O₇

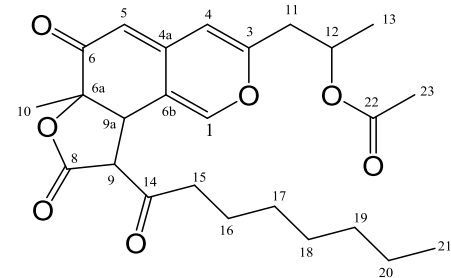
Molecular Weight: 416.47

Acetyl-monasfluol A

24

Table 6-12 The NMR spectra of acetyl-monasfluol B (**25**) (400 MHz , CD₃OD, δ in ppm, J in Hz)

No.	δ_{C}	δ_{H}
1	149.8	7.46 (s, 1H)
3	161.4	
4	110.1	6.27 (s, 1H)
4a	147.9	
5	106.1	5.33 (s, 1H)
6	194.2	
6a	84.1	
6b	116.3	
8	171.0	
9	58.7	3.28 (s, 1H)
9a	43.7	3.89 (s, 1H)
10	23.7	1.51 (s, 3H)
11	40.6	2.65 (d, $J=6.3$, 2H)
12	69.4	5.09 (m, 1H)
13	20.1	1.46 (d, $J=6.4$, 3H)
14	203.9	
15	43.9	2.58 (dt, $J_1=7.3, J_2=18.3$, 1H), 3.11 (dt, $J_1=7.3, J_2=18.3$, 1H)
16	23.5	1.51 (m, 2H)
17	30.2	1.26 (o, 2H)
18	30.0	1.26 (o, 2H)
19	32.1	1.26 (o, 2H)
20	24.0	1.26 (o, 2H)
21	14.4	0.90 (t, $J= 7.1$, 3H)
22	172.0	
25	21.0	1.99 (s, 3H)

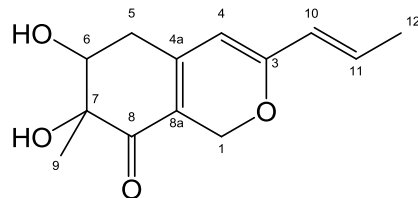


Chemical Formula: C₂₅H₃₂O₇
Molecular Weight: 444.52

Acetyl-Monasfluol B
25

Table 6-13 The NMR spectra of FK17-P2B2 (**35**) (400 MHz , CD₃OD, δ in ppm, J in Hz)

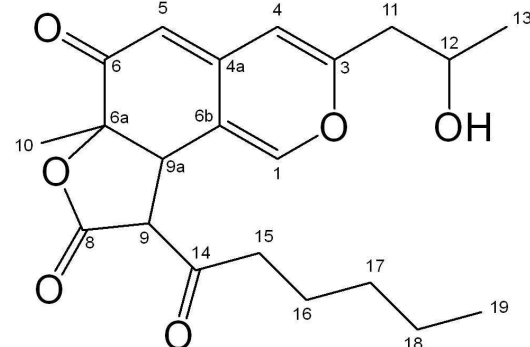
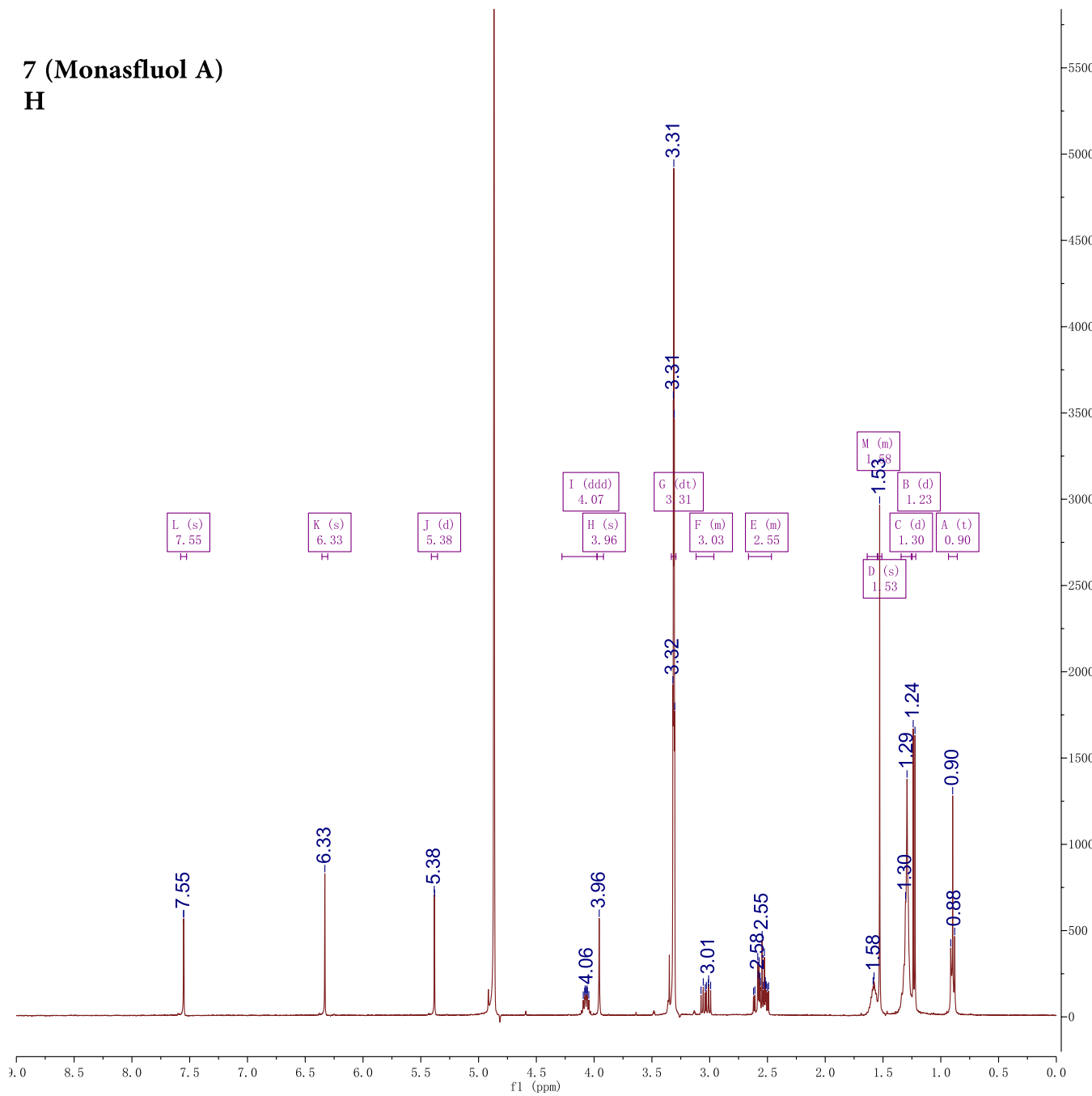
No.	δ_{C}	δ_{H} (m, J_{HH} , area)
1	63.6	4.69 (d, $J=12.4$, 1H), 4.79 (d, $J=12.4$, 1H)
3	161.0	
4	103.9	5.43 (s, 1H)
4a	152.8	
5	33.9	2.45 (dd, $J_1=10.4$, $J_2=14.0$, 1H); 2.66 (dd, $J_1=5.6$, $J_2=14.0$, 1H)
6	71.8	3.92 (dd, $J_1=5.6$, $J_2=10.4$, 1H)
7	77.5	
8	198.5	
8a	136.4	
9	16.8	1.14 (s, 3H)
10	113.7	5.94 (dd, $J_1=1.2$, $J_2=14.0$, 1H)
11	124.1	6.42 (dq, $J_1=7.0$, $J_2=14.0$, 1H)
12	17.7	1.74 (dd, $J_1=1.2$, $J_2=7.2$, 3H)



Chemical Formula: C₁₃H₁₆O₄
Molecular Weight: 236.27

FK17-P2B2
35

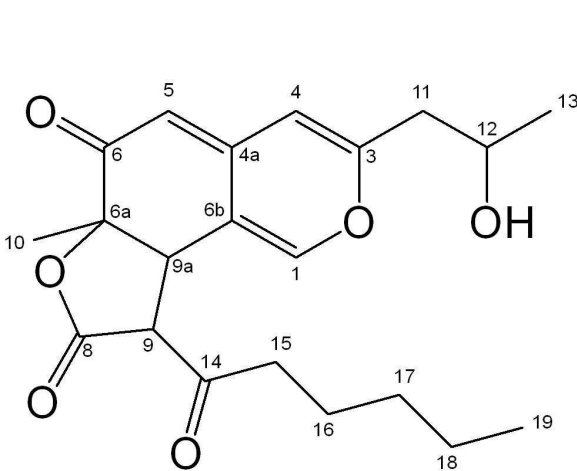
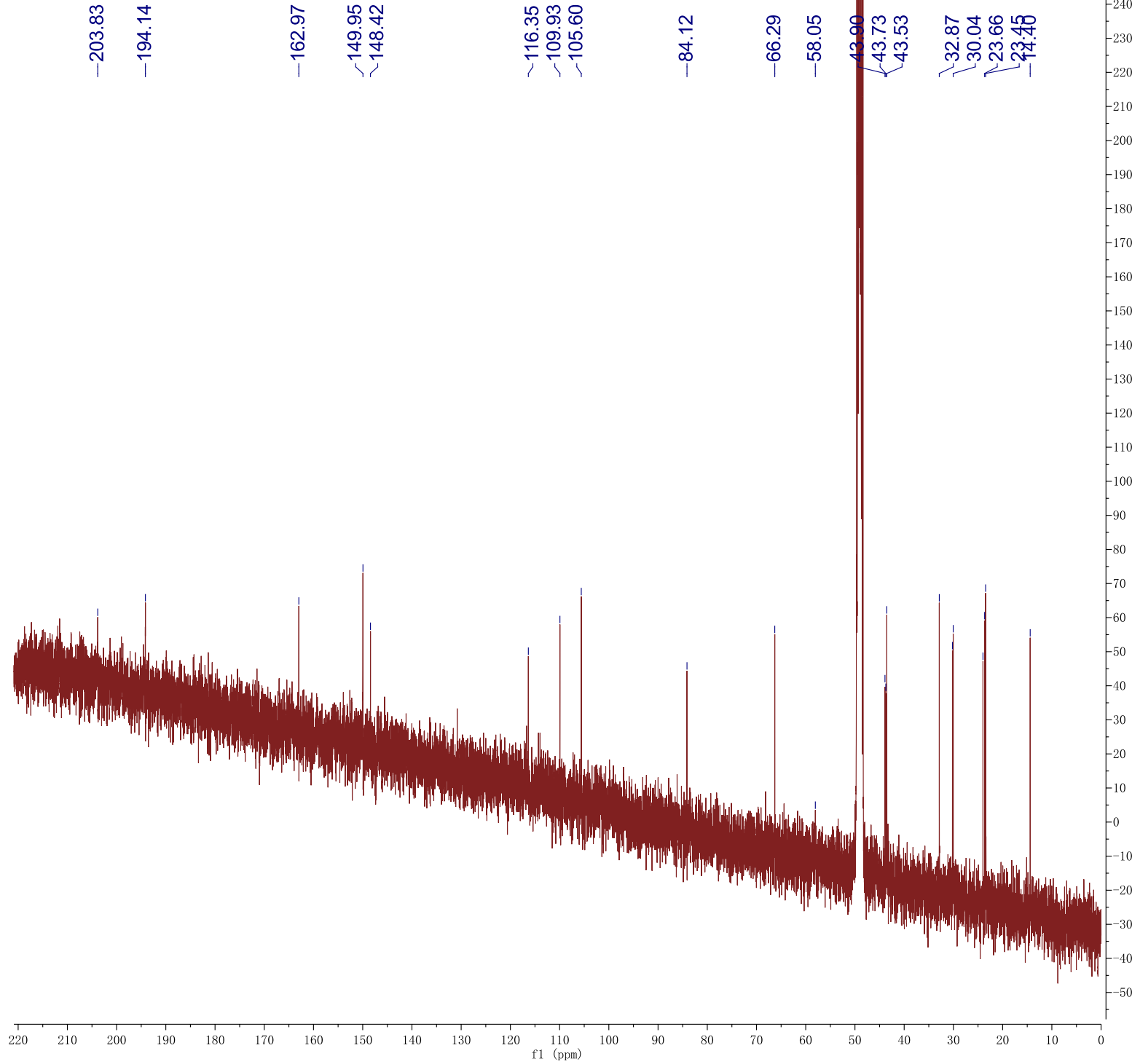
7 (Monasfluol A)
H



Chemical Formula: $C_{21}H_{26}O_6$
Molecular Weight: 374.43

Name	Shift Class	J's
1 L (s)	7.55 s	
2 K (s)	6.33 s	
3 J (d)	5.38 d	1.2
4 I (ddd)	4.07 ddd	4.8, 6.3, 8.0
5 H (s)	3.96 s	
6 G (dt)	3.31 dt	1.6, 1.6, 3.2
7 F (m)	3.03 m	
8 E (m)	2.55 m	
9 M (d)	1.58 d	3.1
10 D (s)	1.53 s	
11 C (d)	1.30 d	5.0
12 B (d)	1.23 d	6.3
13 A (t)	0.90 t	6.9, 6.9

7 (Monasfluol A)
C

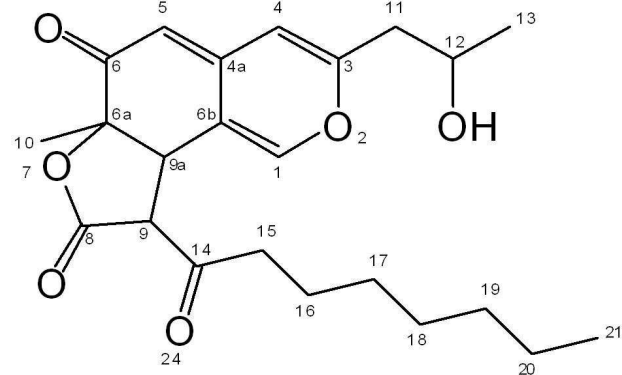
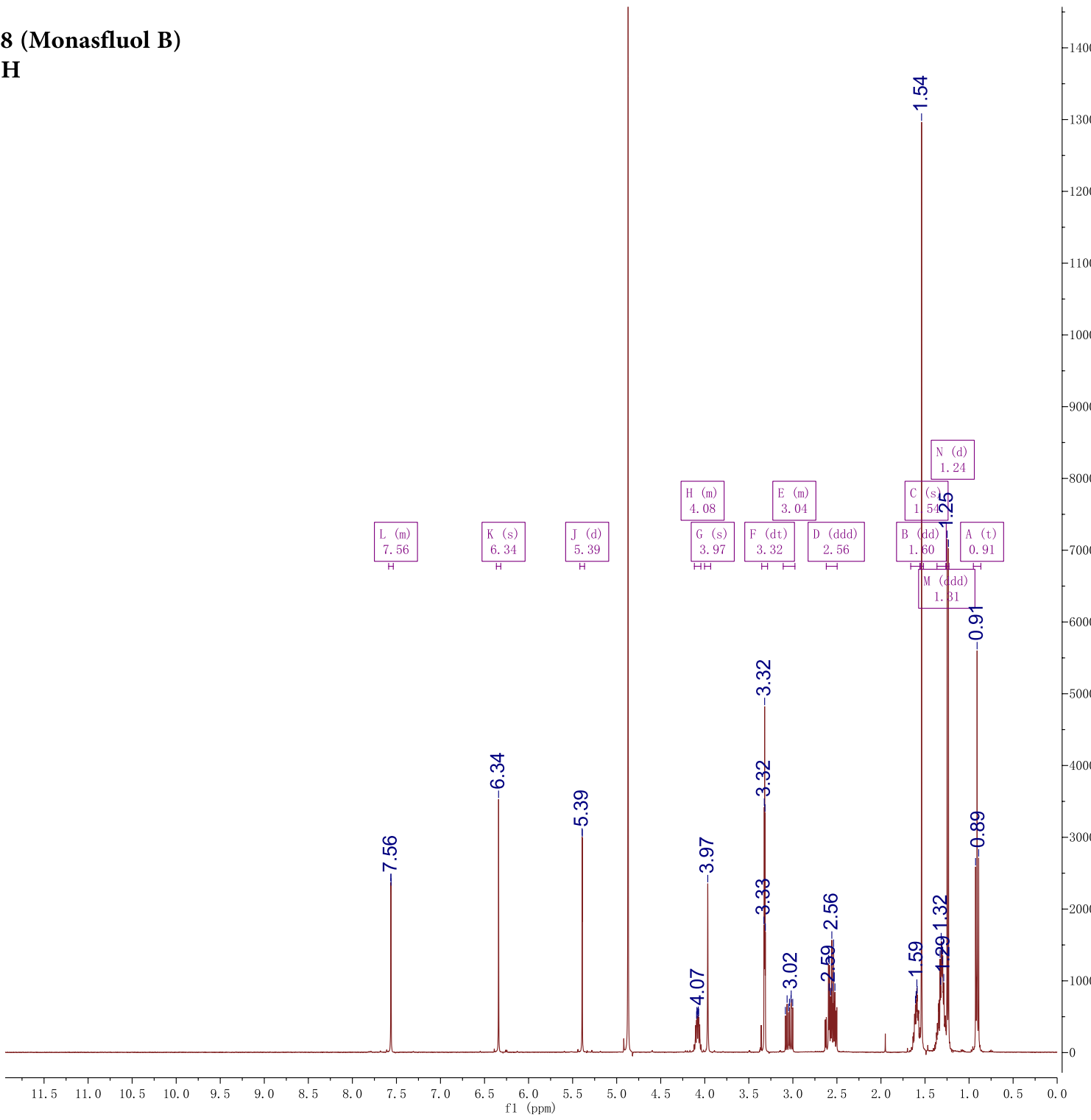


Chemical Formula: C₂₁H₂₆O₆
Molecular Weight: 374.43

	ppm
1	203.83
2	194.14
3	162.97
4	149.95
5	148.42
6	116.35
7	109.93
8	105.60
9	84.12
10	66.29
11	58.05
12	43.90
13	43.73
14	43.53
15	32.87
16	30.19
17	30.04
18	23.99
19	23.66
20	23.45
21	14.40

8 (Monasfluol B)

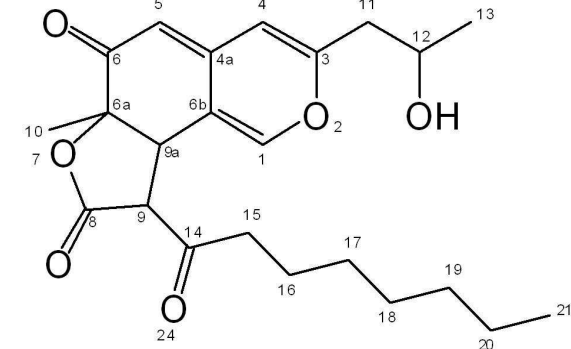
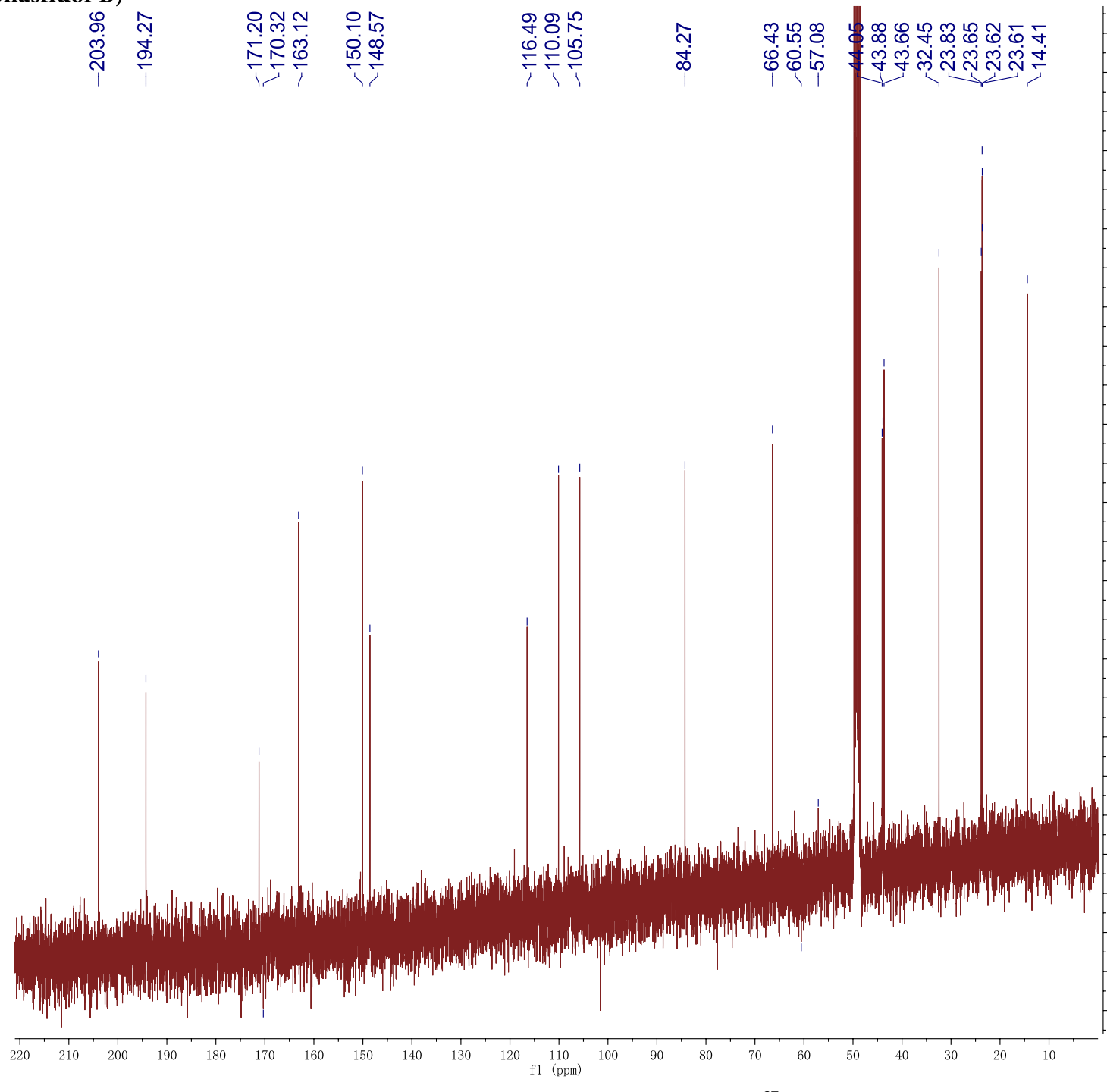
H



Name	Shift Class	J' s
1 L (m)	7.56 m	
2 K (s)	6.34 s	
3 J (d)	5.39 d	1.2
4 H (m)	4.08 m	
5 G (s)	3.97 s	
6 F (dt)	3.32 dt	1.6, 1.6, 3.3
7 E (m)	3.04 m	
8 D (ddd)	2.56 ddd	4.5, 8.5, 14.2
9 B (dd)	1.60 dd	2.2, 5.7
10 C (s)	1.54 s	
11 M (ddd)	1.31 ddd	3.7, 5.6, 8.2
12 N (d)	1.24 d	6.2
13 A (t)	0.91 t	7.1, 7.1

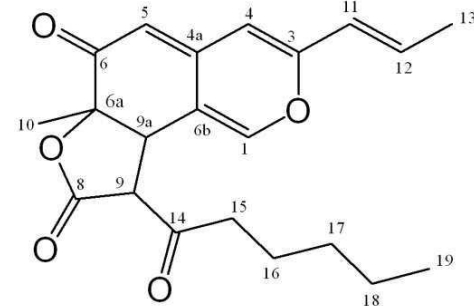
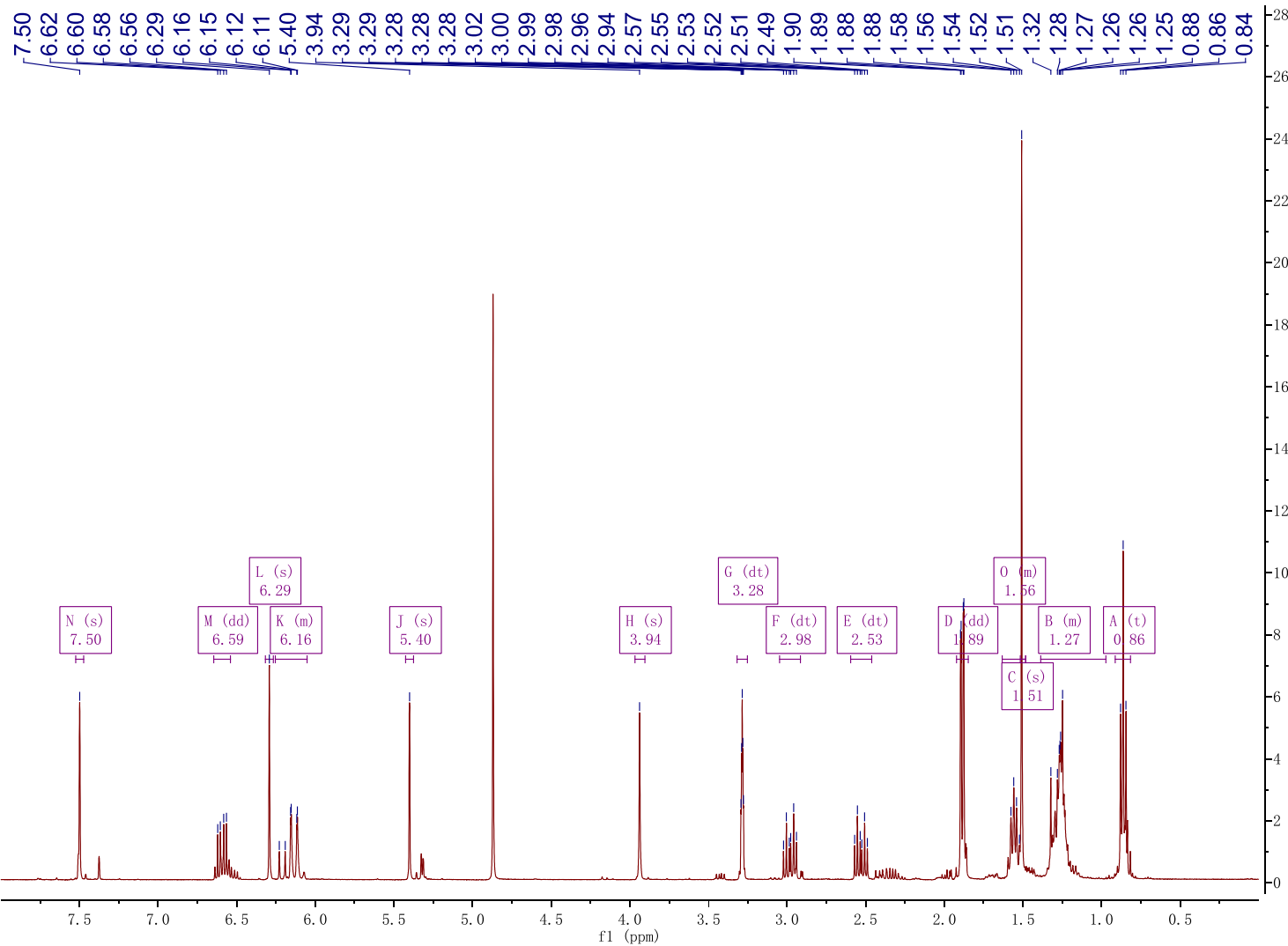
8 (Monasfluol B)

C



	ppm
1	203.96
2	194.27
3	171.20
4	170.32
5	163.12
6	150.10
7	148.57
8	116.49
9	110.09
10	105.75
11	84.27
12	66.43
13	60.55
14	57.08
15	44.05
16	43.88
17	43.66
18	32.45
19	23.83
20	23.65
21	23.62
22	23.61
23	14.41

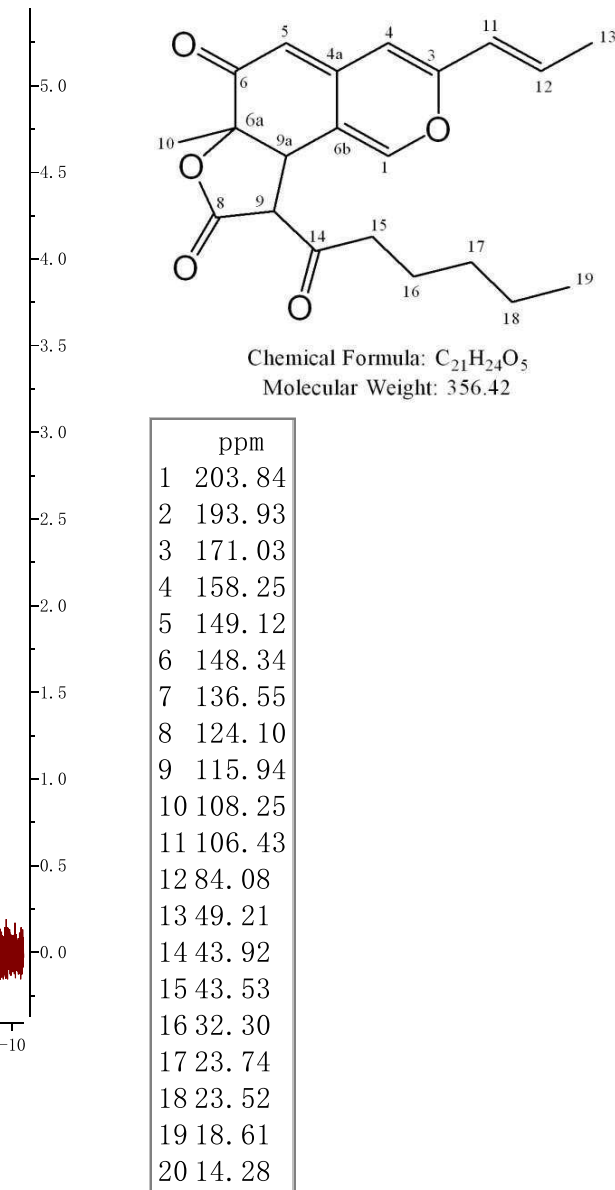
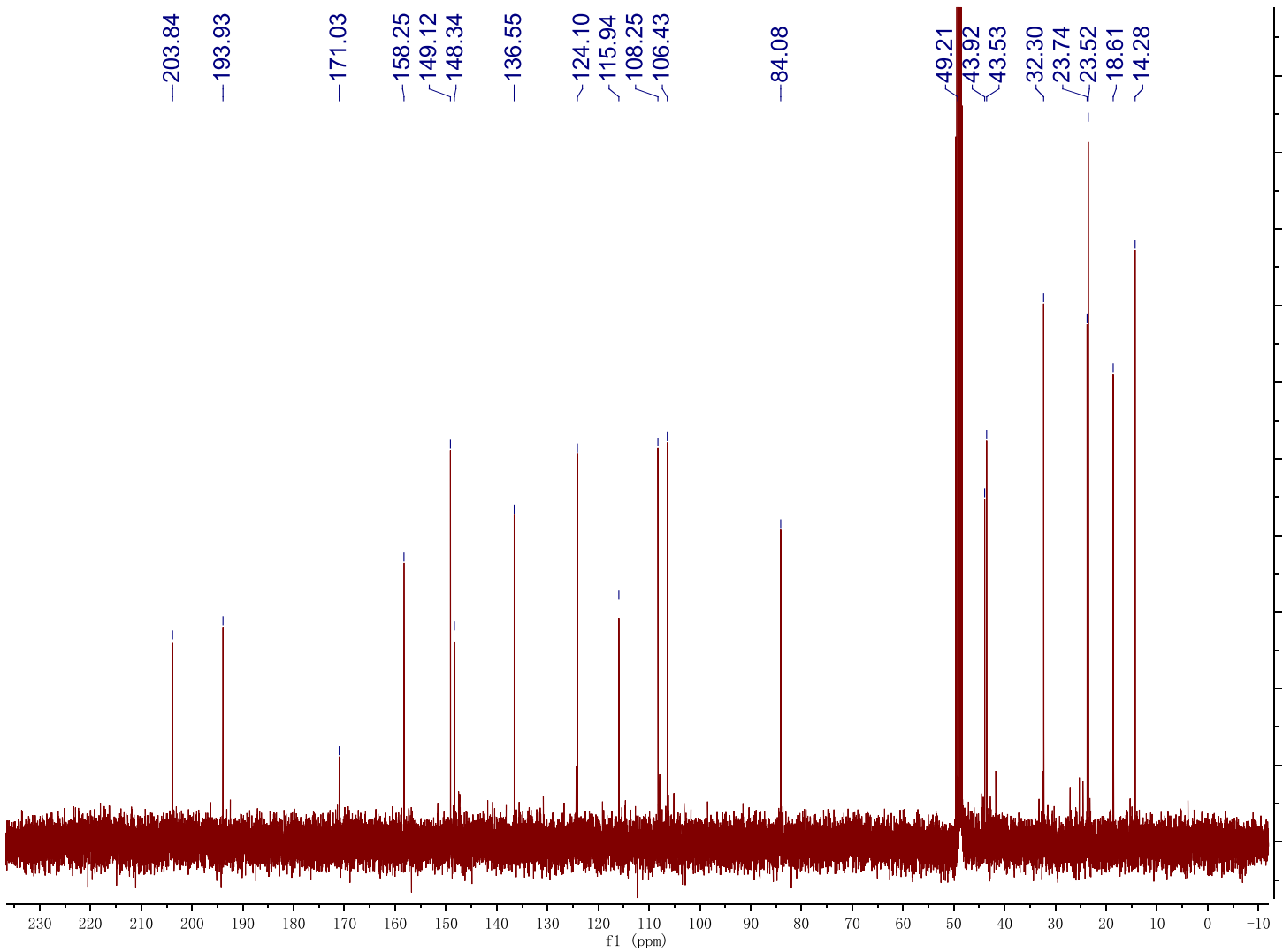
9 (Monasfluore A)
H



Name	Shift	Class	J' s
1	A	(m)	0.85
2	B	(m)	1.27
3	C	(m)	1.54
4	D	(dt)	1.88
5	E	(dd)	2.54
6	F	(dd)	2.97
7	G	(dt)	3.28
8	H	(s)	3.94
9	I	(s)	4.87
10	J	(s)	5.40
11	K	(dd)	6.13
12	L	(s)	6.29
13	M	(dd)	6.59
14	N	(s)	7.50

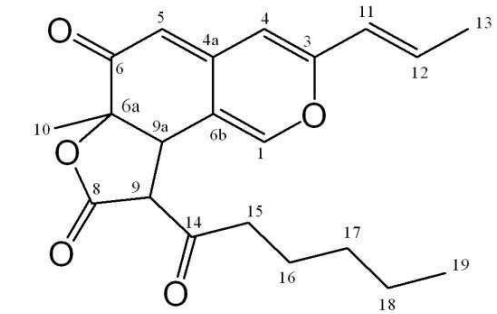
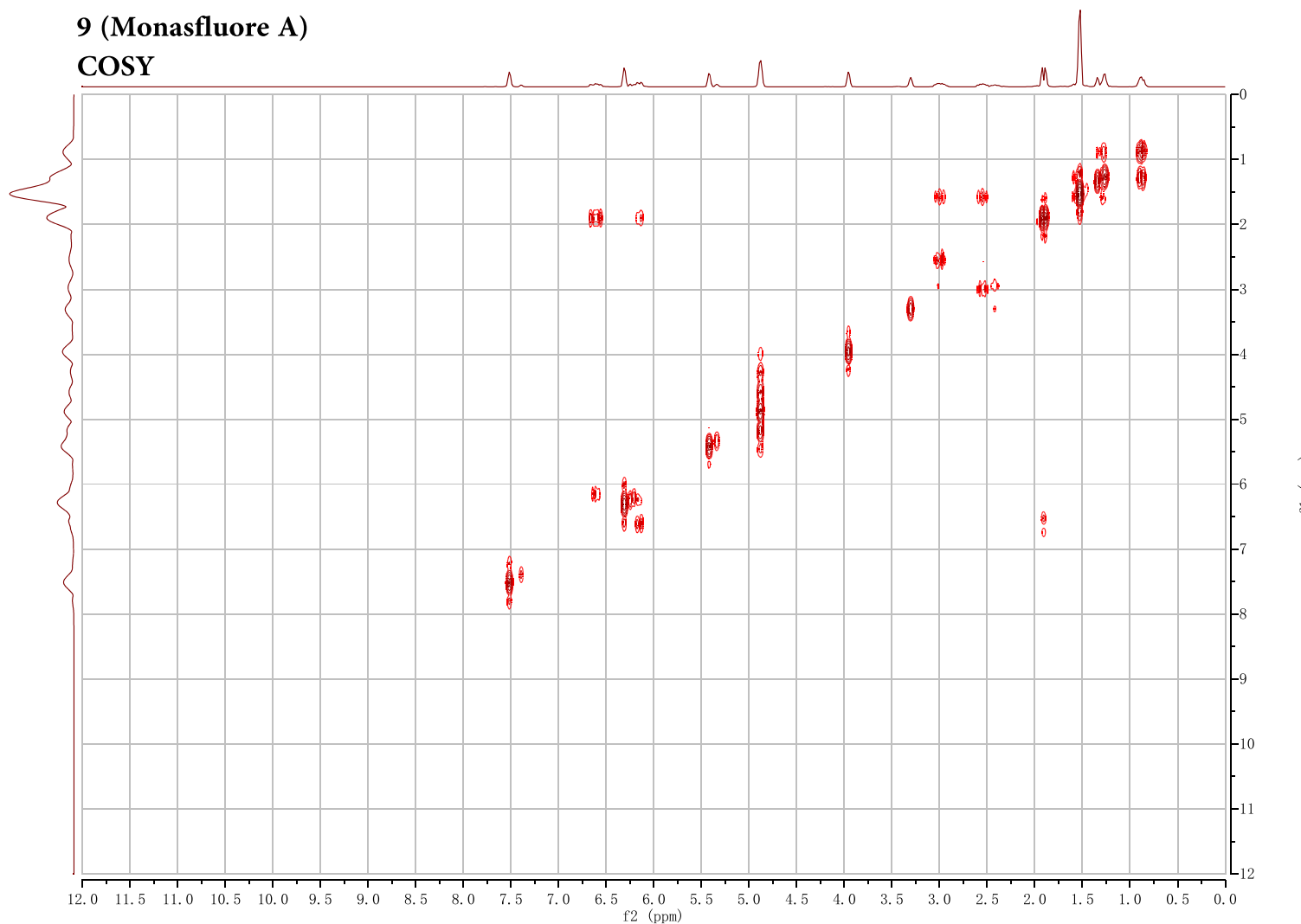
9 (Monasfluore A)

C



9 (Monasfluore A)

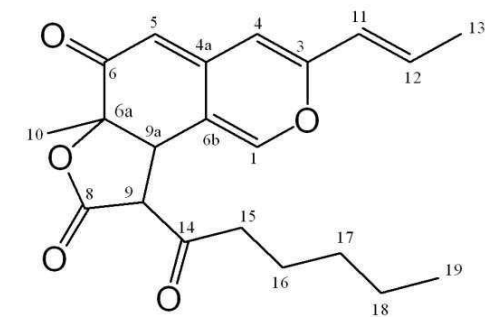
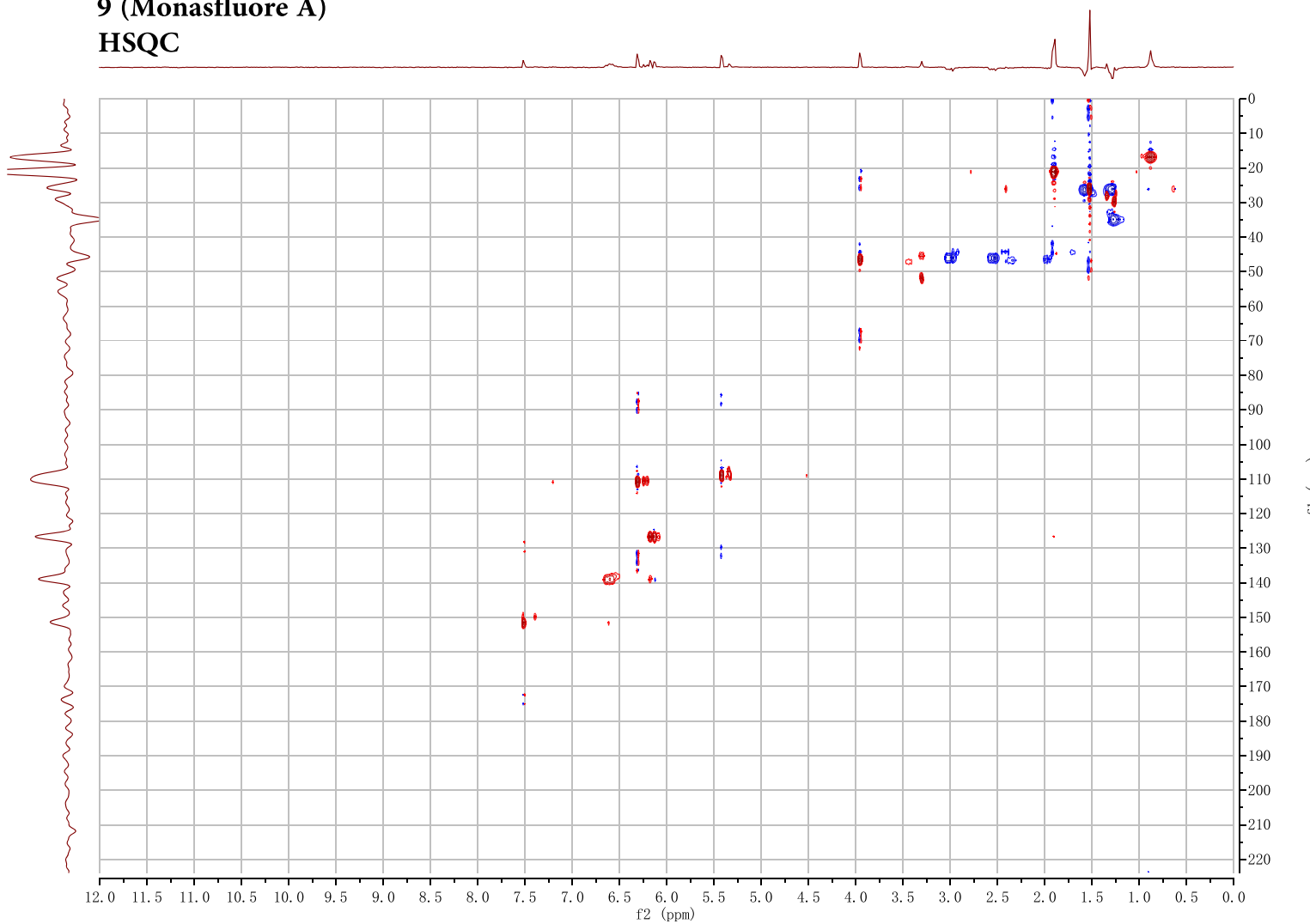
COSY



Chemical Formula: C₂₁H₂₄O₅
Molecular Weight: 356.42

9 (Monasfluore A)

HSQC

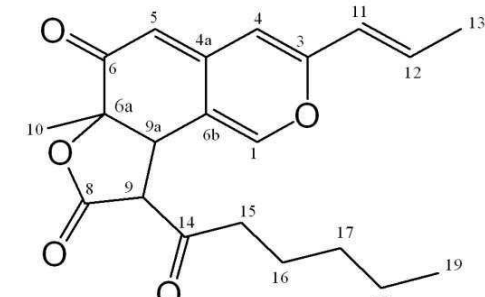
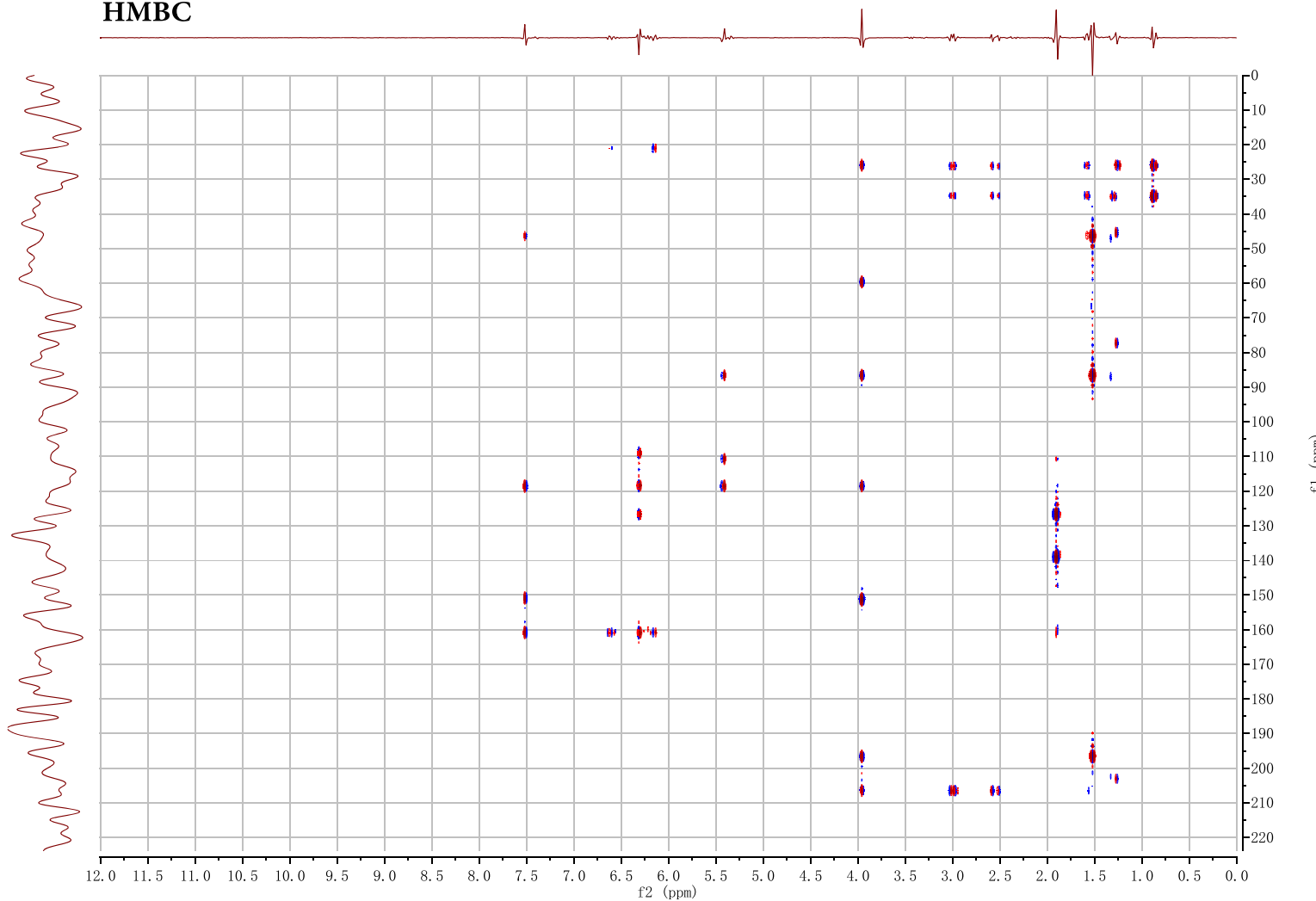


Chemical Formula: C₂₁H₂₄O₅

Molecular Weight: 356.42

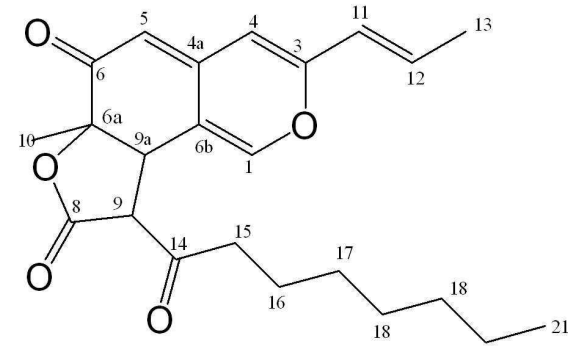
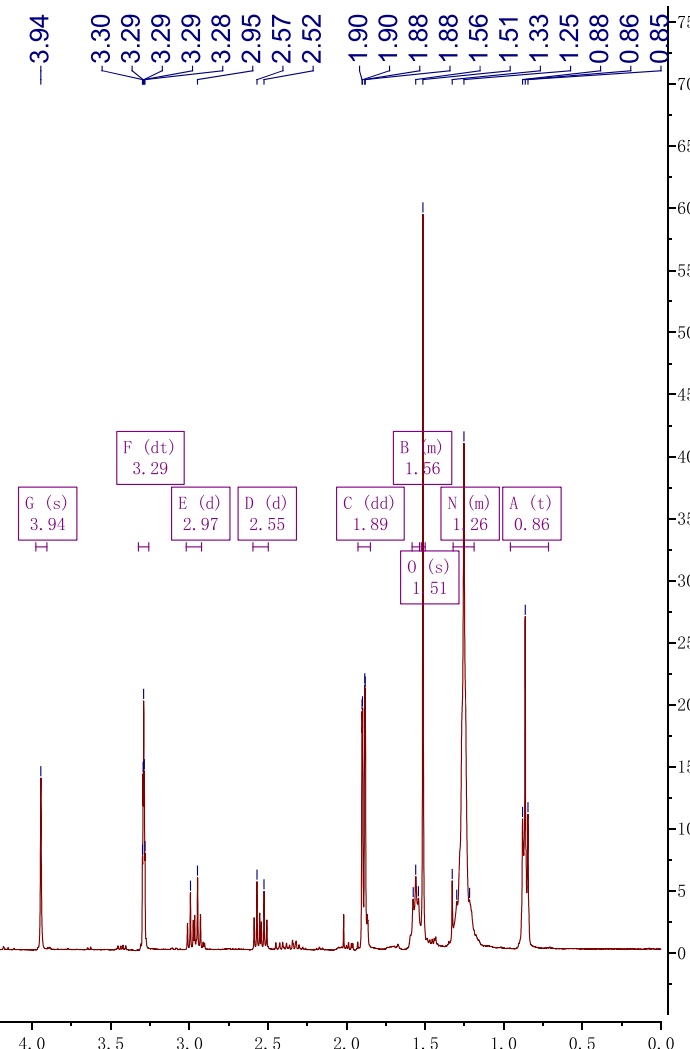
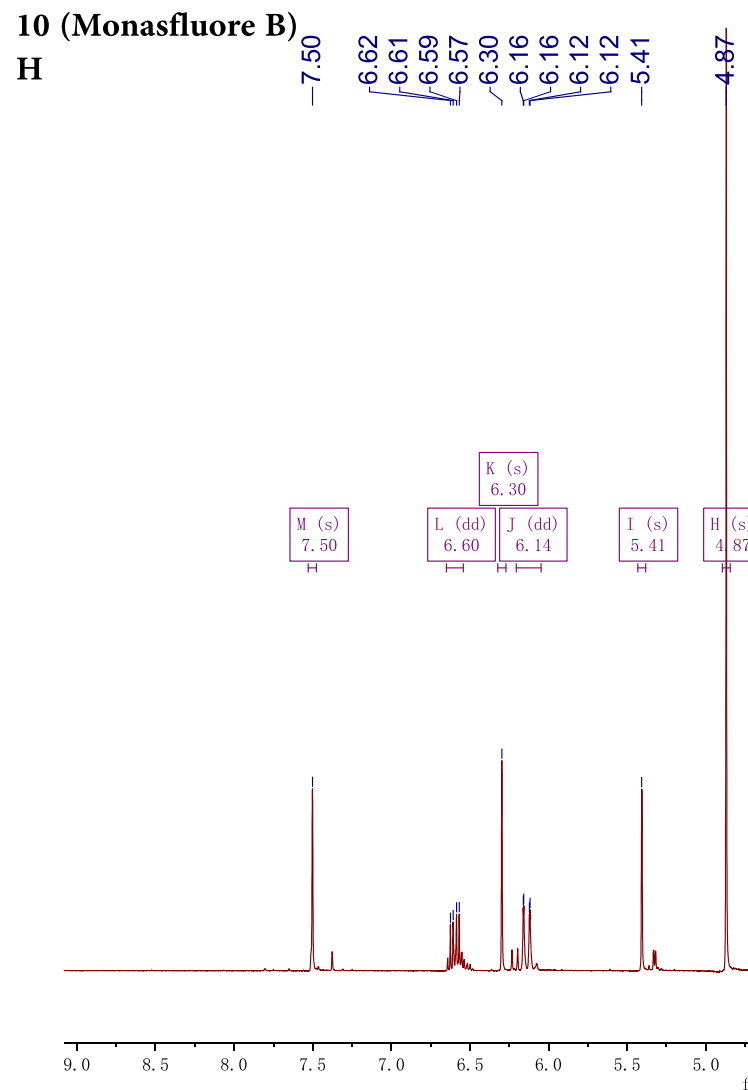
9 (Monasfluore A)

HMBC



Chemical Formula: C₂₁H₂₄O₅

Molecular Weight: 356.42

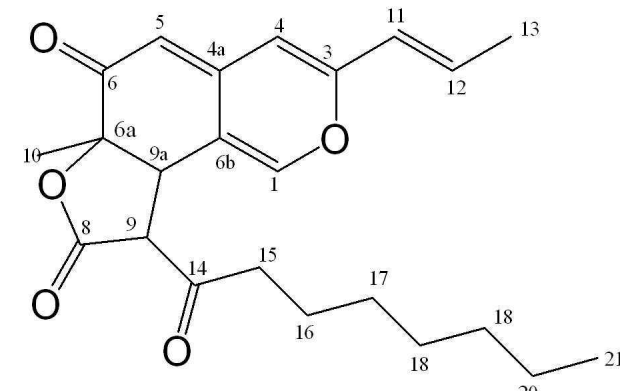
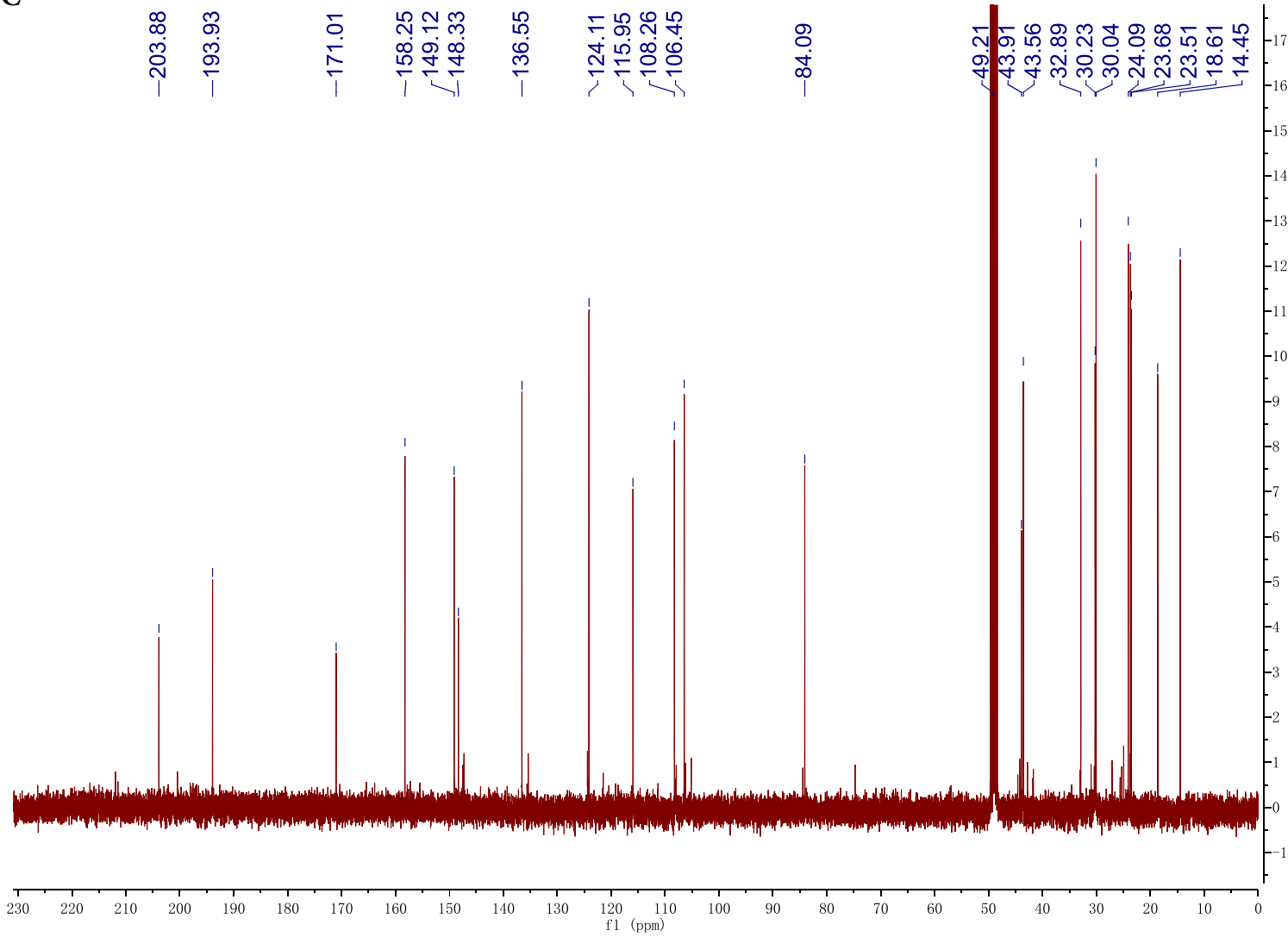


Chemical Formula: C₂₃H₂₈O₅
Molecular Weight: 384.47

Name	Shift	Class	J' s
1 A	0.86	t	6.8, 6.8
2 N	1.26	m	
3 O	1.51	s	
4 B	1.56	m	
5 C	1.89	dd	1.4, 6.9
6 D	2.55	d	18.2
7 E	2.97	d	18.2
8 F	3.29	dt	1.6, 1.6, 3.2
9 G	3.94	s	
10 H	4.87	s	
11 I	5.41	s	
12 J	6.14	dd	1.6, 15.6
13 K	6.30	s	
14 L	6.60	dd	6.9, 15.6
15 M	7.50	s	

10 (Monasfluore B)

C



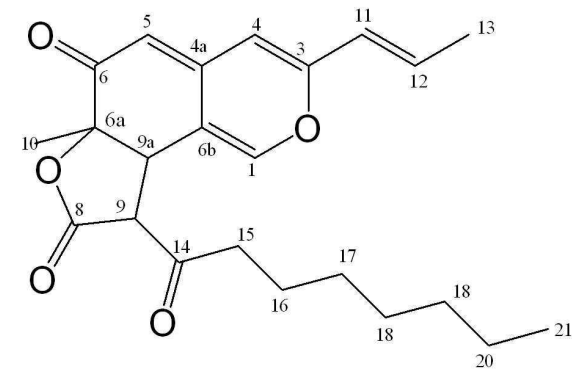
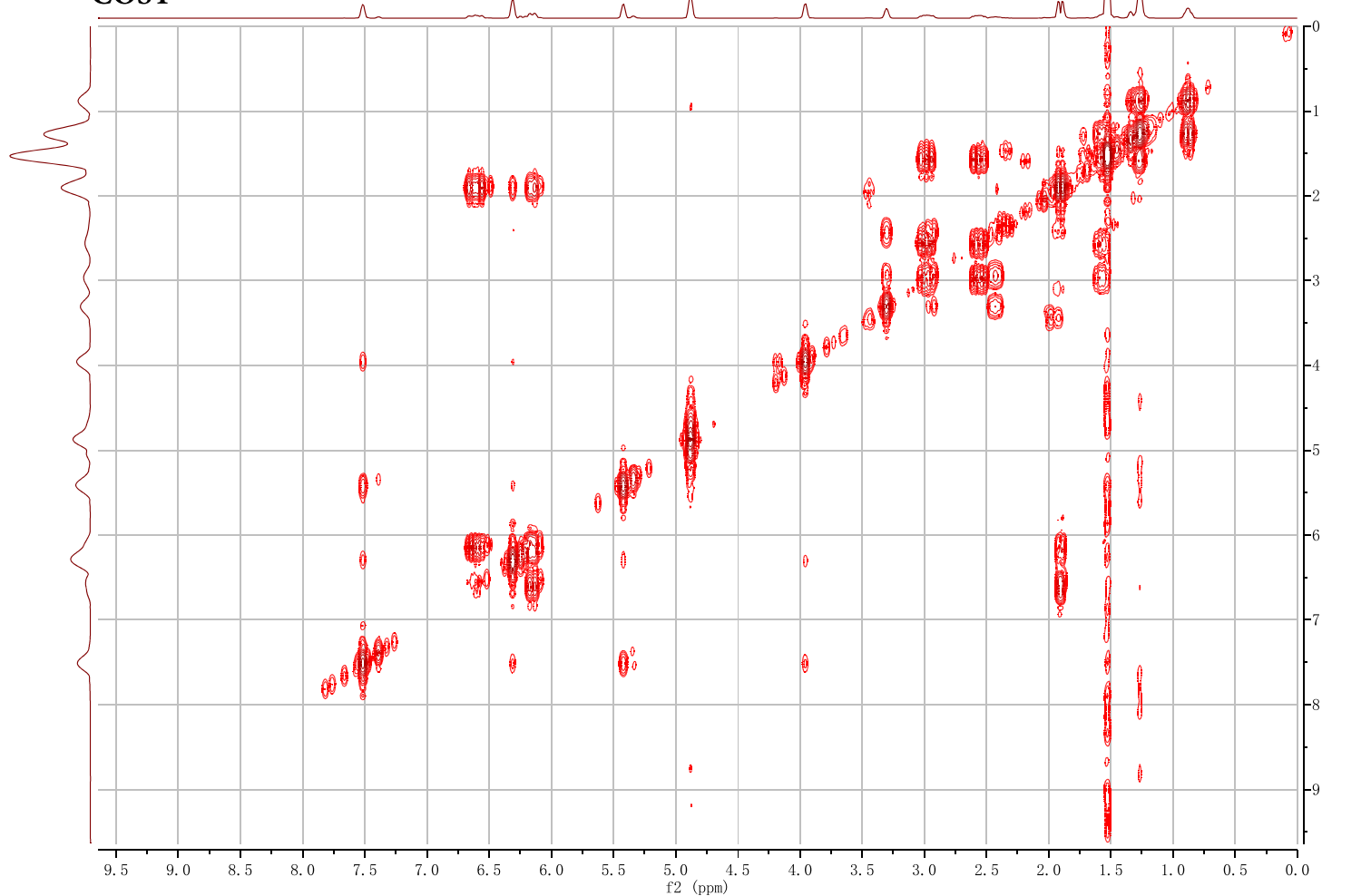
Chemical Formula: C₂₃H₂₈O₅

Molecular Weight: 384.47

	ppm
1	203.88
2	193.93
3	171.01
4	158.25
5	149.12
6	148.33
7	136.55
8	124.11
9	115.95
10	108.26
11	106.45
12	84.09
13	49.21
14	43.91
15	43.56
16	32.89
17	30.23
18	30.04
19	24.09
20	23.68
21	23.51
22	18.61
23	14.45

10 (Monasfluore B)

COSY

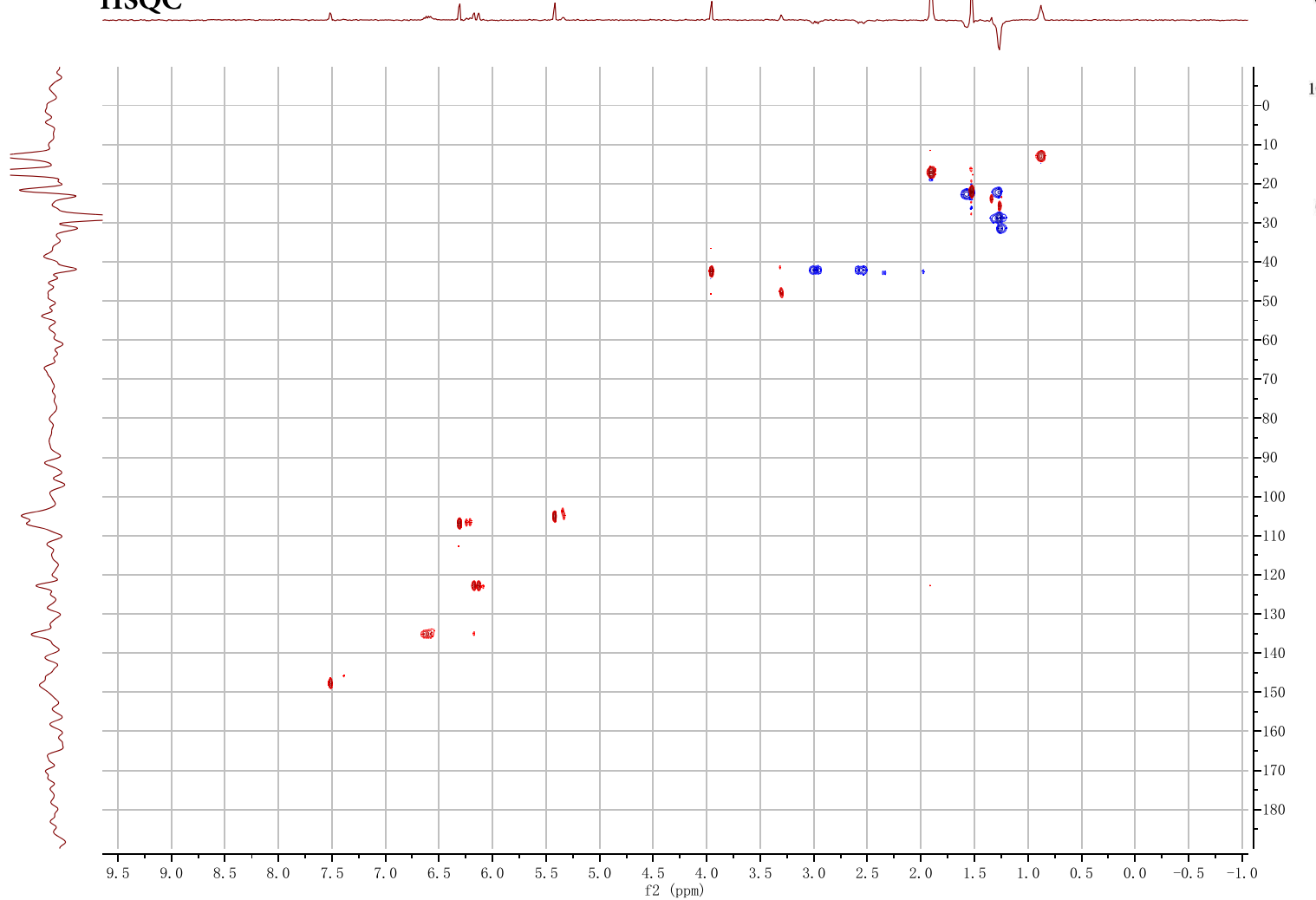


Chemical Formula: C₂₃H₂₈O₅

Molecular Weight: 384.47

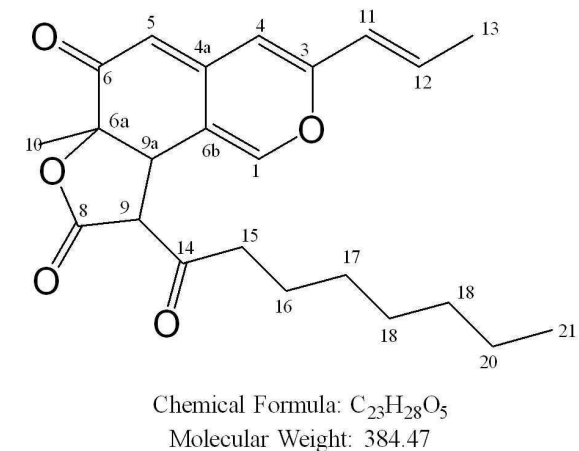
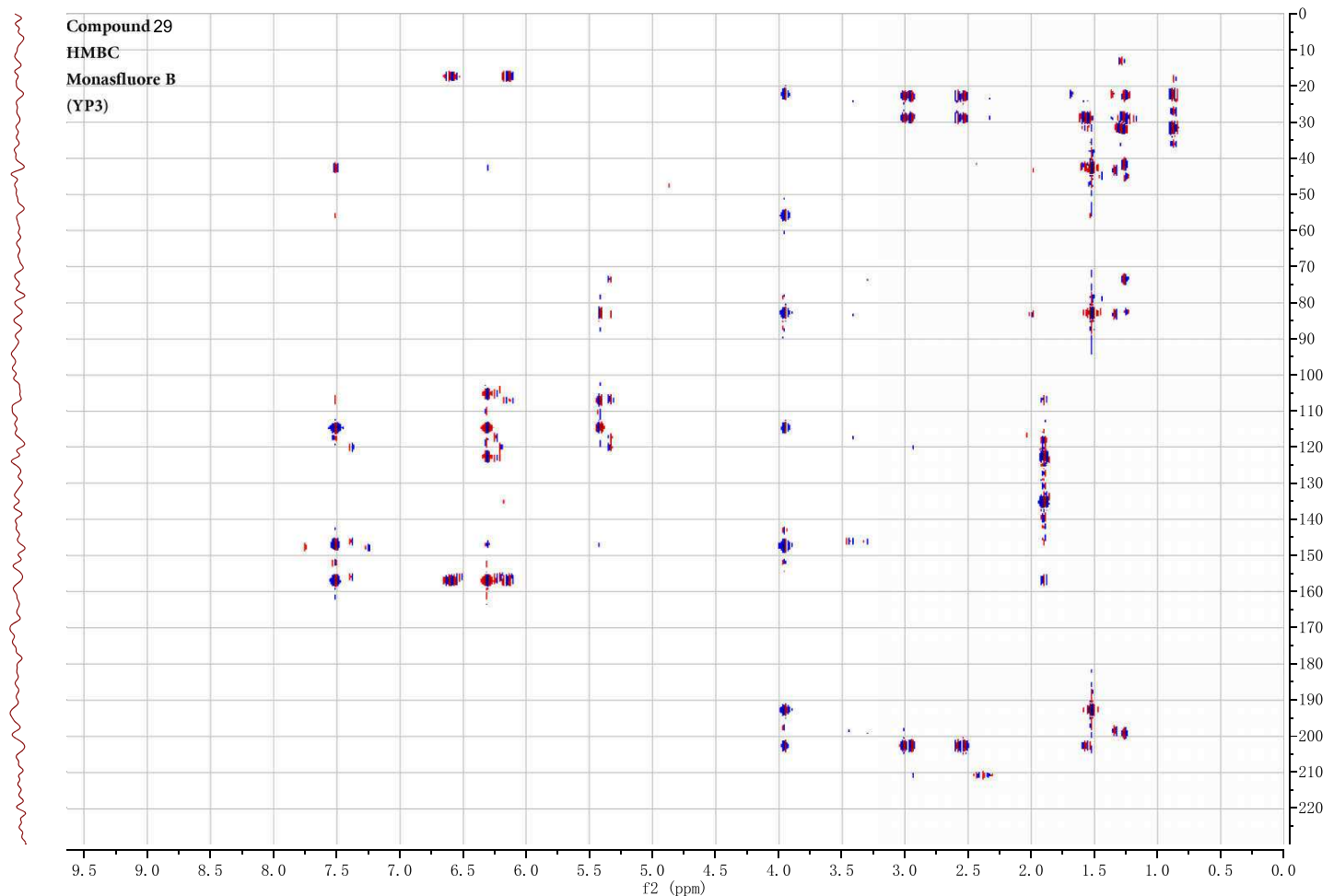
10 (Monasfluore B)

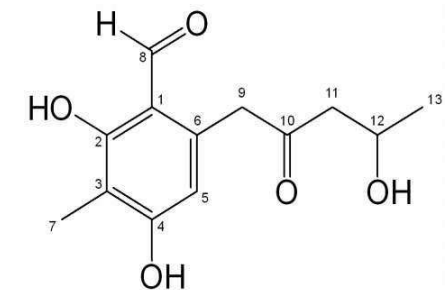
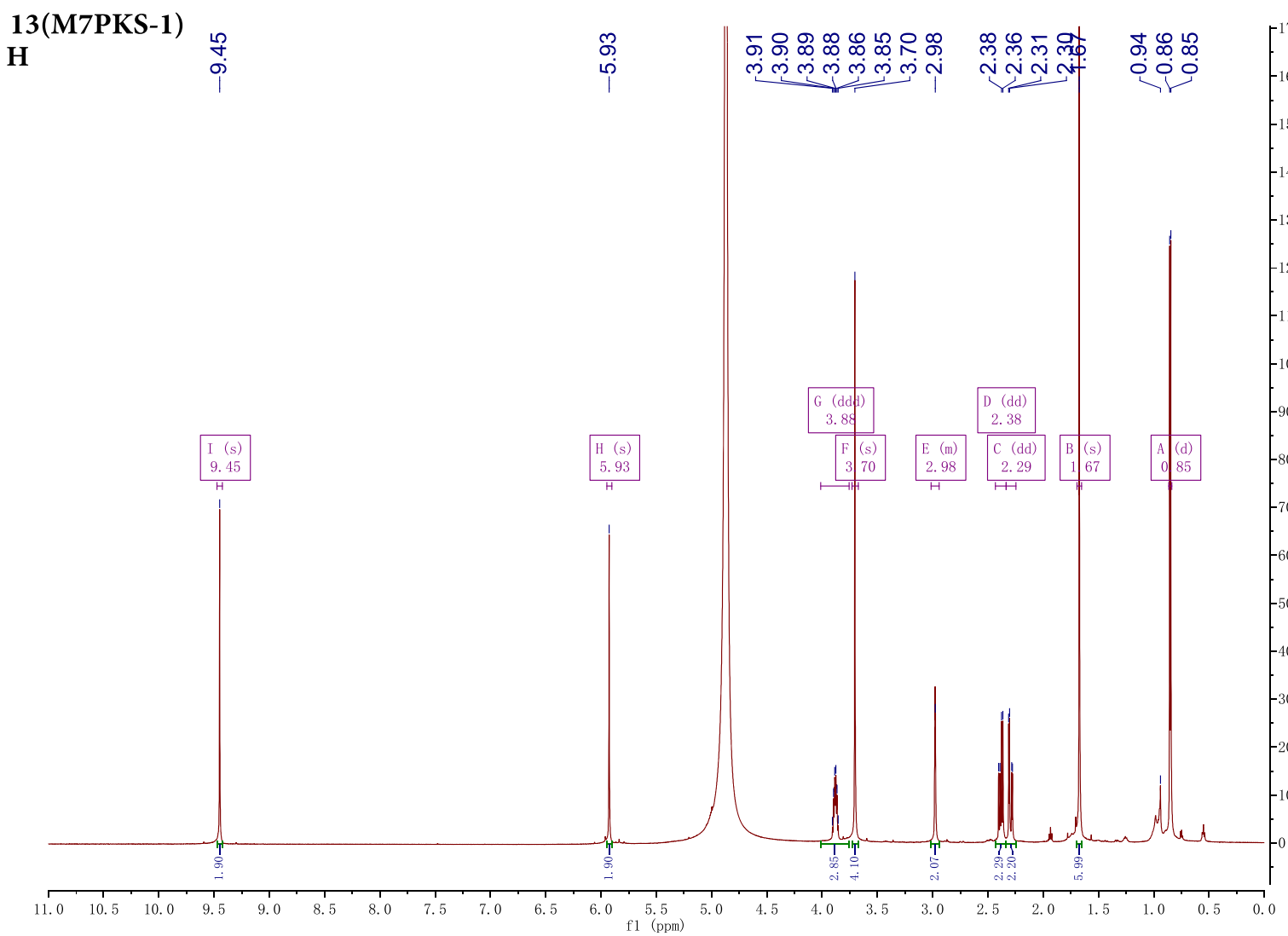
HSQC



10 (Monasfluore B)

HMBC



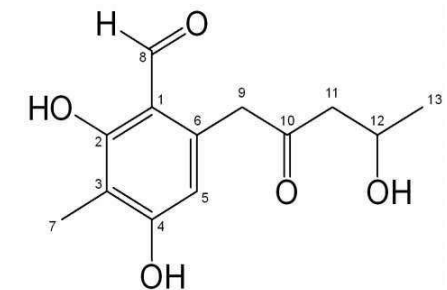
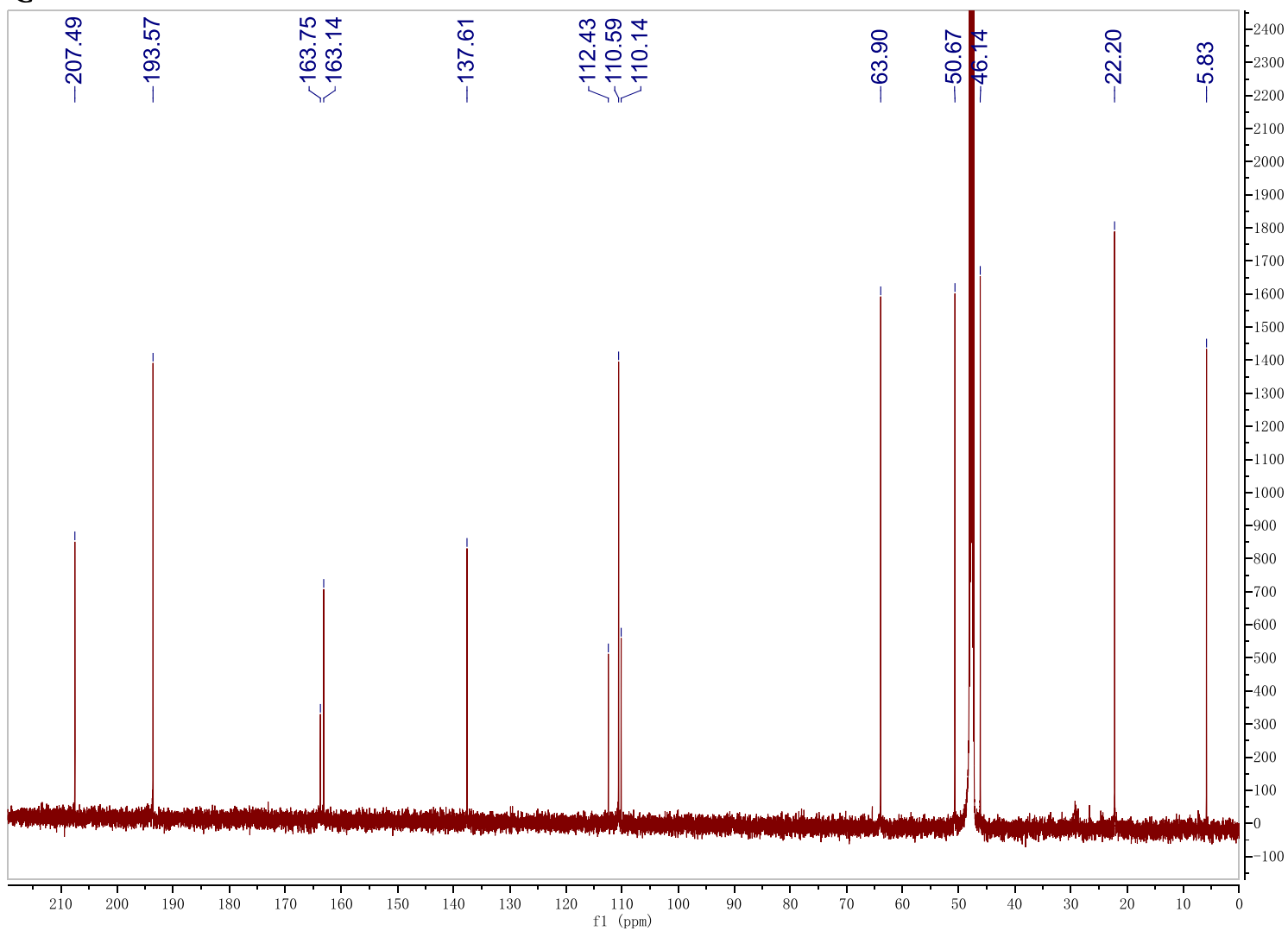


Chemical Formula: C₁₃H₁₆O₅
Molecular Weight: 252.27

Name	Shift	Class	J'	s
1 I (s)	9.45	s		
2 H (s)	5.93	s		
3 G (ddd)	3.88	ddd	4.8,	6.3,
4 F (s)	3.70	s	7.9	
5 E (m)	2.98	m		
6 D (dd)	2.38	dd	8.0,	15.9
7 C (dd)	2.29	dd	4.6,	15.9
8 B (s)	1.67	s		
9 A (d)	0.85	d	6.3	

13 (M7PKS-1)

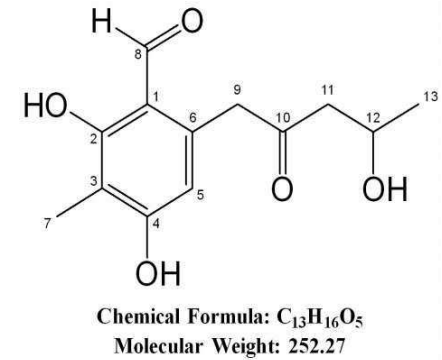
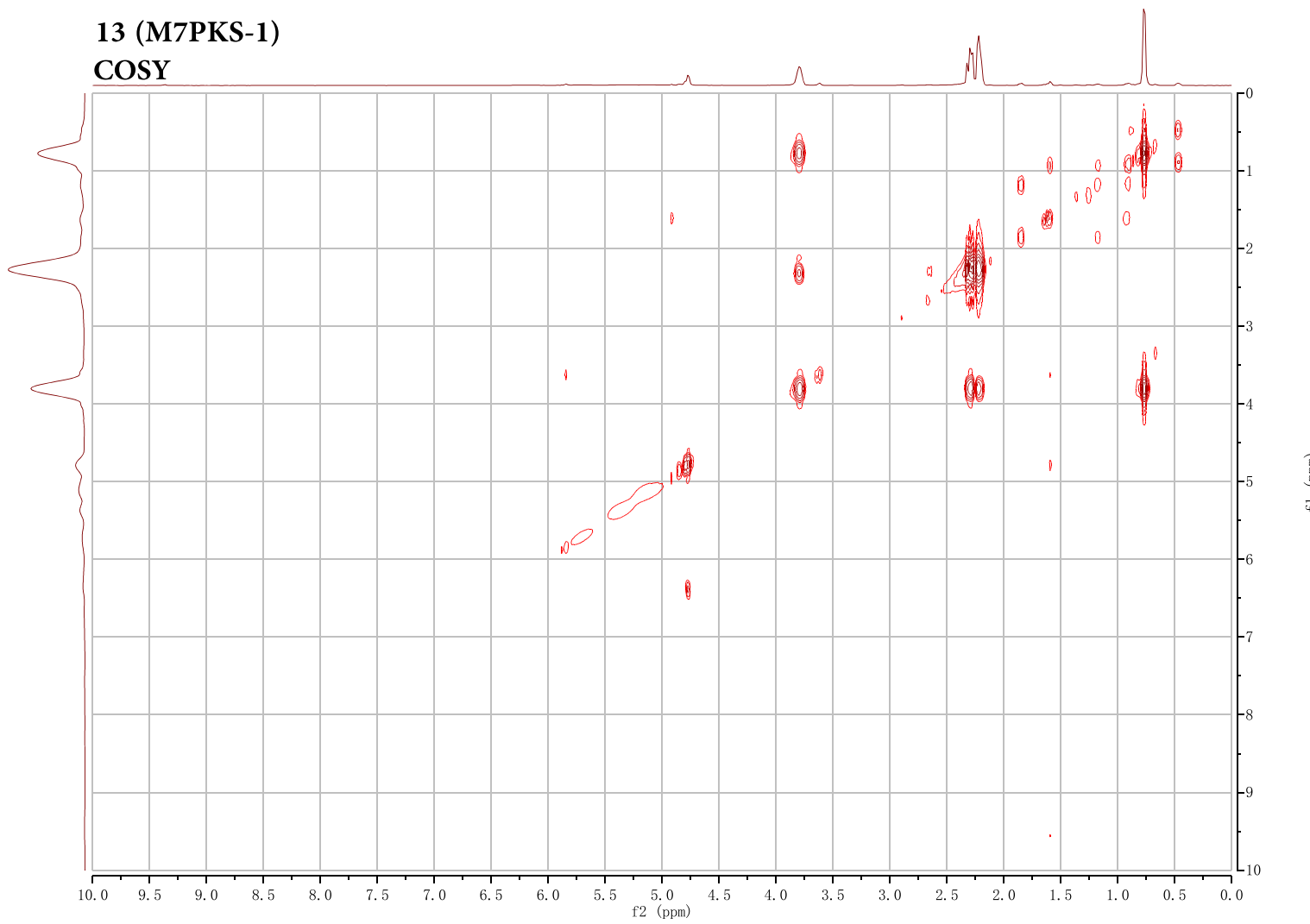
C



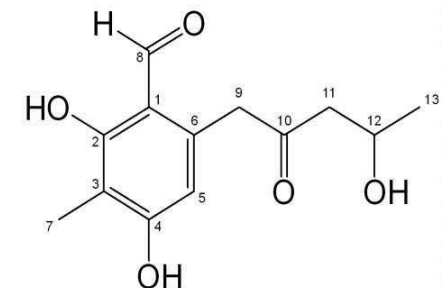
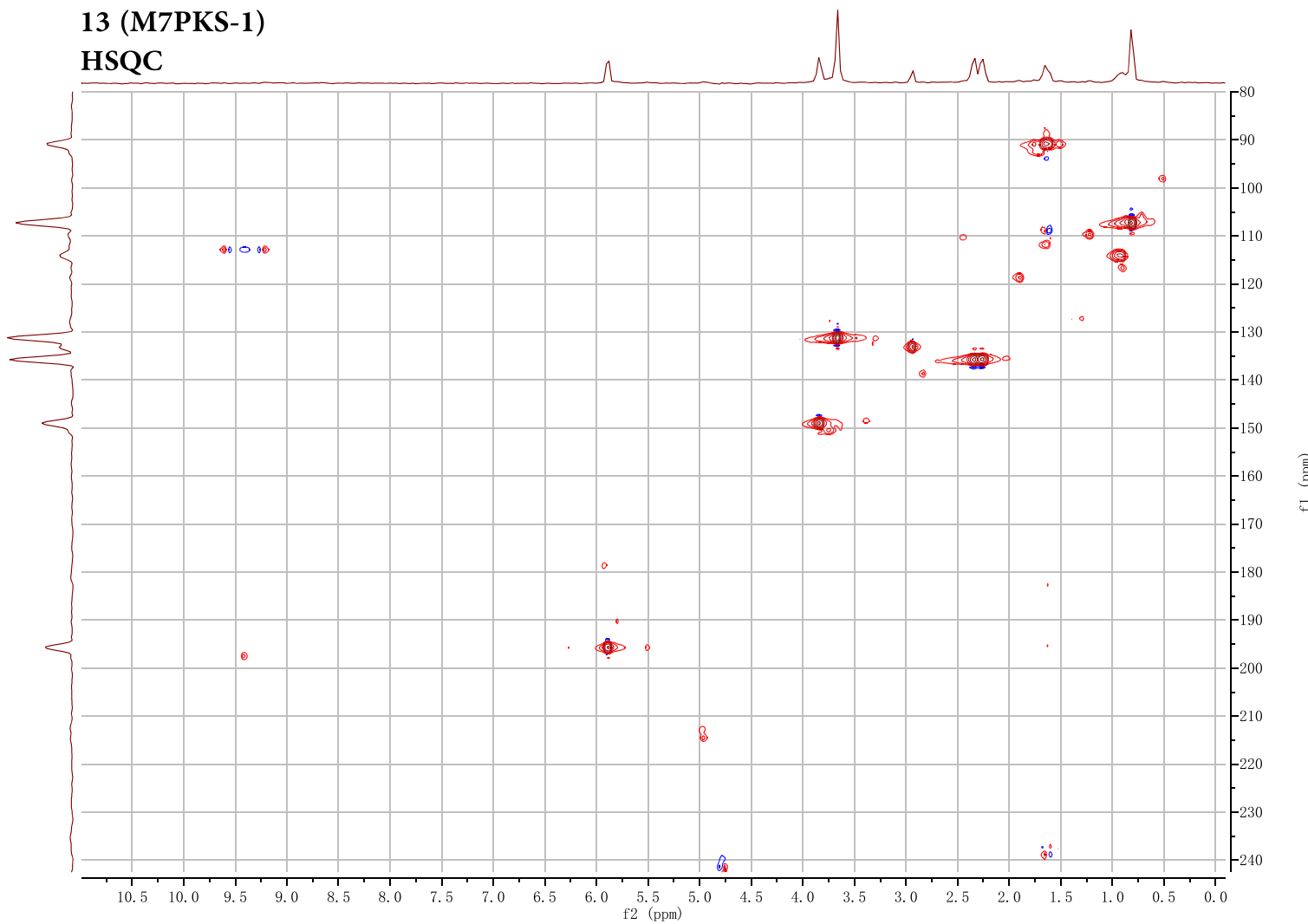
	ppm
1	207.49
2	193.57
3	163.75
4	163.14
5	137.61
6	112.43
7	110.59
8	110.14
9	63.90
10	50.67
11	46.14
12	22.20
13	5.83

13 (M7PKS-1)

COSY



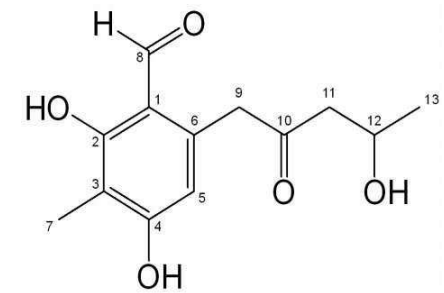
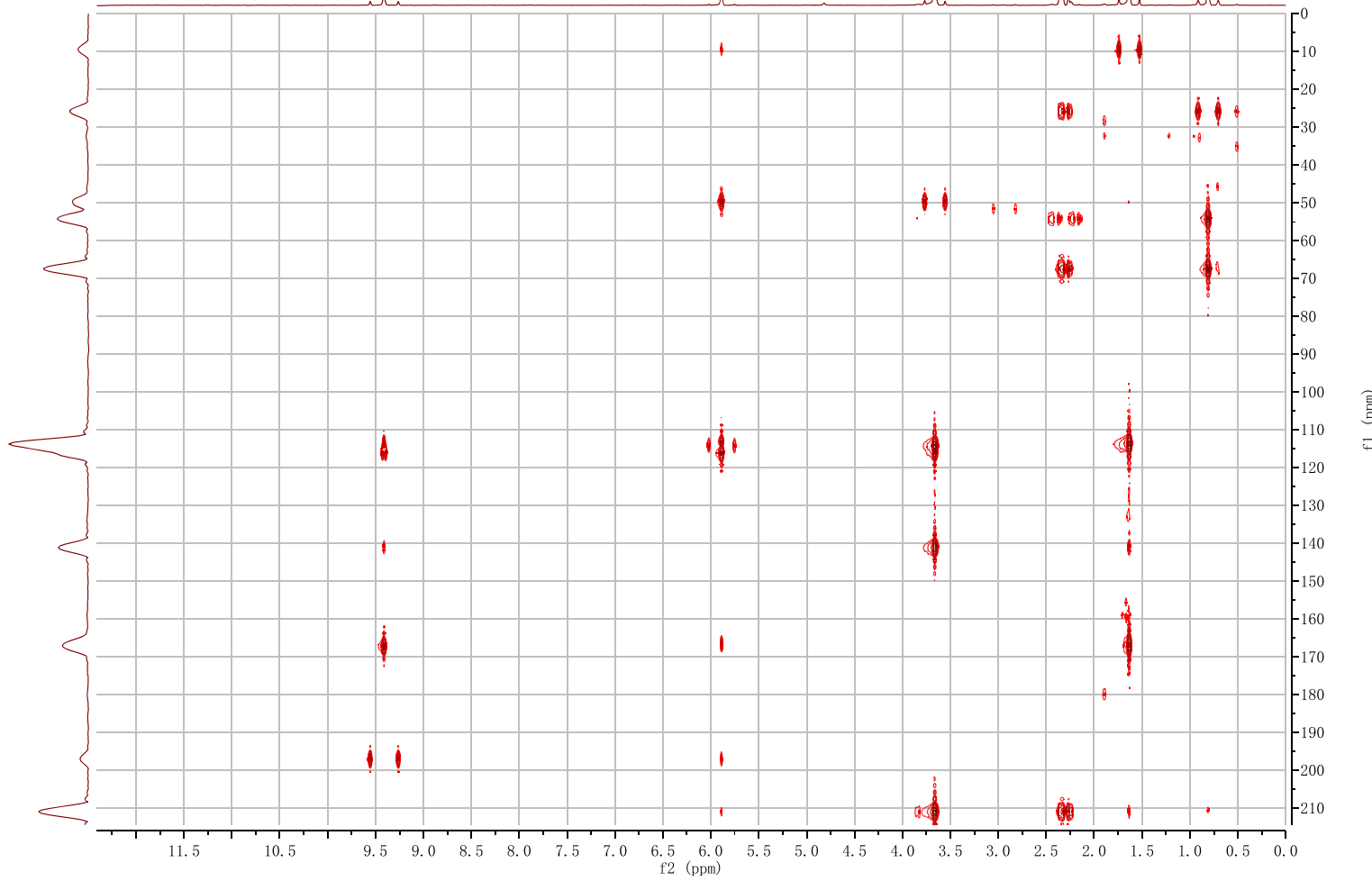
Chemical Formula: C₁₃H₁₆O₅
Molecular Weight: 252.27



Chemical Formula: $\text{C}_{13}\text{H}_{16}\text{O}_5$
Molecular Weight: 252.27

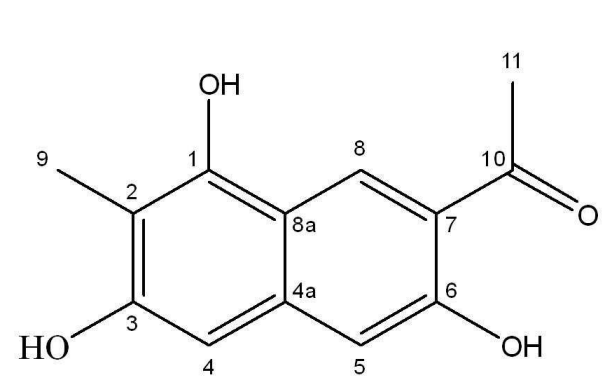
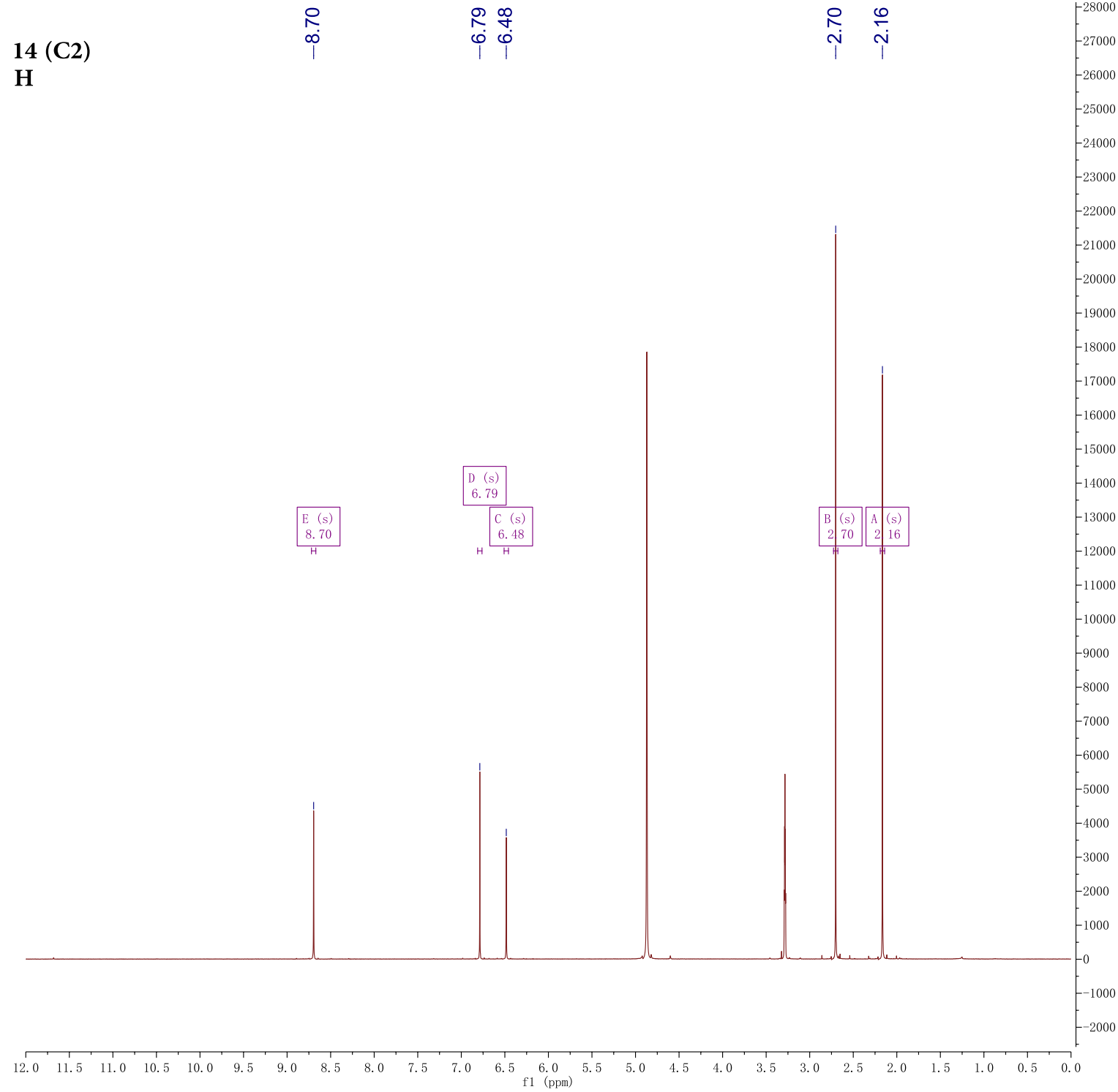
13 (M7PKS-1)

HMBC



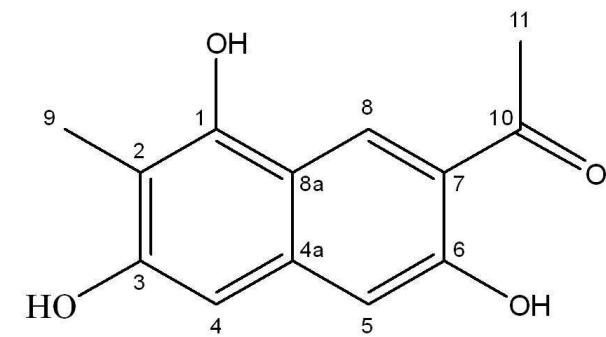
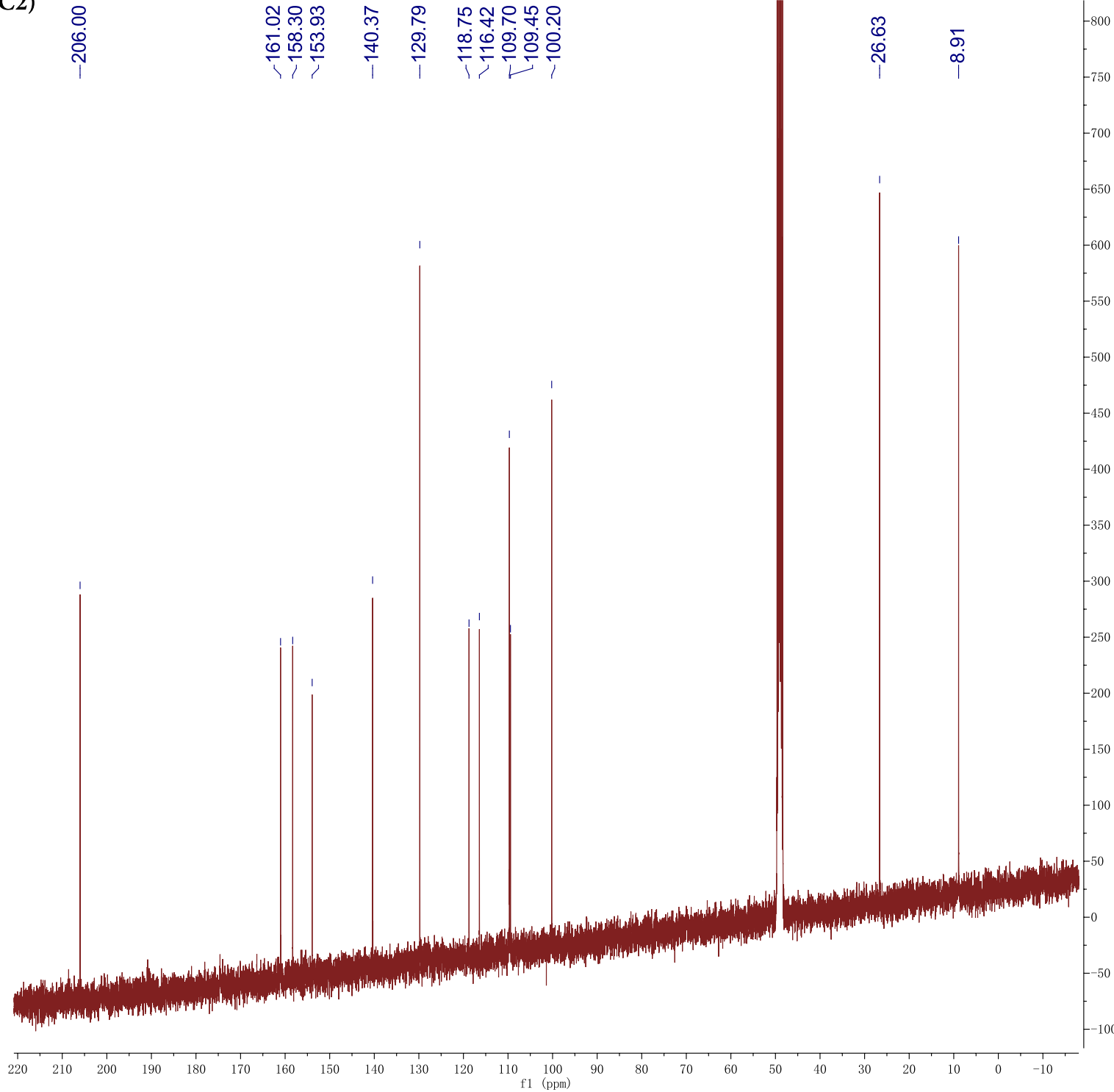
Chemical Formula: C₁₃H₁₆O₅
Molecular Weight: 252.27

14 (C2)
H



Name	Shift	J'	s
1 A	(s)	2.16	
2 B	(s)	2.70	
3 C	(s)	6.48	
4 D	(s)	6.79	
5 E	(s)	8.70	

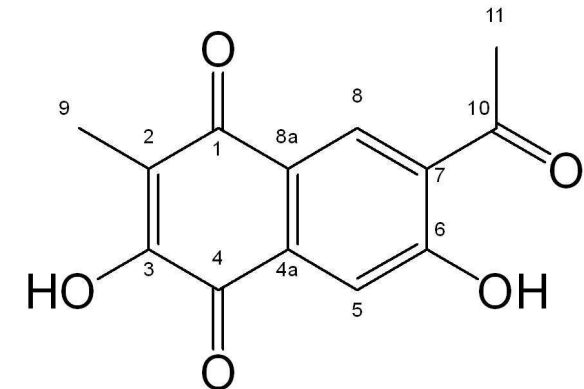
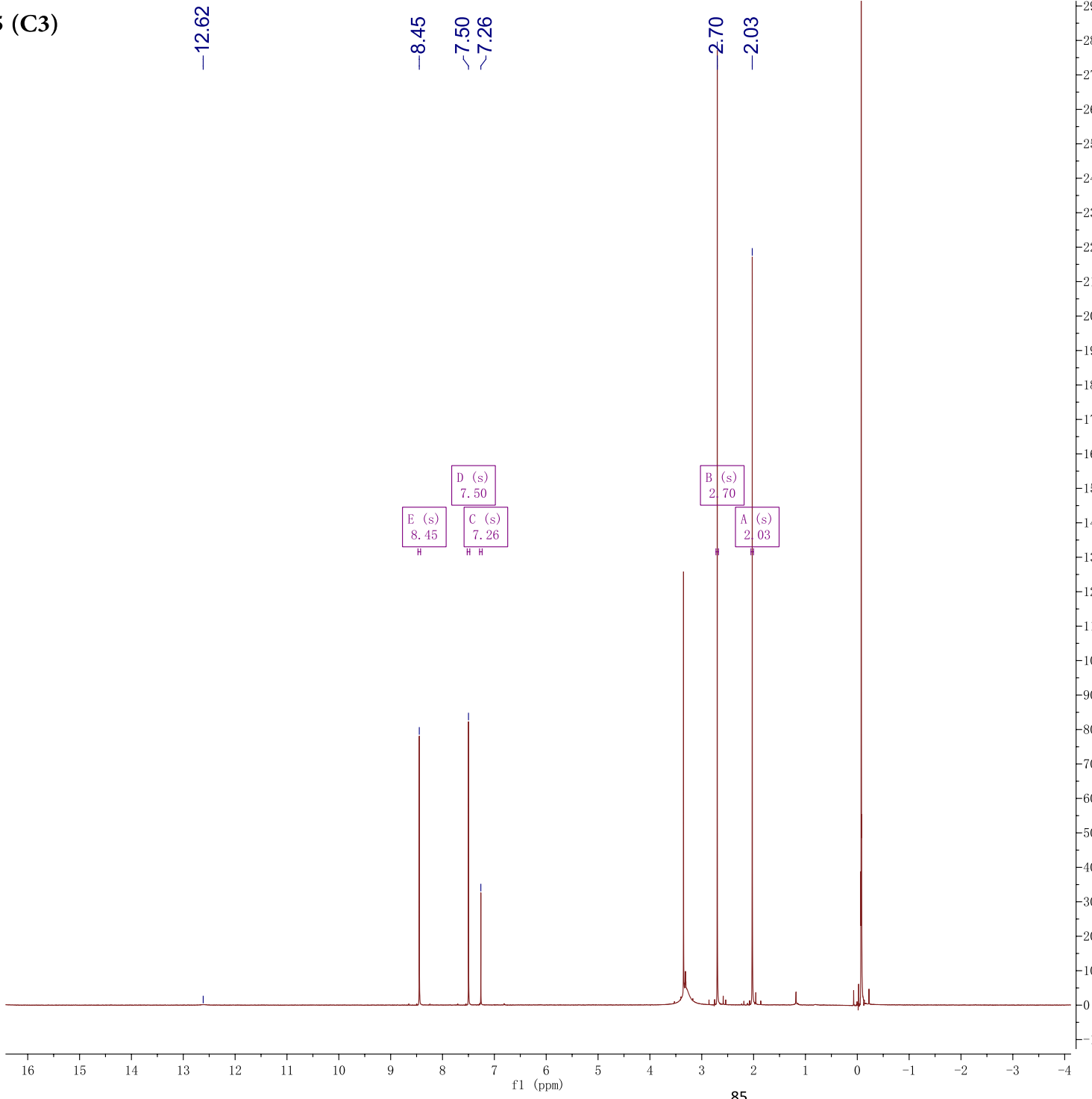
14 (C2)
C



Chemical Formula: C₁₃H₁₂O₄
Molecular Weight: 232.24

	ppm
1	206.00
2	161.02
3	158.30
4	153.93
5	140.37
6	129.79
7	118.75
8	116.42
9	109.70
10	109.45
11	100.20
12	26.63
13	8.91

15 (C3)
H



Chemical Formula: C₁₃H₁₀O₅
Molecular Weight: 246.22

Name	Shift	Class	J's
1 A	(s)	2.03	s
2 B	(s)	2.70	s
3 C	(s)	7.26	s
4 D	(s)	7.50	s
5 E	(s)	8.45	s

15 (C3)
C

-204.94

-183.94
-180.19

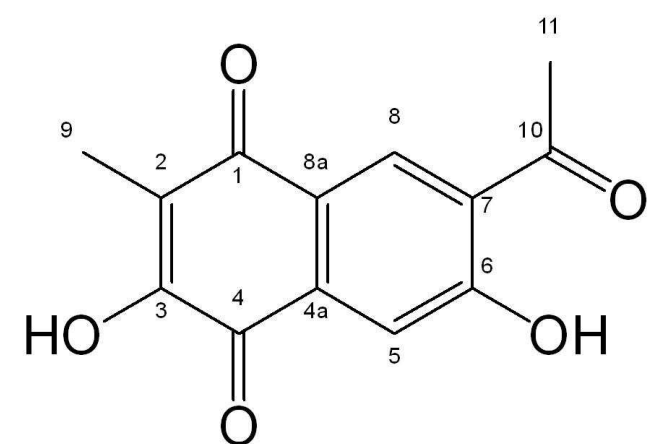
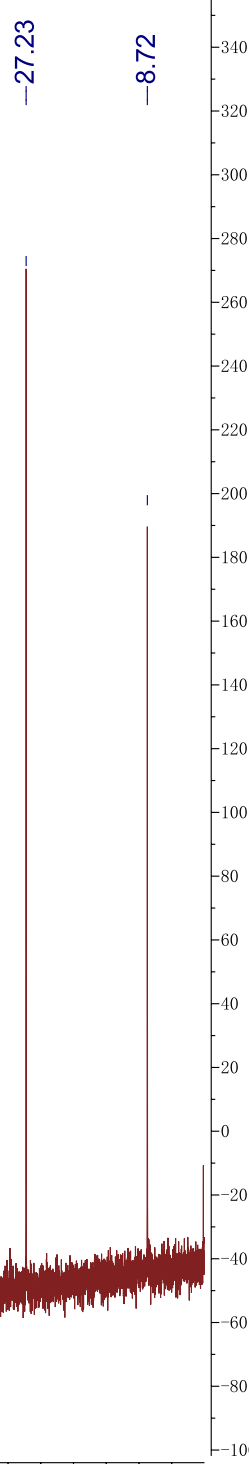
-165.37

-154.85

✓135.32
✓130.41
✓123.95
✓122.34
✓122.26
✓116.14

210 200 190 180 170 160 150 140 130 120 110 100 90 80 70 60 50 40 30 20 10 1 210 200 190 180 170 160 150 140 130 120 110 100 90 80 70 60 50 40 30 20 10 f1 (ppm)

86

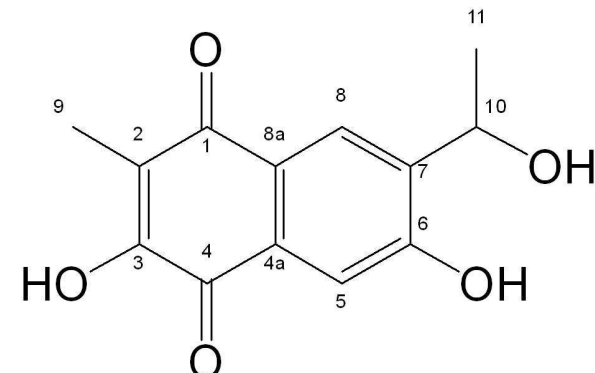
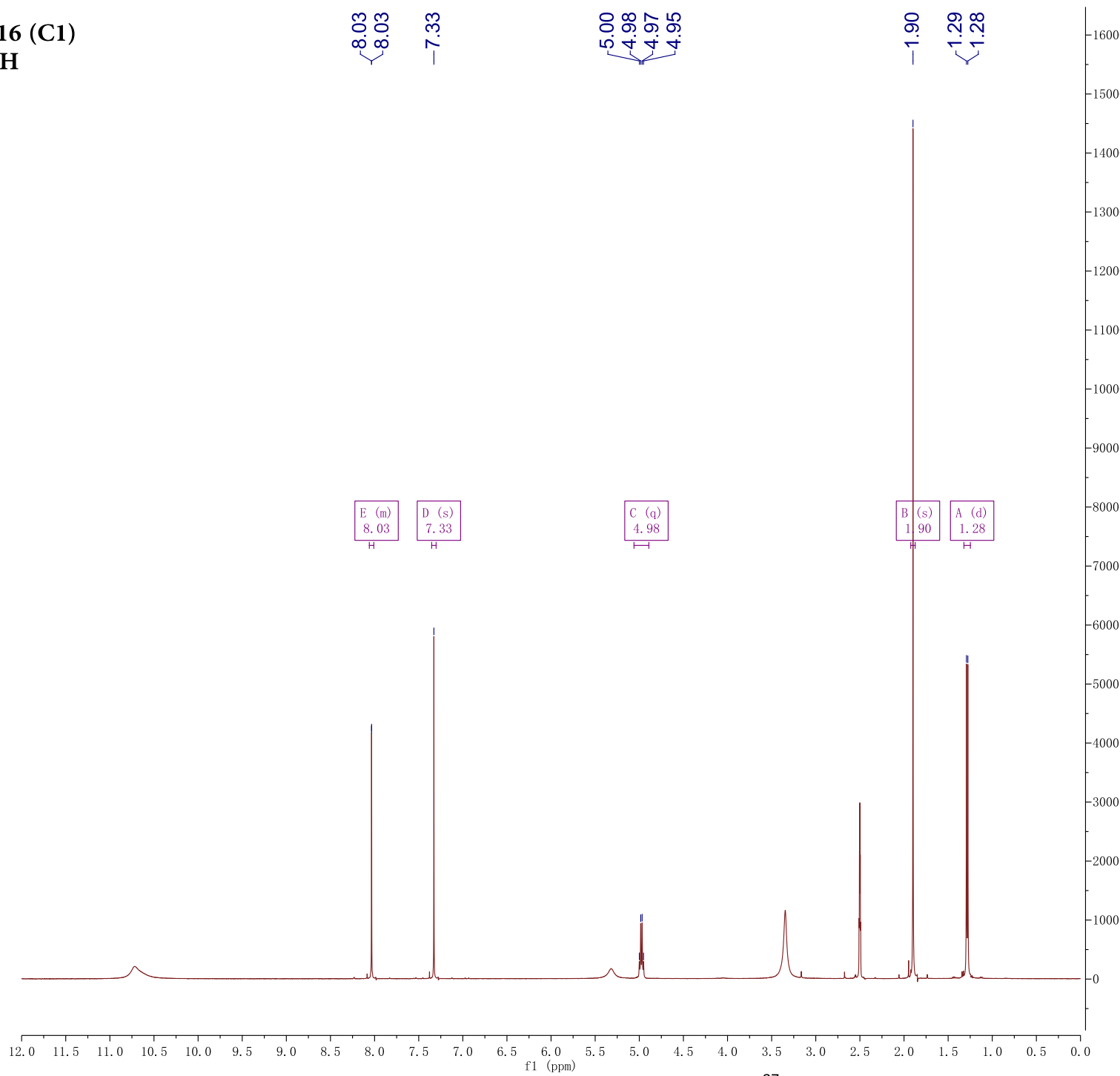


Chemical Formula: C₁₃H₁₀O₅

Molecular Weight: 246.22

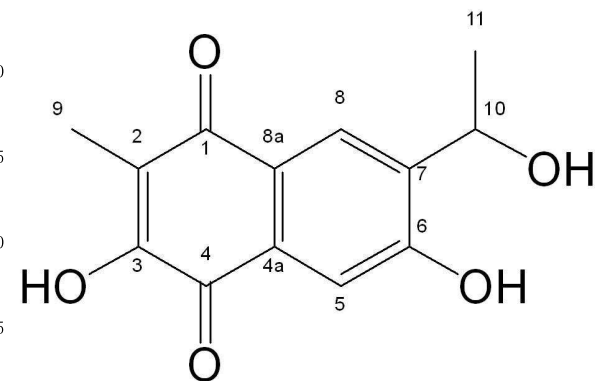
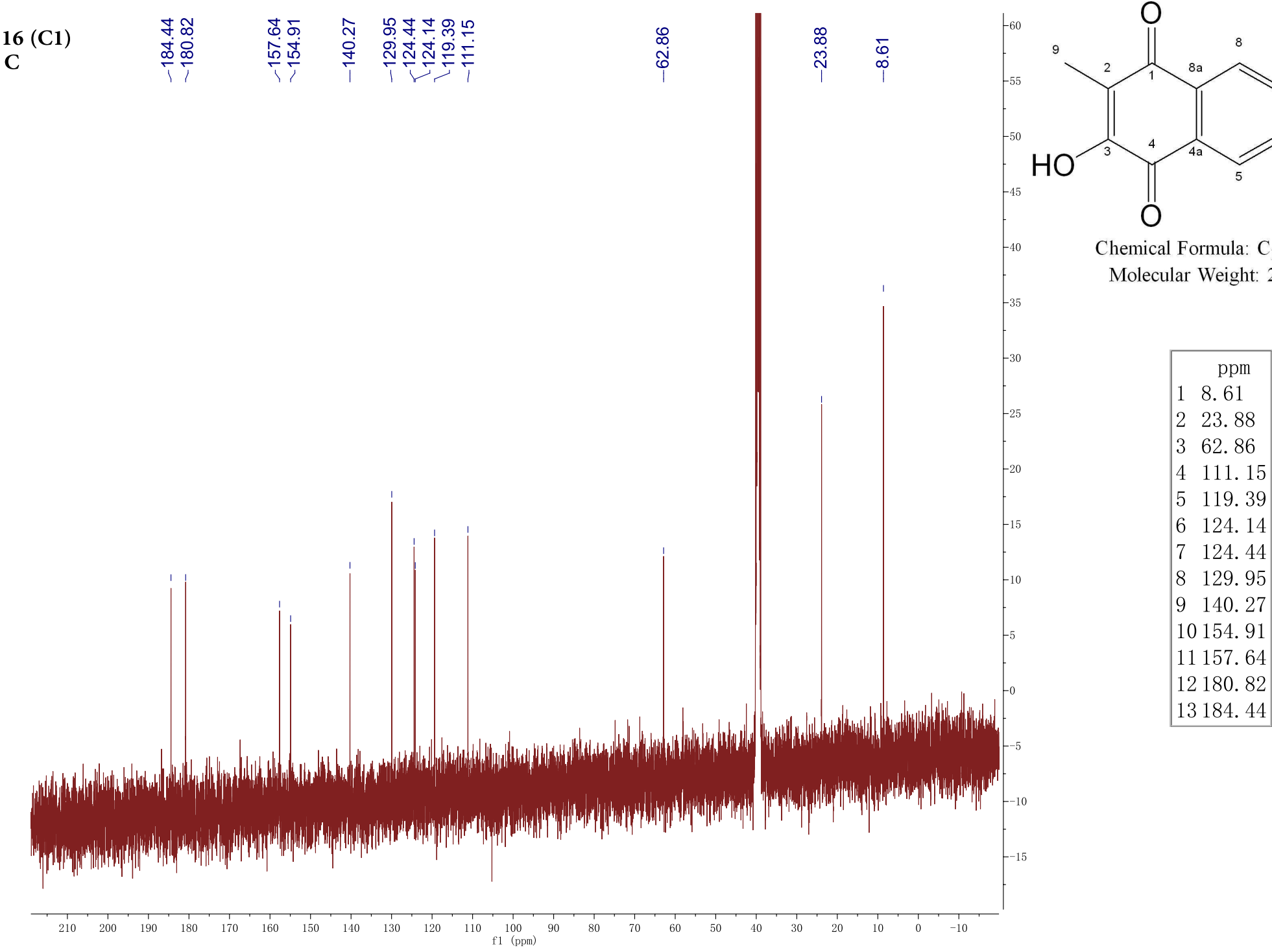
ppm
1 8.72
2 27.23
3 116.14
4 122.26
5 122.34
6 123.95
7 130.41
8 135.32
9 154.85
10 165.37
11 180.19
12 183.94
13 204.94

**16 (C1)
H**



Chemical Formula: C₁₃H₁₂O₅
Molecular Weight: 248.23

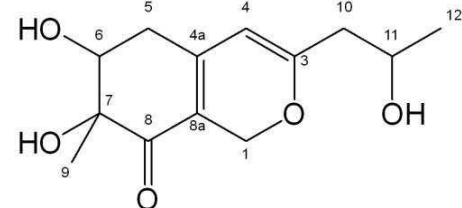
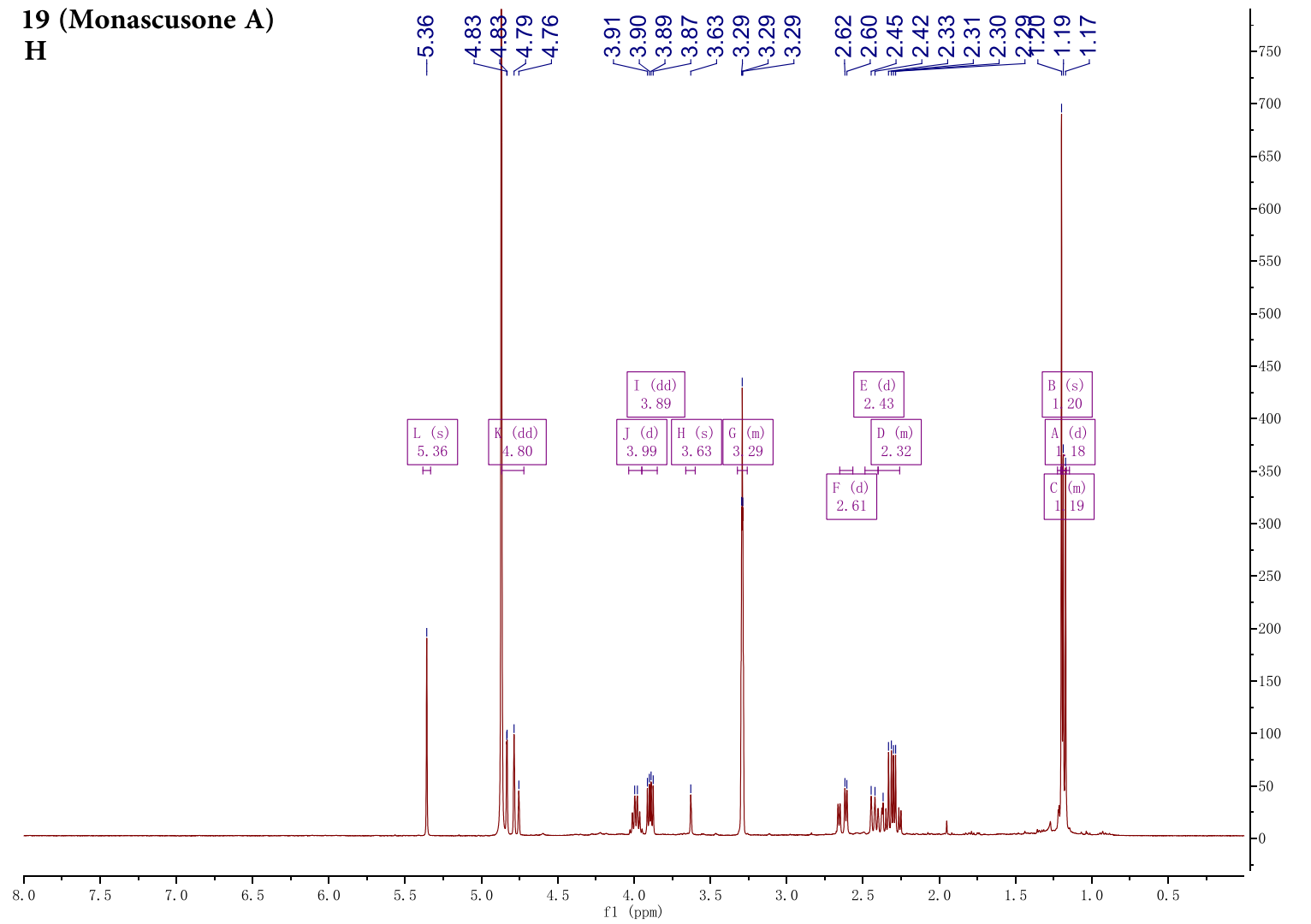
Name	Shift	J'	s
1A	(d)	1.28	6.39
2B	(s)	1.90	
3C	(q)	4.98	6.31, 6.31, 6.31
4D	(s)	7.33	
5E	(m)	8.03	



Chemical Formula: $C_{13}H_{12}O_5$
Molecular Weight: 248.23

	ppm
1	8.61
2	23.88
3	62.86
4	111.15
5	119.39
6	124.14
7	124.44
8	129.95
9	140.27
10	154.91
11	157.64
12	180.82
13	184.44

19 (Monascusone A) H

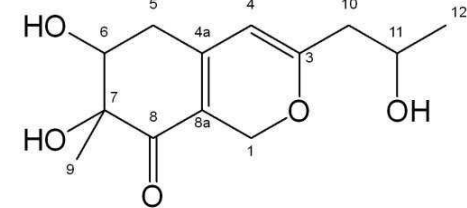
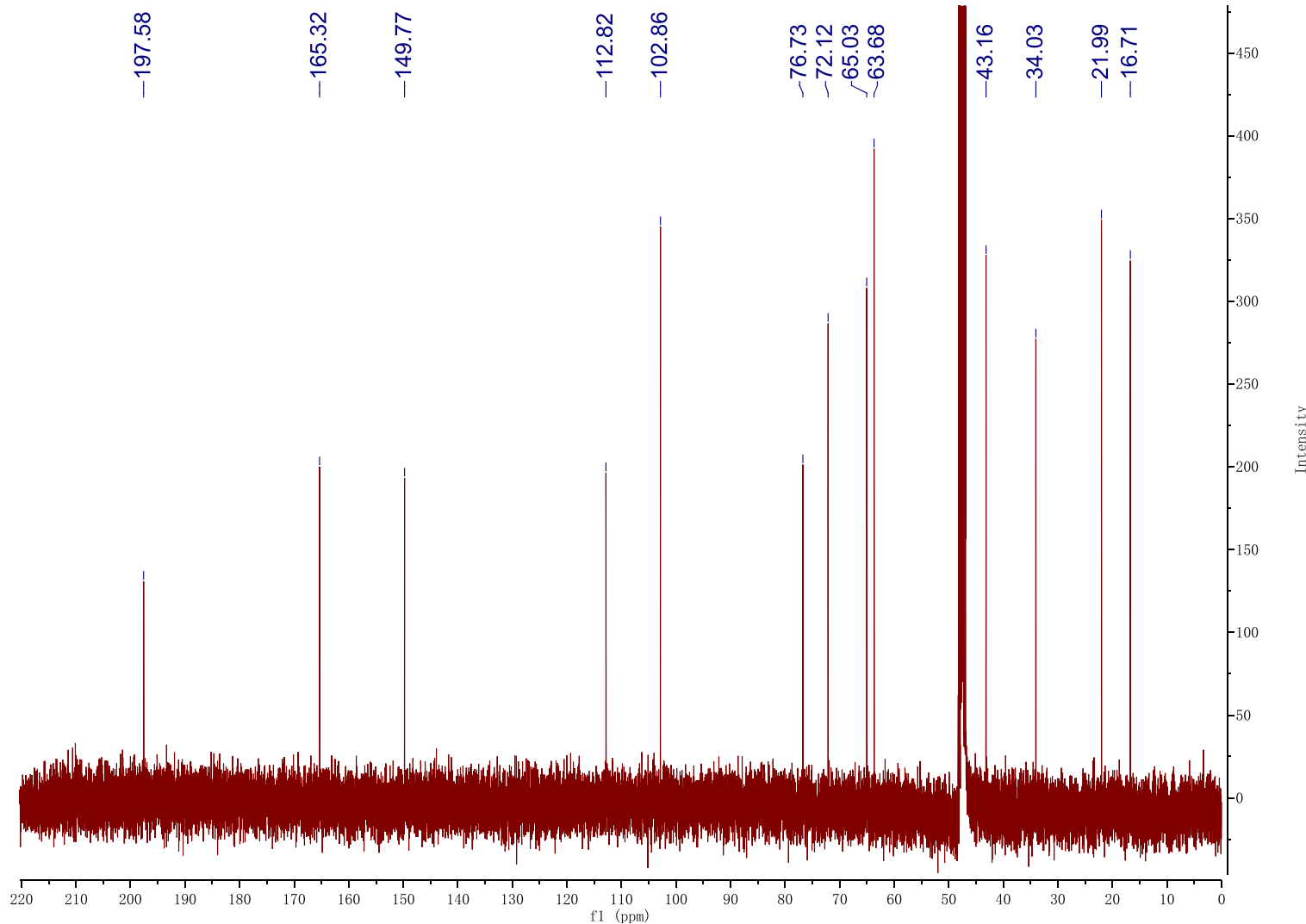


Chemical Formula: C₁₃H₁₈O₅
Molecular Weight: 254.28

	Name	Shift	Class	J'	s
1	A (d)	1. 18	d	6. 2	
2	C (m)	1. 19	m		
3	B (s)	1. 20	s		
4	D (m)	2. 32	m		
5	E (d)	2. 43	d	9. 8	
6	F (d)	2. 61	d		5. 3
7	G (m)	3. 29	m		
8	H (s)	3. 63	s		
9	I (dd)	3. 89	dd	5. 4,	9. 8
10	J (d)	3. 99	d	6. 8	
11	K (dd)	4. 80	dd	6. 8,	25. 0
12	L (s)	5. 36	s		

19 (Monascusone A)

C

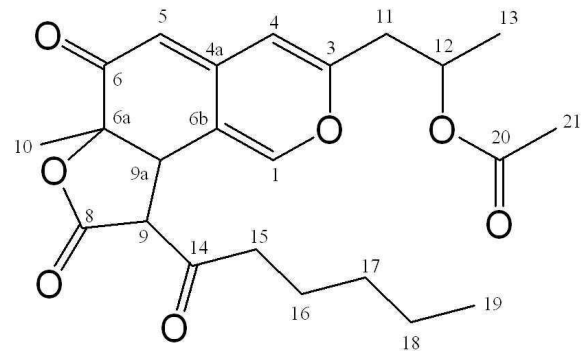
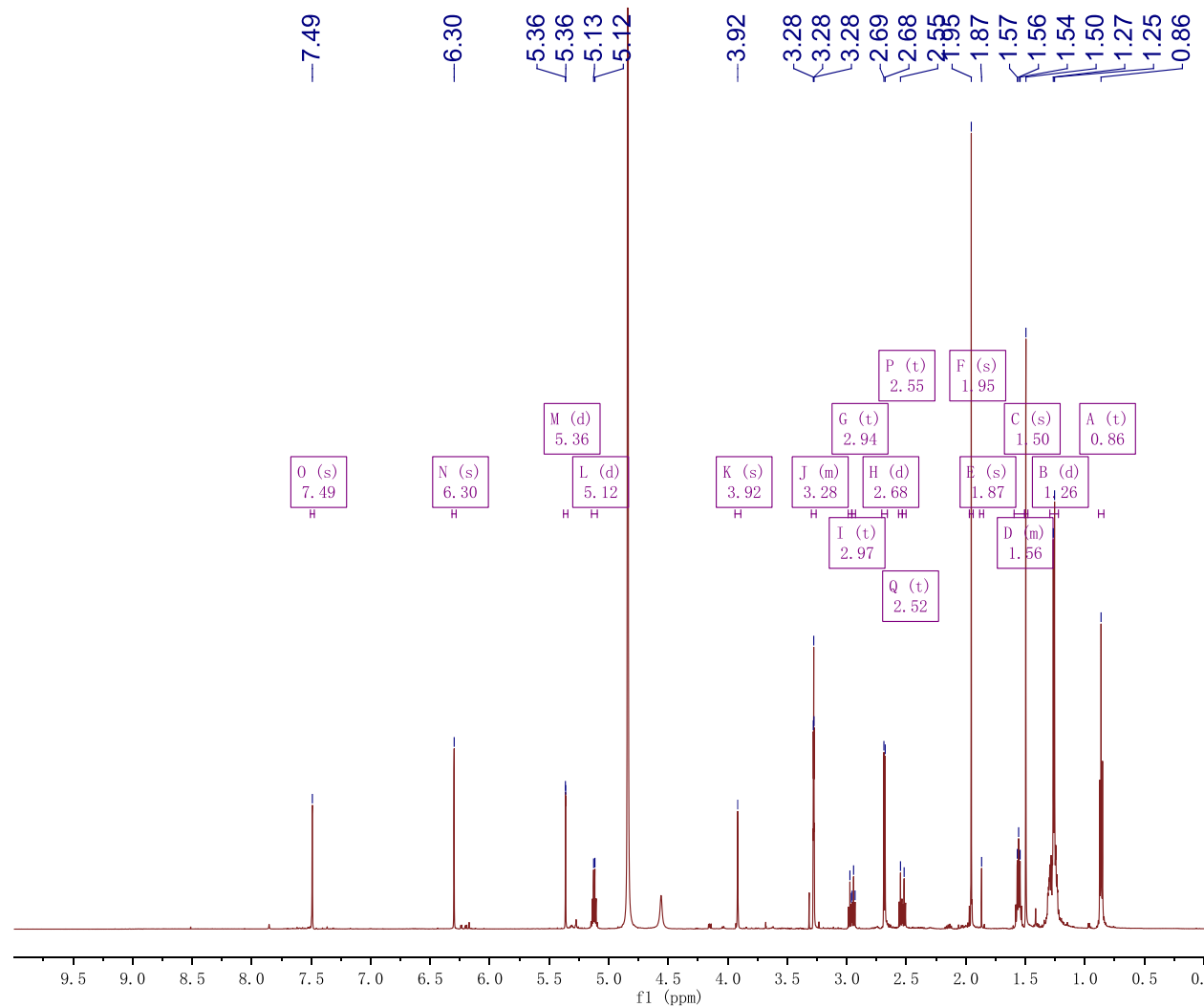


Chemical Formula: $\text{C}_{13}\text{H}_{18}\text{O}_5$
Molecular Weight: 254.28

	ppm
1	197.58
2	165.32
3	149.77
4	112.82
5	102.86
6	76.73
7	72.12
8	65.03
9	63.68
10	43.16
11	34.03
12	21.99
13	16.71

24 (Acetyl-Monasfluol A)

H



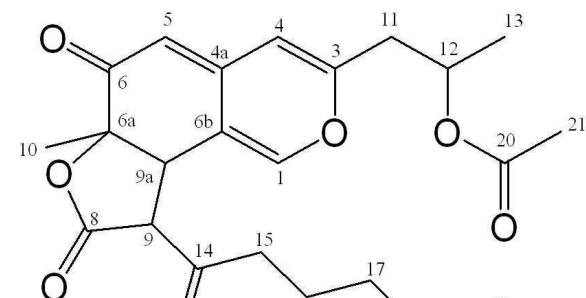
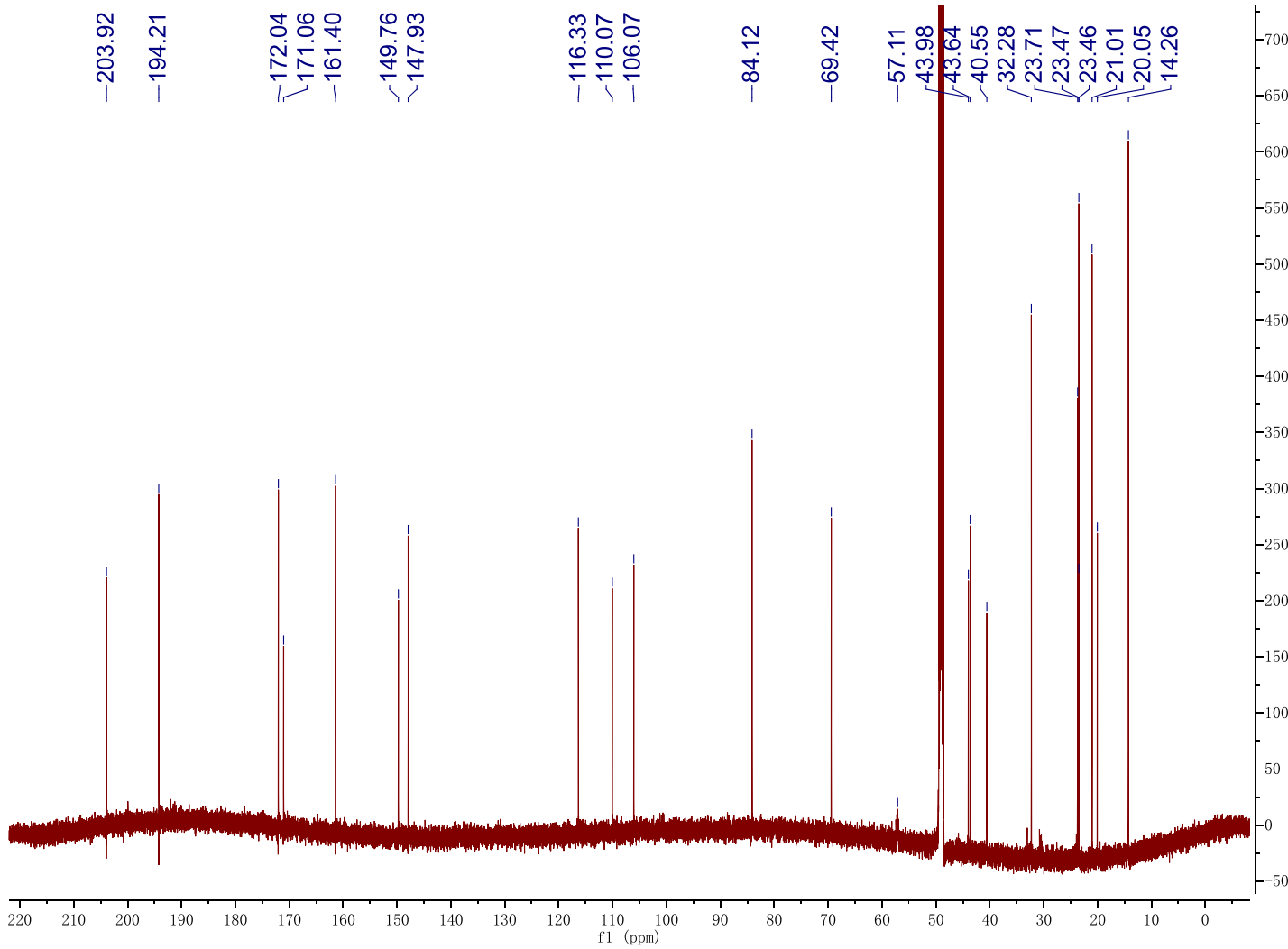
Chemical Formula: C₂₃H₂₈O₇

Molecular Weight: 416.47

	Name	Shift	Class	J's
1	O (s)	7.49	s	
2	N (s)	6.30	s	
3	M (d)	5.36	d	1.0
4	L (d)	5.12	d	6.3
5	K (s)	3.92	s	
6	J (m)	3.28	m	
7	I (t)	2.97	t	7.4
8	G (t)	2.94	t	7.4, 7.4
9	H (d)	2.68	d	6.4
10	P (t)	2.55	t	
11	Q (t)	2.52	t	
12	F (s)	1.95	s	
13	E (s)	1.87	s	
14	D (m)	1.56	m	
15	C (s)	1.50	s	
16	B (d)	1.26	d	6.3
17	A (t)	0.86	t	7.1, 7.1

24 (Acetyl-Monasfluol A)

C



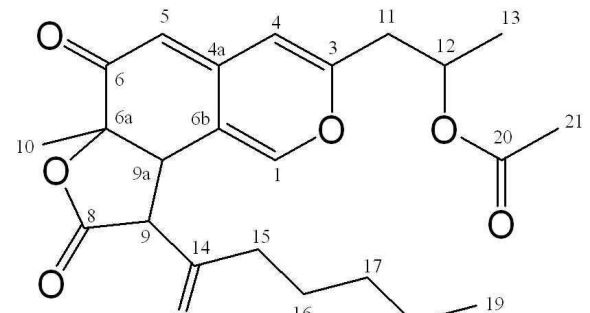
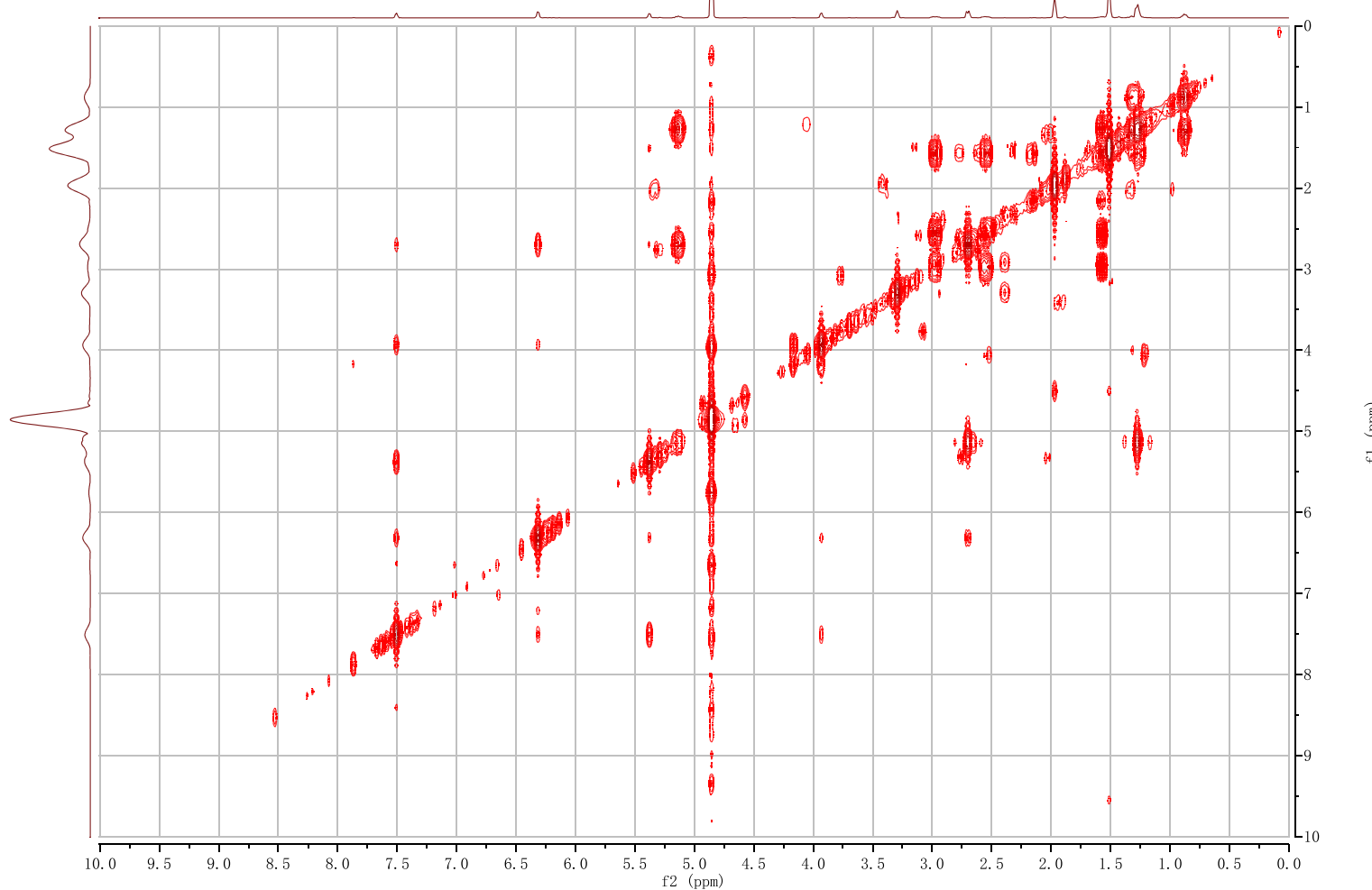
Chemical Formula: C₂₃H₂₈O₇

Molecular Weight: 416.47

	ppm
1	203.92
2	194.21
3	172.04
4	171.06
5	161.40
6	149.76
7	147.93
8	116.33
9	110.07
10	106.07
11	84.12
12	69.42
13	57.11
14	43.98
15	43.64
16	40.55
17	32.28
18	23.71
19	23.47
20	23.46
21	21.01
22	20.05
23	14.26

24 (Acetyl-Monasfluol A)

COSY

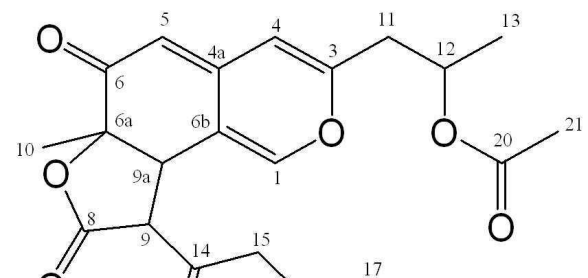
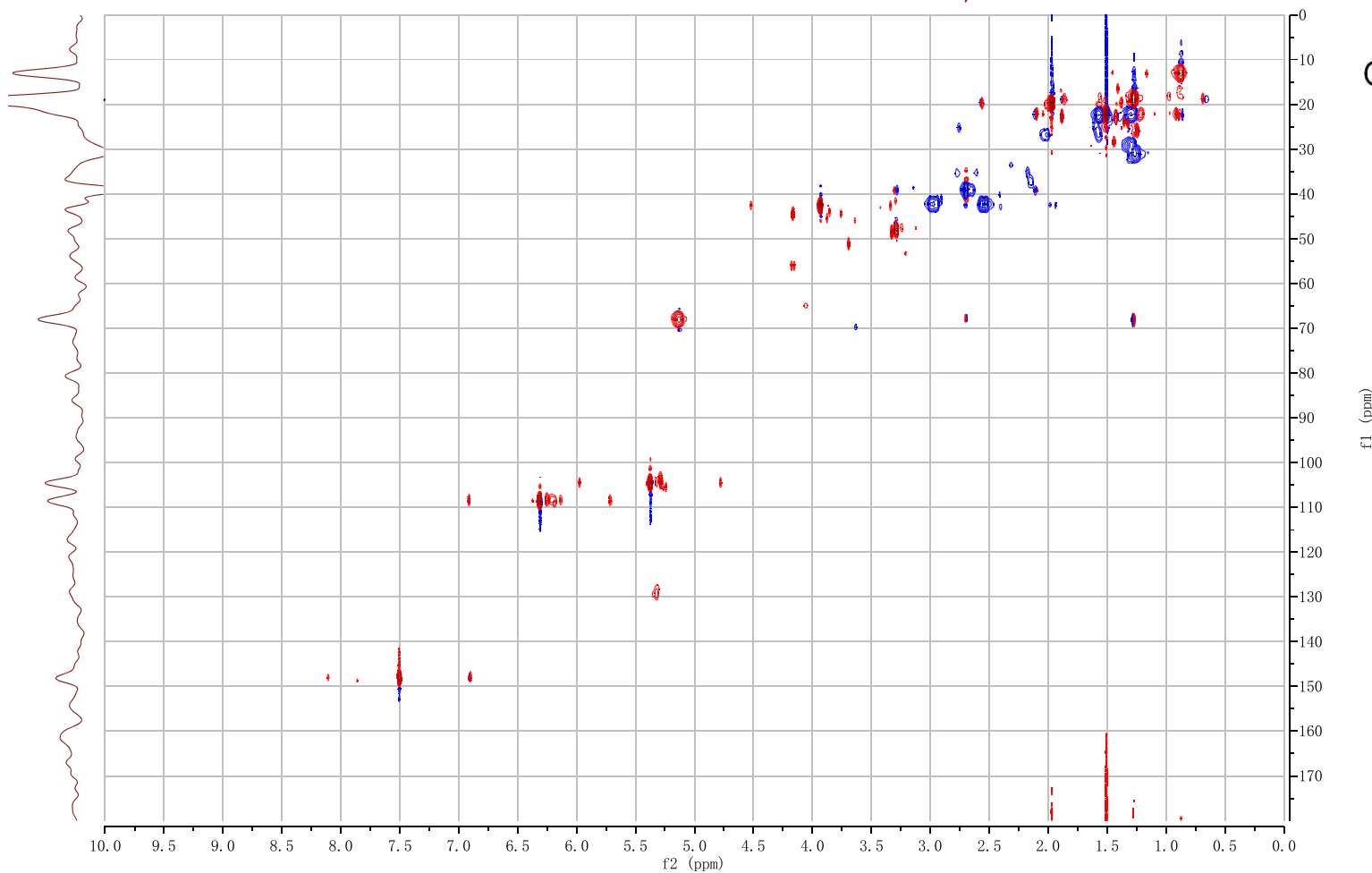


Chemical Formula: $C_{23}H_{28}O_7$

Molecular Weight: 416.47

24 (Acetyl-Monasfluol A)

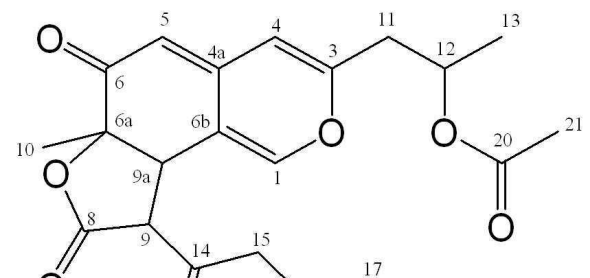
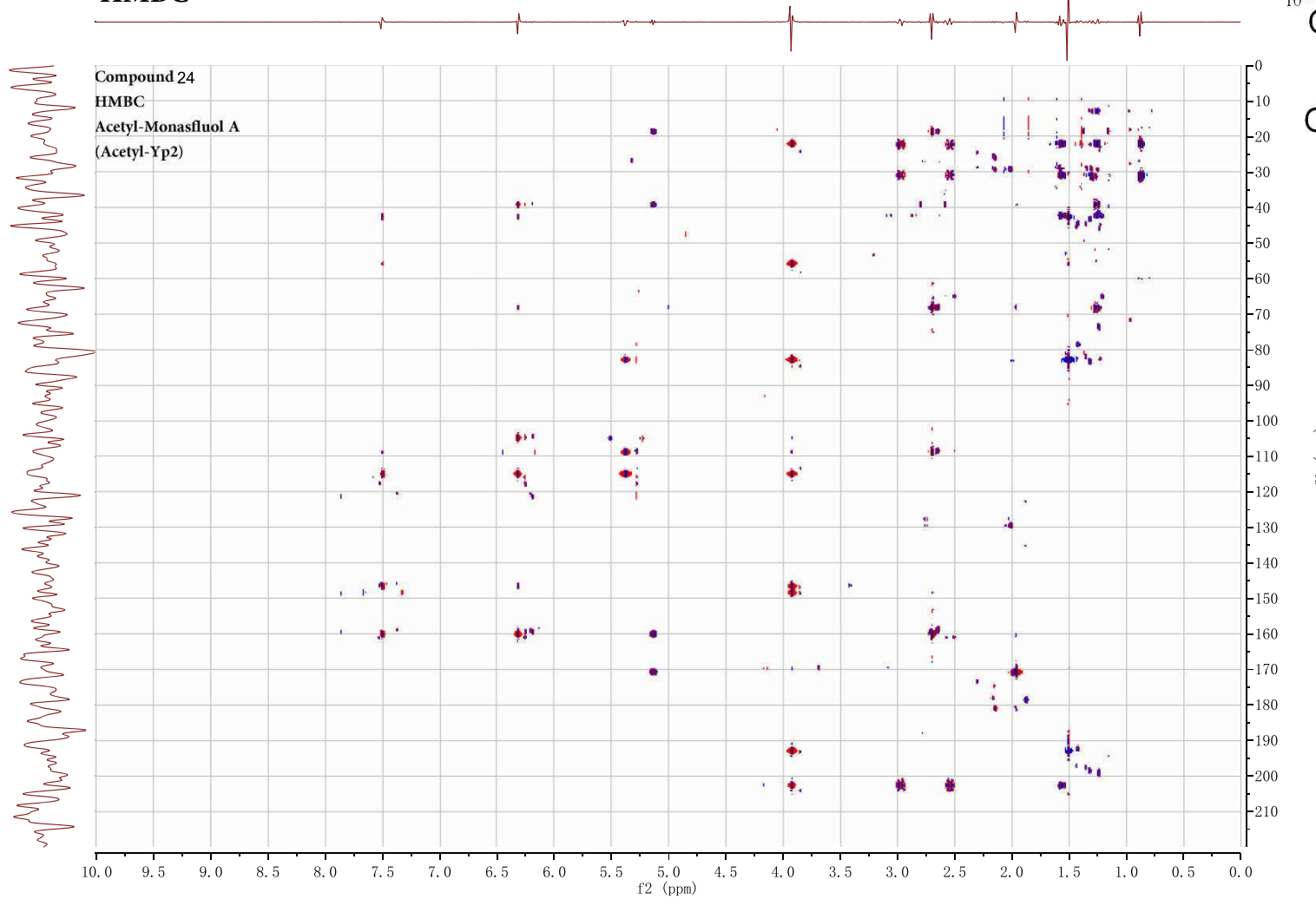
HSQC



Chemical Formula: C₂₃H₂₈O₇

Molecular Weight: 416.47

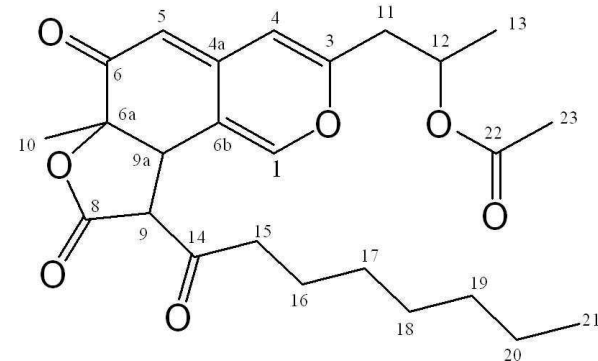
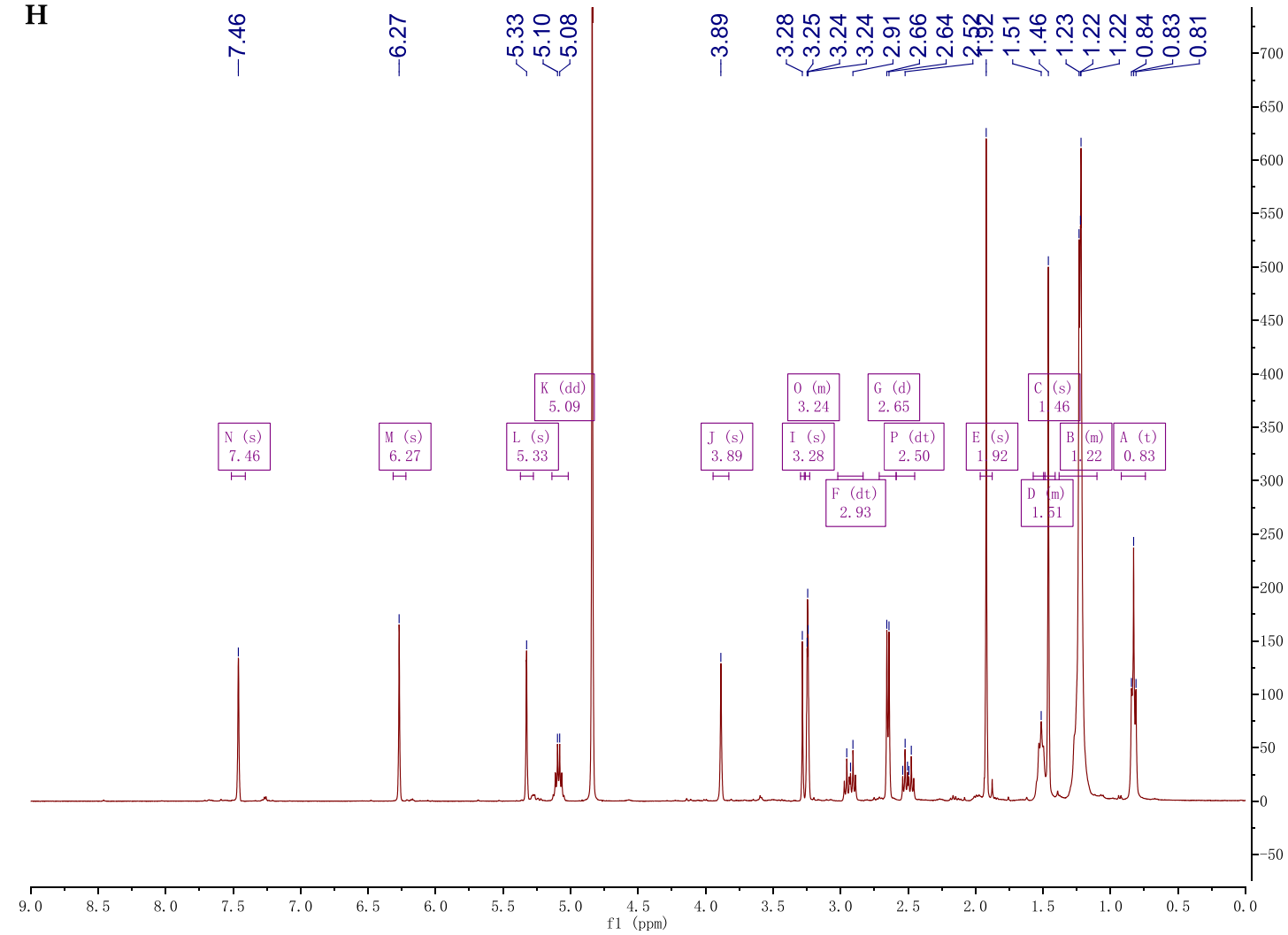
24 (Acetyl-Monasfluol A)
HMBC



Chemical Formula: C₂₃H₂₈O₇
Molecular Weight: 416.47

25 (Acetyl-Monasfluol B)

H



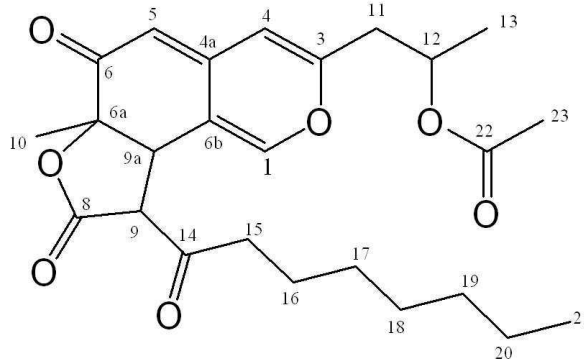
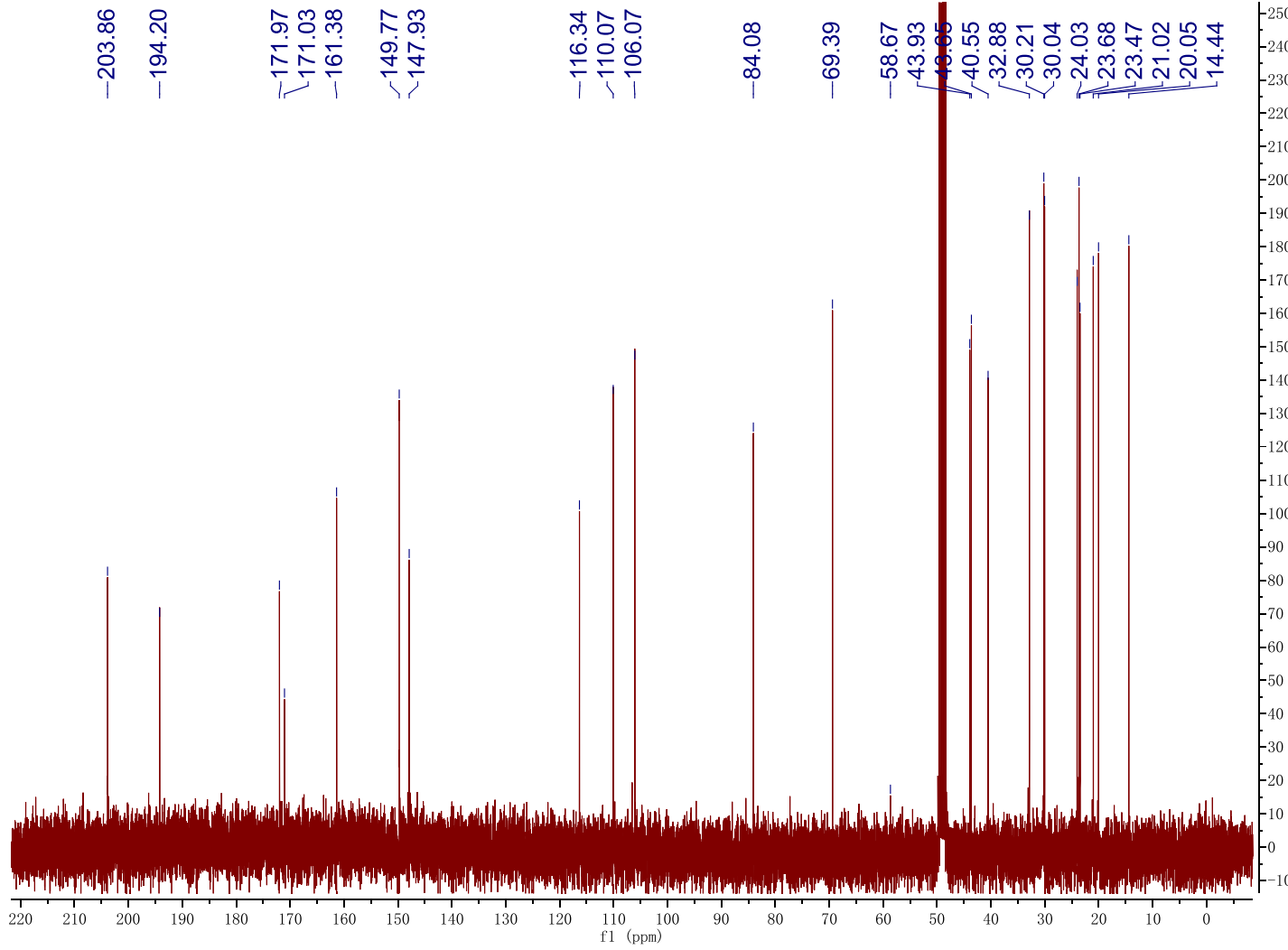
Chemical Formula: $C_{25}H_{32}O_7$

Molecular Weight: 444.52

Name	Shift Class	J' 's
1 N	(s)	7.46
2 M	(s)	6.27
3 L	(s)	5.33
4 K	(dd)	5.09
5 J	(s)	3.89
6 I	(s)	3.28
7 O	(m)	3.24
8 F	(dt)	2.93
9 G	(d)	2.65
10 P	(dt)	2.50
11 E	(s)	1.92
12 D	(m)	1.51
13 C	(s)	1.46
14 B	(m)	1.22
15 A	(t)	0.83
		6.6, 6.6

25 (Acetyl-Monasfluol B)

C

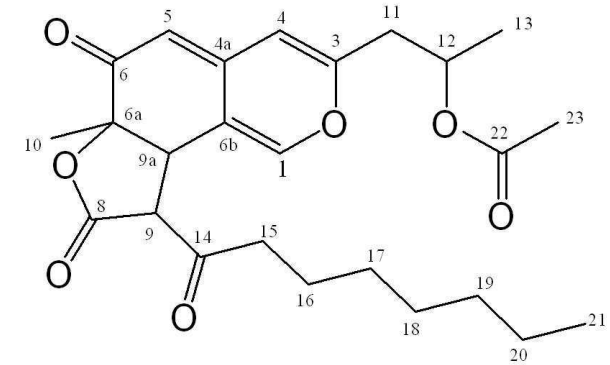
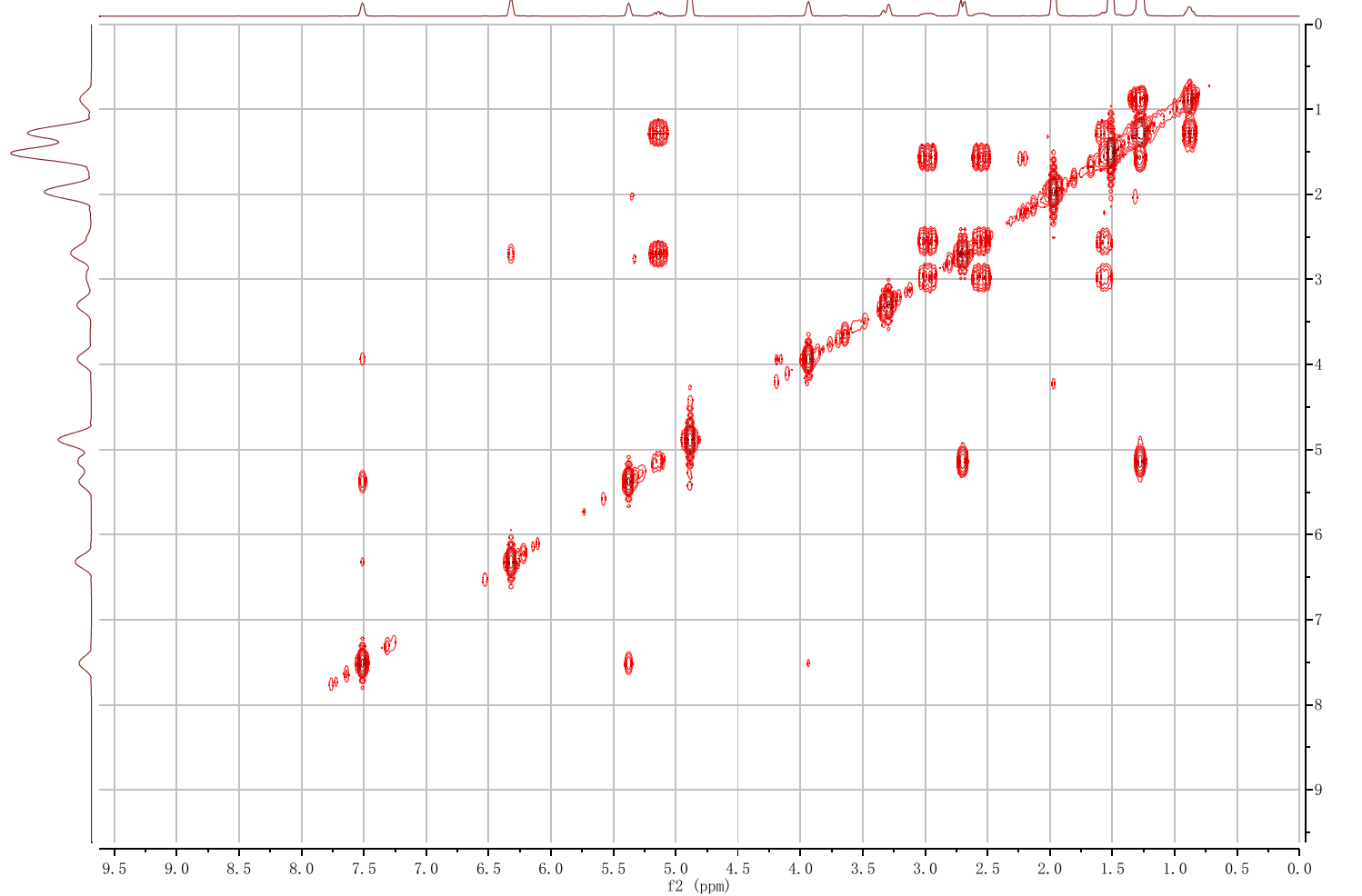


Chemical Formula: $C_{25}H_{32}O_7$

Molecular Weight: 444.52

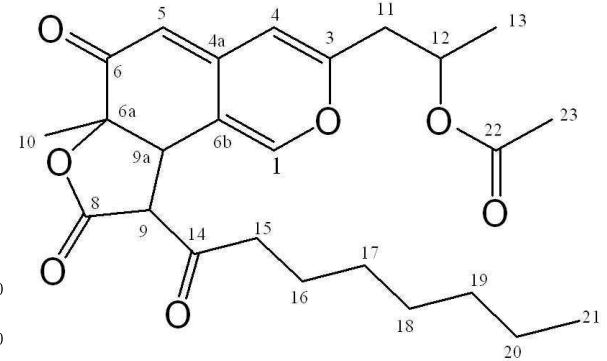
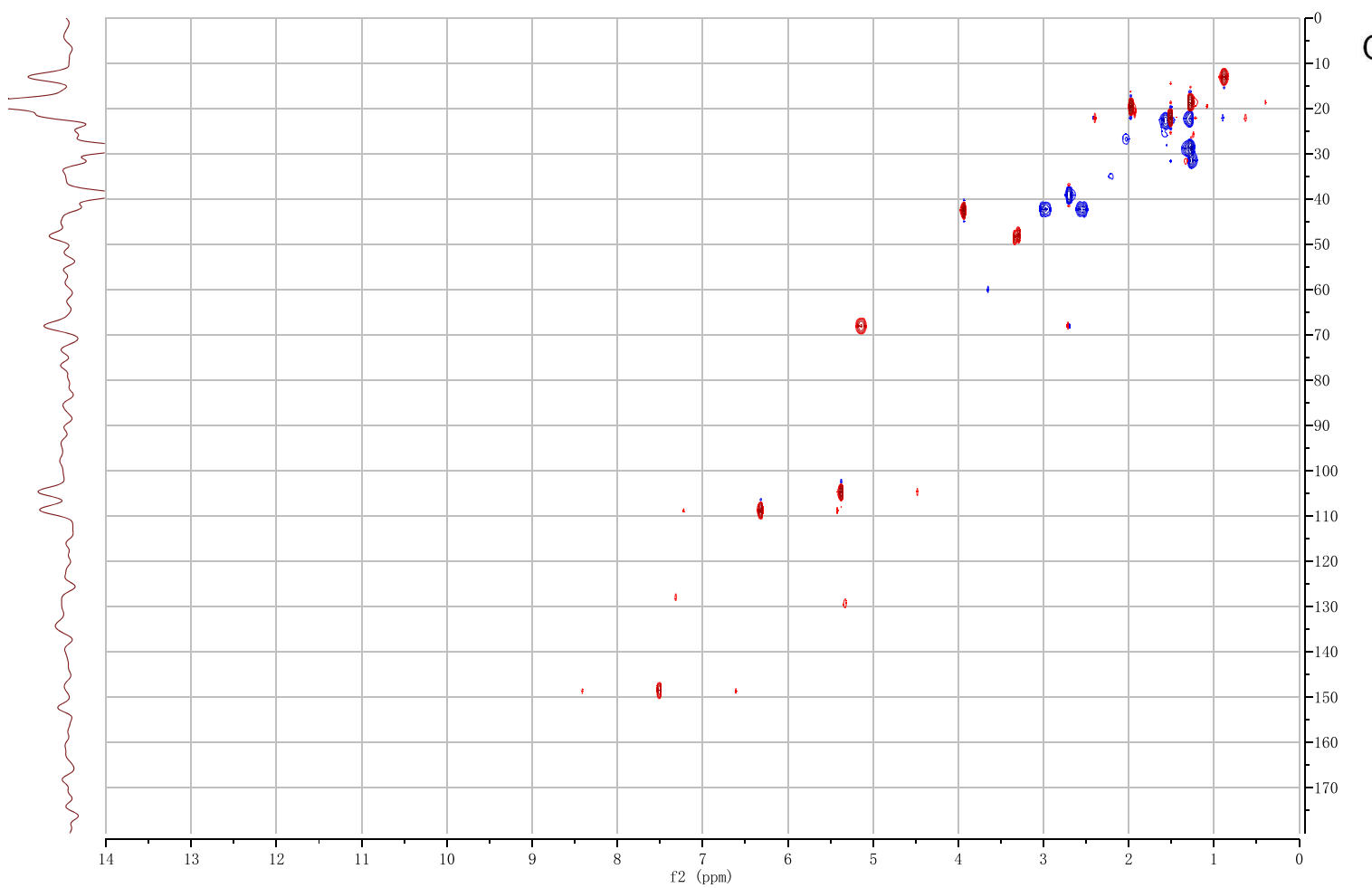
	ppm
1	203.86
2	194.20
3	171.97
4	171.03
5	161.38
6	149.77
7	147.93
8	116.34
9	110.07
10	106.07
11	84.08
12	69.39
13	58.67
14	43.93
15	43.65
16	40.55
17	32.88
18	30.21
19	30.04
20	24.03
21	23.68
22	23.47
23	21.02
24	20.05
25	14.44

25 (Acetyl-Monasfluol B)
COSY



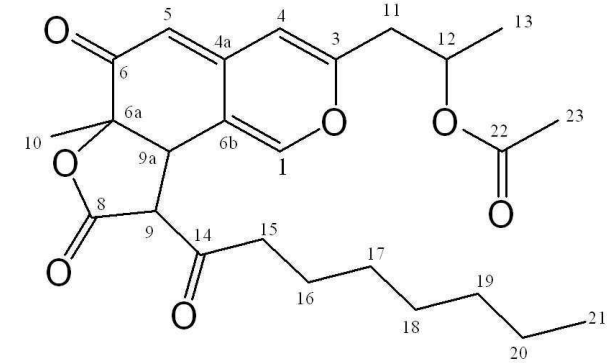
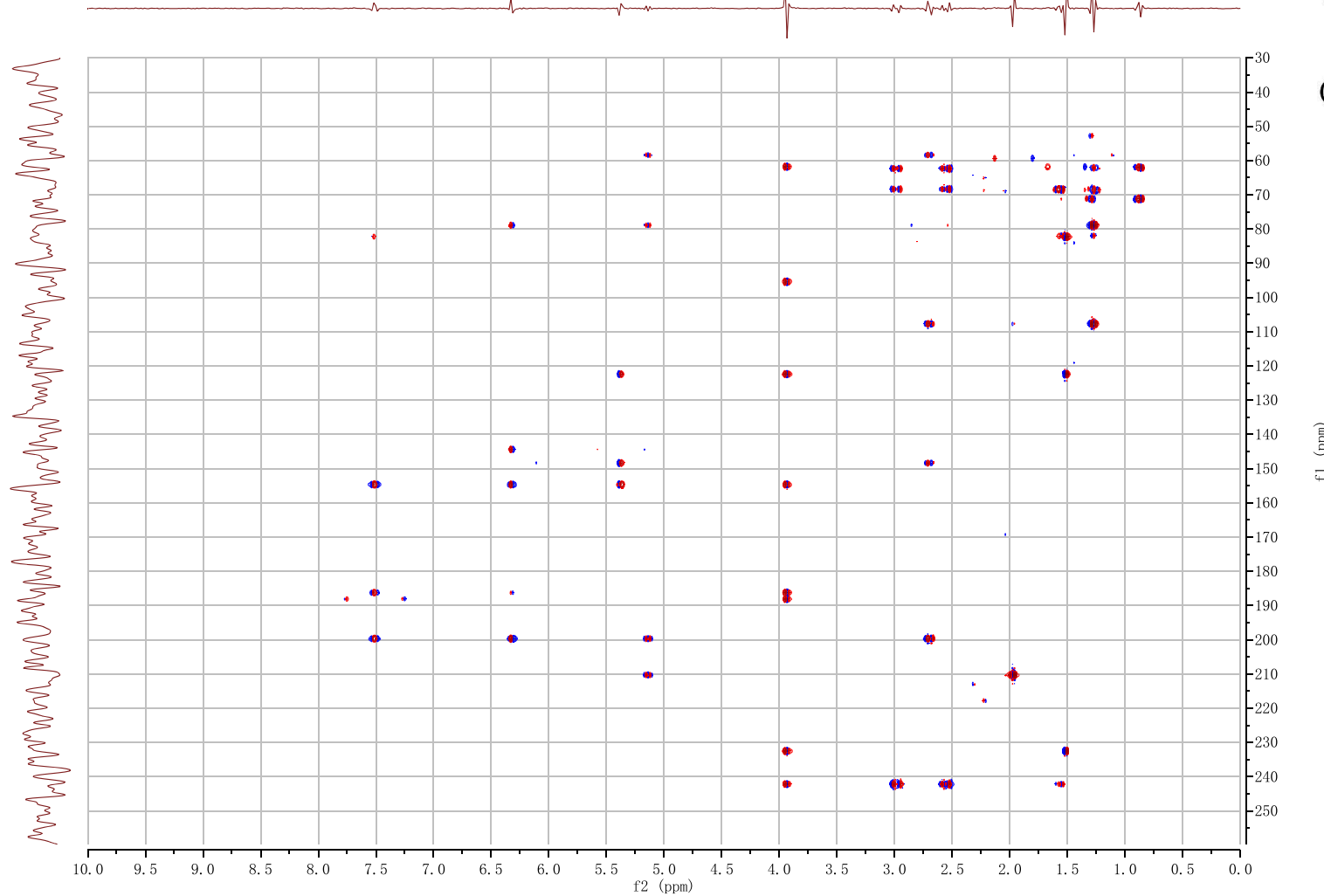
Chemical Formula: C₂₅H₃₂O₇
Molecular Weight: 444.52

25 (Acetyl-Monasfluol B)
HSQC



Chemical Formula: C₂₅H₃₂O₇
Molecular Weight: 444.52

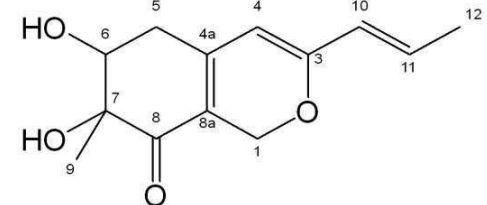
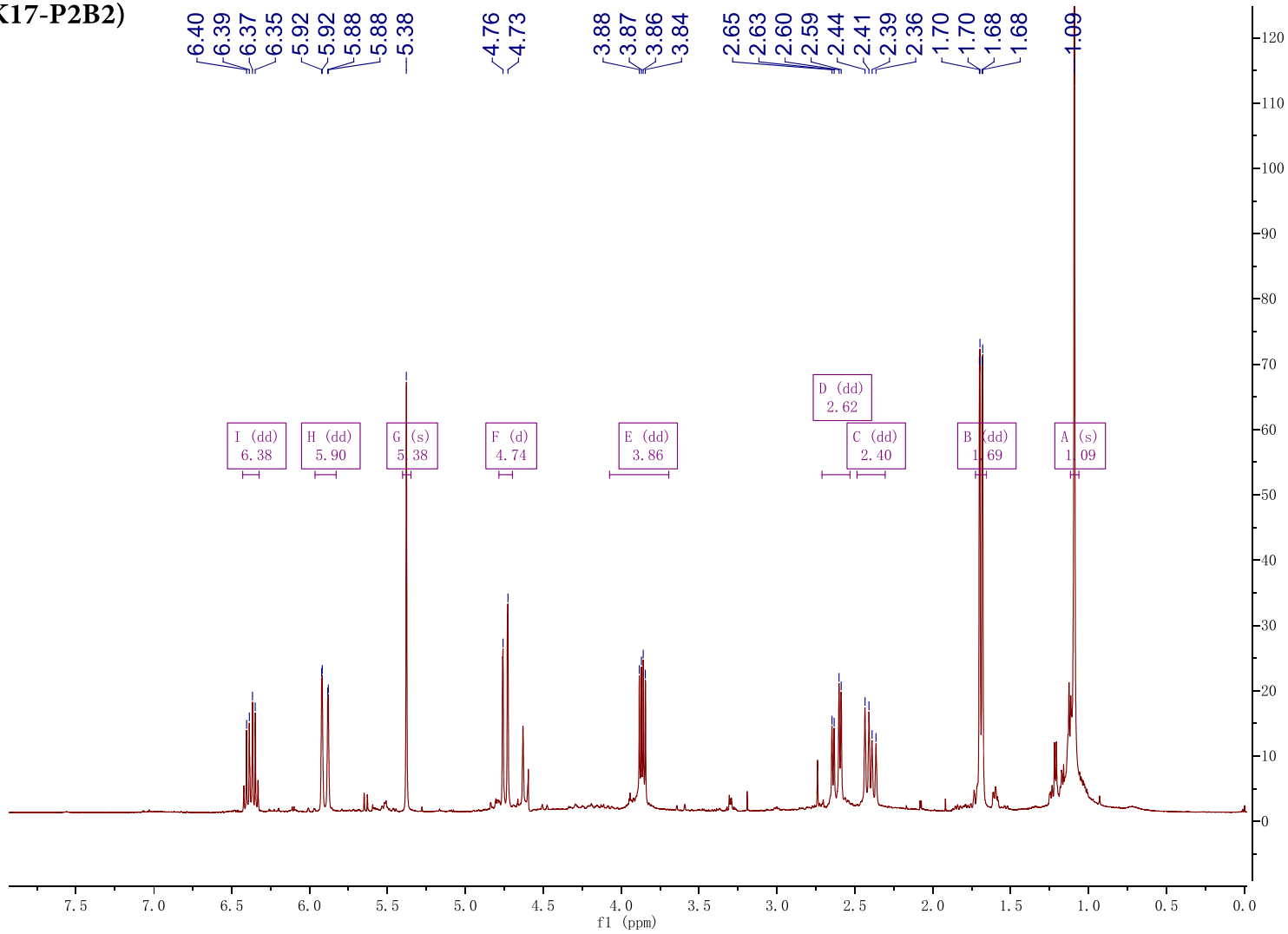
25 (Acetyl-Monasfluol B)
HMBC



Chemical Formula: C₂₅H₃₂O₇

Molecular Weight: 444.52

35 (FK17-P2B2)
H

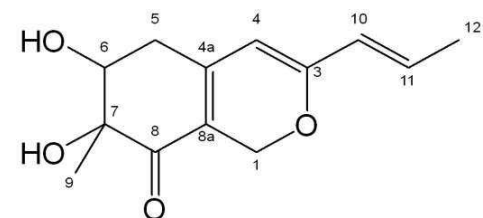
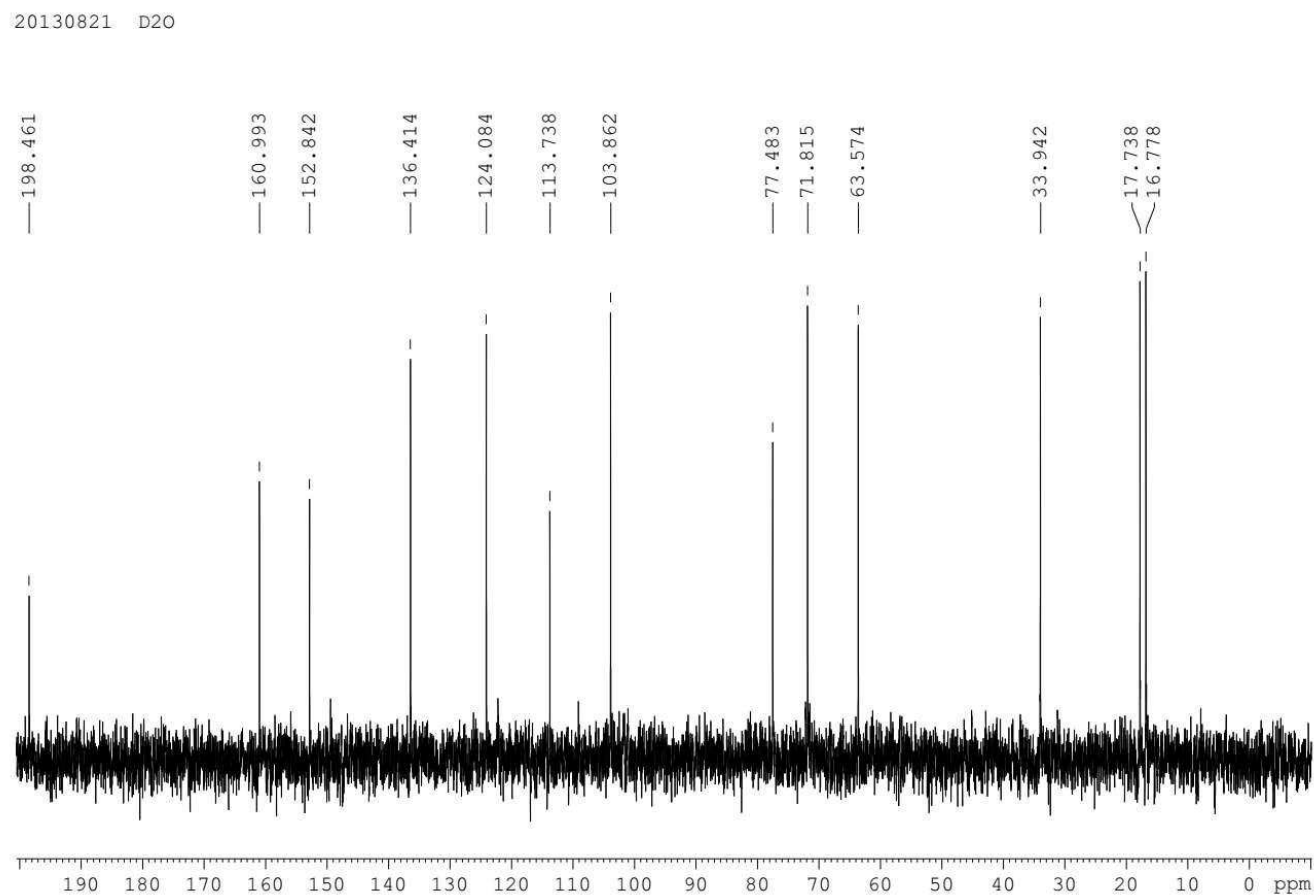


Chemical Formula: $C_{13}H_{16}O_4$
Molecular Weight: 236.27

Name	Shift Class	J's
1 I	(dd)	6.38 dd 7.0, 15.5
2 H	(dd)	5.90 dd 1.5, 15.5
3 G	(s)	5.38 s
4 F	(d)	4.74 d 12.6
5 E	(dd)	3.86 dd 5.5, 10.2
6 D	(dd)	2.62 dd 5.4, 18.1
7 C	(dd)	2.40 dd 10.3, 18.0
8 B	(dd)	1.69 dd 1.1, 7.0
9 A	(s)	1.09 s

35 (FK17-P2B2)

C

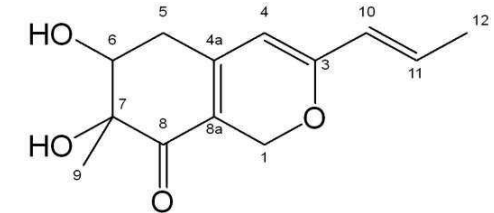
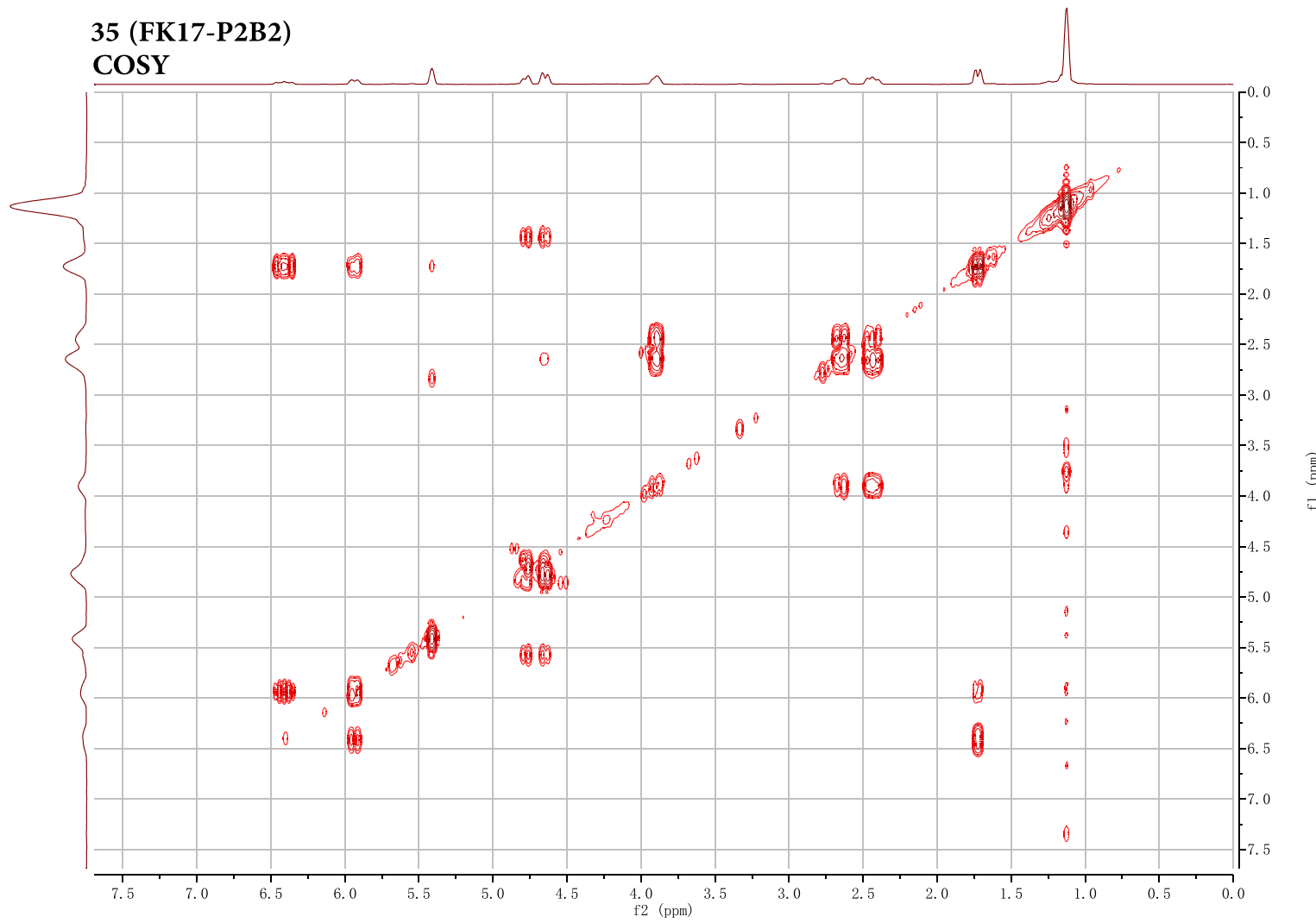


Chemical Formula: C₁₃H₁₆O₄

Molecular Weight: 236.27

	ppm
1	198.46
2	160.99
3	152.84
4	136.41
5	124.08
6	113.74
7	103.86
8	77.48
9	71.82
10	63.57
11	33.94
12	17.74
13	16.78

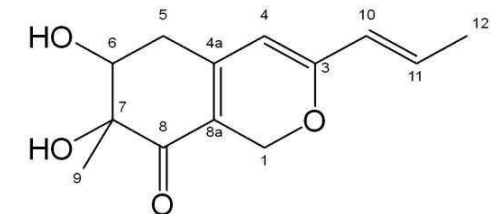
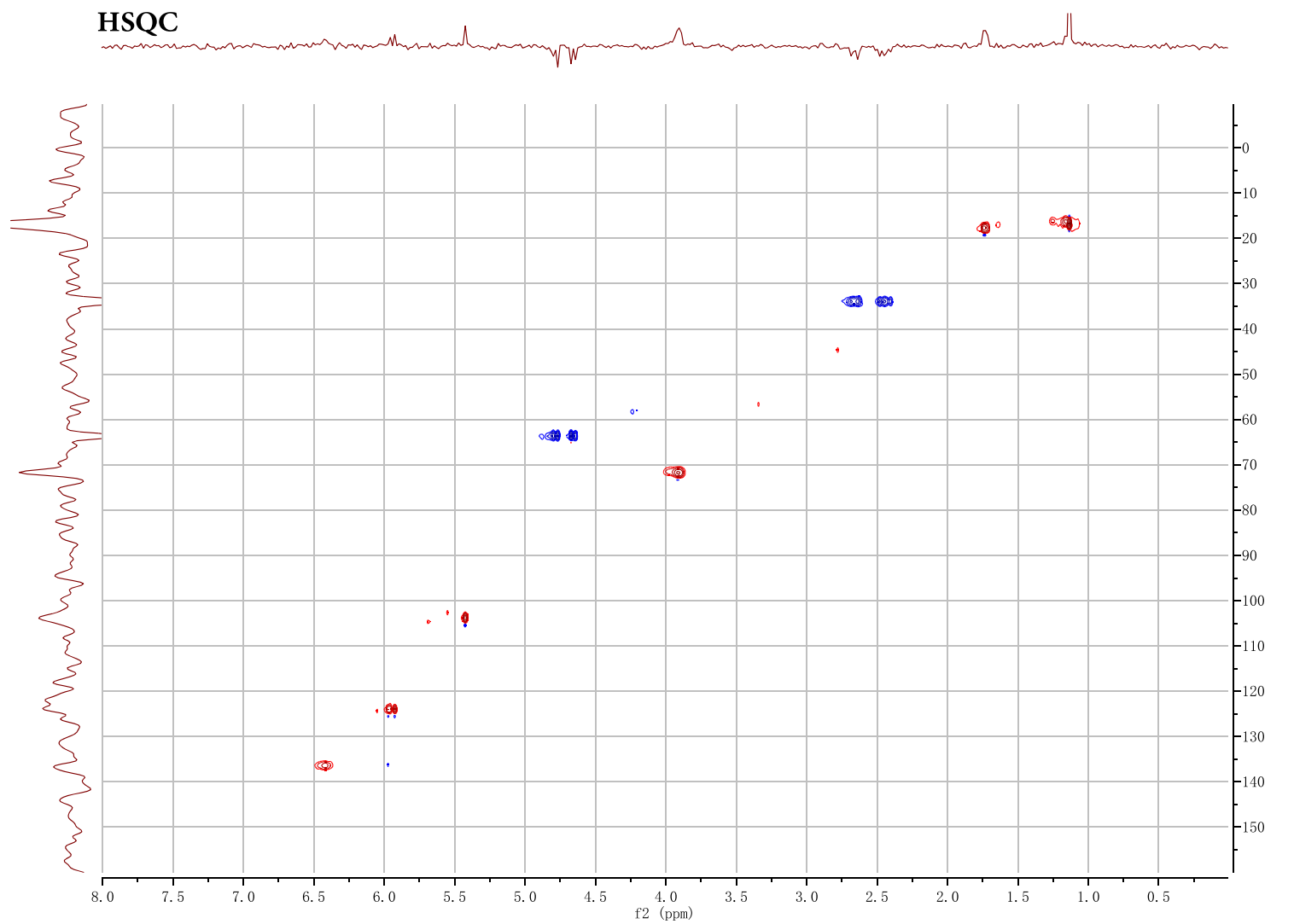
35 (FK17-P2B2)
COSY



Chemical Formula: C₁₃H₁₆O₄
Molecular Weight: 236.27

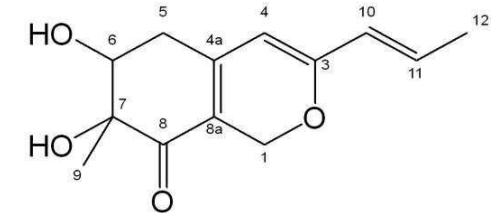
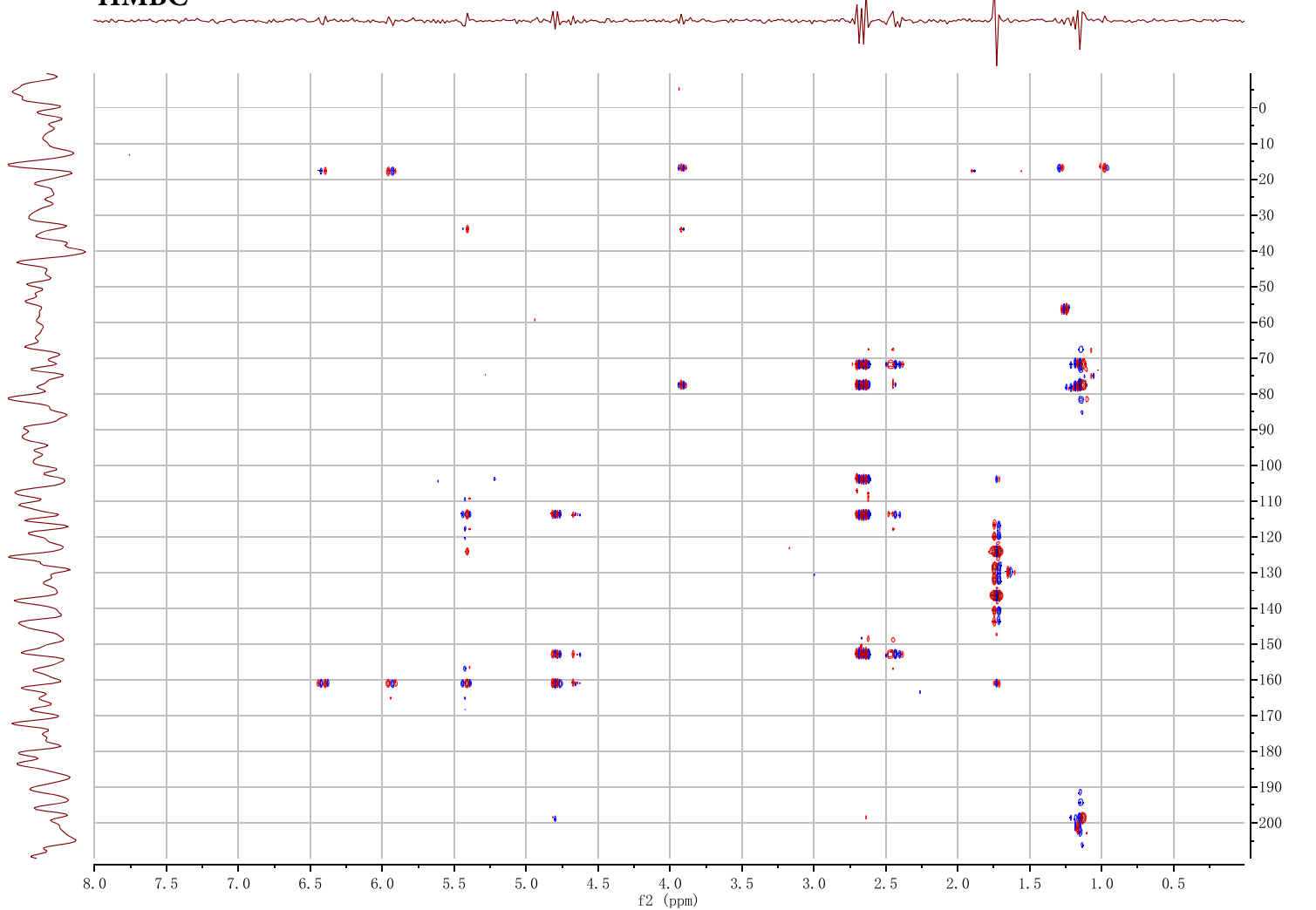
35 (FK17-P2B2)

HSQC



Chemical Formula: $\text{C}_{13}\text{H}_{16}\text{O}_4$
Molecular Weight: 236.27

35 (FK17-P2B2)
HMBC



Chemical Formula: C₁₃H₁₆O₄
Molecular Weight: 236.27

7. Heterologous production of MonAzPs biosynthetic intermediates

7.1. Heterologous expression of *mrpigA* in *Aspergillus oryzae* M-2-3

Heterologous expression of *mrpigA* in *A. oryzae* M-2-3 (arginine auxotroph) followed established protocols (Pahirulzaman et al., 2012). Briefly, the *mrpigA* gene was cloned in the entry plasmid pE-YA (kindly provided by Prof. Colin M. Lazarus, University of Bristol, U.K.) by homologous recombination in *Saccharomyces cerevisiae*. The expression plasmid pT3P-*mrpigA* was obtained by using the LR reaction of the Gateway technology. The expression plasmid was introduced into *A. oryzae* M-2-3 by protoplast-mediated transformation. The colony morphologies of *A. oryzae* M-2-3 and its *mrpigA* transformant *A. oryzae*-A were compared (**Figure 7-1**), and showed an obvious colony color change.

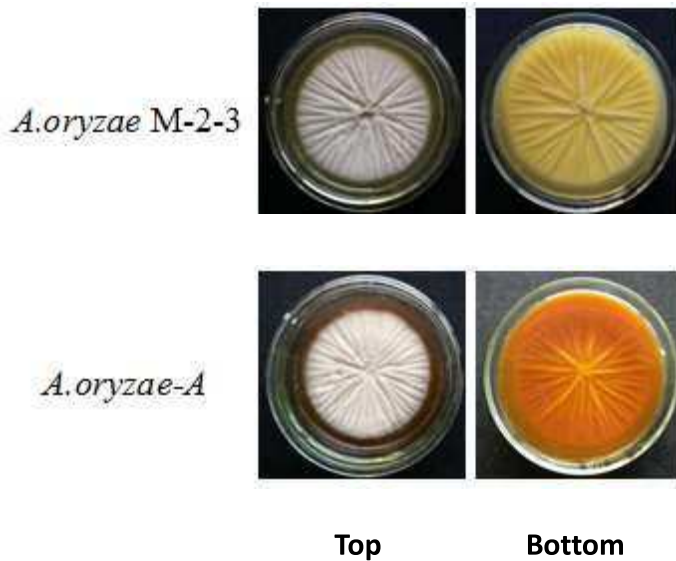


Figure 7-1. Colony morphologies of *A. oryzae* M-2-3 and its *mrpigA* transformant *A. oryzae*-A.

Mycelia of the two strains were incubated on CMP agar medium (3.5% CzapekDox Broth, 2% maltose, 1% polypeptone, 2% agar) at 30°C for 10 days.

The metabolites of *A. oryzae*-A were analyzed by HPLC/MS using *A. oryzae* M-2-3 as a control. The two strains were incubated on CMP agar at 30°C for 5 days. The HPLC conditions are presented in **Table 7-1**. The results showed that the *A. oryzae*-A mainly produced **15** ($m/z=246$). However, the predicted polyketide product of *mrpigA*, compound **14** ($m/z=232$), was found only in minute amounts (**Figure 7-2**).

Table 7-1. The gradient elution profile for analyzing *A. oryzae* transformants by HPLC

Time (min)	Flow rate (mL/ min)	0.5% phosphoric acid (%)	ACN (%)	Deionized water (%)
0	0.8	5	10	85
25	0.8	5	65	30
30	0.8	5	90	5
31	0.8	5	10	85
35	0.8	5	10	85

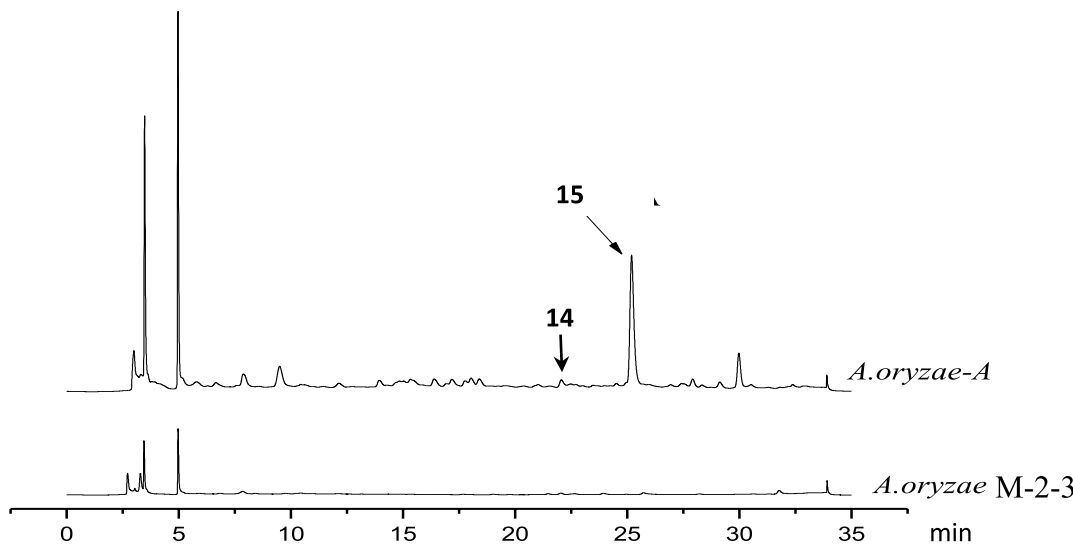


Figure 7-2 HPLC profile of *A. oryzae* M-2-3 and *A. oryzae*-A.

Compounds were detected at 276 nm.

As proposed, the putative ACP-bound benzaldehyde intermediate **11** is released from MrPigA by the expedient aldol cyclization of C10 with the C1 thioester to yield the C10-bicyclic compound **14** and its spontaneously oxidized quinone derivative **15** (**Figure 7-3**). Compounds **14** and **15** are also the main products of the *mrpigC* knockout strain.

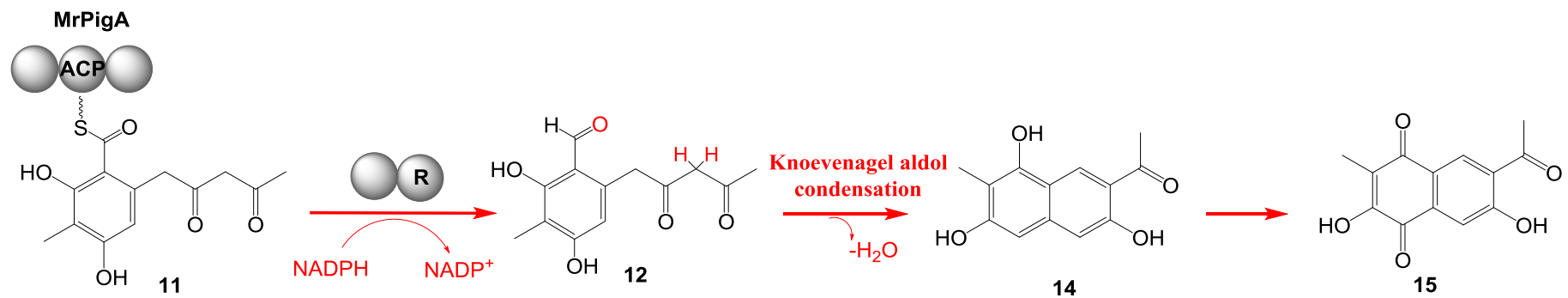


Figure 7-3 The proposed pathway for 14 and 15.

7.2. Heterologous expression of MonAzPs biosynthetic genes in *Saccharomyces cerevisiae*

The intronless *mrpigA* ORF was reconstructed from three parts: a 1,065-bp fragment PCR-amplified with primers MrpigA_1_F and MrpigA_1_R (Table 7-2); a 6,026-bp *KpnI* - *SexAI* restriction fragment of pT3P-*MpigA* (Section 7.1); and a 1,169-bp fragment PCR-amplified with primers MrpigA_2_F and MrpigA_2_R. The PCR fragments were amplified by Phusion polymerase (Thermo Scientific) using the chromosomal DNA of *M. ruber* M7 as the template. The three fragments and the *NdeI* - *PmeI* - digested YEADH2p-FLAG-URA (Xu *et al.*, 2013) vector were transformed into *Saccharomyces cerevisiae* BJ5464-NpgA (Ma *et al.*, 2009) to yield YEPMrPigA by *in vivo* homologous recombination. After plasmid rescue into *E. coli* DH10B, the reconstituted intronless *mrpigA* nrPKS was verified by sequencing.

The plasmid YEPMrPigC was constructed to express the *M. ruber* M7 *mrpigC* gene encoding the MrPigC oxoacyl-[ACP] reductase. The 912-bp intronless *mrpigC* gene was amplified with primers MrpigC_F (*NdeI*) and MrpigC_R (*PmeI*) and cloned into pJET1.2. After sequence verification, the *mrpigC* gene was ligated as an *NdeI* - *PmeI* fragment into the corresponding sites of YEADH2p-FLAG-TRP (Xu *et al.*, 2013) to yield YEPMrPigC.

The plasmid YEPMrPigG was constructed to express the *M. ruber* M7 *mrpigG* gene encoding the MrPigG putative serine hydrolase. The 822-bp intronless *mrpigG* gene was amplified with primers MrpigG_F (*NdeI*) and MrpigG_R (*PmeI*) and cloned into pJET1.2. After sequence verification, the *mrpigG* gene was ligated as an *NdeI* - *PmeI* fragment into the corresponding sites of YEADH2p-FLAG-Leu (Bai *et al.*, 2016) to yield YEPMrPigG.

The plasmids YEPMrPigA, YEPMrPigC, and YEPMrPigG were used to transform *S. cerevisiae* BJ5464-NpgA (Ma *et al.*, 2009) alone or in

combinations. Yeast fermentations and product analysis was conducted as described earlier (Bai *et al.*, 2016; Xu *et al.*, 2014a,b).

Table 7-2. Primers used to construct the yeast expression vectors YE_pMrPigA, YE_pMrPigC and YE_pMrPigG

Primer name	Sequence (5' – 3')
MrpigA_1_F	GGACTACAAAGACGATGACGACAAGCTTCATATGGTCAGTCGGATATTGCGCC
MrpigA_1_R	TCTGGGCCGAAAGAGAGACCAGCACAG
MrpigA_2_F	CTCCTCCCGAAAATGCGTTCTG
MrpigA_2_R	AGTGATGGTGTGGATGTCCGTTAAACTCAGTGCAGGAAACCCAT
MrpigC_F (<i>Nde</i> I)	ATTCCATATGCCCTCCTCCTAGGGGT
MrpigC_R (<i>Pme</i> I)	GCCGCGCCGTTAACCTAGTAGATAAAATTCAC
MrpigG_F (<i>Nde</i> I)	ATTCCATATGCCAGCCAACCGCTC
MrpigG_R (<i>Pme</i> I)	CTTTGTTAAACTCAAATCCGTCTGGAG

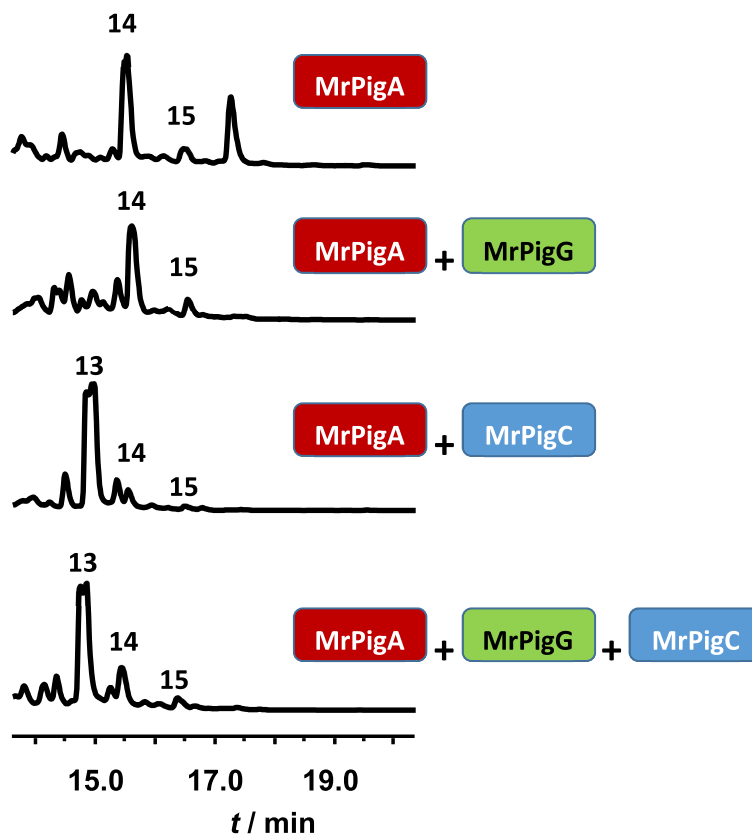


Figure 7-4. Biosynthesis of MonAzPs intermediates in *S. cerevisiae*. HPLC traces were recorded at 300 nm for extracts of *S. cerevisiae* BJ5464-NpgA transformed with the appropriate plasmids. Unlabeled peaks: yeast metabolites unrelated to MonAzPs intermediates.

8. Enzyme assay for MrPigD

8.1. Expression of the *mrpigD* gene in *Escherichia coli*

The *mrpigD* gene was amplified by PCR from cDNA of *Monascus ruber* M7 with primers Mpig D-F: GGAATTCCATATGATGGAGGATCCTGCTCGGACG and Mpig D-R: CCCAAGCTTTCACCCTATATACTCCGCATACG. The resulting PCR product was cloned into pET-28a utilizing the *Nde*I and *Hind*III restriction enzyme sites present in the primers (shown in red). *E. coli* BL21 cells were used as the host for the plasmid pET-28a-MpigD.

E. coli BL21 transformants with pET-28a-MpigD were cultivated in 2TY medium (1% yeast extract, 1.6 % tryptone, 0.5% sodium chloride) with 0.1mM IPTG, with shaking at 200 rpm, 25°C overnight. The harvested cells were resuspended in Tris-HCl buffer (50 mM, pH 7.5) and sonicated. The clarified supernatant was used for the purification of the MrPigD protein using a Ni-NTA column (GE healthcare HisTrapTM FF, 5mL) (**Figure 8-1**).

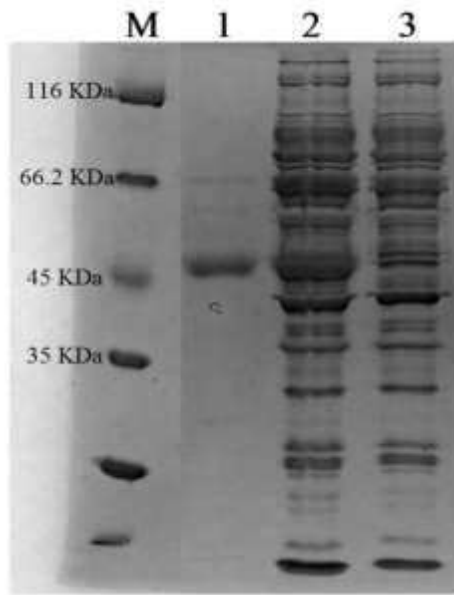
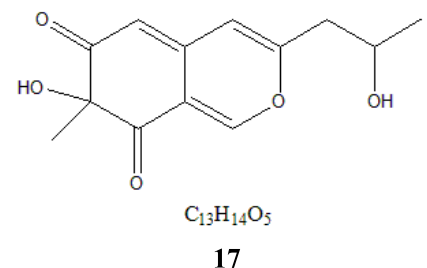


Figure 8-1. SDS-PAGE for purified MrPigD protein (49 kDa, Line 1), induced supernatant with IPTG (Line 2) and supernatant without induction (Line 3)

8.2. Substrate preparation

Preparation of compound 17

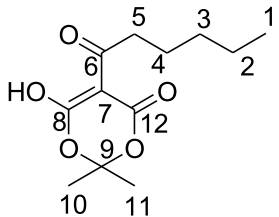
Compound **17** was purified from the PDB culture of the *mrpigD* knockout mutant of *M. ruber* M7.



Semi-Preparative LCMS and compound purification.

Purification of compounds was generally achieved using a Waters mass-directed autopurification system comprising of a Waters 2767 autosampler, Waters 2545 pump system, a Phenomenex Kinetex Axia column (5μ , C₁₈, 100 Å, 21.2 × 250 mm) equipped with a Phenomenex Security Guard precolumn (Luna C₅ 300 Å) eluted at 20 mL/min at ambient temperature. Solvent A, HPLC grade H₂O + 0.05% formic acid; Solvent B, HPLC grade CH₃CN + 0.045% formic acid. The post-column flow was split (100:1) and the minority flow was made up with HPLC grade MeOH + 0.045% formic acid to 1 mL·min⁻¹ for simultaneous analysis by diode array (Waters 2998), evaporative light scattering (Waters 2424) and ESI mass spectrometry in positive and negative modes (Waters SQD-2). Detected peaks were collected into glass test tubes. Combined tubes were evaporated *in vacuo* (vacuum centrifuge), weighed, and residues dissolved directly in NMR solvent for NMR analysis.

Preparation of 5-hexanoyl-6-hydroxy-2,2-dimethyl-4H-1,3-dioxin-4-one



Pyridine (5.0 mmol, 0.8 mL) and DMAP (1.0 mmol, 123.4 mg) were added into a solution of Meldrum's acid (5.0 mmol, 735.4 mg) in CH₂Cl₂ (10 mL) under nitrogen. The mixture was stirred for 10 minutes at room temperature and then cooled on ice. Hexanoyl chloride (5.1 mmol, 686 mg) was added slowly into the mixture at 0 °C. Afterwards, the reaction was stirred at room temperature overnight. To isolate the product, the reaction mixture was washed with 2 M HCl (5 mL) three times and then washed with water (5 mL) three times. The organic phase was concentrated and passed through a silica gel column with Hexane/EtOAc (30:1 first, then 10:1). The product was obtained as an orange oil (726.4 mg, 60 %).

¹H NMR (400 MHz, Chloroform-*d*):

δ (ppm) 3.09 – 2.96 (5-CH₂, m, 2H), 1.69 (10-CH₃, 11-CH₃, s, 6H), 1.67 – 1.59 (4-CH₂, m, 2H), 1.45 – 1.24 (2-CH₂, 3-CH₂, m, 4H), 0.86 (1-CH₃, t, *J* = 7.0 Hz, 2H).

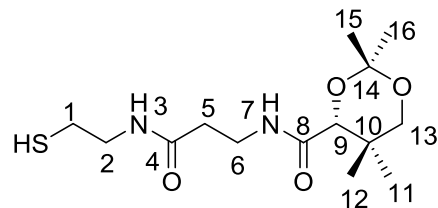
¹³C NMR (101 MHz, Chloroform-*d*):

δ (ppm) 198.16 (8-enol C), 170.50 (6-CO), 160.06 (12-CO), 104.65 (9-C), 91.20 (7-C), 35.58 (5-CH₂), 31.41 (4-CH₂), 26.69 (10-CH₃, 11-CH₃), 25.74 (3-CH₂), 22.21 (2-CH₂), 13.76 (1-CH₃).

HRMS calcd for C₁₂H₁₈O₅ (M+H)⁺ 243.1232, found:243.1283

IR ($\gamma = \text{cm}^{-1}$): 1738, 1661 (C=O). 1572 (-C=C-). 1269, 1202, 1153 (C-O).

Preparation of pantetheine dimethyl ketal



D-pantothenic acid hemi-calcium salt (2.50 g, 5.20 mmol), p-toluenesulfonic acid (2.30 g, 13.00 mmol) and 5 g molecular sieves were suspended in 125 mL dry acetone and stirred at 25 °C for 12 hours under a nitrogen atmosphere. The suspension was filtered with celite and washed with 200 ml acetone. The filtrate was concentrated to a colourless oil, redissolved in 200 ml ethyl acetate and washed two times with brine (25 ml) and dried over MgSO₄. After that the ethyl acetate was removed under vacuum and hexane was added to the flask to precipitate a white solid that was dried under high vacuum. The corresponding D-pantothenic dimethyl ketal (1.90 g, 7.00 mmol) was dissolved in 40 mL dry THF with carbonyldiimidazole (1.70 g, 11.00 mmol) and stirred for one hour at 25 °C. Then cysteamine (1.30 g, 11.00 mmol) was added to the solution and stirred for 12 hours. The solution was concentrated under vacuum and CH₂Cl₂ was added. The organic layer were washed with sat. aq. NH₄Cl (25 mL) and brine (25 mL), dried over MgSO₄ and concentrated under vacuum. The colourless oil was purified by column chromatography (ethyl

acetate) to give a white solid (1.90 g, 6.00 mmol, 86 %). R_f : 0.1 (ethylacetate).

¹H NMR (400 MHz, Chloroform-d):

δ [ppm]: 0.98 (s, 3H, 11-CH₃); 1.05 (s, 3H, 12-CH₃); 1.39 (t, J = 8.6 Hz, 1H, SH); 1.43 (s, 3H, 15-CH₃); 1.47 (s, 3H, 16-CH₃); 2.40 (t, J = 5.8 Hz, 2H, 5-CH₂); 2.64-2.70 (m, 2H, 1-CH₂); 3.29 (d, J = 12.0 Hz, 1H, 13a-CH₂); 3.37-3.63 (m, 4H, 2-6-CH₂); 3.69 (d, J = 12.0 Hz, 1H, 13b-CH₂); 4.09 (s, 1H, 9-CH); 6.37 (bt, J = 5.2 Hz, 1H, 3-NH); 7.03 (bt, J = 5.9 Hz, 1H, 7-NH).

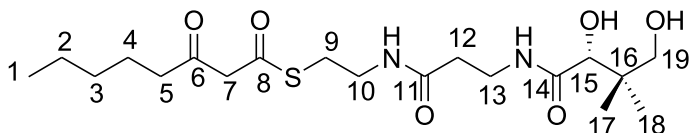
¹³C NMR (101 MHz, Chloroform-d):

δ [ppm]: 18.7 (12-CH₃); 18.9 (11-CH₂); 22.1 (15-CH₃); 24.6 (1-CH₂); 29.5 (15-CH₃); 33.0 (10-C); 34.9 (6-CH₂); 36.2 (5-CH₂); 42.4 (2-CH₂); 71.4 (13-CH₂); 77.2 (9-CH); 99.1 (14-C); 170.3 (4-CO); 171.1 (8-CO).

ES-MS: m/z (%): 319 [M] H⁺ (65%), 261 [M-(CH₃)₂CO] H⁺ (100%).

IR (γ cm⁻¹): 3419 (N-H), 3324 (N-H), 2980 (CH), 2944 (CH), 2872 (CH), 2556 (C-O), 1659 (-C=O)

Preparation of 3-oxooctanoyl pantetheine



A solution of 5-hexanoyl-6-hydroxy-2,2-dimethyl-4H-1,3-dioxin-4-one (0.314 mmol, 76.2 mg) and pantetheine dimethyl ketal (0.157 mmol, 50.0 mg) in toluene (0.314 mL) was stirred at 90 °C under nitrogen for 6 hours, before the solvent was removed *in vacuo*. The mixture was added to 1 N HCl (0.2 mL) in 3 mL of methanol and stirred at room temperature for 4 hours. The solution was neutralized with 1 N NaOH (0.2 mL) to pH 7. The solution was extracted with CH₂Cl₂ (2 mL) 5 times. The concentrated crude product was purified by mass-directed HPLC. The pure product was obtained as a yellow oil (25 mg, 38 %).

¹H NMR (400 MHz, Chloroform-*d*):

δ (ppm) 7.46 (14-NH, t, *J* = 5.9 Hz, 1H), 6.78 (11-NH, t, *J* = 5.9 Hz, 1H), 5.43 (7-enol CH, s), 3.98 (15-CH, s, 1H), 3.69 (7-CH₂, s, 2H), 3.59 – 3.28 (10-CH₂, 13-CH₂, 19-CH₂, m, 6H), 3.05 (9-CH₂, qd, *J* = 7.9, 7.1, 2.8 Hz, 2H), 2.51 (5-CH₂, t, *J* = 7.4 Hz, 2H), 2.42 (12-CH₂, t, *J* = 6.1 Hz, 2H), 2.15 (5-enol CH, t, *J* = 7.7 Hz), 1.56 (4-CH₂, p, *J* = 7.4 Hz, 2H), 1.27 (2-CH₂, 3-CH₂, *J* = m, 4H), 0.98 (18-CH₃, s, 2H), 0.90 (17-CH₃, s, 3H), 0.87 (1-CH₃, t, *J* = 7.0 Hz, 2H).

¹³C NMR (101 MHz, Chloroform-d):

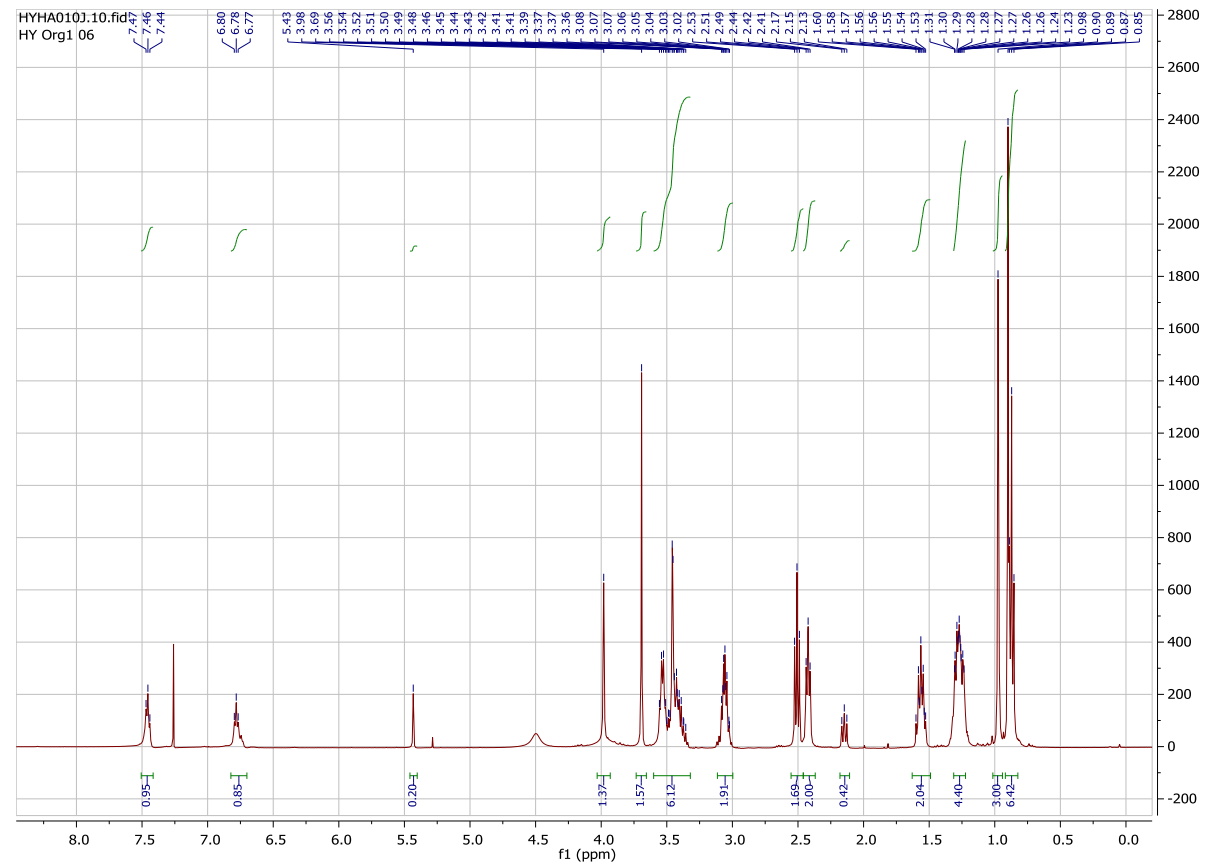
δ (ppm) 202.91 (6-CO), 192.48(8-CO), 173.89 (11-CO), 171.97 (14-CO), 99.11 (7-CH₂), 70.75 (15-CH), 57.04 (19-CH₂), 43.52 (5-CH₂), 39.33 (16-C), 39.07 (10-CH₂), 35.61 (13-CH₂), 35.18 (9-CH₂), 31.09 (12-CH₂), 29.04 (3-CH₂), 23.09 (2-CH₂), 22.36 (2-CH₂), 21.47 (18-CH₃), 20.47 (17-CH₃), 13.88 (1-CH₃).

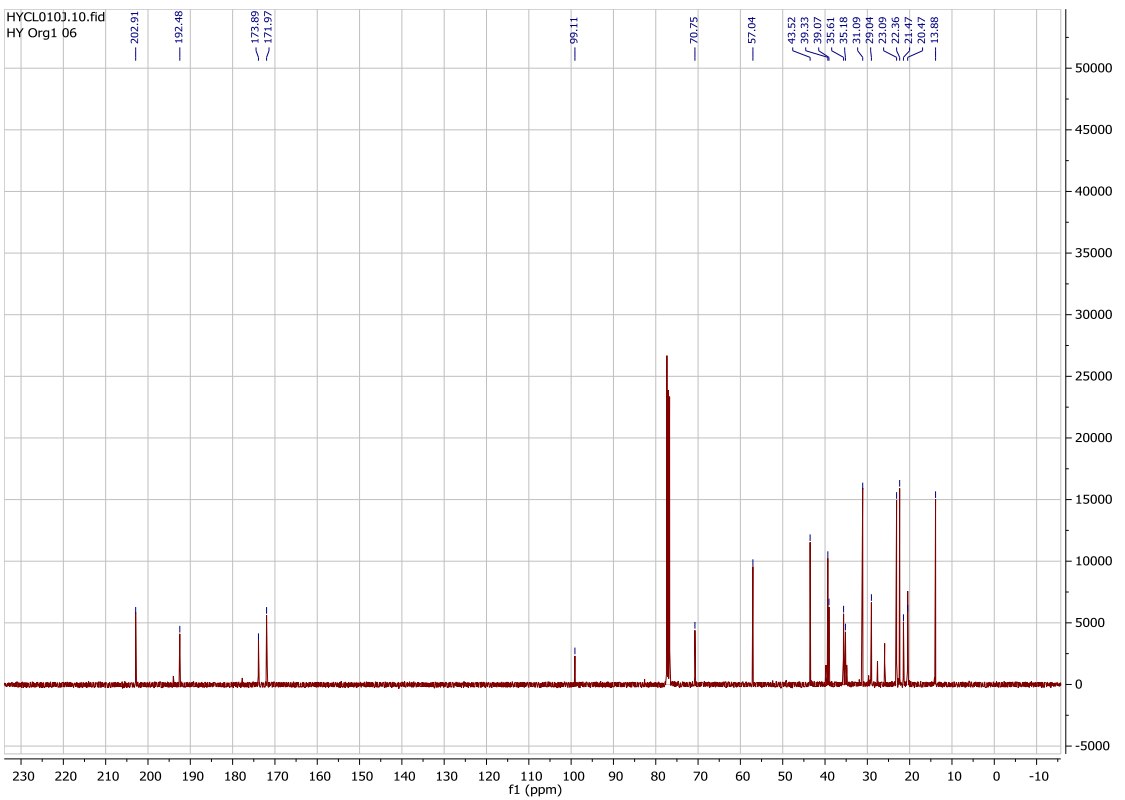
HRMS calcd for C₁₉H₃₄N₂O₆S (M+H)⁺ 419.2216, found:419.2215

IR (γ = cm⁻¹):

3240 (b, N-H, O-H). 1645,1721 (-C=O). 1528 (-CONH-). 1040 (C-O).

NMR of 3-oxooctanoyl pantetheine





8.3. Enzyme assay

Substrates **17** and C₈H₁₃O₂-S-PANT were individually dissolved in water at the concentration of 10 mg/mL. For the enzyme assay, 10 μ L of **17**, 17 μ L C₈H₁₃O₂-S-PANT (molecular ratio of the substrates 1:1) and 5 μ L purified MrPigD protein were mixed with 68 μ L phosphate buffer

(50 mM, pH 7.5). After incubation at 25°C for 2 h, 100 µL CH₃CN was added to stop the reaction, and the reaction was centrifuged to remove the precipitate. 20 µL of supernatant was analyzed by HPLC/MS (**Figure 8-2 and 8-3**).

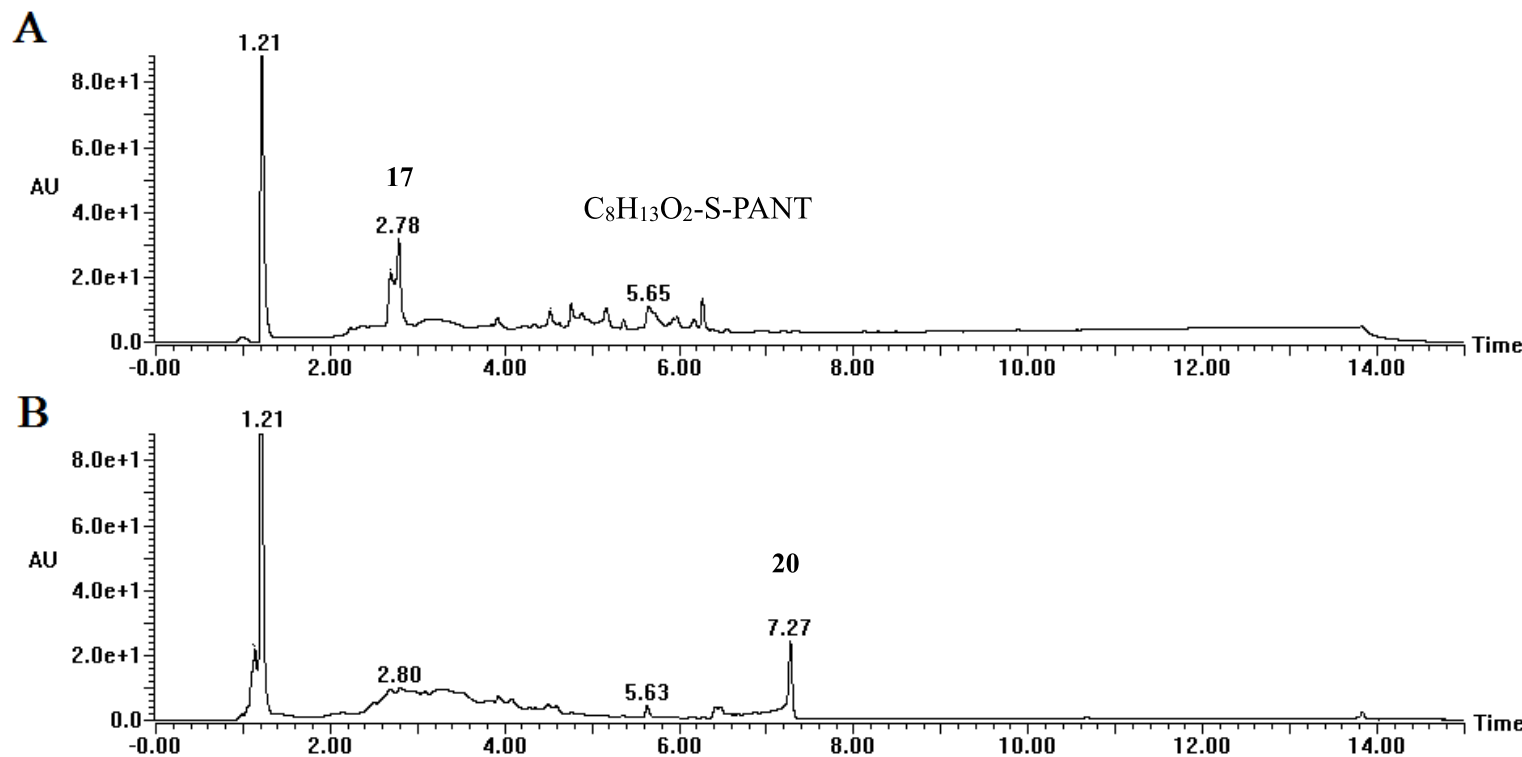


Figure 8-2. HPLC chromatograms of MrPigD enzyme assays. **A:** Enzyme assay with substrates **17** and C₈H₁₃O₂-S-PANT, using boiled (inactivated) MrPigD protein. **B:** Enzyme assay with substrates **17** and C₈H₁₃O₂-S-PANT, using the active MrPigD protein. Compounds were detected at 445 nm.

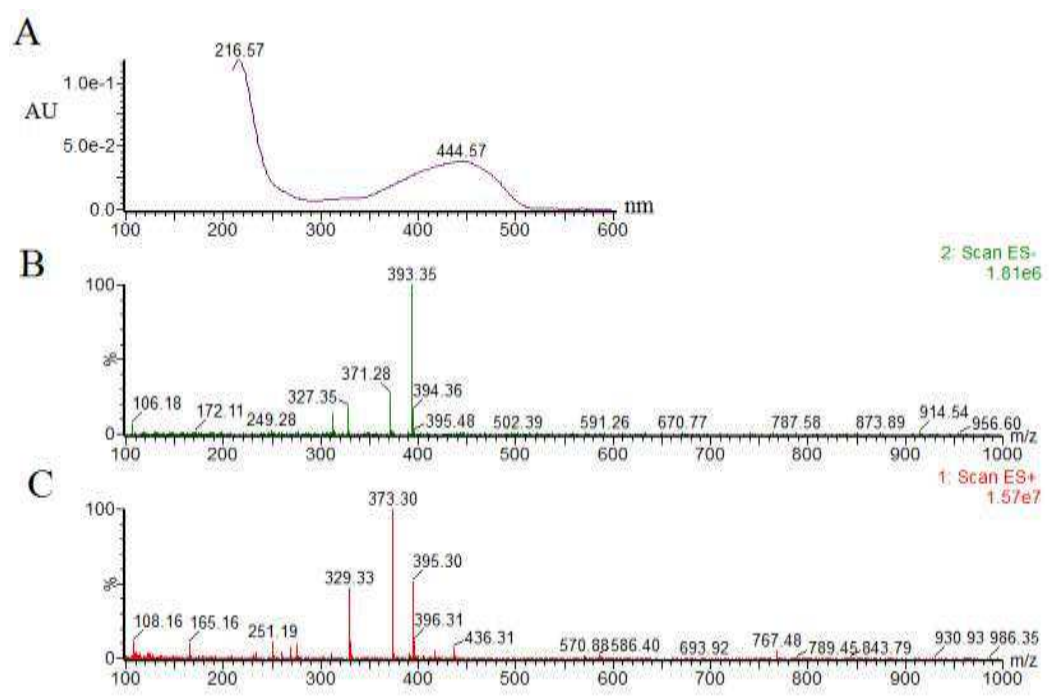


Figure 8-3. UV spectrum (A) and mass spectra (B: negative mode; C: positive mode) for compound 20

In addition to the peaks for substrates **17** and $\text{C}_8\text{H}_{13}\text{O}_2\text{-S-PANT}$, comparison of the two HPLC chromatograms in **Figure 8-2** revealed a new peak (Rt 7.27 min) when the active MrPigD enzyme was present in the reaction. Mass spectrometry shows that the molecular weight of product

20 is 372, identical to that of the assumed reaction product of substrates **17** and C₈H₁₃O₂-S-PANT (**Figure 8-4**). We conclude that MrPigD catalyzes acyl transfer from C₈H₁₃O₂-S-PANT to substrate **17** to form intermediate **18**, followed by spontaneous Knoevenagel cyclization to yield product **20** (**Figure 8-4**).

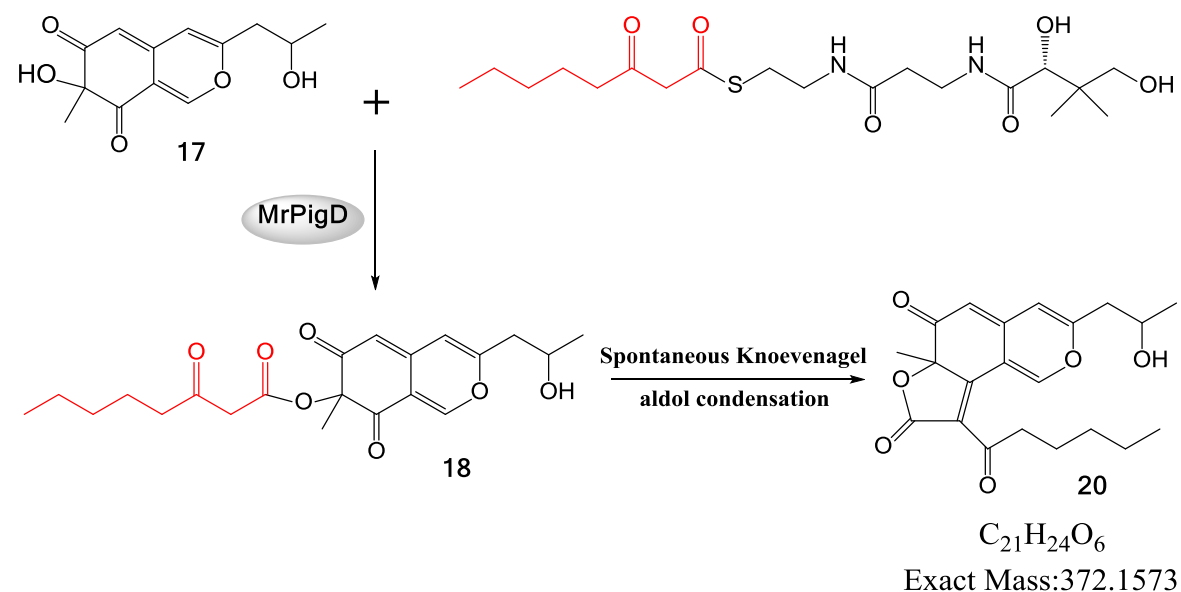


Figure 8-4. *In vitro* assay to verify MrPigD-mediated acyl transfer.

9. *In vitro* reaction of rubropunctatin (3), monascorubrin (4) and monascin (1) with 17 amino acids and ammonia

9.1. Preparation of the substrates

Fresh spore suspensions (10^5 /mL, 100 μ L) of *M. ruber* M7 were inoculated into 30 g of rice medium, and incubated at 28°C for 15 days. Dried fermented rice powder (0.50g) was extracted with 100% methanol (4 mL). Rubropunctatin (3, orange pigment, OP), monascorubrin (4, OP) and monascin (1, yellow pigment, YP) were isolated from the methanol extract by semi-preparative HPLC, using an Intertsil ODS-3 column (250 mm × 10 mm, 5 μ m), an isocratic elution with the mobile phase of 90% methanol, a flow rate of 3 mL/min and an injection volume of 50 μ L. Fractions containing rubropunctatin, monascorubrin and monascin were collected, dried under nitrogen flow, and dissolved in methanol.

Ammonia ($\text{NH}_3 \cdot \text{H}_2\text{O}$, 0.1 mol/L), and 17 different amino acids (Glu, Tyr, Asp, Val, Ile, Gly, Thr, GABA, Phe, Met, The, HyPro, Orn, His, Asn, Arg and Lys) were chosen as substrates. Double-distilled water was used as a negative control.

9.2. Reaction conditions

All amino acids were individually dissolved in double-distilled water at the concentration of 0.1 mol/L, except for Tyr (0.0045 mol/L) and Asp (0.05 mol/L), due to their low solubility. 50 μ L aliquots of the aqueous amino acid solutions (or that of ammonia in double-distilled water) and 50 μ L of 0.35 mmol/L rubropunctatin, monascorubrin or monascin, respectively (all dissolved in methanol) were mixed in PCR tubes, and incubated at 25°C for 10 min.

9.3. Detection methods

Reaction products were analyzed on an Acquity ultra performance liquid chromatograph (UPLC) with an Acquity BEH C18 column (2.1 mm × 100 mm, 1.7 μ m). Isocratic elutions were performed with the mobile phase including solvent A (0.1 % formic acid in water), solvent B (acetonitrile) and solvent C (double-distilled water) (A:B:C volume ratio is 10:50:40), a flow rate of 0.3 mL/min and an injection volume of 2 μ L. Detection was set to 210 nm to 600 nm. The temperatures of chromatographic column and sample were maintained at 40°C and 4°C, respectively.

UPLC-MS analysis of the reaction products was performed on a Waters ACQUITY UPLC system, equipped with a Xevo tandem quadrupole mass spectrometer (Waters, Milford, MA, USA), using the same UPLC method. Two microliters of each sample were injected into the column. Mass spectrometry was performed using a single quadrupole detector equipped with an electrospray ionization source (ESI). Positive ionization was used in the scan mode from 200 to 600 *m/z*. The capillary voltage was set to 2.5 kV, the source and desolvation temperatures were optimized, and kept at 150°C and 350°C, respectively. The desolvation gas was delivered at a flow rate of 10 L/min and the cone gas was set to 1 L/min.

9.4. Results

As shown in **Figure 9-1**, ammonia and some of the amino acids such as Arg and GABA could easily react with the orange pigments rubropunctatin (**3**) and monascorubrin (**4**), as reflected in the obvious color changes of the reaction mixtures compared to the control. In contrary, no significant color change was observed in the reaction with the yellow pigment monascin (**1**) and the tested amino acids and ammonia.

In order to further confirm the reaction of OPs rubropunctatin (**3**) and monascorubrin (**4**) with amino acids and ammonia, we selected their reactions with GABA, Lys and ammonia as representatives and analyzed the reaction products by UPLC-MS. As shown in **Figures 9-2 to 9-7**, GABA, Lys and ammonia directly react with rubropunctatin and monascorubrin to form the expected products, while the UPLC-MS results confirmed that the amino acids and ammonia did not react with the yellow pigment monascin (data not shown).

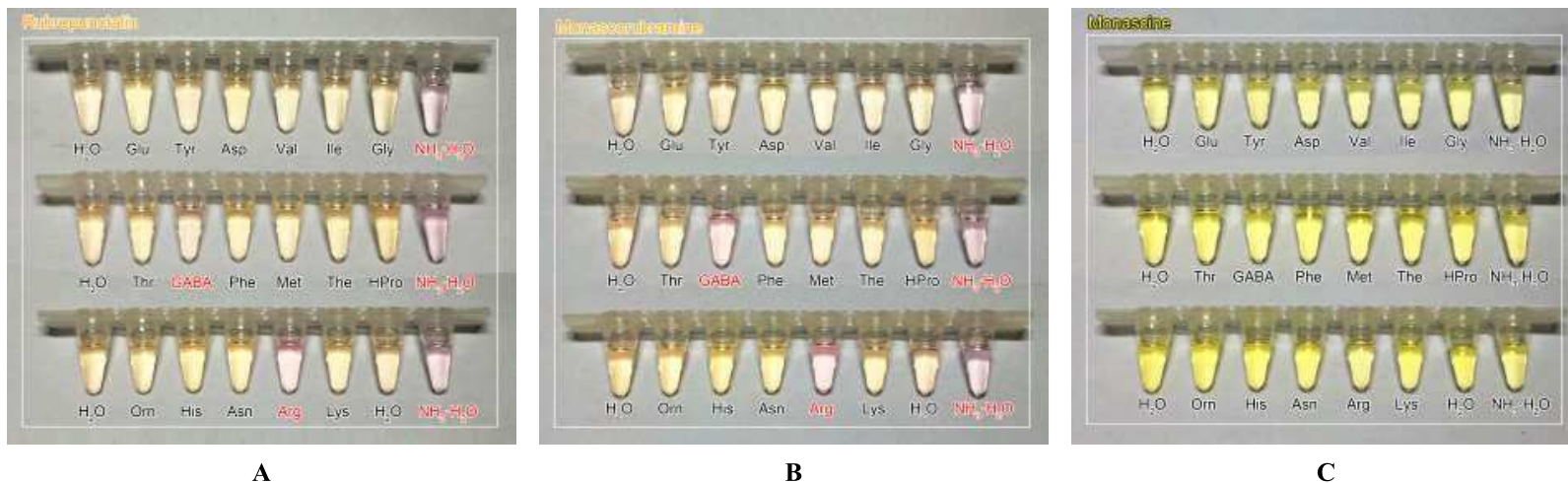
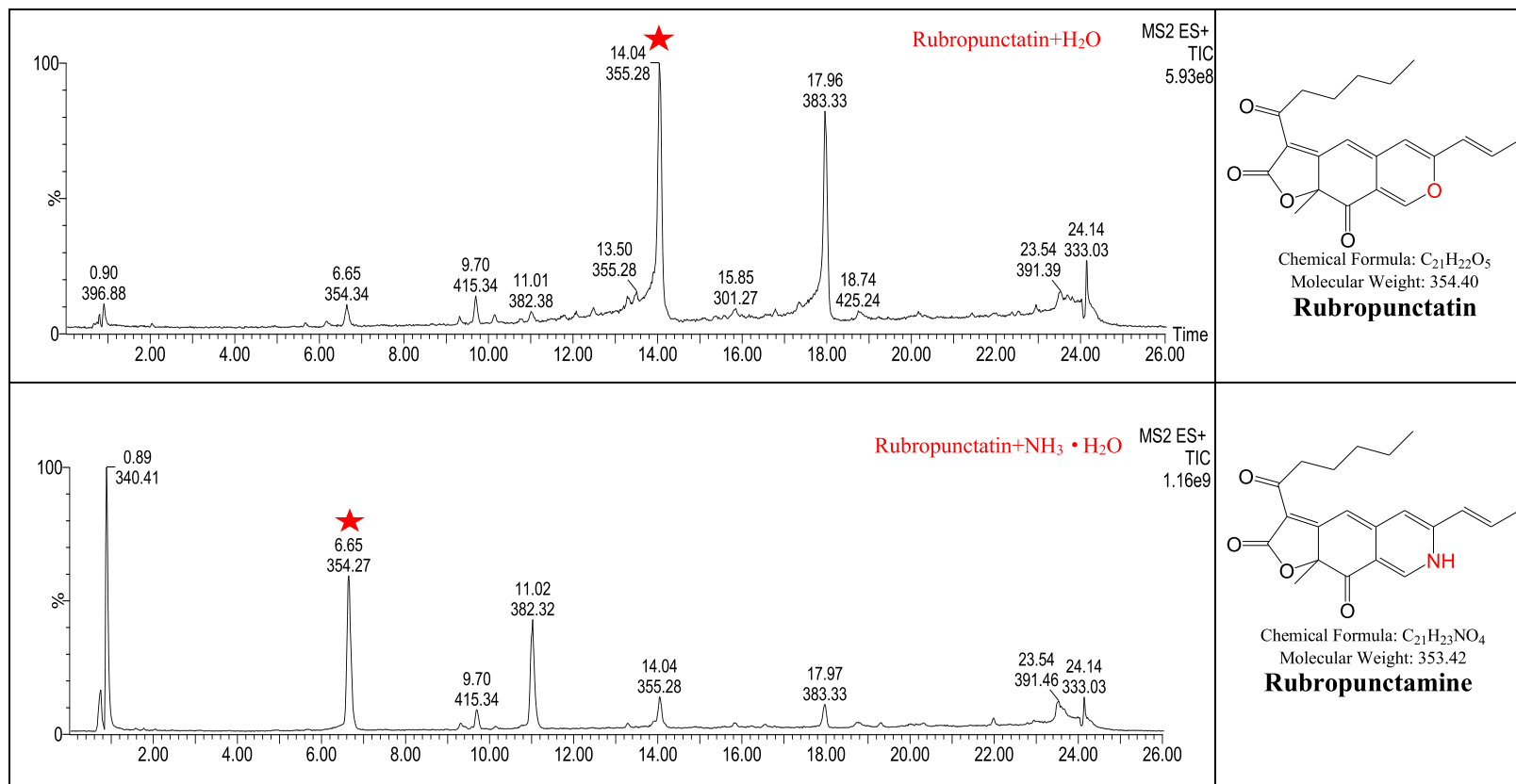


Figure 9-1. *In vitro* reactions between orange and yellow MonAzPs and 17 amino acids and ammonia. **A**, Reaction of rubropunctatin (3) with 17 amino acids and ammonia. **B**, Reaction of monascorubrin (4) with 17 amino acids and ammonia. **C**, Reaction of monascin (1) with 17 amino acids and ammonia.

Figure 9-2. Total ion chromatograms of the reactions of rubropunctatin with H₂O, ammonia, Lys and GABA, respectively. Asterisks indicate the peaks of the listed compounds on the right.



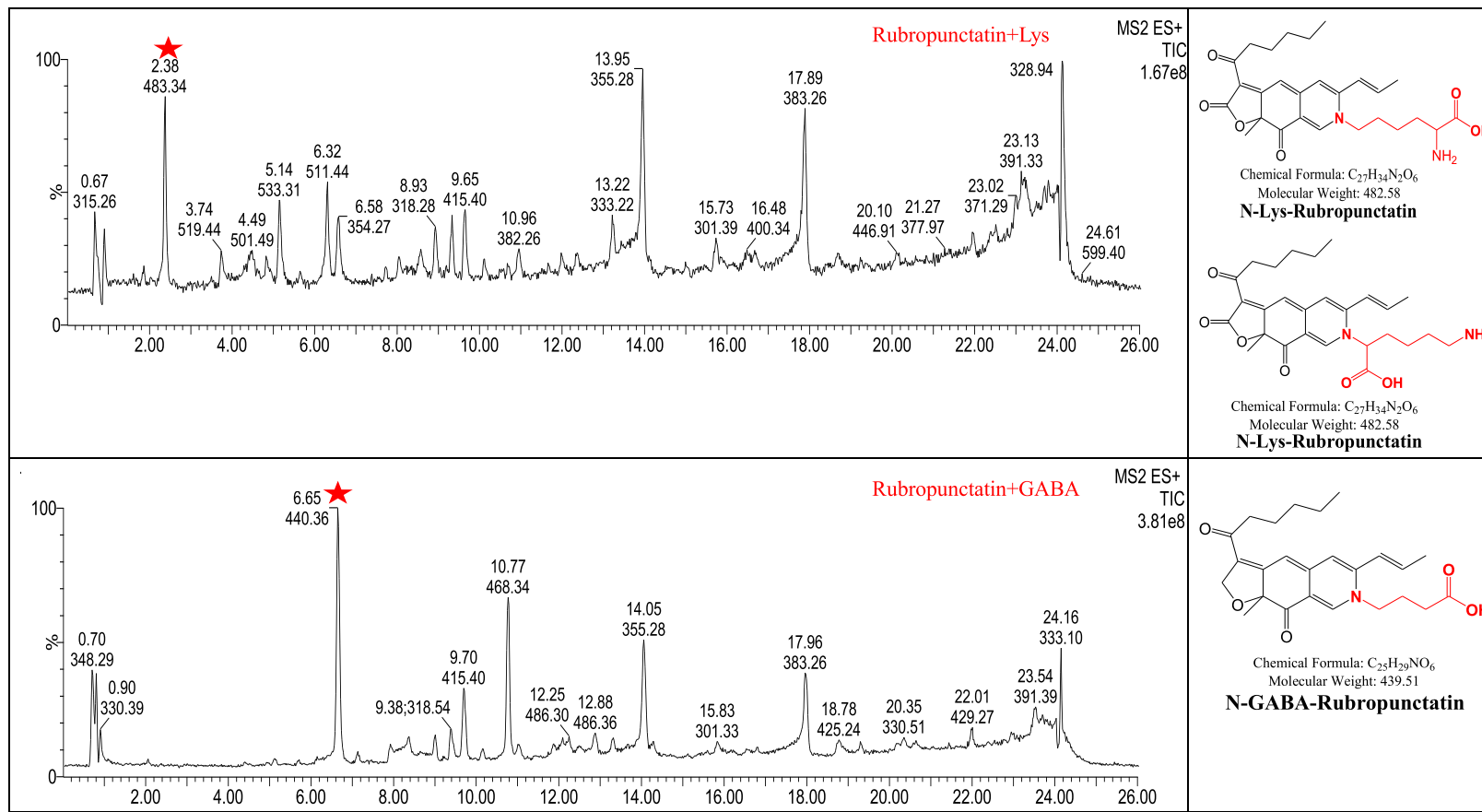
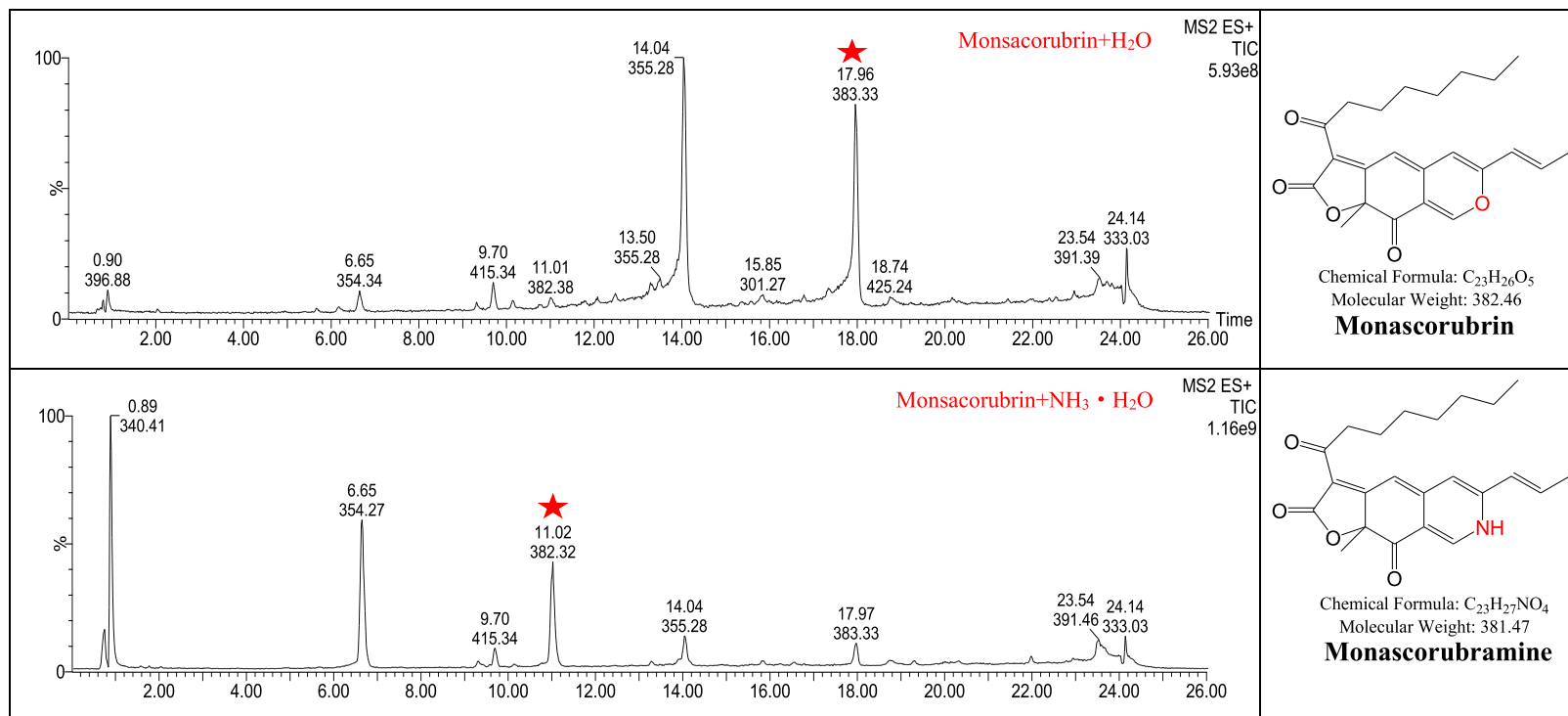


Figure 9-3. Total ion chromatograms of the reactions of monascorubrin with H₂O, ammonia, Lys and GABA, respectively.
 Asterisks indicate the peaks of the listed compounds on the right.



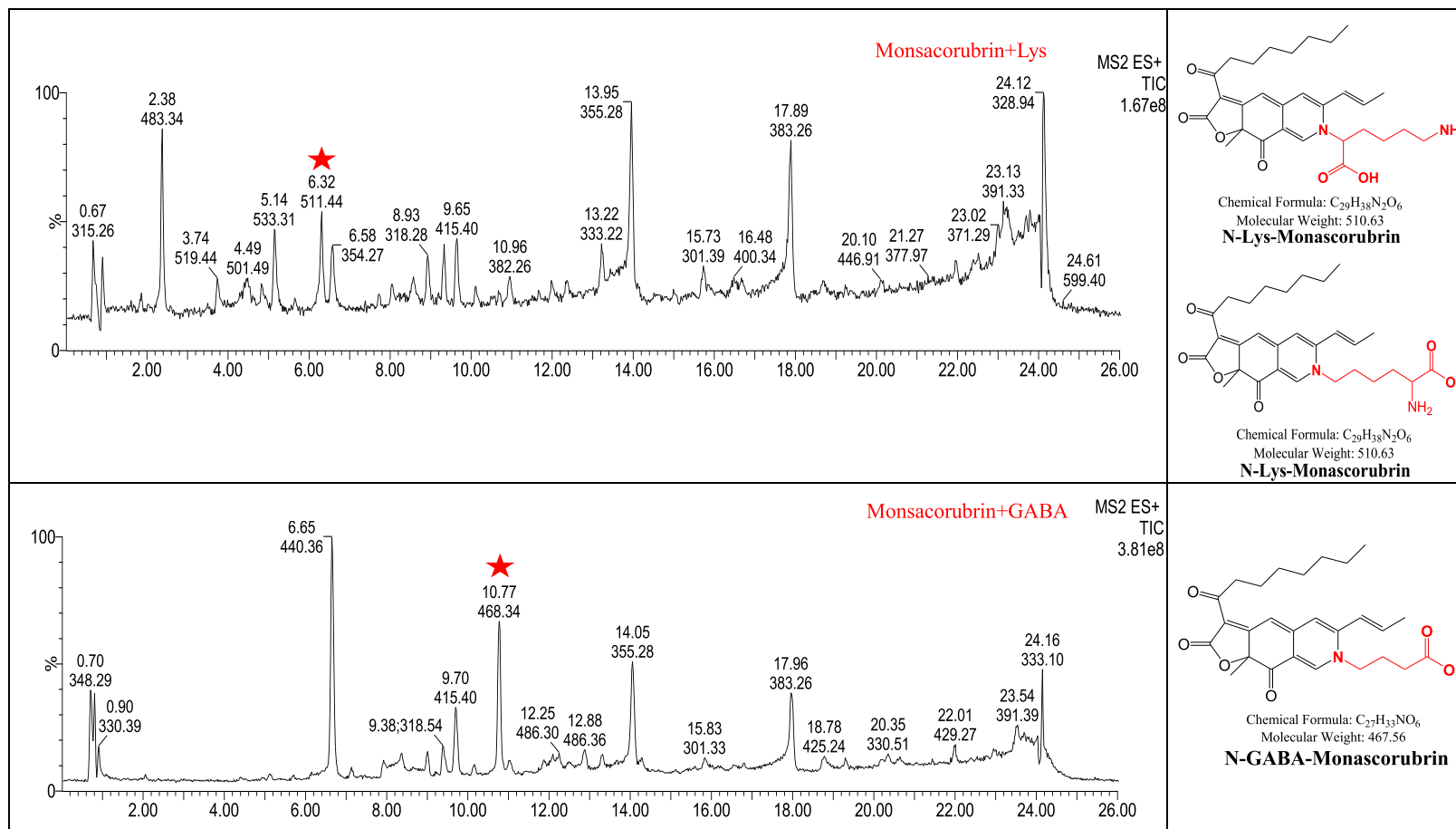
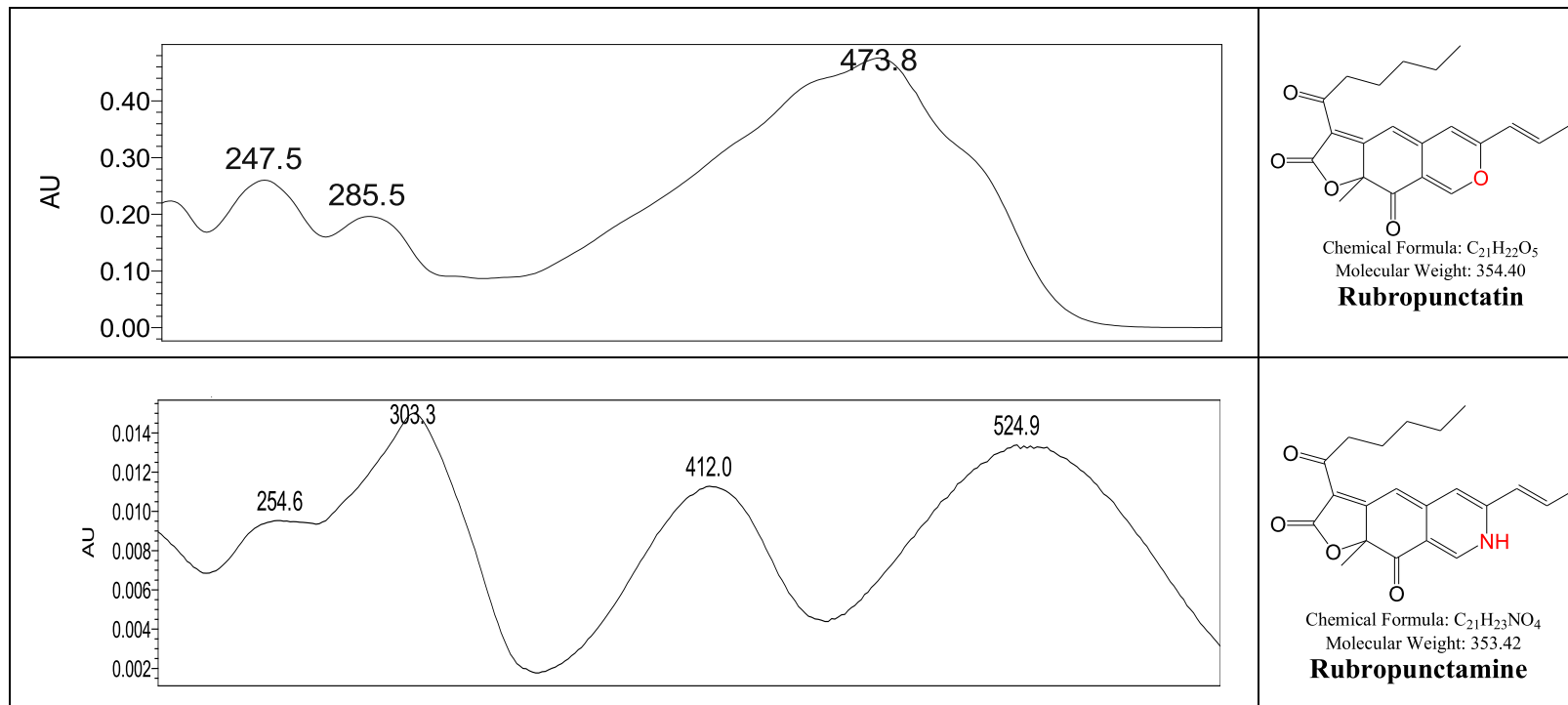
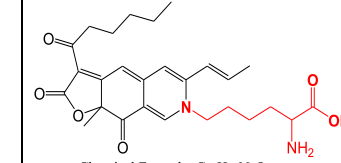
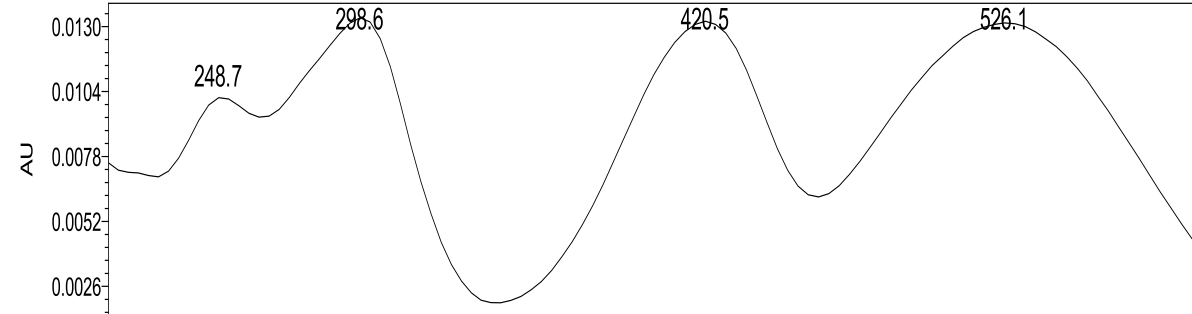
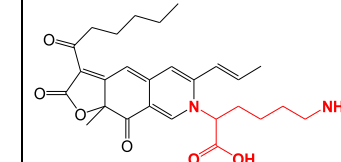


Figure 9-4. UV-VIS spectra of the products of rubropunctatin reacting with H₂O, ammonia, Lys and GABA, respectively.

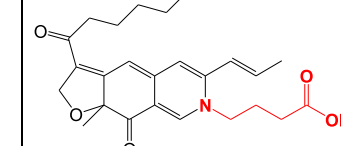
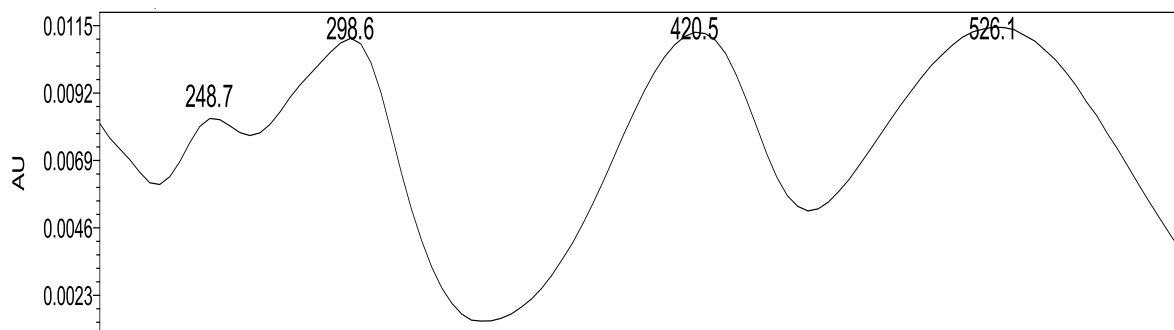




N-Lys-Rubropunctatin

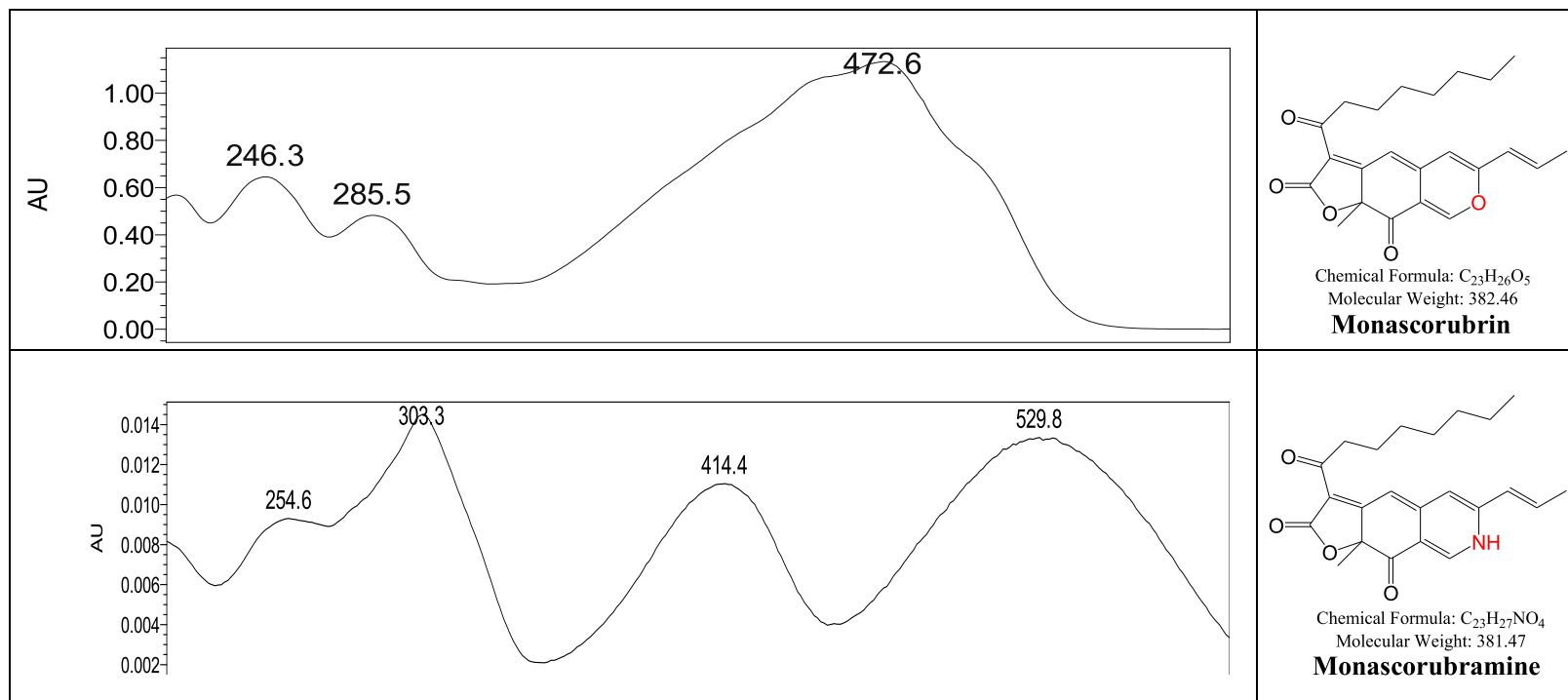


N-Lys-Rubropunctatin



N-GABA-Rubropunctatin

Figure 9-5. UV-VIS spectra of the products of monascorubrin reacting with H₂O, ammonia, Lys and GABA, respectively



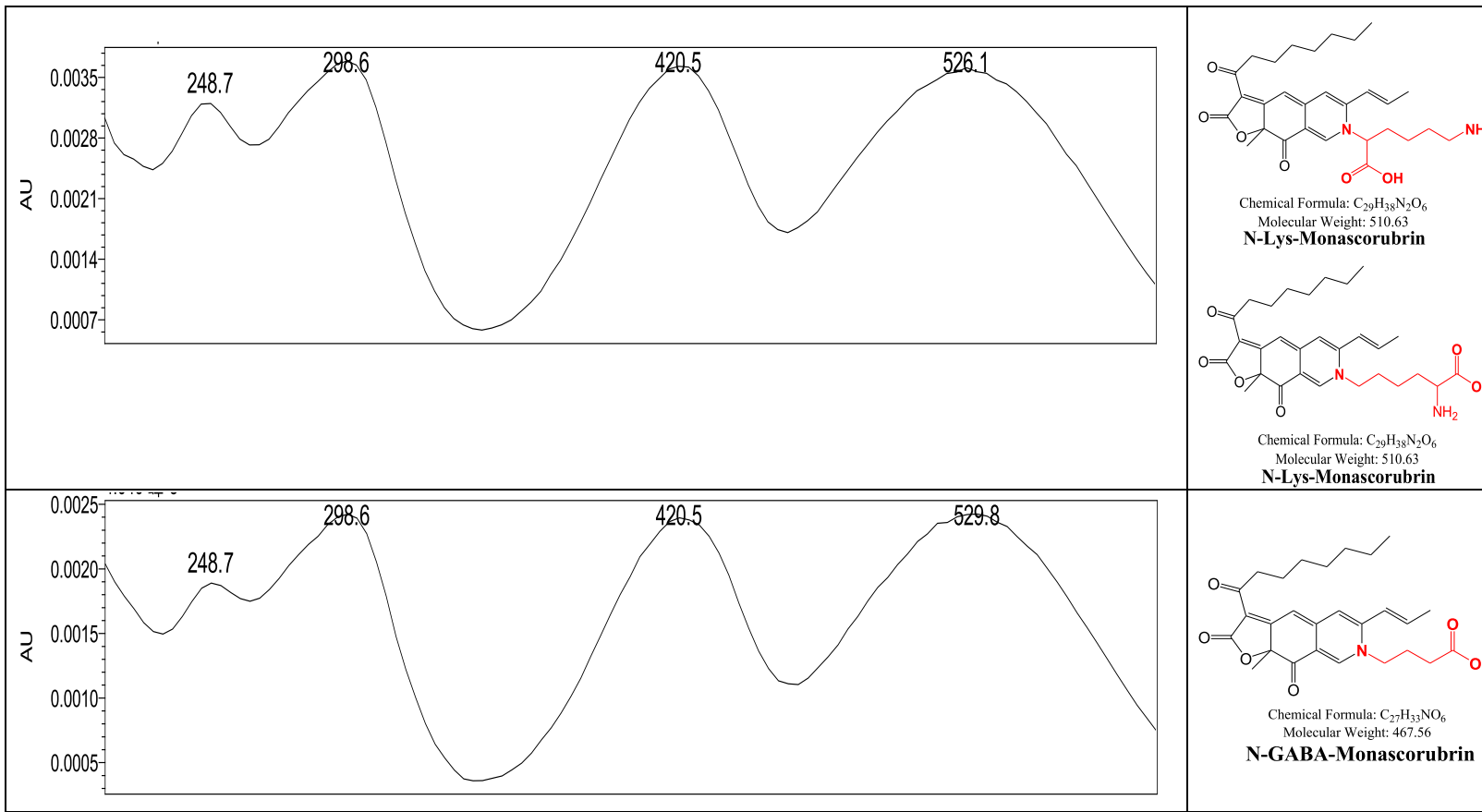
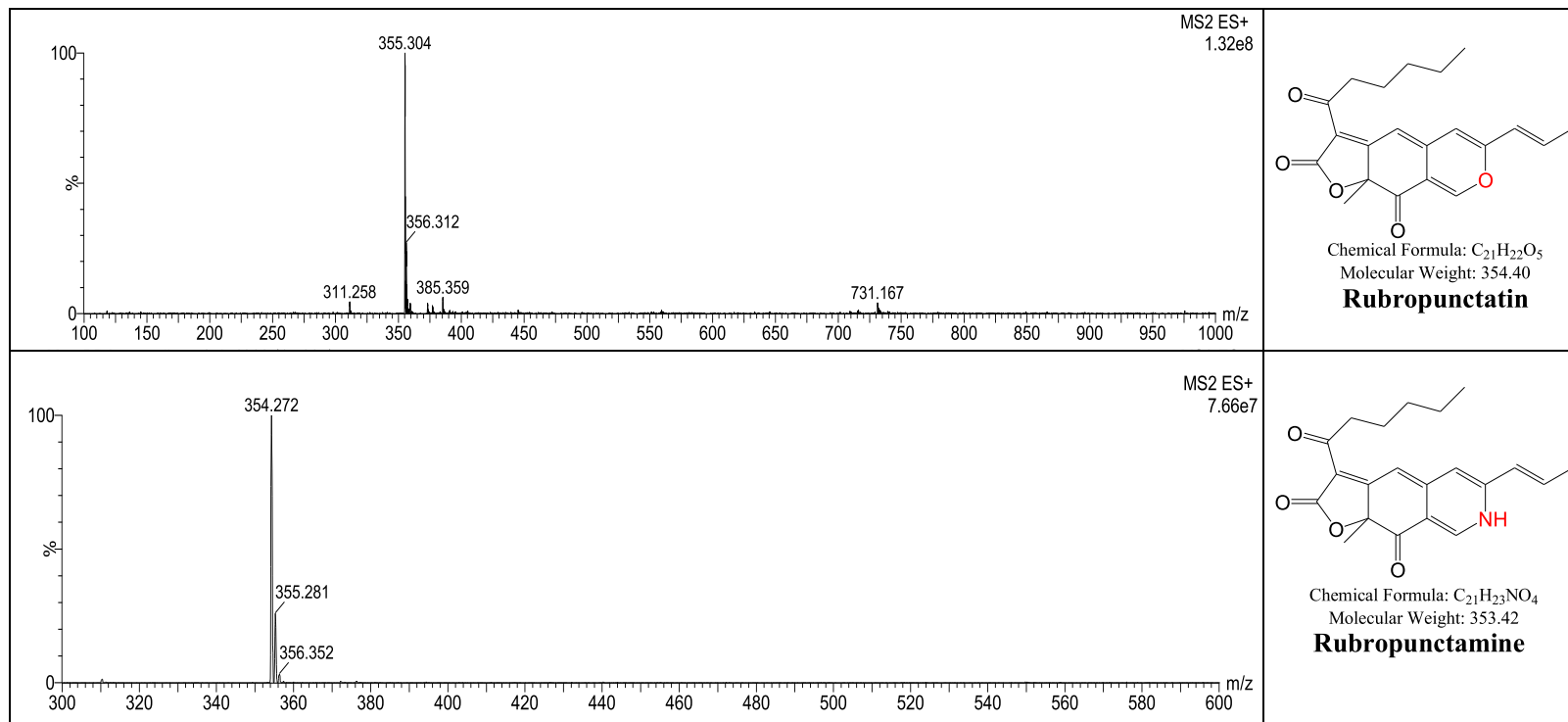


Figure 9-6. Mass spectra of the products of rubropunctatin reacting with H₂O, ammonia, Lys and GABA, respectively.



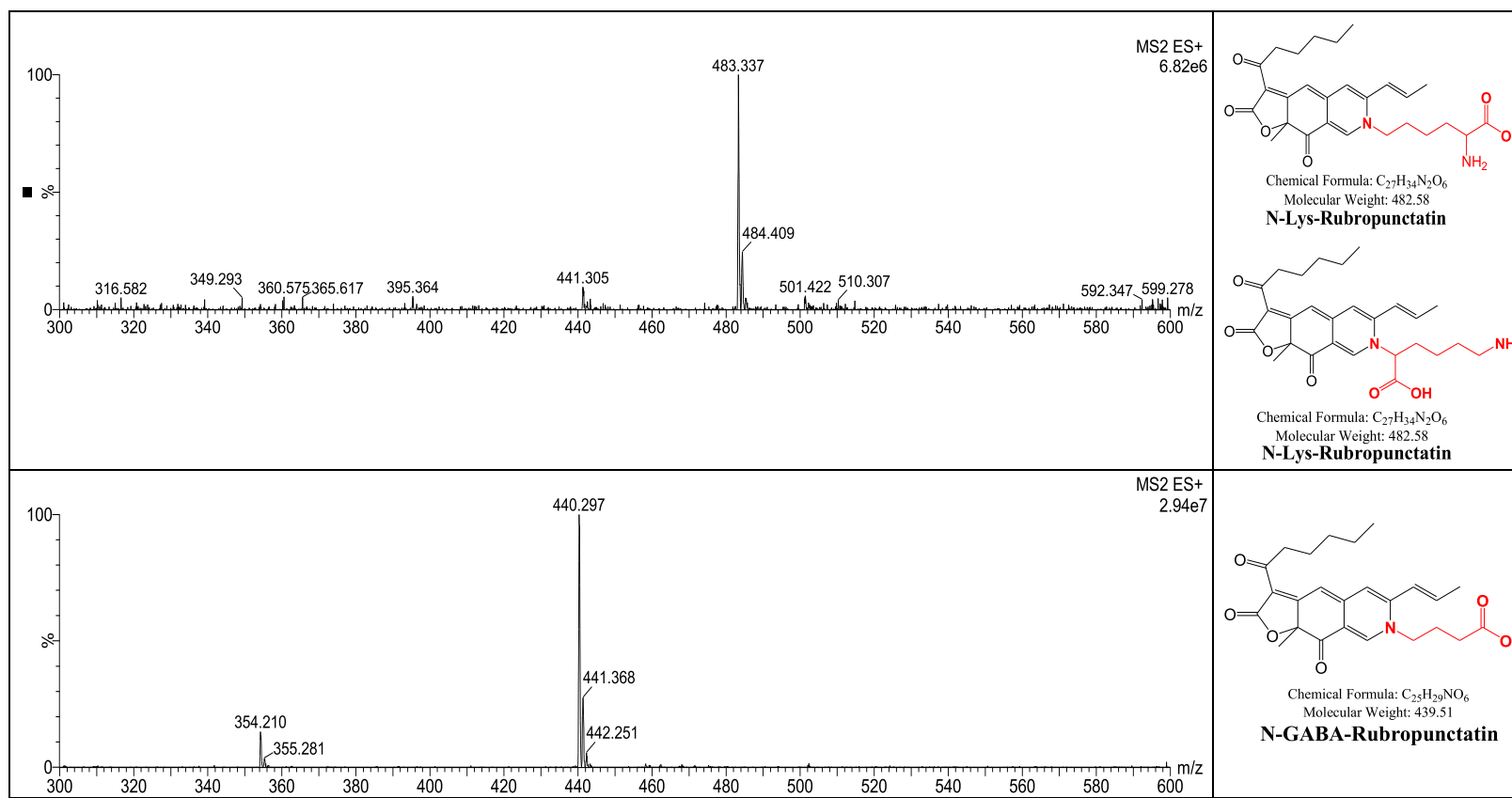
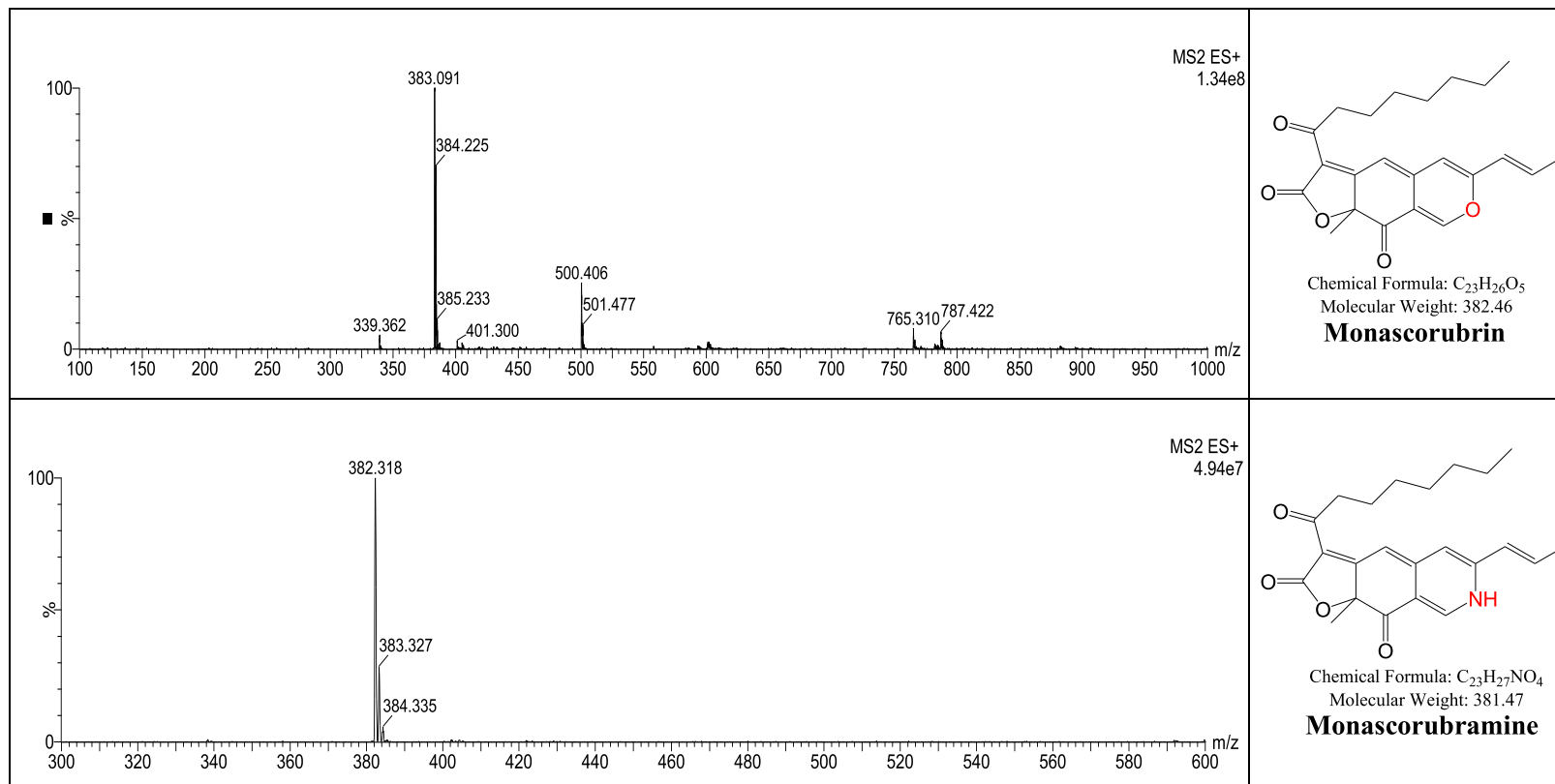
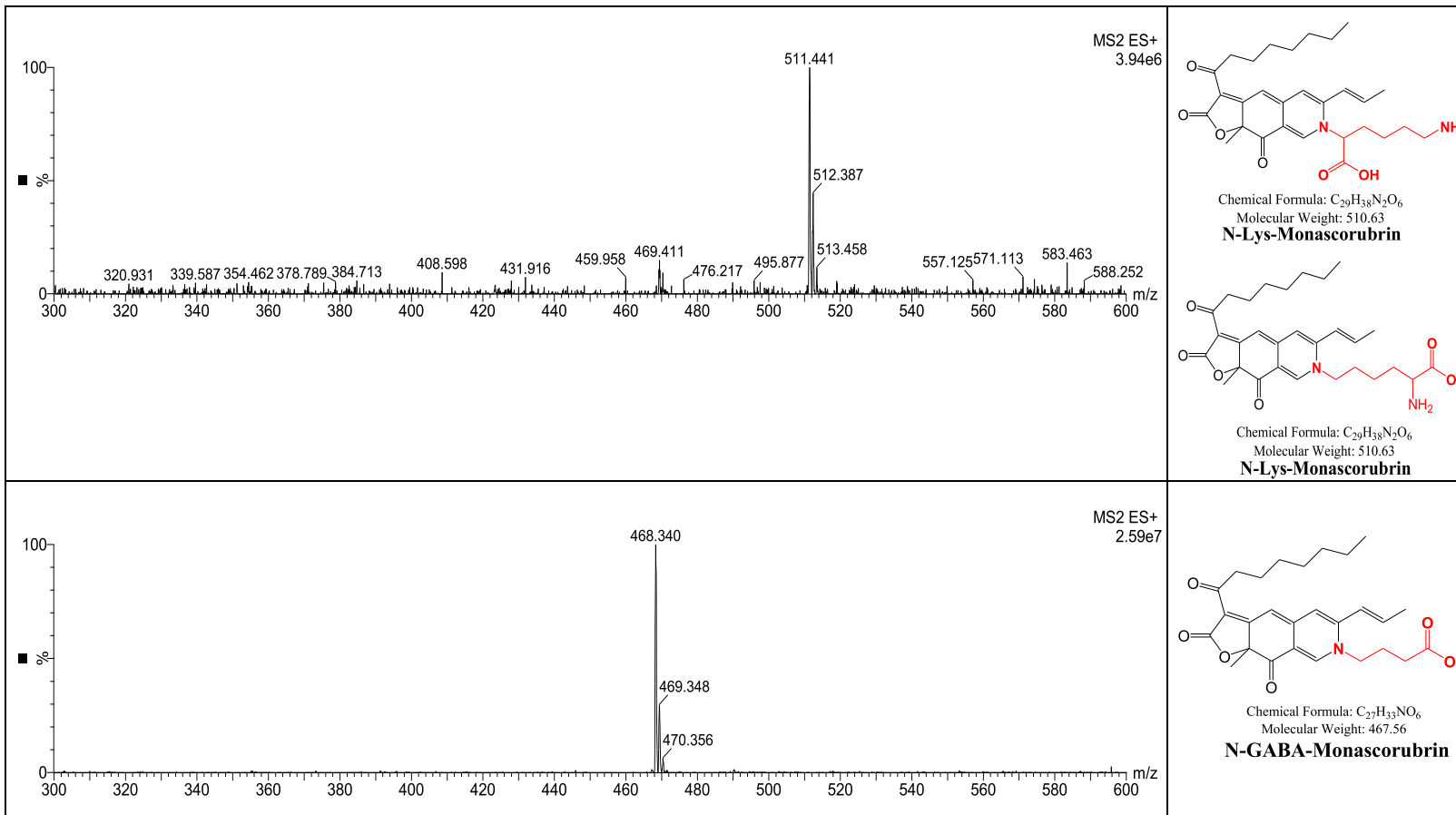
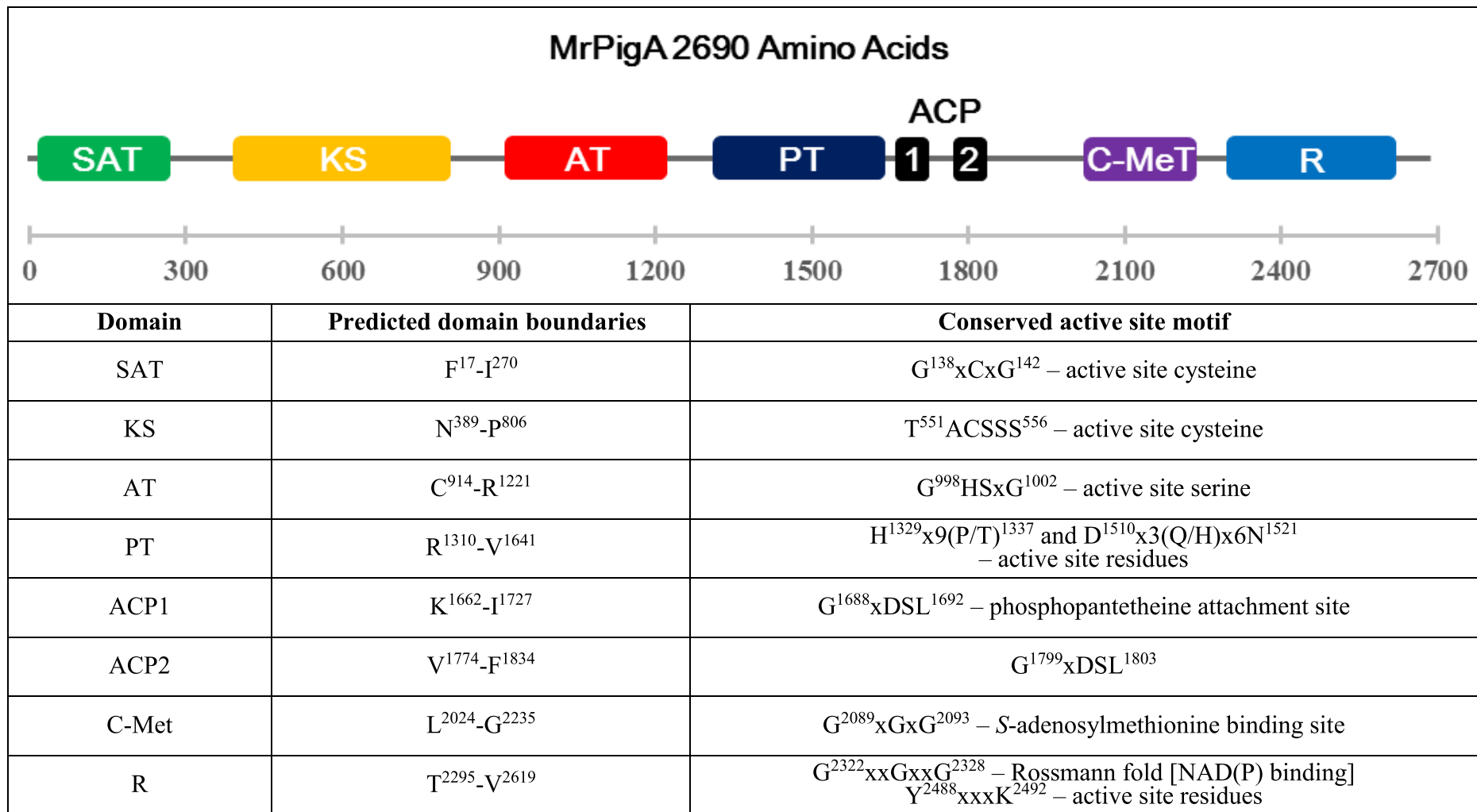


Figure 9-7. Mass spectra of the products of monascorubrin reacting with H₂O, ammonia, Lys and GABA, respectively



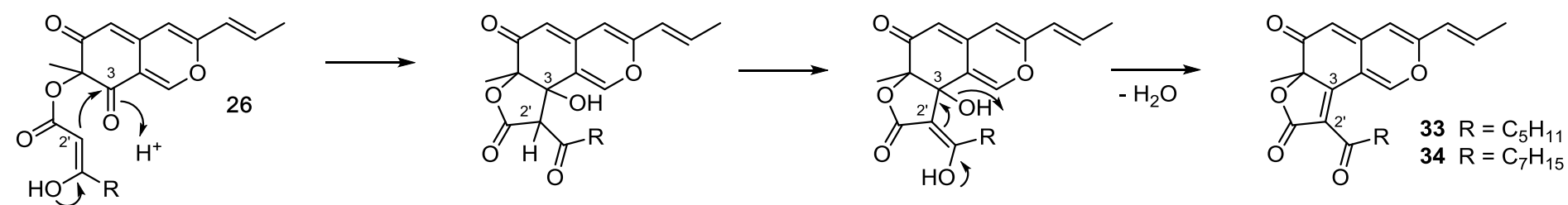


10. Domain analysis of MrPigA, the MonAzPs polyketide synthase from *M. ruber* M7



11. Mechanism of Knoevenagel cyclization

Knoevenagel cyclization plays an important role in MonAzPs production. The following example shows the reaction mechanism of Knoevenagel cyclization.



10. References

- Bai, J., Lu, Y., Xu, Y., Zhang, W., Chen, M., Lin, M., Gunatilaka, A.A., Xu, Y., and Molnár, I. (2016) Diversity-oriented combinatorial biosynthesis of hybrid polyketide scaffolds from azaphilone and benzenediol lactone biosynthons. *Organic Letters* **18**, 1262-1265.
- Bijinu, B., Chandran, R., Park, S.H. and Kwon, H.J. (2015) A new protein factor in the product formation of non-reducing fungal polyketide synthase with a C-Terminus reductive domain. *Journal of Microbiology and Biotechnology* **25**, 1648-1652.
- Bijinu, B., Chen, C.C., Pan, T.M. and Kwon, H.J. (2014) *Mpp7* controls regioselective knoevenagel condensation during the biosynthesis of *Monascus* azaphilone pigments. *Tetrahedron Letters* **55**, 1640-1643.
- Bijinu, B., Suh, J.W., Park, S.H. and Kwon, H.J. (2014) Delineating *Monascus* azaphilone pigment biosynthesis: Oxidoreductive modifications determine the ring cyclization pattern in azaphilone biosynthesis. *RSC Advances* **4**, 59405-59408.
- Campoy, S., Rumbero, A., Martín, J. F. and Liras, P. (2006) Characterization of an hyperpigmenting mutant of *Monascus purpureus* IB1: Identification of two novel pigment chemical structures. *Applied Microbiology and Biotechnology* **70**, 488-496.
- Fielding, B. C., Holker, J. S. E., Jones, D. F., Powell, A. D. G., Richmond, K. W., Robertson, A. and Whalley, W. B. (1961) 898. The chemistry of fungi. Part xxxix. The structure of monascin. *Journal of the Chemical Society (Resumed)*, 4579-4589.
- Haws, E. J., Holker, J. S. E., Kelly, A., Powell, A. D. G. and Robertson, A. (1959) 722. The chemistry of fungi. Part xxxvii. The structure of rubropunctatin. *Journal of the Chemical Society (Resumed)*, 3598-3610.
- He, Y., Liu, Q., Shao, Y. and Chen, F. (2013) *Ku70* and *ku80* null mutants improve the gene targeting frequency in *Monascus ruber* M7. *Applied Microbiology and Biotechnology* **97**, 4965-4976.
- Huang, Z., Xu, Y., Li, L. and Li, Y. (2008) Two new *Monascus* metabolites with strong blue fluorescence isolated from red yeast rice. *Journal of Agricultural and Food Chemistry* **56**, 112-118.
- Jongrungruangchok, S., Kittakoop, P., Yongsmith, B., Bavovada, R., Tanasupawat, S., Lartpornmatulee, N. and Thebtaranonth, Y. (2004) Azaphilone pigments from a yellow mutant of the fungus *Monascus kaoliang*. *Phytochemistry* **65**, 2569-2575.
- Kumasaki, S., Nakanishi, K., Nishikawa, E. and Ohashi, M. (1962) Structure of monascorubrin. *Tetrahedron* **18**, 1171-1184.
- Liu, J., Zhou, Y., Yi, T., Zhao, M., Xie, N., Lei, M., Liu, Q., Shao, Y. and Chen, F. (2016) Identification and role analysis of an intermediate produced by a polygenic mutant of *Monascus* pigments cluster in *Monascus ruber* M7. *Applied Microbiology and Biotechnology* **100**, 7037-7049.

- Liu, Q., Xie, N., He, Y., Wang, L., Shao, Y., Zhao, H. and Chen, F. (2014) *MpigE*, a gene involved in pigment biosynthesis in *Monascus ruber* M7. *Applied Microbiology and Biotechnology* **98**, 285-296.
- Ma, S.M., Li, J.W., Choi, J. W., Zhou, H., Lee, K.K., Moorthie, V.A., Xie, X., Kealey, J.T., Da, Silva, N.A., Vederas, J.C. and Tang, Y. (2009) Complete reconstitution of a highly reducing iterative polyketide synthase. *Science* **326**, 589-592.
- Manchand, P. S., Whalley, W. and Chen, F.C. (1973) Isolation and structure of ankaflavin: A new pigment from *Monascus anka*. *Phytochemistry* **12**, 2531-2532.
- Nierman, W. C., Fedorova-Abrams, N. D. and Andrianopoulos, A. (2015) Genome sequence of the aids-associated pathogen *Penicillium marneffei* (ATCC18224) and its near taxonomic relative *Talaromyces stipitatus* (ATCC10500). *Genome Announcements* **3**, e01559-01514.
- Pahirulzaman, K., Williams, K. and Lazarus, C. M. (2012) A toolkit for heterologous expression of metabolic pathways in *Aspergillus oryzae*. *Methods Enzymol* **517**, 241-260.
- Shao, Y., Ding, Y., Zhao, Y., Yang, S., Xie, B. and Chen, F. (2009) Characteristic analysis of transformants in T-DNA mutation library of *Monascus ruber*. *World Journal of Microbiology and Biotechnology* **25**, 989-995.
- Sweeny, J. G., Estrada-Valdes, M. C., Iacobucci, G. A., Sato, H. and Sakamura, S. (1981) Photoprotection of the red pigments of *Monascus anka* in aqueous media by 1,4,6-trihydroxynaphthalene. *Journal of Agricultural and Food Chemistry* **29**, 1189-1193.
- Woo, P. C. Y., Lam, C. W., Tam, E. W. T., Lee, K. C., Yung, K. K. Y., Leung, C. K. F., Sze, K. H., Lau, S. K. P. and Yuen, K. Y. (2014) The biosynthetic pathway for a thousand-year-old natural food colorant and citrinin in *Penicillium marneffei*. *Scientific Reports* **4**, 6728.
- Wu, M.D., Cheng, M.J., Yech, Y.J., Chen, Y.L., Chen, K.P., Yang, P.H., Chen, I.S. and Yuan, G.F. (2013) Monascusazaphilones A-C, three new azaphilone analogues isolated from the fungus *Monascus purpureus* BCRC 38108. *Natural Product Research* **27**, 1145-1152.
- Xie, N., Liu, Q. and Chen, F. (2013) Deletion of *PigR* gene in *Monascus ruber* leads to loss of pigment production. *Biotechnology Letters* **35**, 1425-1432.
- Xie, N., Zhang, Y. and Chen, F. (2015) Identification of a pigment-polyketide synthase gene deleted mutant of *Monascus ruber* M7. *Acta Microbiologica Sinica* **55**, 863-872.
- Xu, Y., Espinosa-Artiles, P., Schubert, V., Xu, Y. M., Zhang, W., Lin, M., Gunatilaka, A.A., Süßmuth, R. and Molnár, I. (2013) Characterization of the biosynthetic genes for 10,11-dehydrocurvularin, a heat shock response-modulating anticancer fungal polyketide from *Aspergillus terreus*. *Applied and Environmental Microbiology* **79**, 2038-2047.
- Xu, Y., Zhou, T., Espinosa-Artiles,P., Tang, Y., Zhan, J., and Molnár, I. (2014a) Insights into the biosynthesis of 12-membered resorcylic acid lactones from heterologous production in *Saccharomyces cerevisiae*. *ACS Chemical Biology* **9**, 1119–1127.
- Xu, Y., Zhou, T., Zhang, S., Espinosa-Artiles, P., Wang, L., Zhang, W., Lin, M., Gunatilaka, A.A., Zhan, J., Molnár, I. (2014b) Diversity-oriented combinatorial biosynthesis of benzenediol lactone scaffolds by subunit shuffling of fungal polyketide synthases. *Proceedings of the National Academy of Sciences* **111**, 12354-12359.
- Yu, J.H., Hamari, Z., Han, K.H., Seo, J.A., Reyes-Domínguez, Y. and Scazzocchio, C. (2004) Double-joint PCR: A PCR-based molecular tool for gene manipulations in

filamentous fungi. *Fungal Genetics and Biology* **41**, 973-981.

Zabala, A. O., Xu, W., Chooi, Y.H. and Tang, Y. (2012) Characterization of a silent azaphilone gene cluster from *Aspergillus niger* ATCC 1015 reveals a hydroxylation-mediated pyran-ring formation. *Chemistry & Biology* **19**, 1049-1059.